

Université de Montréal

Le rôle des interneurones GABAergiques dans l'hippocampe normal
et dans un modèle expérimental d'épilepsie chez le rat

par

France Morin

Département de physiologie

Faculté de médecine

Thèse présentée à la Faculté des études supérieures
en vue de l'obtention du grade de
Philosophiae Doctor (Ph.D.)
en sciences neurologiques

novembre, 1998

©France Morin, 1998



W
4
U58
1999
V.052

Библиотека Университета

Библиотека Университета
имени Ахмета Насырова им. Ахмета Насырова

2002

Библиотека

имени Ахмета Насырова

Алматы, Казахстан

Библиотека им. Ахмета Насырова
имени Ахмета Насырова
имени Ахмета Насырова



Библиотека
имени Ахмета Насырова

Université de Montréal
Faculté des études supérieures

Cette thèse intitulée :

Le rôle des interneurones GABAergiques dans l'hippocampe normal
et dans un modèle expérimental d'épilepsie chez le rat

présentée par :

France Morin

a été évaluée par un jury composé des personnes suivantes :

Dr. Vincent Castellucci (président-rapporteur)

Dr. Denis Paré (examinateur externe)

Dr. Caterina Psarropoulou (membre du jury)

Dr. Jean-Claude Lacaille (directeur de recherche)

Dr. Roger Godbout (représentant du doyen)

Thèse acceptée le : 26 février 1999

SOMMAIRE

Dans cette thèse, nous avons caractérisé les changements qui surviennent dans les circuits excitateurs et inhibiteurs de la région CA1 de l'hippocampe dans le modèle d'épilepsie de l'acide kaïnique (AK) chez le rat.

Les propriétés intrinsèques et les courants synaptiques des cellules pyramidales et des interneurones ont été caractérisés électrophysiologiquement chez le rat normal. Les propriétés intrinsèques étaient différentes dans les cellules pyramidales et les interneurones, mais étaient semblables dans groupes d'interneurones. Les courants synaptiques non-NMDA, NMDA et GABA_A étaient similaires dans les interneurones et cellules pyramidales, à l'exception des courants NMDA dont la cinétique différait dans les interneurones de la couche oriens et l'alveus (O/A).

Les mécanismes contribuant à l'hyperexcitabilité des cellules pyramidales après le traitement à l'AK ont ensuite été étudiés. L'effet du traitement sur le nombre d'interneurones GABAergiques a été étudié en utilisant l'immunocytochimie contre la décarboxylase de l'acide glutamique (DAG). Le traitement a provoqué une perte sélective des interneurones DAG dans la couche O/A, mais pas dans les couches radiatum et lacunosum-moleculare (LM). Une perte similaire d'interneurones a été observée en utilisant une méthode de coloration de Nissl. Cette perte sélective d'interneurones GABAergiques contribuerait à l'hyperexcitabilité dans l'hippocampe après le traitement.

L'effet du traitement à l'AK sur les propriétés intrinsèques et les courants synaptiques des interneurones et cellules pyramidales a aussi été examiné. Les propriétés intrinsèques étaient intactes suite au traitement, mais les réponses synaptiques étaient modifiées. Les courants postsynaptiques excitateurs étaient réduits spécifiquement dans

les interneurones LM. La conductance des courants GABA_A monosynaptiques n'était pas diminuée dans les cellules pyramidales, mais leur cinétique était plus rapide. La réduction des courants excitateurs dans les interneurones LM pourrait contribuer à la diminution de l'inhibition polysynaptique des cellules pyramidales, tandis que les modifications de cinétique des courants inhibiteurs suggèrent des changements compensatoires au niveau des synapses inhibitrices des cellules pyramidales.

L'effet du traitement à l'AK sur les synapses périsomatiques GABAergiques et non-GABAergiques des cellules pyramidales et interneurones a ensuite été examiné en utilisant la méthode d'immunocytochimie du GABA. Après le traitement, la longueur moyenne des synapses GABA des cellules pyramidales était augmentée, ainsi que le nombre et la longueur totale des synapses GABA sur le soma des interneurones LM. Aucun changement n'a été observé aux synapses non-GABAergiques. L'inhibition périsomatique semble donc augmentée dans les interneurones LM et les cellules pyramidales suite au traitement à l'AK.

Finalement, une technique de fixation a été mise au point pour permettre une préservation adéquate de tissu prélevé lors de résection de foyer épileptique chez l'humain. Cette méthode a permis une fixation supérieure du tissu cortical prélevé chez l'humain et un marquage des synapses GABAergiques à l'aide de l'immunocytochimie du GABA après-enrobage. Cette méthode de fixation pourrait permettre une analyse quantitative des contacts synaptiques GABAergiques dans le tissu épileptique humain.

Ainsi, nos travaux indiquent la présence de changements multiples et spécifiques dans les circuits inhibiteurs du CA1 qui peuvent contribuer à l'hyperexcitabilité des cellules pyramidales dans le modèle expérimental de l'épilepsie de l'AK.

TABLE DES MATIÈRES

SOMMAIRE.....	III
LISTE DES TABLEAUX.....	IX
LISTE DES FIGURES.....	X
LISTE DES ABRÉVIATIONS	XIII
REMERCIEMENTS	XIV
INTRODUCTION GÉNÉRALE ET OBJECTIFS DE LA THÈSE	1
1. INTRODUCTION GÉNÉRALE	2
<i>1.1 Les syndromes épileptiques</i>	<i>2</i>
<i>1.2 L'hippocampe du rat témoin</i>	<i>4</i>
<i>1.2.1 Le réseau neuronal de l'hippocampe</i>	<i>4</i>
<i>1.2.2 La classification des interneurones par leur morphologie</i>	<i>6</i>
<i>1.2.3 La caractérisation des interneurones par la co-localisation de neuropeptides</i>	<i>11</i>
<i>1.2.4 La caractérisation des interneurones par la co-localisation de protéines liant le Ca²⁺</i>	<i>12</i>
<i>1.2.5 La caractérisation des interneurones par le type d'inhibition</i>	<i>14</i>
<i>1.2.6 Les propriétés physiologiques des interneurones</i>	<i>16</i>
<i>1.2.7 Les réponses synaptiques dans les cellules pyramidales</i>	<i>17</i>
<i>1.2.8 Les réponses synaptiques dans les interneurones.....</i>	<i>19</i>
<i>1.3 L'hippocampe épileptique.....</i>	<i>22</i>
<i>1.3.1 Le modèle de l'acide kainique</i>	<i>22</i>
<i>1.3.2 L'hyperexcitabilité de la région CA1 chez le traité à l'AK.....</i>	<i>23</i>

<i>1.3.3 La perte de neurones inhibiteurs dans l'hippocampe épileptique.....</i>	25
<i>1.3.4 L'inhibition polysynaptique est diminuée chez le rat</i>	
<i>traité à l'AK.....</i>	26
<i>1.3.5 Les propriétés intrinsèques des neurones chez le rat</i>	
<i>traité à l'AK.....</i>	27
<i>1.4 Les objectifs de la thèse</i>	27
2. PROPRIÉTÉS MEMBRANAIRES ET COURANTS SYNAPTIQUES	
GÉNÉRÉS DANS DES SOUS-TYPES D'INTERNEURONES DE LA	
RÉGION CA1 DANS DES TRANCHES D'HIPPOCAMPE	
CHEZ LE RAT.....	35
3. PERTE SÉLECTIVE DES NEURONES GABA DANS LA RÉGION	
CA1 DE L'HIPPOCAMPE CHEZ LE RAT APRÈS INJECTION	
INTRAVENTRICULAIRE DE L'ACIDE KAÏNIQUE.....	97
4. ALTERATIONS SPÉCIFIQUES DES PROPRIÉTÉS SYNAPTIQUES	
DES INTERNEURONES DE LA RÉGION CA1 DE L'HIPPOCAMPE	
APRÈS LE TRAITEMENT À L'ACIDE KAÏNIQUE.....	116
5. ALTÉRATIONS DES SYNAPSES PÉRISOMATIQUES GABA DANS	
LES INTERNEURONES INHIBITEURS ET LES CELLULES	
PYRAMIDALES DE LA RÉGION CA1 DE L'HIPPOCAMPE DANS	
LE MODÈLE D'ÉPILEPSIE DE L'ACIDE KAÏNIQUE.....	168
6. UNE PROCÉDURE DE FIXATION POUR L'INVESTIGATION	
ULTRASTRUCTURALE DES CONNEXIONS SYNAPTIQUES DANS	

LE CORTEX HUMAIN PRÉLEVÉ PAR RÉSECTION.....	210
7. DISCUSSION GÉNÉRALE.....	237
7.1 <i>L'hippocampe du rat normal.....</i>	238
7.1.1 <i>La caractérisation morphologique des cellules pyramidales et des interneurones</i>	238
7.1.2 <i>Les propriétés intrinsèques des cellules pyramidales et des interneurones</i>	239
7.1.2.1 <i>Potentiel d'action, résistance d'entrée et après-hyperpolarisation</i>	239
7.1.2.2 <i>Réponses produites par injection de courant</i>	241
7.1.3 <i>Les courants postsynaptiques excitateurs dans les cellules pyramidales et les interneurones</i>	244
7.1.4 <i>Les courants postsynaptiques inhibiteurs dans les cellules pyramidales et les interneurones</i>	245
7.2 <i>L'hippocampe du rat traité à l'acide kaïnique.....</i>	247
7.2.1 <i>La perte de cellules dans l'hippocampe épileptique</i>	247
7.2.2 <i>Les propriétés intrinsèques des cellules pyramidales et des interneurones après le traitement à l'AK</i>	249
7.2.3 <i>Les modifications de la transmission synaptique excitatrice suite au traitement à l'AK.....</i>	250
7.2.4 <i>Les modifications des synapses GABAergiques après le traitement à l'AK</i>	252
7.2.5. <i>Les contacts synaptiques GABA sur les interneurones et</i>	

<i>le traitement à l'AK</i>	257
<i>7.2.7 L'épilepsie du lobe temporal chez l'humain.....</i>	258
<i>7.2.8 Perspectives d'avenir</i>	259
8. BIBLIOGRAPHIE GÉNÉRALE	264
9. APPENDICE	288
9.1 Contribution de l'étudiante	289

LISTE DES TABLEAUX**CHAPITRE 1**

Table 1-1. Caractéristiques des interneurones.....	15
---	----

CHAPITRE 2

Table 2-1. Membrane properties of interneuron subtypes and pyramidal cells	95
Table 2-2. Properties of synaptic currents in interneuron subtypes and pyramidal cells	96

CHAPITRE 4

Table 4-1. Membrane properties of interneurons and pyramidal cells from control and kainate-treated rats	154
Table 4-2. Properties of evoked EPSCs in interneurons and pyramidal cells from control and kainate-treated rats	155
Table 4-3. Properties of evoked IPSCs in interneurons and pyramidal cells from control and kainate-treated rats	156

CHAPITRE 5

Table 5-1. GABA and non-GABA synapses on pyramidal cells and interneuron subtypes of control and kainate-treated rats	209
---	-----

LISTE DES FIGURES

CHAPITRE 1

Figure 1-1. Schéma du circuit trisynaptique excitateur de l'hippocampe.....	31
Figure 1-2. Schéma des interneurones et des cellules pyramidales de la région CA1 de l'hippocampe	33

CHAPITRE 2

Figure 2-1. Biocytin-filled interneurons and pyramidal cells	85
Figure 2-2. Membrane and firing properties of interneurons and pyramidal cells	86
Figure 2-3. Postsynaptic potentials in interneurons and pyramidal cells.....	87
Figure 2-4. Non-NMDA EPSCs in interneurons	88
Figure 2-5. Decay of non-NMDA EPSCs in interneurons.....	89
Figure 2-6. NMDA EPSCs in an O/A interneuron	90
Figure 2-7. Slower rise time of NMDA EPSCs in O/A interneurons.....	91
Figure 2-8. Decay time constant of NMDA EPSCs in an O/A interneuron	92
Figure 2-9. GABA _A IPSCs in an O/A interneuron	93
Figure 2-10. Voltage sensitivity of the decay of GABA _A IPSCs in an O/A interneuron	94

CHAPITRE 3

Figure 3-1. Distribution of GAD-immunopositive cells in O/A and R/LM

of control and kainate-treated rats..... 110

Figure 3-2. Distribution of Nissl-stained cells in O/A and R/LM of control
and kainate-treated rats 111

CHAPITRE 4

Figure 4-1. Nissl-stained sections of the hippocampus in control and
kainate-treated rats 162

Figure 4-2. Field recordings in slices of control and kainate-treated rats..... 163

Figure 4-3. Compound postsynaptic currents in a LM and pyramidal cell of
control and kainate-treated rats 164

Figure 4-4. Changes in EPSCs after kainate treatment..... 165

Figure 4-5. Changes in monosynaptic GABA_A IPSCs after kainate treatment 166

Figure 4-6. Alterations in hippocampal CA1 inhibitory circuits after kainate
treatment 167

CHAPITRE 5

Figure 5-1. Ultrastructure of an O/A interneuron in a control rat..... 204

Figure 5-2. Ultrastructure of a LM interneuron in a control rat..... 205

Figure 5-3. Ultrastructure of a pyramidal cell in a control rat..... 206

Figure 5-4. Ultrastructure of a LM interneuron in a kainate-treated rat 207

Figure 5-5. Frequency of synaptic contact length of GABA and non-GABA
synapses for cell types in control and kainate-treated rats..... 208

CHAPITRE 6

Figure 6-1. Effect of osmolarity.....	232
Figure 6-2. Effect of temperature.....	233
Figure 6-3. Effect of dimethyl sulfoxide.....	234
Figure 6-4. Overall appearance of human neocortical tissue fixed with the proposed protocol.....	235
Figure 6-5. GABA immunoreactivity in human neocortical tissue fixed with the proposed protocol.....	236

LISTE DES ABRÉVIATIONS

Chapitres 1-7

- ACSF: artificial cerebrospinal fluid
 AHP: afterhyperpolarization
 AK: acide kaïnique
 Alv: alveus
 AMPA: α -amino-3-hydroxy-5-methyl-4-isoxazole propionic acid
 AP5: (\pm)-2-amino-5-phosphonopentanoic acid
 BIC: bicuculline
 CCK: cholecystokinine
 CNQX : 6-cyano-7-nitroquinoxaline-2,3-dione
 CPSE: courant postsynaptique excitateur
 DAG: décarboxylase de l'acide glutamique
 DMSO: dimethyl sulfoxide
 EPSC: excitatory postsynaptic current
 EPSP: excitatory postsynaptic potential
 GABA: acide gamma-aminobutyrique
 GAD: glutamic acid decarboxylase
 IPSC: inhibitory postsynaptic current
 IPSP: inhibitory postsynaptic potential
 IS: interneuron-selective
 KA: kainic acid
 L_L -GABA: length of GABA synapses per unit length
 $L_{L\text{-non-GABA}}$: length of non-GABA synapses per unit length
 LM: lacunosum-moleculare
 N_L -GABA: number of GABA synapses per unit length
 $N_{L\text{-non-GABA}}$: number of non-GABA synapses per unit length
 NMDA: *N*-methyl-*D*-aspartate
 NPY: neuropeptide Y
 N_V : numerical density
 O/A: oriens/alveus
 Ori: oriens
 PIV: polypeptide intestinal vasoactif
 PPSE: potentiel postsynaptique excitateur
 PPSI: potentiel postsynaptique inhibiteur
 PSC: postsynaptic current
 PV: parvalbumin
 PYR: pyramidale
 Rad: radiatum
 R/LM: radiatum/lacunosum-moleculare
 SOM: somatostatine
 str.: stratum
 TLE: temporal lobe epilepsy

REMERCIEMENTS

J'aimerais remercier ici toutes les personnes qui m'ont aidée dans la réalisation de ce travail :

Mon superviseur Jean-Claude Lacaille pour ses conseils et son enseignement au cours de mes études doctorales.

Mon ancien co-superviseur Clermont Beaulieu pour l'enthousiasme et les idées qu'il a su me communiquer au cours de mes travaux.

À ma famille et mes amis, qui m'ont encouragée au cours de mes études.

À Kent, qui m'a encouragée pendant les moments difficiles.

Enfin, je tiens à remercier la Fondation Savoy, la Faculté des études supérieures et les docteurs Jean-Claude Lacaille et Clermont Beaulieu pour leur soutien financier.

CHAPITRE 1

INTRODUCTION GÉNÉRALE ET OBJECTIFS DE LA THÈSE

1 INTRODUCTION GÉNÉRALE

1.1 Les syndromes épileptiques

L'épilepsie est un syndrome neurologique, affligeant plus de 1 % de la population (Engel 1989), causé par l'hyperactivité et la synchronisation des neurones dans une ou plusieurs régions du cerveau (Engel 1989). Deux classes de crises d'épilepsie sont identifiées selon une classification internationale: les crises généralisées notamment les crises d'absence, tonico-cloniques, myocloniques ainsi que les crises partielles comme les crises du lobe temporal (Fukuzako et Izumi 1991; Shin et McNamara 1994). Dans cette thèse, les mécanismes associés aux crises d'épilepsie du lobe temporal seront abordés. Chez l'humain, les crises du lobe temporal sont étroitement liées à une perte cellulaire extensive (sclérose) dans la corne d'Ammon (CA), région de l'hippocampe correspondant aux aires CA1 à CA4, et à l'hyperexcitabilité des cellules pyramidales (excitatriques) qui survivent dans cette région (Nadler 1981; Ben-Ari 1985).

Afin d'étudier les mécanismes cellulaires qui sont impliqués dans ces deux phénomènes, plusieurs modèles animaux ont été développés : injection d'acide kaïnique (Nadler 1981; Ben-Ari 1985) et de pilocarpine (Turski et al. 1989), stimulation du faisceau perforant (Sloviter 1983) et *status epilepticus* (Lothman et al. 1989) ainsi que le modèle du *kindling* (Goddard et al. 1969; Wasterlain et al. 1986). Dans la présente thèse, le modèle du rat traité à l'acide kaïnique (AK) sera considéré. L'acide kaïnique administré dans les ventricules latéraux des deux hémisphères du rat

produit une perte sélective des neurones du hile et des cellules pyramidales du CA3 ainsi qu'un état d'hyperexcitabilité des cellules pyramidales de la région CA1. Comparativement à l'injection intraventriculaire, l'injection systémique d'AK chez le rat provoque aussi une perte de certains neurones du hile et des cellules pyramidales de la région CA3, mais en plus endommage les cellules pyramidales de la région CA1 ainsi que les neurones du cortex pyriforme, de l'amygdale et du thalamus (Nadler 1981). Un des mérites du modèle d'injection intraventriculaire de l'AK est qu'il reproduit, chez le rat, la pathologie observée dans l'hippocampe de plusieurs patients souffrant d'épilepsie (Nadler 1981; Ben-Ari 1985). De plus, le modèle de l'AK reproduit l'activité épileptiforme dans l'hippocampe et le système limbique qui peut ensuite provoquer des changements au niveau des circuits de l'hippocampe (Nadler 1981). Toutefois, une des limitations de ce modèle est que c'est une condition expérimentale artificielle où l'injection d'un analogue du glutamate endommage certaines régions hippocampiques et corticales chez le rat. De plus, le modèle de l'AK est un modèle d'épilepsie chez le rat, qui reproduit certaines caractéristiques observées dans l'hippocampe chez des patients épileptiques, mais qui demeure toutefois un modèle animal où les changements observés dans les circuits hippocampiques peuvent être différents de ceux qui surviennent chez l'humain.

Des études ont démontré qu'une semaine après le traitement à l'AK, il y avait une déafférentation importante au niveau des dendrites des cellules pyramidales dans la couche radiatum du CA1 (Nadler et al. 1980), et que les cellules pyramidales étaient hyperexcitables (Turner et Wheal 1991). Toutefois, d'autres travaux ont indiqué qu'il y avait une réinnervation des dendrites des cellules pyramidales de six à huit

semaines après le traitement à l'AK (Nadler et al. 1980), et que l'hyperexcitabilité des cellules pyramidales était diminuée deux à quatre mois après le traitement à l'AK (Franck et al. 1988). Ainsi, l'étude des circuits inhibiteurs, deux à quatre semaines après le traitement à l'AK, permet de déterminer les changements observés dans les circuits inhibiteurs durant un état chronique d'hyperexcitabilité suite au traitement à l'AK.

Afin de mieux comprendre les mécanismes cellulaires reliés à l'hyperexcitabilité des cellules pyramidales et à l'activité épileptiforme de l'hippocampe, les circuits excitateurs et inhibiteurs de l'hippocampe doivent être d'abord considérés chez l'animal témoin.

1.2 L'hippocampe du rat témoin

1.2.1 *Le réseau neuronal de l'hippocampe*

L'hippocampe est constitué d'un réseau trisynaptique excitateur : les fibres du faisceau perforant, provenant du cortex entorhinal, font des contacts synaptiques sur les dendrites des cellules granulaires du gyrus dentelé; les axones des cellules granulaires (fibres moussues) projettent ensuite aux dendrites apicales des cellules pyramidales de la région CA3; tandis que les fibres de Schaffer (axones des cellules pyramidales du CA3) font des contacts synaptiques sur les dendrites des cellules pyramidales de la région CA1 (Figure 1) (Ramón y Cajal 1911; Lorente de Nō 1934). Les cellules granulaires et pyramidales de ce réseau sont des neurones

excitateurs et libèrent le neurotransmetteur glutamate. Les cellules pyramidales ont un corps cellulaire de forme triangulaire d'où émerge une dendrite primaire apicale qui traverse la couche radiatum (rad) en donnant des branches secondaires, qui se subdivisent ensuite en plusieurs branches (Figure 1) (Ramón y Cajal 1911; Lorente de Nō 1934). Ces branches, de plus petit calibre, forment des arborisations dans les couches radiatum et lacunosum-moleculare (lm) jusqu'à la fissure hippocampique. Les cellules pyramidales possèdent aussi des dendrites basales se ramifiant dans la couche oriens (ori) et à la bordure de l'alveus (alv). Les dendrites des cellules pyramidales sont couvertes d'épines. L'axone des neurones pyramidaux de la région CA1 prend origine du corps cellulaire du neurone, ou parfois d'une dendrite basale, traverse la couche oriens jusqu'à l'alveus et se dirige vers le subiculum, le septum latéral et d'autres régions limbiques (Ramón y Cajal 1911; Lorente de Nō 1934; Freund et Buzsāki 1996).

En plus des cellules pyramidales qui sont situées côte à côte dans une couche définie, plusieurs types de neurones inhibiteurs, qui libèrent l'acide gamma-aminobutyrique (GABA), sont présents dans les différentes couches de la région CA1 (Figure 2) (Ramon y Cajal 1911; Lorente de Nō 1934). Les neurones inhibiteurs, aussi appelés interneurones, forment une classe hétérogène de cellules qui règulent l'activité neuronale de l'hippocampe en inhibant les cellules pyramidales (Andersen et al. 1964; Alger et Nicoll 1982). Grâce à la mise au point d'anticorps contre l'enzyme de synthèse du GABA, la décarboxylase de l'acide glutamique (DAG), ainsi que contre le GABA, on a pu identifier, à l'aide de la technique d'immunocytochimie, les neurones GABAergiques de l'hippocampe (Ribak et al. 1978). Des données

quantitatives suggèrent que les interneurones constituent environ 10% de la population neuronale de l'hippocampe et du gyrus dentelé, et que la majorité (80-95%) des interneurones de l'hippocampe sont GABAergiques, et donc inhibiteurs (Freund et Buzsáki 1996).

1.2.2 La classification des interneurones par leur morphologie

L'utilisation de différentes techniques de marquage comme celle de Golgi et l'injection intracellulaire de colorant a permis d'identifier plusieurs types d'interneurones qui peuvent être classés selon leur arborisation dendritique et axonale (Ramón y Cajal 1911; Freund et Buzsáki 1996).

Dans la région CA1, les neurones axo-axoniques (A) (Figure 2), aussi appelés chandeliers, ont leur corps cellulaire dans la couche pyramidale. Ils sont caractérisés par une arborisation dendritique multi-laminaire. Ils possèdent des dendrites qui traversent la couche radiatum, et s'arborisent profusément dans la couche lacunosum-moleculare, ainsi que des dendrites basales se ramifiant dans la couche oriens et l'alveus (Buhl et al. 1994; Freund et Buzsáki 1996). Leurs dendrites n'ont pas d'épines mais possèdent quelquefois des varicosités. L'arborisation dendritique des neurones axo-axoniques les rend susceptibles à plusieurs types d'afférences, notamment les fibres de Schaffer, commissurales et celles provenant du cortex entorhinal. L'axone des neurones axo-axoniques prend origine au niveau du corps cellulaire ou d'une dendrite primaire, et s'arborise profusément dans les couches pyramidale et oriens (Buhl et al. 1994). Les contacts synaptiques formés par ces neurones sont localisés

exclusivement au segment initial de l'axone des cellules pyramidales (Figure 2) (Somogyi et al. 1983; Buhl et al. 1994).

Le neurone à panier (Pa) (Figure 2), ou *basket cell*, est un autre type de neurone inhibiteur dont le corps cellulaire est situé dans la couche pyramidale (Schwartzkroin et Mathers 1978; Schwartzkroin et Kunkel 1985; Buhl et al. 1995). Les dendrites des neurones à panier ressemblent à celles des neurones axo-axoniques: dendrites apicales s'arborisant dans les couches radiatum et lacunosum-moleculare et dendrites basales situées dans l'oriens et l'alveus. De plus, les dendrites des neurones à panier ne possèdent généralement pas d'épines. L'arborisation dendritique des neurones à panier favorise aussi leur activation de plusieurs sources : fibres de Schaffer, commissurales et entorhinales. L'axone des cellules à panier forme des contacts synaptiques principalement dans la couche pyramidale et dans la région proximale des couches oriens et radiatum, ciblant ainsi les corps cellulaires et dendrites proximaux des neurones pyramidaux (Figure 2) (Schwartzkroin et Mathers 1978; Schwartzkroin et Kunkel 1985; Buhl et al. 1995).

Les interneurones horizontaux (H) (Figure 2), que l'on appelle aussi interneurones O-LM, ont leur corps cellulaire dans la couche oriens (Maccaferri et McBain 1995; Blasco-Ibanez et Freund 1995; Freund et Buzsaki 1996). Ces neurones inhibiteurs ont des dendrites qui se prolongent horizontalement dans la couche oriens et dans l'alveus, et qui se subdivisent en plusieurs branches. Des travaux ont montré qu'après un événement ischémique qui cause une mort cellulaire sélective des neurones pyramidaux de la région CA1, presque tous les contacts synaptiques asymétriques (excitateurs) sur les interneurones O-LM étaient perdue (Blasco-

Ibanez et Freund 1995). Ces auteurs en ont conclu que les principales afférences des interneurones O-LM étaient des fibres collatérales des axones des cellules pyramidales de la région CA1. L'axone des interneurones horizontaux projette dans la couche radiatum jusqu'à la couche lacunosum-moleculare, où plusieurs collatéraux forment des contacts synaptiques sur les dendrites distales des cellules pyramidales (Figure 2) (Blasco-Ibanez et Freund 1995; Maccaferri et McBain 1995; Freund et Buzsáki 1996).

Les interneurones verticaux (V) (Figure 2), qui incluent les neurones bistratifiés (Buhl et al. 1996; Halasy et al. 1996) et trilaminaires (Sik et al. 1995), constituent un autre type d'interneurone dont le corps cellulaire est situé dans les couches pyramidale ou oriens (Lacaille et al. 1987; Lacaille et Williams 1990). Contrairement aux interneurones horizontaux, les dendrites de ces interneurones sont distribuées horizontalement dans la couche oriens et dans l'alveus, ainsi que verticalement dans les couches radiatum et lacunosum-moleculare (Figure 2) (Lacaille et al. 1987; Lacaille et Williams 1990; Freund et Buzsáki 1996). L'arborisation dendritique multi-laminaire de ces interneurones rend possible leur activation par les fibres commissurales et de Schaffer, ainsi que par celles provenant du cortex entorhinal. Toutefois, ces neurones sont aussi activés par les fibres collatérales des axones des cellules pyramidales de la région CA1. L'axone des interneurones bistratifiés forme des arborisations dans les couches oriens ainsi que radiatum, tandis que celui des neurones trilaminaires donne en plus des ramifications dans la couche pyramidale (Freund et Buzsáki 1996) (Figure 2). Ainsi, ces arborisations axonales indiquent que ces deux types d'interneurones forment en

grande partie des contacts synaptiques avec les dendrites des cellules pyramidales (Freund et Buzsáki 1996).

Les interneurones étoilés (É) (Figure 2) sont un autre type d'interneurone dont le corps cellulaire est situé à la bordure des couches radiatum et lacunosum-moleculare (Misgeld et Frotscher 1986; Kunkel et al. 1988; Lacaille et Schwartzkroin 1988a). Ces interneurones possèdent des dendrites dépourvues d'épines formant des arborisations dans les couches oriens, radiatum et lacunosum-moleculare, ainsi que parfois dans la couche moléculaire du gyrus dentelé. Des travaux étudiant la dégénérescence de terminaisons ont démontré que les afférences des interneurones étoilés provenaient des fibres de Schaffer, commissurales ainsi que du cortex entorhinal ipsilatéral (Kunkel et al. 1988). Ces interneurones ont une arborisation axonale très étendue surtout dans les couches radiatum et lacunosum-moleculare et font principalement des contacts synaptiques sur les dendrites des cellules pyramidales (Figure 2). Un autre type d'interneurone, dont le corps cellulaire est localisé dans la couche radiatum, possède des dendrites formant des arborisations principalement dans la couche radiatum, mais aussi moins fréquemment dans les couches pyramidale et oriens (non illustré dans la Figure 2) (Gulyas et al. 1993). Leur arborisation dendritique rend possible l'activation de ces interneurones par les fibres de Schaffer et commissurales. L'axone des interneurones de la couche radiatum est localisé dans la couche radiatum, toutefois quelques collatéraux pénètrent dans les couches pyramidale et oriens. Des travaux en microscopie électronique ont indiqué que les axones de ces interneurones forment des contacts synaptiques sur les

dendrites ainsi que sur les épines dendritiques des cellules pyramidales (Gulyas et al. 1993).

Grâce à la technique d'immunocytochimie, trois autres types d'interneurones contenant un neuropeptide appelé polypeptide intestinal vasoactif (PIV) ont pu être identifiés. L'axone de ces interneurones forment des contacts synaptiques uniquement avec d'autres interneurones, d'où leur appellation de cellules *interneuron-selective* (IS-1, IS-2, et IS-3) (Figure 2) (Acsady et al. 1996a,b; Guylas et al. 1996). Le premier type d'interneurone, IS-1, a un corps cellulaire situé dans les couches radiatum, pyramidale ou oriens. Ces interneurones possèdent des dendrites démunies d'épines qui s'étendent dans les couches radiatum, lacunosum-moleculare et oriens (Figure 2). Ces cellules forment des contacts dendrodendritiques entre elles où deux ou trois dendrites peuvent être entrelacées sur une distance d'environ 100 µm (Gulyas et al. 1996; Acsady et al. 1996b). L'arborisation axonale des cellules IS-1 est généralement dans la couche radiatum (Figure 2). D'après leur arborisation dendritique et axonale, ces interneurones reçoivent probablement des afférences des fibres de Schaffer, commissurales et entorhinales, et projettent aux interneurones qui forment des contacts synaptiques sur les dendrites des cellules pyramidales (Figure 2). Le deuxième type d'interneurone, IS-2, a un corps cellulaire situé dans la couche radiatum près de la couche lacunosum-moleculare, des dendrites dépourvues d'épines arborisant profusément dans la couche lacunosum-moleculare, et un axone qui projette dans la couche radiatum jusqu'à la couche pyramidale (Figure 2) (Acsady et al. 1996a,b). Les afférences des interneurones IS-2 proviennent du cortex entorhinal, tandis que leurs cibles semblent être les interneurones qui font des contacts

synaptiques sur les dendrites des cellules pyramidales au niveau de la couche radiatum. Le dernier type d'interneurone, IS-3, a un corps cellulaire, dans la couche pyramidale ou radiatum (Figure 2) (Acsady et al. 1996a,b). Son arborisation dendritique est bipolaire, avec un axe dendritique projetant vers la couche lacunosum-moleculare, et un autre vers la couche oriens. L'axone des neurones IS-3 prend origine au niveau du corps cellulaire ou d'une dendrite primaire, et projette vers la couche oriens, donnant plusieurs collatéraux à la bordure de l'alveus. Les afférences de ces interneurones sont les fibres entorhinales, tandis que leurs axones ciblent les interneurones de la couche oriens, qui eux font des contacts synaptiques sur les dendrites des cellules pyramidales (Figure 2).

1.2.3 La caractérisation des interneurones par la co-localisation de neuropeptides

Les interneurones peuvent aussi être caractérisés selon la co-localisation sélective de certains neuropeptides, notamment la somatostatine (SOM), le neuropeptide Y (NPY), le polypeptide intestinal vasoactif (PIV), et la cholecystokinine (CCK) avec le GABA (Somogyi et al. 1984; Sloviter et Naviler 1987; Kosaka et al. 1988; Buckmaster et al. 1994). La somatostatine a été trouvée dans les interneurones de la couche oriens et de l'alveus, et des travaux en immunocytochimie ont suggéré qu'elle était plus spécifiquement associée aux interneurones horizontaux (Kunkel et Schwartzkroin 1988; Blasco-Ibanez et Freund 1995; Freund et Buzsaki 1996), puisque les neurones marqués par la somatostatine étaient aussi marqués par un anticorps contre le récepteur métabotrope, mGluR1,

spécifiquement retrouvé dans les interneurones horizontaux (Baude et al. 1993). D'autres interneurones dont le corps cellulaire est situé dans les couches pyramidale ou oriens démontrent une co-localisation du GABA et du neuropeptide Y. Il s'agit probablement d'interneurones horizontaux, car leurs arborisations dendritiques et axonales sont semblables (Freund et Buzsäki 1996). Tel que décrit précédemment, le neuropeptide PIV a été identifié dans les cellules *interneuron selective* (IS-1, IS-2 et IS-3), toutefois il est aussi présent dans les cellules à panier (Acsady et al. 1996a,b; Freund et Buzsäki 1996). Finalement, la cholecystokinine est un autre neuropeptide qui a été identifié principalement dans les interneurones de la couche radiatum, moins fréquemment dans ceux des couches pyramidale et oriens, et rarement dans ceux de la couche lacunosum-moleculare (Freund et Buzsäki 1996). Des travaux de double marquage ont suggéré que la cholecystokinine est présente dans certains interneurones à panier et axo-axoniques de la couche pyramidale, puisqu'ils sont aussi immunopositifs pour une protéine intracellulaire liant le Ca^{2+} , que l'on appelle la parvalbumine (Gulyas et al. 1991).

1.2.4 La caractérisation des interneurones par la co-localisation de protéines liant le Ca^{2+}

En utilisant les techniques d'immunocytochimie, certains interneurones de la région CA1 peuvent être différenciés selon les protéines liant le Ca^{2+} (*calcium binding proteins*) qu'ils contiennent (Kosaka et al. 1987; Gulyas et al. 1991; Freund et Buzsäki 1996). La parvalbumine est une de ces protéines qui a été identifiée dans les

interneurones de l'hippocampe (Baimbridge et Miller 1982). La proportion des interneurones des régions CA1, CA3 et du gyrus dentelé qui contiennent la DAG et la parvalbumine est d'environ 20% (Kosaka et al. 1987). Une étude immunocytochimique a suggéré que 50% des neurones immunopositifs pour la parvalbumine étaient situés dans la couche pyramidale et correspondent aux neurones à panier et axo-axoniques (Kosaka et al. 1987). Par contre, des travaux en microscopie électronique ont montré que les contacts synaptiques de forme symétrique localisés au corps cellulaire, aux dendrites proximales ainsi qu'au segment initial de l'axone de cellules pyramidales n'étaient pas toujours immunopositifs pour la parvalbumine (Ribak et al. 1990). Par ailleurs, il existe des interneurones à panier qui contiennent les neuropeptides CCK et PIV mais qui ne contiennent pas de parvalbumine (Gulyas et al. 1991; Acsady et al. 1996a,b). Les études immunocytochimiques indiquent donc que les interneurones à panier et axo-axoniques ne contiennent pas tous de la parvalbumine. De plus, 30 à 40% des interneurones de la couche oriens et 3 à 6% de ceux de la couche radiatum contiennent de la parvalbumine (Kosaka et al. 1987), tandis que les interneurones de la couche lacunosum-moleculare ne contiennent pas de parvalbumine (Kosaka et al. 1987).

Une autre protéine liant le Ca^{2+} , aussi appelée calbindine, est présente dans les interneurones, mais aussi dans les cellules pyramidales de la région CA1 de l'hippocampe (Baimbridge et Miller 1982; Sloviter 1989; Toth et Freund 1992). Les interneurones contenant la calbindine sont situés dans la couche radiatum ainsi qu'à la bordure des couches radiatum et lacunosum-moleculare (Gulyas et al. 1991; Toth

et Freund 1992). Certains interneurones des couches oriens, pyramidale et lacunosum-moleculare contiennent aussi, mais plus rarement, la calbindine. D'après leur arborisation dendritique et axonale, certains interneurones contenant la calbindine correspondraient aux interneurones bistratifiés, aux interneurones de la couche radiatum ainsi qu'aux interneurones situés à la bordure des couches radiatum et lacunosum-moleculare (Freund et Buzsaki 1996).

Finalement, la calrétinine est une autre protéine intracellulaire liant le Ca^{2+} présente dans les interneurones qui forment préférentiellement des contacts synaptiques sur les autres interneurones (IS-1, IS-2 et IS-3) (Gulyas et al. 1996).

Ainsi, la co-localisation dans les interneurones du GABA et d'autres substances, comme les neuropeptides ou les protéines intracellulaires liant le Ca^{2+} , suggère que les interneurones inhibiteurs de la région CA1 de l'hippocampe constituent une classe de neurones très hétérogène.

1.2.5 La caractérisation des interneurones par le type d'inhibition

Trois grandes classes d'interneurones peuvent aussi être identifiées selon le type d'inhibition qu'ils produisent dans les cellules pyramidales. Les cellules verticales (V; Figure 2) (Lacaille et al. 1987; Lacaille et Williams 1990), axo-axoniques (A; Figure 2) (Buhl et al. 1994) et à panier (Pa; Figure 2) (Knowles et Schwartzkroin 1981) ont une arborisation dendritique multi-laminaire et sont activées par les fibres afférentes de la région CA1. Ces interneurones sont donc activés de manière proactive. Ces interneurones reçoivent aussi des afférences des fibres collatérales des axones des

Caractéristiques des interneurones de la région CA1 de l'hippocampe (Freund et Buzsaki 1996)

Type de cellule	Dendrites	Axone	Cibles	Afférences	Protéines liant le Ca ²⁺	Neuropeptides
Axo-axonique	alv., ori., pyr. rad., lm.	ori., pyr.	axone	CA3, CA1, CE	PV	CCK
Cellule à panier	alv., ori., pyr. rad., lm.	ori., pyr.	soma, dend.prox.	CA3, CA1, CE	PV	CCK, PIV
Verticale	alv., ori., pyr. rad., lm.	ori., pyr., rad.	soma, dend.prox., dend.dist.	CA3, CA1, CE	CB	NPY
Horizontale	alv., ori.	lm.	dend.dist.	CA1	CB	SOM, NPY
Étoilée	pyr., rad., lm.	rad., lm.	dend.dist.	CA3, CE	CB	-
Radiatum	ori., pyr., rad.	ori., pyr., rad.	dend.dist.	CA3	CB	CCK
IS-1	ori., rad., lm.	rad.	soma, dend. prox., dend.dist.	CA3, CE	CR	PIV
IS-2	lm.	pyr., rad.	soma, dend. prox., dend.dist.	CE	CR	PIV
IS-3	alv., ori., pyr., rad., lm.	alv., ori.	soma, dend. prox., dend dist.	CA3, CA1, CE	CR	PIV

Alv.; alveus, CB; calbindine, CCK; cholécystokinine, CE; cortex entorhinal, CR; calrétinine, dend.dist.; dendrite distale, dend.prox.; dendrite proximale, lm; stratum lacunosum-moleculare, NPY; neuropeptide Y, ori.; stratum oriens, PIV; polypeptide intestinal vasoactif, PV; parvalbumine, pyr.; stratum pyramidale, rad.; stratum radiatum, SOM; somatostatine.

cellules pyramidales de la région CA1 et sont donc également activés de manière rétroactive (Figure 2). Ainsi, ces interneurones inhibent les cellules pyramidales de façon proactive et rétroactive. Par contre, la majorité des contacts synaptiques excitateurs des interneurones horizontaux (H; Figure 2) proviennent de collatéraux des axones des cellules pyramidales (Blasco-Ibanez et Freund 1995), ce qui indique que ces interneurones génèrent seulement une inhibition rétroactive dans les cellules pyramidales (Blasco-Ibanez et Freund 1995; Maccaferri et McBain 1995) (Figure 2). Finalement, les interneurones étoilés situés à la bordure des couches radiatum et lacunosum-moleculare (É; Figure 2) reçoivent des afférences des fibres de Schaffer et du cortex entorhinal ipsilateral, et non des cellules pyramidales de la région CA1. Ils inhibent donc les cellules pyramidales uniquement de manière proactive (Schwartzkroin et Mathers 1978; Kawaguchi et Hama 1988; Lacaille et Schwartzkroin 1988b) (Figure 2).

1.2.6 *Les propriétés physiologiques des interneurones*

Les propriétés membranaires des cellules pyramidales et de différents types d'interneurones ont été caractérisées lors d'enregistrements intracellulaires de neurones dans des tranches d'hippocampe maintenues *in vitro*. Ces travaux ont mis en évidence des différences entre les propriétés intrinsèques des cellules pyramidales et des interneurones (Schwartzkroin et Mathers 1978; Lacaille et Schwartzkroin 1988a,b). De plus, ces études ont suggéré que deux types d'interneurones pouvaient être différenciés selon leurs propriétés physiologiques (Kawaguchi et Hama 1988;

Lacaille et al. 1989). Comparativement aux cellules pyramidales, les cellules à panier, axo-axoniques et verticales ont démontré un potentiel d'action de courte durée, une après-hyperpolarisation prononcée, et peu d'accomodation de la fréquence de décharge durant une dépolarisation soutenue (Schwartzkroin et Mathers 1978; Lacaille et al. 1987; Buhl et al. 1994). Ces propriétés correspondent à un profil de cellule à décharge rapide ou *fast spiking cell*.

Une deuxième classe d'interneurones, les neurones étoilés situés à la bordure des couches radiatum et lacunosum-moleculare, possèdent aussi des propriétés physiologiques différentes de celles des cellules pyramidales (Lacaille et Schwartzkroin 1988a; Lacaille et al. 1989). Comparativement aux cellules pyramidales, ces interneurones ont un potentiel d'action de même durée, une après-hyperpolarisation prononcée, peu d'accomodation de la fréquence de décharge au potentiel membranaire de repos et des bouffées de potentiels d'action sensibles au voltage (Lacaille et Schwartzkroin 1988a; Lacaille et al. 1989). Ces interneurones possèdent donc des propriétés physiologiques différentes de celles des cellules pyramidales et des autres interneurones, et sont identifiés comme des cellules à décharge non-rapide ou *non-fast spiking cell* (Kawaguchi et Hama 1988; Lacaille et Schwartzkroin 1988a; Lacaille et al. 1989).

1.2.7 Les réponses synaptiques dans les cellules pyramidales

Lors d'enregistrements intracellulaires, la stimulation électrique des afférences de la région CA1 provoque des potentiels postsynaptiques excitateurs (PPSE) et

inhibiteurs (PPSI) dans les cellules pyramidales. La réponse excitatrice est produite par l'activation des récepteurs ionotropes au glutamate de type α -amino-3-hydroxy-5-methyl-4-isoxazole propionic acid (AMPA) et *N*-methyl-*D*-aspartate (NMDA) (Collingridge et al. 1988). Ces deux types de récepteurs sont des récepteurs-canaux perméables aux cations. Les récepteurs-canaux AMPA sont perméables aux ions Na^+ et K^+ , tandis que leur perméabilité au Ca^{2+} est négligeable (Collingridge et al. 1988). Par contre, les récepteurs-canaux NMDA sont perméables aux ions Na^+ , K^+ et Ca^{2+} (Collingridge et al. 1988). Les récepteurs NMDA sont sensibles au voltage, puisque les ions Mg^{2+} bloquent le canal à des potentiels membranaires négatifs (Ascher et Nowak 1988). Ainsi, le passage d'ions à travers les récepteurs NMDA requiert la liaison du neurotransmetteur au récepteur et la dépolarisation du neurone postsynaptique pour enlever le blocage du canal par les ions Mg^{2+} . Les réponses AMPA et NMDA peuvent aussi être différenciées par leur cinétique : l'activation des récepteurs AMPA est responsable de la composante rapide de la réponse, tandis que l'activation des récepteurs NMDA cause la composante lente (Collingridge et al. 1988). Ces deux composantes ont pu être isolées pharmacologiquement en utilisant des antagonistes des récepteurs NMDA ((\pm)-2-amino-5-phosphonopentoanoic acid, AP5) et non-NMDA (6-cyano-7-nitroquinoxaline-2,3-dione, CNQX) (Davies et al. 1981; Honore et al. 1988). L'utilisation de la technique de *patch clamp* en configuration cellule entière a permis d'enregistrer avec une meilleure résolution les courants postsynaptiques excitateurs (CPSE) dans les cellules pyramidales (Hestrin et al. 1990). La courbe courant-voltage (I-V) des CPSE AMPA est linéaire et a un

potentiel d'inversion d'environ zéro, tandis que la courbe I-V des CPSE NMDA démontre une région linéaire, avec un potentiel d'inversion près de zéro, mais aussi une région de pente négative entre les potentiels membranaires de -30 et -70 mV. La région de pente négative est due à un blocage du canal NMDA par les ions Mg^{2+} qui est dépendant du voltage (Hestrin et al. 1990).

La stimulation électrique des afférences de la région CA1 provoque une activation des interneurones GABAergiques qui causent des réponses inhibitrices polysynaptiques dans les cellules pyramidales (Alger et Nicoll 1982; Alger 1984). Les réponses inhibitrices possèdent également deux composantes : une composante rapide provoquée par la liaison du neurotransmetteur GABA aux récepteurs $GABA_A$, et une composante lente produite par l'activation des récepteurs $GABA_B$. Le récepteur $GABA_A$ est un récepteur-canal sélectivement perméable aux ions Cl^- , tandis que le récepteur $GABA_B$ est un récepteur lié aux protéines G qui sont couplées à une ouverture de canaux K^+ (Thompson 1994). Ces deux composantes inhibitrices ont pu être caractérisées en les isolant pharmacologiquement soit avec de la bicuculline, un antagoniste du récepteur $GABA_A$ (Curtis et al. 1970) ou le CGP 55845A, un antagoniste des récepteurs $GABA_B$ (Davis et al. 1993).

1.2.8 Les réponses synaptiques dans les interneurones

À l'aide d'enregistrements intracellulaires, il a été démontré que la stimulation des fibres afférentes dans la région CA1 produit également des potentiels postsynaptiques excitateurs (PPSE) et inhibiteurs (PPSI) dans les interneurones situés dans les couches pyramidale (Schwartzkroin et Mathers 1978; Knowles et Schwartzkroin

1980; Ashwood et al. 1984; Lacaille 1991), oriens (Lacaille et al. 1987) et lacunosum-moleculare (Kawaguchi et Hama 1988; Lacaille et Schwartzkroin 1988a,b). Lors d'enregistrements intracellulaires simultanés d'interneurones O/A ou LM et de cellules pyramidales, il a été démontré que la stimulation des fibres de Schaffer provoque des PPSE différents dans les interneurones et les cellules pyramidales (Lacaille et al. 1987; Lacaille et Schwartzkroin 1988b). Comparativement à ceux des cellules pyramidales, les PPSE des interneurones ont une plus grande amplitude, un seuil de stimulation moindre et un temps de montée plus rapide (Lacaille et al. 1987; Lacaille et Schwartzkroin 1988b). Ces données suggèrent donc une activation proactive des interneurones comparativement aux cellules pyramidales (Lacaille et al. 1987, Lacaille et Schwartzkroin 1988b). De plus, d'autres observations ont démontré que la stimulation des fibres de Schaffer provoque, dans les interneurones de la couche pyramidale, des PPSE rapides et lents, dus à l'activation des récepteurs AMPA et NMDA, ainsi que des PPSI précoces et tardifs, produits par l'activation des récepteurs GABA_A et GABA_B, des réponses semblables à celles des cellules pyramidales (Lacaille 1991).

Des enregistrements de *patch clamp* en configuration cellule entière ont indiqué que les réponses excitatrices des interneurones des couches pyramidale et oriens chez le rat juvénile sont composées de courants AMPA et NMDA (Sah et al. 1990). De plus, des données physiologiques et moléculaires récentes ont montré que les récepteurs AMPA diffèrent entre les interneurones inhibiteurs et les cellules pyramidales (Geiger et al. 1995). Dans les interneurones, les récepteurs AMPA sont perméables au Ca²⁺ et se désensibilisent rapidement, tandis que dans les cellules

pyramidales, les récepteurs AMPA ont une faible perméabilité au Ca^{2+} et se désensibilisent moins rapidement (Geiger et al. 1995). Dans la région CA3 de l'hippocampe, d'autres travaux ont aussi montré que la relation courant-voltage et la cinétique des courants postsynaptiques AMPA spontanés diffèrent dans deux types d'interneurones de la couche radiatum : l'un étant compatible avec l'activation de récepteurs AMPA qui sont perméables au Ca^{2+} , et l'autre avec l'activation de récepteurs AMPA qui sont imperméables au Ca^{2+} (McBain et Dingledine 1993). Par ailleurs, d'autres études physiologiques ont indiqué que les courants postsynaptiques NMDA diffèrent dans certains interneurones et dans les cellules pyramidales chez le rat juvénile (Perouansky et Yaari 1993). En effet, un temps de montée des CPSE NMDA plus lent a été observé dans les interneurones de la couche oriens que dans ceux de la couche lacunosum-moleculare ou dans les cellules pyramidales (Perouansky et Yaari 1993). Par contre, le temps de descente des courants postsynaptiques NMDA est plus rapide dans les interneurones des couches O/A et LM que dans les cellules pyramidales (Perouansky et Yaari 1993). Ces données suggèrent donc que les courants postsynaptiques AMPA et NMDA diffèrent entre les interneurones et les cellules pyramidales, et que ces courants postsynaptiques peuvent également différer entre certains types d'interneurones.

En conclusion, la stimulation des afférences de la région CA1 provoque des réponses postsynaptiques excitatrices dans les cellules pyramidales, ainsi que des réponses inhibitrices indirectes, via l'activation de différents types d'interneurones. Un équilibre entre les réponses excitatrices et inhibitrices des cellules pyramidales est nécessaire au maintien de l'activité normale des cellules principales. Ainsi, un

déséquilibre entre ces diverses composantes pourrait favoriser des conditions anormales et contribuer au développement de l'activité épileptiforme des circuits neuronaux de l'hippocampe.

1.3 L'hippocampe épileptique

1.3.1 *Le modèle de l'acide kaïnique*

Dans le modèle d'épilepsie du rat traité à l'AK, les conséquences électrophysiologiques et morphologiques du traitement à l'AK ont d'abord été caractérisées dans le gyrus dentelé. Des travaux anatomiques et physiologiques ont démontré que l'injection d'AK (intraventriculaire ou systémique) provoque une perte de cellules dans le hile, une diminution de l'inhibition polysynaptique des cellules granulaires (Sloviter 1991, 1992) ainsi qu'une hyperexcitabilité du gyrus dentelé (Tauck et Nadler 1985). L'hyperexcitabilité des cellules granulaires est accompagnée d'un bourgeonnement extensif de fibres collatérales des axones des cellules granulaires (Tauck et Nadler 1985; Cronin et al. 1992; Sloviter 1992; Sundstrom et al. 1993). Des observations en microscopie électronique ont indiqué que ce bourgeonnement axonal peut causer la formation de synapses excitatrices aberrantes sur les dendrites des cellules granulaires et ainsi contribuer à l'hyperexcitabilité des cellules granulaires en créant une excitation récurrente de ces cellules (Represa et al. 1993). De plus, Sloviter (1991) a démontré que les neurones GABAergiques sont toujours présents dans le gyrus dentelé, et que lorsque stimulés de façon adéquate, l'inhibition des cellules granulaires peut être rétablie. Ainsi, il a proposé que

l'hyperexcitabilité des cellules granulaires peut être causée par des interneurones inhibiteurs dormants (Sloviter 1991). Cette hypothèse suggère que la perte des cellules moussues du hile, qui normalement sont la source principale d'afférences excitatrices aux interneurones GABAergiques, produit une déafférentation des interneurones à panier, causant donc une perte d'inhibition polysynaptique et une hyperexcitabilité des cellules granulaires (Sloviter 1991).

La désinhibition ne semble pas permanente, puisque l'inhibition récurrente produite par les interneurones à panier semble rétablie deux mois après le traitement à l'AK (Sloviter 1992). Il a été proposé que le bourgeonnement axonal des cellules granulaires puisse contribuer à la formation de nouvelles synapses excitatrices sur les neurones inhibiteurs (Cronin et al. 1992; Sloviter 1992). Ainsi, ce phénomène de néosynaptogenèse pourrait représenter un mécanisme de compensation pour contrôler l'hyperexcitabilité du gyrus dentelé (McNamara 1994).

1.3.2 L'hyperexcitabilité de la région CA1 chez le rat traité à l'AK

Le traitement à l'AK provoque une perte cellulaire au niveau de la région CA3 (Nadler 1981). Suite à ce traitement, les cellules pyramidales de la région CA1 ne sont pas lésées mais deviennent partiellement déafférentées (Nadler 1981; Ben-Ari 1985). Lors d'enregistrements extracellulaires dans des tranches d'hippocampe de rats traités à l'AK, la stimulation des fibres afférentes aux cellules pyramidales de la région CA1 provoque des réponses épileptiformes constituées de bouffées de potentiels d'action (Herron et al. 1985; Ashwood et Wheal 1986, 1987). Des études pharmacologiques ont montré que cette activité épileptiforme est en partie due à

l'activation de récepteurs NMDA, puisque l'application d'un antagoniste NMDA diminue ces réponses en bouffées (Lancaster et Wheal 1984; Ashwood et Wheal 1986). Des observations lors d'enregistrements intracellulaires ont confirmé que les PPSE lents produits par l'activation des récepteurs NMDA sont augmentés de manière significative dans les cellules pyramidales hyperexcitables de la région CA1 chez les rats traités à l'AK (Turner et Wheal 1991; Williams et al. 1993).

Certains travaux suggèrent que l'augmentation des réponses NMDA peut être due à la formation de synapses aberrantes causée par le bourgeonnement axonal des fibres récurrentes des cellules pyramidales de la région CA1 suite au traitement à l'AK (Nadler et al. 1980). En effet, la stimulation des fibres de l'alveus, qui active antidromiquement les axones des cellules pyramidales de la région CA1, provoque des bouffées épileptiformes de potentiels d'action dans les tranches d'hippocampe des animaux traités à l'AK (Franck et al. 1988). En revanche, la même stimulation en présence d'une concentration élevée de magnésium et diminuée de calcium (ce qui bloque la transmission synaptique) ne provoque pas de bouffées épileptiformes de potentiels d'action, mais un seul potentiel d'action antidromique (Franck et al. 1988). Ces données suggèrent que les bouffées épileptiformes de potentiels d'action observées chez les animaux traités à l'AK peuvent être liées à la présence de nouvelles synapses excitatrices formées par les collatéraux récurrents des axones des cellules pyramidales de la région CA1. Donc, l'hyperexcitabilité de la région CA1 semble être causée en partie par une augmentation des réponses postsynaptiques excitatrices NMDA (Turner et Wheal 1991; Williams et al. 1993), et par la formation de nouvelles synapses excitatrices aberrantes sur les cellules pyramidales de la région

CA1 (Nadler et al. 1980; Franck et al. 1988; Perez et al. 1996). D'autres mécanismes comme des changements aux récepteurs GABA_A ou aux canaux calciques, des modifications du milieu extracellulaire produisant des variations de pH et d'ions K⁺, ou la présence de couplage électrotonique, peuvent aussi contribuer à l'activité épileptiforme des neurones hippocampiques (Schwartzkroin 1997).

1.3.3 La perte de neurones inhibiteurs dans l'hippocampe épileptique

Chez les patients épileptiques, les observations qui suggèrent une perte de neurones inhibiteurs sont controversées. Quelques travaux ont rapporté que le nombre d'interneurones immunopositifs pour la somatostatine est diminué dans l'hippocampe des épileptiques (de Lanerolle et al. 1989; Robbins et al. 1991). Par contre, des travaux en immunocytochimie ont indiqué que les neurones et contacts synaptiques inhibiteurs immunopositifs pour la DAG sont toujours présents (Babb et al. 1989).

Chez les rats traités à l'AK, des études immunocytochimiques ont suggéré que le nombre d'interneurones contenant de la parvalbumine et de la somatostatine est significativement diminué dans la région CA1 (Best et al. 1993). Cette diminution est corrélée à une perte des contacts synaptiques immunopositifs pour la parvalbumine sur le corps cellulaire et les dendrites proximales des cellules pyramidales de la région CA1 (Best et al. 1994). Puisque les interneurones contenant de la parvalbumine sont GABAergiques et donc inhibiteurs, cette perte de cellules pourrait donc contribuer à l'hyperexcitabilité des cellules pyramidales de la région CA1. Par contre, d'autres études immunocytochimiques ont démontré que les interneurones

immunopositifs pour la DAG sont toujours présents dans les couches pyramidale, radiatum et lacunosum-moleculare suite au traitement à l'AK (Franck et al. 1988).

1.3.4 L'inhibition polysynaptique est diminuée chez le rat traité à l'AK

L'inhibition semble être compromise au niveau des mécanismes synaptiques chez le rat traité à l'AK. Des enregistrements intracellulaires dans des tranches d'hippocampe ont démontré que la stimulation des fibres afférentes de la région CA1 produit des PPSI polysynaptiques significativement diminués en amplitude dans les cellules pyramidales de rat traité à l'AK (Franck et Schwartzkroin 1985; Ashwood et Wheal 1986; Franck et al. 1988; Williams et al. 1993). Par ailleurs, l'inhibition monosynaptique produite par l'activation directe des interneurones inhibiteurs en présence d'antagonistes AMPA et NMDA est intacte dans les cellules pyramidales (Nakajima et al. 1991; Williams et al. 1993). La présence d'inhibition monosynaptique dans les cellules pyramidales suite à l'activation directe des interneurones suggèrent donc que les synapses inhibitrices de la région CA1 sont intactes chez les rats traités à l'AK et qu'une diminution de l'activation des interneurones peut être responsable de la perte d'inhibition polysynaptique (Williams et al. 1993).

1.3.5 Les propriétés intrinsèques des neurones chez le rat traité à l'AK

Chez les rats traités à l'AK, les changements des propriétés intrinsèques qui peuvent causer l'hyperexcitabilité des cellules pyramidales de la région CA1 sont aussi controversés. Des enregistrements intracellulaires ont démontré une diminution des après-hyperpolarisations lentes et une augmentation de la résistance d'entrée des cellules pyramidales de la région CA1 chez l'animal traité à l'AK (Franck et Schwartzkroin 1985; Franck et al. 1988; Nakajima et al. 1991), toutefois ces changements n'ont pas été confirmés (Williams et al. 1993).

Pour ce qui est des propriétés des interneurones inhibiteurs, deux études intracellulaires n'ont rapporté aucun changement des propriétés intrinsèques dans les interneurones de la couche pyramidale chez l'animal traité à l'AK (Franck et al. 1988; Nakajima et al. 1991). Aucune étude n'a examiné les propriétés intrinsèques des autres types d'interneurones de la région CA1 après traitement à l'AK.

1.4 LES OBJECTIFS DE LA THÈSE

Le but de cette thèse est de caractériser les changements qui surviennent dans les circuits excitateurs et inhibiteurs de la région CA1 et qui contribuent à l'hyperexcitabilité des cellules pyramidales dans le modèle d'épilepsie de l'acide kaïnique (AK).

Dans un premier temps, les propriétés intrinsèques et les courants postsynaptiques excitateurs et inhibiteurs seront caractérisés dans les cellules pyramidales et trois groupes d'interneurones, i) dans la couche oriens et l'alveus

(O/A), ii) dans la couche pyramidale (PYR), et iii) à la bordure des couche radiatum et lacunosum-moleculare (LM) chez le rat normal juvénile. Les différents types de cellules seront visualisés dans des tranches d'hippocampe par vidéo-microscopie infrarouge et étudiés à l'aide d'enregistrement de *patch-clamp* en configuration cellule entière. De plus, un marquage intracellulaire avec la biocytine lors des enregistrements permettra d'analyser la morphologie des différents neurones étudiés. Ainsi, ces données permettront de corrélérer les propriétés intrinsèques, les courants synaptiques et la morphologie de différents types d'interneurones.

Dans un deuxième temps, puisque des travaux en immunocytochimie ont rapporté que le nombre d'interneurones contenant de la parvalbumine et de la somatostatine est significativement diminué dans la région CA1 chez les rats traités à l'AK, nous déterminerons si le nombre d'interneurones immunopositifs pour l'enzyme de synthèse du GABA, la décarboxylase de l'acide glutamique (DAG), est réduit dans la région CA1. La technique d'immunocytochimie contre la DAG sera utilisée sur des coupes d'hippocampe de rats témoins et de rats traités à l'AK. Nous quantifierons les neurones immunopositifs pour la DAG dans différentes couches de la région CA1 à l'aide d'une méthode stéréologique qui tient compte de l'épaisseur de la coupe, de la grosseur des neurones et de l'aire de la région où les cellules seront échantillonnées. Le but de cette étude sera de déterminer si certains interneurones GABAergiques sont préférentiellement endommagés par le traitement à l'AK.

Bien que l'effet du traitement à l'AK sur les propriétés intrinsèques et les réponses postsynaptiques excitatrices et inhibitrices des cellules pyramidales de la région CA1 ait déjà été décrit, très peu de travaux ont examiné les propriétés des

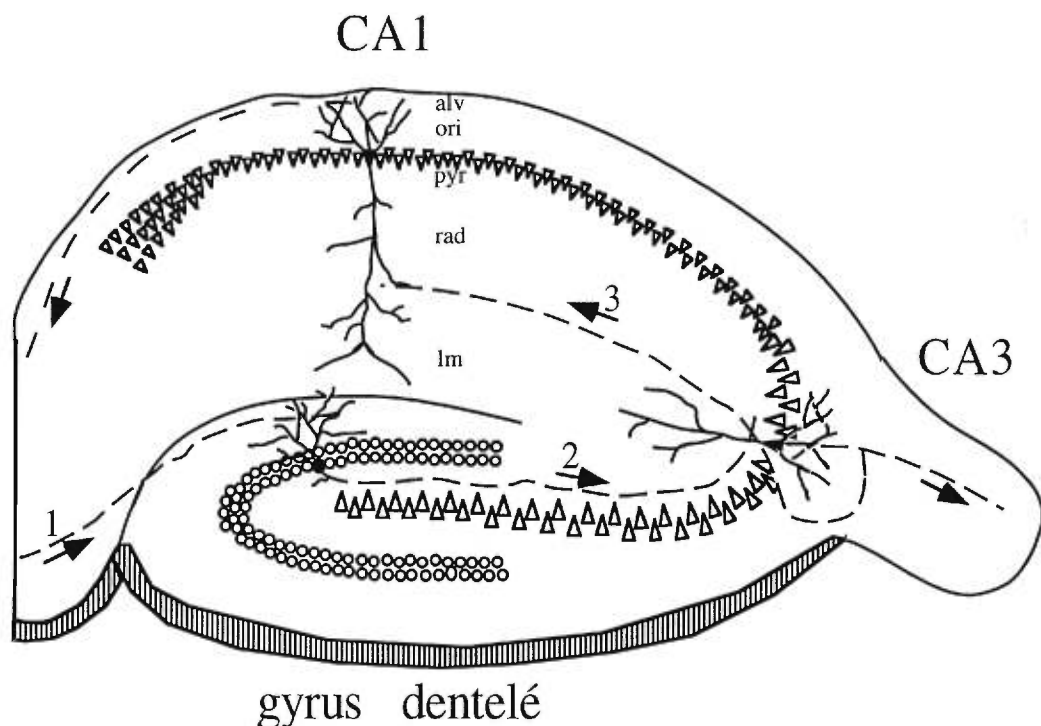
différents interneurones de la région CA1 suite au traitement à l'AK. Ainsi, dans un troisième temps, des enregistrements de *patch clamp* en configuration cellule entière seront utilisés afin d'examiner les propriétés intrinsèques et les courants postsynaptiques excitateurs et inhibiteurs de différents interneurones de la région CA1 dans le modèle de rats traités à l'AK. Cette étude permettra de déterminer si l'hyperexcitabilité des cellules pyramidales est due à des altérations de l'excitabilité des interneurones ou de leurs mécanismes synaptiques.

Dans un quatrième temps, certaines données anatomiques et physiologiques ont suggéré qu'il pourrait y avoir une perte de synapses inhibitrices sur les cellules pyramidales et une déafférentation des synapses excitatrices sur les interneurones GABAergiques chez les rats traités à l'AK. Nous déterminerons l'effet du traitement à l'AK sur les contacts synaptiques GABAergiques (inhibiteurs) et non-GABAergiques (excitateurs) situés sur le corps cellulaire et les dendrites proximales de cellules pyramidales et des interneurones de la région CA1. Les contacts synaptiques GABA seront identifiés en microscopie électronique en utilisant la méthode d'immunocytochimie du GABA après-enrobage. Les contacts synaptiques GABA et non-GABA seront caractérisés premièrement dans les différents types d'interneurones de la région CA1 chez l'animal témoin et ensuite l'effet du traitement à l'AK sur ces contacts synaptiques sera évalué. Ces données nous permettront d'examiner au niveau ultrastructural les changements synaptiques survenant suite au traitement à l'AK.

Dans un cinquième temps, afin de pouvoir éventuellement étudier, en microscopie électronique, les circuits GABAergiques dans le cortex humain épileptique, nous mettrons au point une technique de fixation qui permettra une

préservation adéquate de tissu cortical prélevé lors de résection chirurgicale de foyer épileptique du lobe temporal. Différentes méthodes de fixation seront d'abord testées sur le tissu prélevé chez le rat adulte anesthésié. Ensuite, la technique de fixation produisant une préservation optimale sera utilisée pour fixer le tissu cortical prélevé chez l'humain et sera couplée à l'immunocytochimie du GABA après-enrobage pour identifier les synapses GABAergiques dans ce tissu. La mise au point de cette méthode de fixation pourrait éventuellement permettre une analyse quantitative des contacts synaptiques GABA dans le tissu épileptique humain.

Schéma du circuit trisynaptique de l'hippocampe



- 1) faisceau perforant
- 2) fibres moussues
- 3) collatéraux de Schaffer

Figure 1

Figure 1 : Représentation schématique du circuit trisynaptique excitateur de l’hippocampe dans une coupe transverse de l’hippocampe. Les fibres du faisceau perforant (1) forment des contacts synaptiques excitateurs sur les dendrites des cellules granulaires du gyrus dentelé. Ensuite, les axones des cellules granulaires, que l’on appelle aussi fibres moussues (2), projettent aux dendrites des cellules pyramidales de la région CA3. Finalement, les axones des cellules pyramidales de la région CA3, que l’on nomme aussi collatéraux de Schaffer (3), forment des contacts synaptiques excitateurs sur les dendrites des cellules pyramidales de la région CA1. alv, alveus; ori, oriens; pyr, pyramidale; rad, radiatum et lm, lacunosum-moleculare. Les lignes pointillées représentent les fibres axonales.

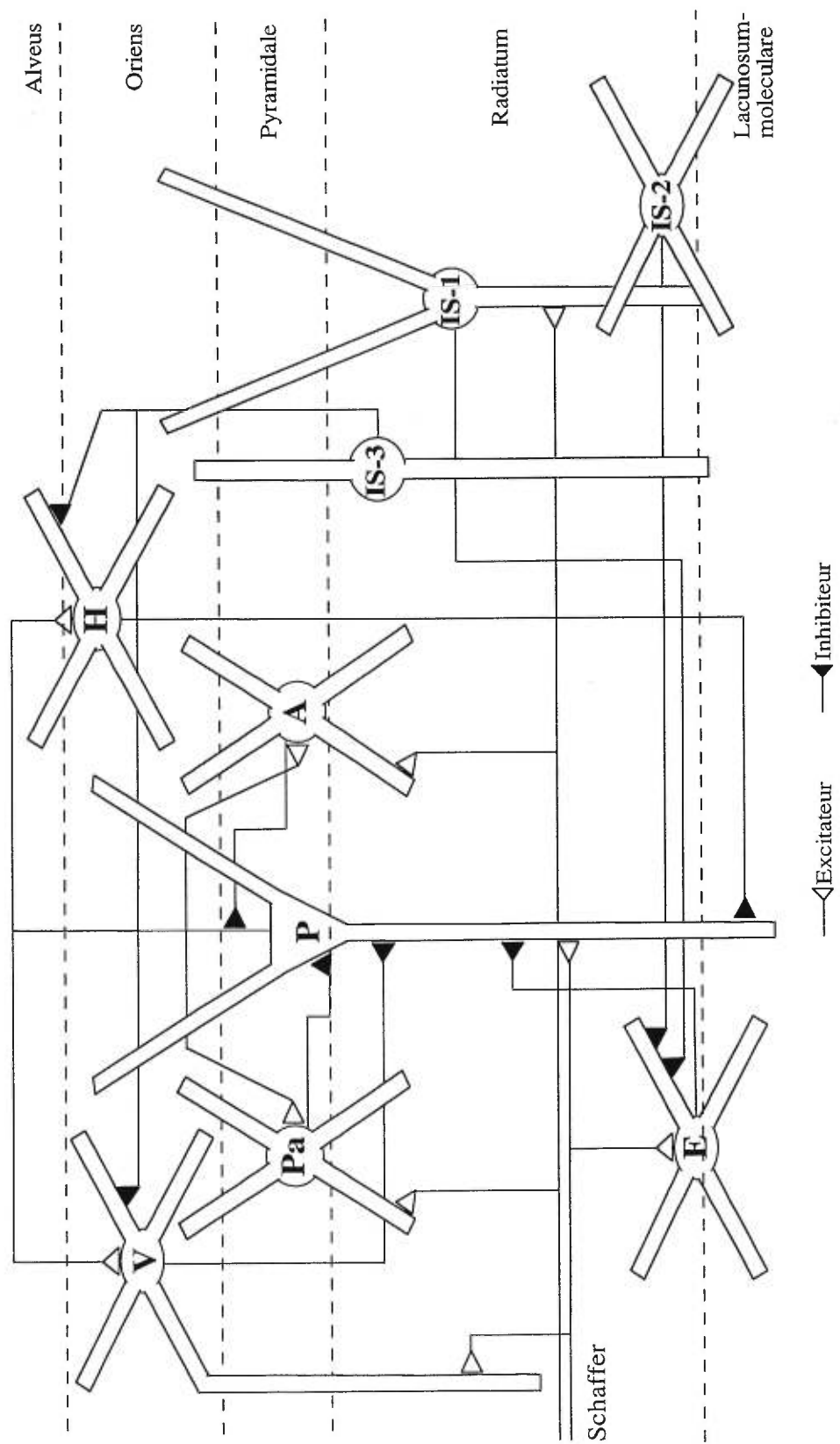


Figure 2

Figure 2 : Représentation schématique des interneurones impliqués dans l'inhibition proactive et rétroactive des cellules pyramidales de la région CA1 de l'hippocampe. L'inhibition proactive, produite par l'activation des fibres afférentes de la région CA1, recrute plusieurs populations d'interneurones : les interneurones verticaux (V), neurones à panier (Pa), cellules axo-axoniques (A), neurones étoilés (É) et les cellules *interneuron-selective* (IS-1). L'inhibition rétroactive, produite par l'activation des collatérales excitatrices des cellules pyramidales (P), implique aussi plusieurs sous-types d'interneurones : les interneurones verticaux (V) et horizontaux (H), neurones à panier (Pa), et les cellules axo-axoniques (A). Certaines populations d'interneurones inhibent préférentiellement d'autres interneurones : les cellules *interneuron-selective* (IS-1, IS-2 et IS-3). Les couches de la région CA1 sont indiquées par les lignes pointillées (alveus, oriens, pyramidale, radiatum et lacunosum-moleculare). Les synapses excitatrices sont représentées par des triangles blancs, et les synapses inhibitrices, par des triangles noirs.

CHAPITRE 2

**PROPRIÉTÉS MEMBRANAIRES ET COURANTS SYNAPTIQUES
ÉVOQUÉS DANS DES SOUS-TYPES D'INTERNEURONES DE LA RÉGION
CA1 DANS DES TRANCHES D'HIPPOCAMPE CHEZ LE RAT**

**Membrane Properties and Synaptic Currents Evoked in CA1 Interneuron
Subtypes in Rat Hippocampal Slices**

France Morin^{1,2}, Clermont Beaulieu² and Jean-Claude Lacaille¹

Centre de recherche en sciences neurologiques and Départements de physiologie¹ et
de pathologie², Université de Montréal, Montréal, Québec, Canada, H3C 3J7.

publié dans

Journal of Neurophysiology, 76: 1-16, 1996.

ABSTRACT

1. Intrinsic membrane properties and pharmacologically isolated excitatory and inhibitory postsynaptic currents (EPSCs and IPSCs, respectively) were characterized with the use of whole cell current- and voltage-clamp recordings, in combination with biocytin labeling, in different subtypes of CA1 interneurons and pyramidal cells in rat hippocampal slices.
2. Three classes of interneurons were selected on the basis of their soma location in the CA1 region: (1) in stratum (str.) oriens near the alveus, (2) near str. pyramidale and (3) near the border of str. radiatum and lacunosum-moleculare. Each class of biocytin-labeled cells demonstrated specific cellular morphology. The somata of all interneurons were non-pyramidal in shape and usually multipolar. However, the pattern of dendritic and axonal arborizations of labeled interneurons differed in each class.
3. In current-clamp recordings, all interneuron subtypes had shorter-duration and smaller-amplitude action potentials than pyramidal cells. Fast- and medium-duration afterhyperpolarizations were larger in amplitude in interneurons. Cell input resistance was greater and membrane time constant was faster in all interneuron subtypes than in pyramidal cells.

4. Depolarizing current pulses evoked regular firing in all classes of interneurons, whereas burst firing was observed in 50% of pyramidal cells. With hyperpolarizing current pulses, all nonpyramidal and pyramidal cell types displayed inward rectification followed by anodal break excitation.

5. Electrical stimulation of nearby afferents evoked excitatory postsynaptic potentials (EPSPs) in all cells. EPSPs were of short duration and usually followed by inhibitory postsynaptic potentials (IPSPs). EPSPs were mediated by glutamate since they were blocked by non-N-methyl-D-aspartate (non-NMDA) and NMDA antagonists (6-cyano-7-nitroquinoxaline-2,3-dione (CNQX) and (\pm)-2-amino-5-phosphonopentanoic acid (AP5), respectively). In the presence of these antagonists, IPSPs were evoked in isolation and reversed near -72 mV.

6. In voltage-clamp recordings, non-NMDA EPSCs were isolated pharmacologically in the presence of AP5 and the GABA_A antagonist bicuculline (BIC). Their properties were similar in all interneuron subtypes and pyramidal cells. Current-voltage (*I-V*) relations were linear, and mean reversal potentials were near 5 mV. Non-NMDA EPSCs were reversibly antagonized by CNQX.

7. NMDA EPSCs were pharmacologically isolated during CNQX and BIC application and were observed in all cell types. *I-V* relations of NMDA EPSCs

demonstrated a region of negative slope at membrane potentials between -80 and -20 mV and their reversal potential was near 7 mV. The rise time of NMDA EPSCs was significantly slower in O/A interneurons than in other cell types. NMDA EPSCs were reversibly antagonized by AP5.

8. GABA_A IPSCs were pharmacologically isolated in AP5 and CNQX and their properties were similar in all cell types. *I-V* relations of GABA_A IPSCs were linear with mean reversal potentials near -32 mV. GABA_A IPSCs were reversibly blocked by BIC.

9. In conclusion, morphologically different subtypes of interneurons located in O/A, near str. pyramidale and near the str. radiatum/lacunosum-moleculare border displayed intrinsic membrane properties that were distinct from pyramidal cells, but were similar among them. In contrast, the properties of non-NMDA, NMDA and GABA_A postsynaptic currents were similar between interneurons and pyramidal cells, except for NMDA EPSCs which had slower rise times in O/A interneurons.

INTRODUCTION

The hippocampus is composed of a principal excitatory trisynaptic circuit consisting of granule cells of the dentate gyrus, large pyramidal cells of the CA3 region and small pyramidal cells of the CA1 region (Lorente de Nò 1934; Ramon y Cajal 1911). The presence of numerous local circuit cells (interneurons) has also been described within each of these regions (Amaral 1978; Lorente de Nò 1934; Ramon y Cajal 1911). Contrary to the principal cells, which are excitatory neurons, a large majority of interneurons are GABAergic and therefore inhibitory in function (Babb et al. 1988; Ribak et al. 1978; Woodson et al. 1989). These GABAergic interneurons provide powerful inhibition of principal cells and act to regulate excitation in the principal circuit (Buhl et al. 1994a; Lacaille et al. 1989; Schwartzkroin and Prince 1980; Traub et al. 1987).

Local circuit cells in the dentate gyrus and hippocampus proper are morphologically and physiologically heterogeneous. In the CA1 region, different subtypes of interneurons with distinctive dendritic and axonal arborizations have been investigated with combined intracellular recordings and morphological analysis: basket, axo-axonic, vertical, horizontal and stellate cells. These interneuron subtypes have been differentiated based on their soma location within the hippocampal layers. Basket cells (Schwartzkroin and Kunkel 1985; Schwartzkroin and Mathers 1978) and axo-axonic cells (Buhl et al. 1994b) are located in or near stratum (str.) pyramidale (PYR); vertical (Lacaille and Williams 1990; Lacaille et al. 1987) and horizontal cells (McBain et al. 1994) are located in str. oriens near the alveus (O/A); and stellate cells

are located near the junction of str. radiatum and str. lacunosum-moleculare (L-M) (Kawaguchi and Hama 1987; Lacaille and Schwartzkroin 1988a; Misgeld and Frotscher 1986). These interneurons fall into two broad classes on the basis of their physiological properties. Basket, axo-axonic and vertical cells display similar short-duration action potentials, pronounced spike afterhyperpolarizations, and little frequency accommodation, characterizing them as "fast spiking" cells (Schwartzkroin and Mathers 1978). In contrast, stellate cells have longer-duration action potentials and show voltage-dependent burst firing, identifying them as "non-fast spiking" cells (Kawaguchi and Hama 1988; Lacaille and Schwartzkroin 1988a). Similarly, these interneurons display two types of local circuit interactions with pyramidal cells. Vertical (Lacaille et al. 1987), axo-axonic (Buhl et al. 1994b) and basket cells (Knowles and Schwartzkroin 1981) inhibit pyramidal cells and receive reciprocal excitatory inputs from them; they can thus mediate both feedforward and feedback inhibition of the principal cells. In contrast, stellate cells inhibit pyramidal cells but do not receive excitatory inputs from them; therefore they may only mediate feedforward inhibition of pyramidal cells (Lacaille and Schwartzkroin 1988b). Furthermore, heterogeneity among local circuit cells has also been documented on the basis of their differences in pre- and postsynaptic properties (Buhl et al. 1994a; Lambert and Wilson 1993), receptor subunit expression (Gao and Fritschy 1994; McBain and Dingledine 1993), content of peptides (Somogyi et al. 1984) and Ca^{2+} binding proteins (Gulyas et al. 1991); however, the functional significance of these differences remains unclear.

The combination of whole cell recording and visual identification of cells in brain slices (Edwards et al. 1989) has provided powerful tools to study synaptic currents (Perouansky and Yaari 1993; Sah et al. 1990) and membrane properties (Williams et al. 1994) of interneurons. However, no comparative study has yet examined, with the use of whole cell recordings in combination with morphological identification of cells in hippocampal slices, the membrane properties and synaptic currents of various subtypes of interneurons and pyramidal cells. The aim of the present study was therefore to characterize and directly compare the intrinsic properties and postsynaptic currents of morphologically identified interneuron subtypes located in three different regions of the CA1 area: 1) O/A, 2) PYR, and 3) L-M. The properties of these interneurons were also compared with those of pyramidal cells. Preliminary reports of this work have been presented in abstract form (Morin et al. 1995).

METHODS

Hippocampal slices

Hippocampal slices were obtained as described previously (Ouardouz and Lacaille 1995; Williams et al. 1994). Briefly, young male Sprague-Dawley rats (14-22 days) were deeply anesthetized with ether and killed by decapitation. The brain was quickly removed from the skull and placed in cold (4°C) fresh artificial cerebrospinal fluid (ACSF) containing (in mM) 124 NaCl, 5 KCl, 1.25 NaH₂PO₄, 2 MgSO₄, 2 CaCl₂, 26 NaHCO₃ and 10 dextrose. A block of tissue containing the hippocampus was glued with cyanoacrylate to the tissue holder of a vibratome

(Campden Instruments). Transverse hippocampal slices (300 μm thick) were cut and transferred to a container filled with oxygenated ACSF at room temperature. After a recovery period of ~ 1 hour, a slice was positioned in a recording chamber and maintained submerged with a U-shaped platinum wire (Edwards et al. 1989). Slices were continuously perfused with oxygenated ACSF (3-4 ml/min) at room temperature (22°-24°C). The recording chamber was mounted on an upright microscope (Zeiss Axioskop) equipped with a long-range water immersion objective (40x) (Nomarski optics), and an infrared charge-coupled device camera (Cohu 6500). Under these conditions, pyramidal cells and various subtypes of interneurons located in different hippocampal layers were easily distinguishable upon visual inspection and were then selected for whole cell recordings.

Recordings

For current-clamp experiments, patch electrodes ($5\text{-}10\text{ M}\Omega$) were filled with (in mM): 140 potassium gluconate, 5 NaCl, 2 MgCl₂, 10 *N*-2-hydroxyethylpiperazine-*N*-2-ethanesulfonic acid (HEPES), 0.5 ethylene glycol-bis(β -aminoethyl ether)-*N,N,N,N*-tetraacetic acid (EGTA), 2 ATP-tris, 0.4 GTP-tris, pH adjusted to 7.4 with KOH. For voltage-clamp experiments, to improve the space clamp and block K⁺ and Na⁺ currents (Nathan et al. 1990), the internal solution of the patch electrodes contained (in mM) 120 Cs-methane sulphonate, 20 lidocaine *N*-ethyl- bromide (QX-314; Research Biochemicals, RBI), 8 NaCl, 1 MgCl₂, 10 HEPES, 1 EGTA, 2 ATP-tris, 0.4 GTP-tris, pH adjusted to 7.4 with

CsOH. In all experiments, 0.1% biocytin was added to the recording solution to intracellularly label the cell and allow later morphological characterization.

Tight-seals ($>1\text{ G}\Omega$) were formed on cell bodies of chosen neurons and whole cell recordings were obtained by rupturing the cell membrane with negative pressure (Hamill et al. 1981). Current- and voltage-clamp recordings were made with the use of an Axopatch 1D amplifier (Axon Instruments) with low-pass filtering at 10 KHz (-3db), displayed on an oscilloscope (Gould 1604), and digitized at 22 KHz for storage on a video cassette recorder (Neurocorder DR-886). Recordings were also digitized and analyzed with a PC-DOS microcomputer equipped with a data acquisition system (TL-125 and pClamp, Axon Instruments). Recordings were considered acceptable if series resistance and capacitance could be properly compensated, and if membrane potential (current-clamp) or holding current (voltage-clamp) were stable. Mean series resistance was 22.1 ± 0.9 (SE) $\text{M}\Omega$ ($n=87$). Liquid junction potentials were measured at the end of the experiments after withdrawal from the cell and membrane potentials were corrected accordingly.

Postsynaptic responses were evoked by electrical stimulation (constant current, 0-300 μA , 0.05 ms pulses) of nearby afferent fibers with the use of a monopolar tungsten microelectrode (Frederick Haer Co.), positioned either in str. radiatum for pyramidal cells, or 150-250 μm laterally from the cell soma (within the same layer) for interneurons. The analysis of postsynaptic currents was performed on averaged ($n=3$) excitatory and inhibitory postsynaptic currents (EPSCs and IPSCs,

respectively). In all experiments, the CA1 and CA3 regions were disconnected by a surgical cut.

Statistical analysis

Statistical differences between means of groups of cells were assessed with one-way analysis of variance (ANOVA) tests. When significant differences were found ($p<0.05$), pairwise comparisons were made using the Student's Newman-Keuls test. When not significantly different, values from different interneuron subtypes were pooled and compared with those of pyramidal cells with Student's t-tests ($p<0.05$). Statistical difference between paired data was assessed with paired Student's t-tests ($p<0.05$). All data are given as mean \pm SE. Values given in the text refer to pooled data for interneurons, whereas those in tables refer to data for each interneuron subtype.

Pharmacology

Stock solutions of the non-*N*-methyl-D-aspartate (non-NMDA) antagonist 6-cyano-7-nitroquinoxaline-2,3-dione (CNQX; 3.1 mM, RBI), the NMDA antagonist (\pm)-2-amino-5-phosphonopentanoic acid (AP5; 7.7 mM, Sigma) and the GABA_A antagonist bicuculline methiodide (BIC; 3.3 mM, Sigma) were prepared in distilled water and stored frozen in 1-ml aliquots. Before each experiment, antagonists were diluted in ACSF to their final concentration (CNQX, 20 μ M; AP-5, 50 μ M; BIC, 25 μ M). Antagonists were applied by perfusion in the bath through a three-way valve.

Histology

After completion of physiological recordings, the slices were put in a fixative solution containing 4% paraformaldehyde, 1% glutaraldehyde, 2.5% dimethyl sulfoxide (DMSO), 3.0 mM CaCl₂ in 0.1 M cacodylate buffer (pH 7.4) for 4 h. Slices were then thoroughly rinsed and left overnight in 0.1 M cacodylate buffer. Subsequently, slices were embedded in 1% agarose and cut on a vibratome in 60 µm-thick sections. The sections were treated with 1% H₂O₂ for 20 min to eliminate endogenous peroxidase, and were washed in phosphate-buffered saline (4x5 min) and then in phosphate-buffered saline containing 2.5% dimethyl sulfoxide (4x5 min). Slices were incubated in the avidin biotin complex (ABC kit, Vector Labs) at a concentration of 1:200 for 24 h at room temperature and the peroxidase product was revealed according to a modified protocol using tetramethylbenzidine (Llewellyn-Smith et al. 1993). Briefly, slices were incubated for 20 min in a solution of phosphate buffer (0.1 M, pH 6.0) containing 0.4% ammonium chloride (Sigma) and 0.001% tetramethylbenzidine (Sigma). The blue reaction was visualized by adding 0.5% H₂O₂ to the first incubating solution. To stabilize the tetramethylbenzidine product, slices were incubated 15 min in a solution of phosphate buffer (0.1 M, pH 6.0) containing 0.4% NH₄Cl, 1% cobalt chloride (CoCl₂, Sigma), 0.1% diaminobenzidine, and 0.05% H₂O₂. Sections were then mounted for light microscopy. The dendritic and axonal arborizations of the cells were reconstructed with the use of a camera lucida at a final magnification of about X400.

RESULTS

Cells were visually identified with Nomarski optics in slices and selected for recordings on the basis of their location in specific layers of the CA1 region and their morphology (soma and primary dendrites). A first group of interneurons consisted of cells located in the inferior part of O/A ($n=20$). A second group was composed of interneurons found within $\sim 75 \mu\text{m}$ of str. pyramidale (PYR; $n=20$). To differentiate the latter from pyramidal cells, interneurons with large ($\sim 30 \mu\text{m}$) nonpyramidal somata were selected. The identification of PYR interneurons was subsequently confirmed on the basis of their nonpyramidal membrane characteristics (see below). A third group of interneurons was comprised of cells located at L-M ($n=21$). Finally, recordings were also obtained from 25 CA1 pyramidal cells.

Morphology of biocytin-filled cells

The morphological profiles of cells labeled with biocytin were relatively similar within each group. For labeled O/A cells ($n=11$), their multipolar soma was usually oriented horizontally and their dendritic processes were varicosed and aspinous (Fig. 1A). In general, major dendrites were directed horizontally within str. oriens and the alveus, but few dendritic branches also coursed vertically in str. oriens and occasionally in str. radiatum ($n=4$). Labeled axons of O/A cells could be followed ($n=2$) originating from a proximal dendrite and coursing either through the pyramidal cell layer, through str. radiatum and str. lacunosum-moleculare, or into the pyramidal cell layer. For PYR interneurons (Fig. 1B), labeled cell somata were

located in str. radiatum (n=7) or oriens (n=2). Their dendrites usually extended in many CA1 layers: str. oriens/radiatum/lacunosum-moleculare (n=2), str. radiatum/lacunosum-moleculare (n=3), str. radiatum/oriens (n=1). In three of these interneurons, however, dendrites were confined to str. radiatum. Labeled axons of PYR interneurons were seen either residing within the pyramidal cell layer only (n=2) or additionally extending in str. radiatum and lacunosum-moleculare (n=2). Somata of L-M interneurons were multipolar and their dendrites were smooth and varicosed (n=11). Dendritic processes extended radially within str. lacunosum-moleculare and radiatum, occasionally coursed in str. pyramidale (n=4) and oriens (n=3), and in one case crossed the hippocampal fissure (Fig. 1C). Labeled L-M cell axons usually covered a large surface of str. radiatum and lacunosum-moleculare with some collaterals extending in the pyramidal cell layer (n=5). The morphology of interneurons of each group was clearly different from labeled CA1 pyramidal cells (n=13), which displayed typical spiny dendritic arborizations and axonal processes (Fig. 1D).

Membrane properties in current-clamp

Whole cell recordings were obtained in current-clamp mode to examine the intrinsic membrane properties of interneurons and pyramidal cells (n=24). Except for some characteristics of afterhyperpolarizations, membrane properties were similar in subtypes of interneurons (Table 1). Mean resting membrane potential did not differ significantly between interneurons and pyramidal cells, but other membrane properties clearly did (Table 1). In interneurons, action potential amplitude was

significantly smaller (82 vs 95 mV in pyramidal cells; $p<0.05$), duration of action potentials, measured at the base, was significantly shorter (1.9 vs 3.0 ms in pyramidal cells; $p<0.001$) (Fig. 2A, B), and cell input resistance was significantly greater (236.1 vs 135.6 M Ω in pyramidal cells; $p<0.05$).

Afterhyperpolarizations following individual action potentials (AHPs) were more pronounced in interneurons (Fig. 2). As in pyramidal cells, AHPs in interneurons consisted of fast-duration (*f*AHP) and medium-duration (*m*AHP) components (Storm 1989). In interneurons, *f*AHPs were significantly larger in amplitude (-13.2 vs -0.1 mV in pyramidal cells; $p<0.001$) and had significantly shorter peak latency (2.8 vs 3.6 ms in pyramidal cells; $p<0.05$) and significantly longer recovery time (1.8 vs 1.3 ms in pyramidal cells; $p<0.05$) (Table 1). The mean amplitude of the *m*AHP was significantly greater in interneurons (-5.4 mV) than in pyramidal cells (1.1 mV; $p<0.01$) (Table 1). The mean peak latency of the *m*AHP differed significantly between PYR and L-M interneurons, but not between other cell types (Table 1). Mean recovery times of the *m*AHP were not different between cell types (Table 1).

Interneurons and pyramidal cells also responded differently to injection of depolarizing and hyperpolarizing current pulses (300-400 ms in duration) (Fig. 2). In all interneurons, depolarizing pulses elicited nondecrementing train of action potentials (Fig. 2C). Voltage-dependent burst firing, previously reported in interneurons in L-M (Lacaille and Schwartzkroin 1988a), was not observed in any interneurons. In pyramidal cells, depolarizing pulses evoked either regular ($n=5$) or

burst firing ($n=4$; Fig. 2D). During small hyperpolarizing current pulses (0-200 pA), the membrane potential gradually increased to a maximum steady level. Membrane time constants were obtained by fitting an exponential function to the responses to small hyperpolarizing current pulses. Mean time constants did not differ among interneuron subtypes, but were significantly faster for interneurons (28.9 ms) than for pyramidal cells (46.0 ms, $p<0.05$) (Table 1). During injection of larger-amplitude hyperpolarizing pulses (> 300 pA), the membrane potential reached an initial peak value and then returned slowly to a more depolarized steady level (Fig. 2C, D). This inward rectification was observed in all interneurons and pyramidal cells. When inward rectification was present, anodal break excitation was observed after the end of the current pulse. To quantify inward rectification, the membrane potential was measured at the peak and at the end of the pulse for series of stimulation with different current intensities (Fig. 2). Cell input resistances were obtained from the slopes of the voltage-current regression lines (Fig. 2E, F). The presence of inward rectification was clearly seen from the reduction in input resistance at the end of the pulse (Fig. 2E, F) (Table 1). Mean rectification ratios, obtained from the ratio of peak input resistance to end input resistance, were not different between interneurons and pyramidal cells (Table 1).

Synaptic responses in current clamp

Electrical stimulation of nearby axons evoked postsynaptic potentials in all cells. Short-latency excitatory postsynaptic potentials (EPSPs) were elicited in all interneurons ($n=14$) and pyramidal cells ($n=8$) tested (Fig. 3 and Table 1). Near

resting membrane potential, higher intensities of stimulation evoked one or two action potentials. EPSP amplitude increased when evoked at hyperpolarized membrane potentials. EPSPs were reversibly blocked with the addition of non-NMDA and NMDA antagonists (20 μ M CNQX, and 50 μ M AP5) to the perfusion medium. In the presence of these antagonists, inhibitory postsynaptic potentials (IPSPs) were observed in isolation in 7 out of 11 interneurons and in 6 of 7 pyramidal cells (Fig. 3). IPSPs were pronounced near resting membrane potentials and reversed at a mean membrane potential of -72.4 ± 2.9 mV (data not shown, n=13 cells).

Synaptic responses in voltage clamp

Because prominent NMDA and non-NMDA EPSPs and GABA_A-like IPSPs were observed in interneurons during current-clamp recordings, voltage-clamp experiments were carried out in 47 interneurons and 16 pyramidal cells during pharmacological manipulation to characterize in isolation each of the synaptic currents. Cells were initially voltage clamped near -80 mV and postsynaptic currents were evoked by stimulation of nearby afferent fibers (0-300 μ A). The intensity of stimulation was then set to evoke a response at 80% of maximal amplitude and perfusion with pharmacological antagonists was initiated.

Non-NMDA EPSCs

Non-NMDA EPSCs were pharmacologically isolated in the presence of 50 μ M AP5 and 25 μ M BIC, and were evoked in cells voltage clamped at membrane

potentials between -100 and 60 mV (Fig. 4A). The properties of non-NMDA EPSCs were similar in different interneuron subtypes and pyramidal cells (Table 2). The current-voltage (I-V) relationship of averaged non-NMDA EPSCs was mostly linear except at most extreme membrane potentials (Fig. 4B). The mean reversal potential of non-NMDA EPSCs varied between -1.2 and 8.6 mV in interneurons and was 2.5 mV in pyramidal cells (Table 2). The mean conductance of the non-NMDA EPSCs, obtained from the slope of the linear portion of the I-V relationship (eg. Fig. 4B), was 4.0 nS in interneurons and 4.9 nS in pyramidal cells (Table 2).

Bath application of the non-NMDA antagonist CNQX (20 μ M) reversibly blocked non-NMDA EPSCs (Fig. 4C). In CNQX, the mean peak amplitude of the non-NMDA EPSCs evoked near -85 mV was significantly reduced by $95.0 \pm 0.9\%$ ($n=17$ interneurons; $p<0.05$). This antagonism was reversible ($22.9 \pm 6.7\%$ of control; $n=3$ cells). At positive holding potentials (near 50 mV), the mean peak amplitude of non-NMDA EPSCs was significantly decreased by $78.6 \pm 4.4\%$ ($n=16$ interneurons; $p<0.05$) in CNQX, and the effect was reversible (amplitude $44.8 \pm 29.1\%$ of control after wash; $n=3$ cells). In pyramidal cells, non-NMDA EPSCs were also reversibly reduced during CNQX application by $91.9 \pm 2.5\%$ at negative (near -80 mV; $n=6$) and by $84.6 \pm 6.7\%$ at positive (near 50 mV; $n=4$) holding potentials.

The 10-90% rise time of non-NMDA EPSCs, evoked at membrane potentials near -80 mV, was similar between interneurons (8.4 ± 1.4 ms) and pyramidal cells (8.4 ± 1.1 ms) (Table 2). Non-NMDA EPSCs generally decayed as a single exponential function in all cell types (Table 2). In some cases ($n=3$ cells), the decay was better described with a biexponential function, but these cells were not included

in the analysis. At membrane potentials near -80 mV, the decay time constant of non-NMDA EPSCs was similar in interneurons (30.0 ± 6.8 ms) and pyramidal cells (32.2 ± 3.4 ms) (Table 2). A positive correlation was found between the rise time and decay time constant of non-NMDA EPSCs, but it was not statistically significant ($n=13$ cells, $r=0.31$; Fig. 5E).

NMDA EPSCs

NMDA EPSCs were evoked in the presence of $20 \mu\text{M}$ CNQX and $25 \mu\text{M}$ BIC in ACSF containing Mg^{2+} (Fig. 6). All cell types showed prominent NMDA EPSCs that were voltage dependent between -80 mV and 60 mV (Table 2). NMDA EPSCs were almost null near -80 mV but were large near 50 mV (Fig. 6). The I-V graph of peak NMDA EPSCs demonstrated a negative slope between -80 and -20 mV ($n=18$ cells; eg. Fig. 6B). The mean reversal potential of NMDA EPSCs was similar in interneurons and pyramidal cells and varied between 2.4 and 11.8 mV (Table 2). The conductance of NMDA EPSCs was estimated from the slope of the linear portion of I-V relations (eg. Fig. 6B), and was not significantly different between interneurons and pyramidal cells (5.2 and 5.1 nS, respectively). Bath application of the selective NMDA antagonist AP5 antagonized NMDA EPSCs evoked at depolarized potentials in interneurons (by $84.9 \pm 2.9\%$, $n=9$ cells; $p<0.05$) (Fig. 6C) and in pyramidal cells (by $62.4 \pm 8.9\%$, $n=5$ cells; $p<0.05$). The effects of AP5 were reversible in interneurons ($35.4 \pm 15.3\%$ of control amplitude; $n=2$) and in pyramidal cells ($86.0 \pm 11.4\%$ of control amplitude; $n=3$).

Differences were found in the kinetics of NMDA EPSCs in interneurons (Table 2). The 10-90% rise time of NMDA EPSCs, evoked at membrane potentials near 50 mV, was three- to fourfold slower in O/A interneurons than in other cell types. The rise time was significantly slower for NMDA EPSCs evoked near 50 mV (Fig. 7, Table 2, $p<0.05$). In contrast, the decay of NMDA EPSCs was similar in interneurons and pyramidal cells (Table 2). NMDA EPSCs, evoked at membrane potential near 50 mV, decayed with a single-exponential time constant of 290 ± 36 ms in interneurons (Fig. 8A, B; Table 2). A positive, but non-significant, correlation ($r=0.34$) was found between the decay time constant and the rise time of NMDA EPSCs in interneurons ($n=14$ cells; Fig. 8).

GABA_A IPSCs

GABA_A IPSCs were pharmacologically isolated during bath application of 50 μ M AP5 and 20 μ M CNQX (Table 2). These IPSCs are likely monosynaptic responses, because they were evoked in the presence of antagonists of non-NMDA and NMDA glutamate receptors. In all cell types, GABA_A IPSCs were inward at negative holding potentials (near -60 mV) and outward at positive potentials (near 50 mV). The I-V relationship of the peak GABA_A IPSCs was mostly linear (Fig. 9). The mean reversal potential of GABA_A IPSCs was similar in all cell types and varied between -28.6 and -34.3 mV (Table 2). The mean conductance of GABA_A IPSCs, obtained from the slope of the linear portion of the I-V relationship, was not significantly different among interneurons and pyramidal cells (6.7 and 11.3 nS, respectively; Table 2). The GABA_A nature of these IPSCs was confirmed using the

GABA_A antagonist BIC (Fig. 8C). In interneurons (n=11 cells), the peak amplitude of outward IPSCs evoked near 50 mV and of inward IPSCs elicited near -60 mV were significantly reduced by $84.4 \pm 3.3\%$ and $82.6 \pm 4.7\%$, respectively ($p < 0.05$). The effects of BIC were reversible ($64.8 \pm 9.7\%$ of control, n=9 and $66.0 \pm 11.8\%$ of control, n=8; respectively). BIC similarly antagonized IPSCs in pyramidal cells (by $89.4 \pm 3.1\%$ near 50 mV and by $92.0 \pm 1.9\%$ near -60 mV; n=2 cells; $p < 0.05$).

The kinetics of GABA_A IPSCs were similar in interneuron subtypes and pyramidal cells (Table 2). The mean rise time of GABA_A IPSCs was not sensitive to voltage (holding potentials near -60 vs 50 mV) and varied between 5.1 and 7.4 ms in interneurons versus 7.0 ms in pyramidal cells (Table 2). The decay time constant of GABA_A IPSCs, obtained from a single-exponential fit of the decay phase, was not different between the various cell types (Table 2), but was voltage sensitive (Fig. 10B). For interneurons (n=12 cells), the decay time constant of GABA_A IPSCs was slower near 50 mV (154 ± 11 ms) than near -60 mV (72 ± 5 ms, $p < 0.001$). In pyramidal cells, GABA_A IPSCs also decayed more slowly at depolarized holding potentials (Table 2). No significant correlation was found between decay time constant and rise time of GABA_A IPSCs (n=12 cells, $r = 0.20$; Fig. 10).

DISCUSSION

Membrane properties and synaptic currents were characterized, with the use of whole cell recordings, and compared in three groups of interneurons selected on the basis of their soma location in specific layers of the hippocampal CA1 region: (1)

O/A, (2) PYR and (3) L-M. The major findings were that, in hippocampal slices of young animals, the intrinsic membrane properties of interneurons were different from those of pyramidal cells, but these properties were generally similar among the various interneuron subtypes. In contrast, pharmacologically isolated non-NMDA and NMDA EPSCs and GABA_A IPSCs were similar in the various interneurons and pyramidal cells, except for NMDA EPSCs, which displayed distinct kinetics in O/A interneurons.

Morphology

The morphology of biocytin-labeled interneurons was different for each group of interneurons, confirming their different subtypes. The somata of all interneurons were nonpyramidal in shape and usually multipolar. The dendritic arborization of labeled interneurons differed markedly. Dendrites of cells in O/A arborized greatly in str. oriens and sometimes in str. radiatum. Those of interneurons near PYR usually extended both in str. radiatum and oriens. Dendrites of L-M cells usually ramified extensively in str. radiatum and lacunosum-moleculare. Biocytin-labeled axons were seen only in a few cells of each group, but in each case also indicated distinctive arborization patterns: in str. oriens, pyramidale and radiatum for O/A cells; in str. radiatum and pyramidale for PYR interneurons; and in str. radiatum and lacunosum-moleculare for L-M cells. The distinctive dendritic and axonal arborizations observed in each group of interneurons are generally similar to the specific morphology previously reported in intracellular studies in adult slices for interneurons in O/A (Lacaille and Williams 1990; Lacaille et al. 1987), near PYR

(Buhl et al. 1994a; Kawaguchi and Hama 1988; Schwartzkroin and Kunkel 1985), and in L-M (Kawaguchi and Hama 1988; Lacaille and Schwartzkroin 1988a). Similar distinctive morphology has been reported for interneurons labeled during whole cell recordings in slices of young rats in the O/A (McBain et al. 1994) and L-M (Williams et al. 1994) regions. The lower incidence of axonal labeling observed in the present study may be due to the reduced thickness of slices for whole cell recordings, which may favor damage to interneuron axons during sectioning.

Membrane properties

Significant differences in intrinsic membrane properties were found between interneurons and pyramidal cells. First, resting membrane potentials were similar in all cell types, which is in general agreement with previous reports from interneurons in O/A (McBain et al. 1994) and L-M (Williams et al. 1994), and from pyramidal cells (Spigelman et al. 1992) in slices of young animals. The membrane properties that were significantly different in all interneuron subtypes compared with pyramidal cells were action potential amplitude and duration, afterhyperpolarizations, membrane time constant, cell input resistance, and evoked firing. Action potential duration was significantly shorter in interneurons than in pyramidal cells, which is in accordance with previous studies with intracellular recordings from interneurons in or near PYR (Kawaguchi and Hama 1987; Lacaille 1991; Schwartzkroin and Mathers 1978) and in O/A (Lacaille and Williams 1990; Lacaille et al. 1987), and with whole cell recordings from interneurons in L-M (Williams et al. 1994). Action potential amplitude was significantly smaller in interneurons than in pyramidal cells. These

findings are in agreement with previous intracellular studies of PYR (Lacaille 1991; Schwartzkroin and Mathers 1978), O/A (Lacaille and Williams 1990; Lacaille et al. 1987), and L-M interneurons (Lacaille and Schwartzkroin 1988a) that reported action potentials with little overshoot in interneurons. Cell input resistance was significantly greater in interneurons than in pyramidal cells. Our results confirmed, with whole cell recordings, the previously reported higher cell input resistance of interneurons near PYR (Schwartzkroin and Mathers 1978), O/A (Lacaille et al. 1987) and L-M (Lacaille and Schwartzkroin 1988a), and further suggest that cell input resistance is not significantly different between these interneuron subtypes.

Afterhyperpolarizations also showed marked differences in interneurons and pyramidal cells. Although afterhyperpolarizations consisted of *fAHP* and *mAHP* components in interneurons and pyramidal cells, both components were larger in amplitude in interneurons. In interneurons, pronounced AHPs have been reported as distinctive features of cells in O/A (Lacaille et al. 1987; Zhang and McBain 1995), PYR (Schwartzkroin and Mathers 1978) and L-M (Kawaguchi and Hama 1987; Lacaille and Schwartzkroin 1988a), but the previously reported AHPs were usually monophasic. Dual-component AHPs have been characterized previously in pyramidal cells (Storm 1989, 1990). Our results confirm the presence of *fAHPs* and *mAHPs* in L-M cells (Williams et al. 1994) and further show that other subtypes of interneurons in O/A and PYR also display such AHPs with dual components. Although the presence of afterdepolarizing potentials may partially mask AHPs in pyramidal cells, differences in potassium current kinetics may underlie the more pronounced *fAHPs* and *mAHPs* in interneurons (Zhang and McBain 1995).

Interneurons and pyramidal cells also responded differently to current injections. First, membrane time constants were significantly faster in all interneuron subtypes. In previous intracellular studies in conventional slices, membrane time constants were also faster in interneurons than pyramidal cells (Lacaille and Schwartzkroin 1988a; Lacaille et al. 1987; Schwartzkroin and Mathers 1978). Second, when depolarizing current pulses were applied near resting membrane potential, the firing pattern was different in interneurons and pyramidal cells. Current pulses evoked regular firing in all classes of interneurons but produced burst firing in 50% of pyramidal cells. Furthermore, the pattern of firing observed in L-M and other types of interneurons did not change at hyperpolarized membrane potential. This is in contrast to the voltage-dependent burst firing previously reported with intracellular recordings in L-M cells in conventional slices (Kawaguchi and Hama 1988; Lacaille and Schwartzkroin 1988a). The present results confirm the reported lack of voltage-dependent burst firing in L-M interneurons with whole cell recordings (Williams et al. 1994). The present observations were performed with a similar whole cell recording solution that was previously used to record low-threshold Ca^{2+} spikes in neocortical interneurons (Kawaguchi 1993). It remains unclear why the previously reported voltage-dependent pattern of firing was not observed in the present study, but significant differences in the experimental paradigm like the age of animals, low recording temperatures, and/or the use of whole cell recordings may play a role (Williams et al. 1994).

Interneurons and pyramidal cells displayed inward rectification during hyperpolarizing current pulses. Rectification ratios were similar in all cell types. Our results confirm previous reports of inward rectification in O/A interneurons (Lacaille and Williams 1990), and further extend these observations to PYR interneurons. In a previous study of L-M interneurons, rectification was less pronounced (Williams et al. 1994). However, in the present study, the use of longer-duration and larger-amplitude current pulses clearly indicated that L-M cells display inward rectification similar to that of other cell types. Interneurons and pyramidal cells also displayed anodal break excitation after hyperpolarizing current pulses. In pyramidal cells of adult animals, both the inward rectification and the rebound excitation are thought to be mediated by the inward rectifier current I_Q (Storm 1990). Preliminary reports suggest that some interneurons may also possess this current (Maccaferri and McBain 1995), which may account for the similarity of inward rectification and anodal break excitation between interneurons and pyramidal cells.

In general, the present results confirm with whole cell recordings that CA1 interneurons display membrane properties that are significantly different from pyramidal cells (Kawaguchi and Hama 1988; Lacaille and Schwartzkroin 1988a; Lacaille et al. 1987; Schwartzkroin and Mathers 1978). These results suggest that interneurons display their characteristic nonpyramidal intrinsic properties in young animals (14-22 days postnatally). Our results also show that the properties of interneurons in L-M are not significantly different from those of other interneurons. This is in contrast to findings that L-M cells displayed longer-duration action

potentials and a distinctive voltage-dependent firing pattern different from interneurons in O/A and PYR in slices of adult animals (Kawaguchi and Hama 1988; Lacaille and Schwartzkroin 1988a). Thus in young animals L-M interneurons may have developed their nonpyramidal membrane properties, but they may not yet have expressed their distinctive membrane properties, which differentiate them from other interneurons in adult animals.

Synaptic responses

Stimulation of nearby afferents evoked short-duration EPSPs mediated by non-NMDA and NMDA glutamate receptors, as well as IPSPs mediated by GABA_A receptors, in interneurons and pyramidal cells. No evidence of GABA_B responses was obtained because IPSPs reversed at -72 mV. These results are in contrast with postsynaptic responses previously studied in conventional slices of adult animals, which were largely excitatory in interneurons in O/A (Lacaille et al. 1987) and L-M (Lacaille and Schwartzkroin 1988a), but are similar to the excitatory and inhibitory responses recorded in interneurons in PYR (Lacaille 1991).

Non-NMDA EPSCs

Voltage-clamp techniques and pharmacological antagonists were used to characterize in isolation evoked non-NMDA, NMDA, and GABA_A postsynaptic responses. Non-NMDA EPSCs evoked in interneurons and pyramidal cells demonstrated a linear I-V, as well as similar reversal potential and sensitivity to

CNQX. Our results are consistent with a previous study showing non-NMDA components of EPSCs that were similar in interneurons of str. oriens and in pyramidal cells (Sah et al. 1990). The present results further extend this similarity of non-NMDA EPSCs to interneurons in L-M and near PYR. In the previous study (Sah et al. 1990), the time course of the non-NMDA EPSCs was generally faster than in the present study. The similarity in time course of non-NMDA EPSCs evoked in interneurons and pyramidal cells in the present study is also in contrast to the more rapid kinetics of spontaneous EPSCs in interneurons compared with pyramidal cells of the CA3 region (McBain and Dingledine 1993) and of the visual cortex (Hestrin 1993), and to the faster rise time and decay time constant of non-NMDA EPSCs in aspiny interneurons in comparison with mossy cells of the hilus (Livsey and Vicini 1992). The similarity in time course of non-NMDA EPSCs between CA1 interneurons and pyramidal cells may reflect regional and cellular differences, or discrepancies between evoked and spontaneous synaptic events (e.g., asynchronous release and postsynaptic summation of a large number of homo- and heterogenous individual events). Dendritic filtering could have also influenced the rise time and decay of synaptic responses in the present study. However, intracellular solutions containing cesium and QX-314 were used to minimize this filtering; in addition, rise time and decay of non-NMDA EPSCs were positively but not significantly correlated.

NMDA EPSCs

NMDA-mediated EPSCs were characterized in CNQX and BIC. With no added glycine and in the presence of extracellular Mg^{2+} , large outward NMDA EPSCs were evoked at positive membrane potentials (50 mV). Except for their slower time course in O/A interneurons, NMDA EPSCs were generally similar in interneurons and pyramidal cells. In all cells, I-V relation of NMDA EPSCs demonstrated a region of negative slope at membrane potentials between -80 and -20 mV, and was linear at membrane potentials more positive than -20 mV. NMDA EPSCs were antagonized by AP5 in all cell types. At depolarized membrane potentials (50 mV), the rise time of NMDA EPSCs was significantly slower in interneurons of O/A (31.6 ms) than in other types of cells (8.6 ms), whereas the decay was similar in all cell types. The present results are in agreement with previous findings of NMDA EPSCs with a slower rise time in O/A interneurons than in L-M interneurons or pyramidal cells (Perouansky and Yaari 1993). Our results further suggest that the slower rise time may be a property limited to NMDA EPSCs of O/A interneurons, because interneurons near PYR showed NMDA EPSCs with faster rise time. The cause of this difference remains unknown, but two mechanisms have been proposed to account for the slower rise time of NMDA EPSCs: diffusion of transmitter to neighboring synaptic or extrasynaptic NMDA receptors, or slower activation kinetics of NMDA channels in O/A interneurons (Perouansky and Yaari 1993). It is also possible that the slower rise time may be due to a different electrotonic location of NMDA synapses on O/A cells, compared with other cell

types. In such a case, however, the decay would also be expected to be slower, which was not the case in our experiments.

Thus these results suggest that synaptic excitation in pyramidal cells and in various subtypes of interneurons involves generally similar non-NMDA and NMDA mechanisms. However, the unique time course of NMDA EPSCs in interneurons in O/A may suggest some heterogeneous NMDA synaptic mechanism in this subtype of interneurons. It is interesting that parvalbumin-positive interneurons located in stratum oriens are lost after kainate seizures (Best et al. 1993). Thus it is possible that the presence of distinct NMDA mechanisms in interneurons of str. oriens may play a role in their selective vulnerability to excitotoxic insults.

GABA_A IPSCs

GABA_A IPSCs were pharmacologically isolated during application of AP5 and CNQX. They were antagonized by BIC and displayed similar properties in all cell types. I-V relations of GABA_A IPSCs were linear and the mean reversal potential was -32 mV. The reversal potential of GABA_A IPSPs recorded in current clamp was -72 mV in interneurons and pyramidal cells. A similar value was reported for GABA_A IPSPs in L-M cells (Williams et al. 1994). The shift in a depolarized direction of the reversal potential for GABA_A IPSCs in our voltage-clamp experiments may have been caused by the inclusion of QX-314 (bromide salt) in the intracellular solution and the contribution of Br⁻ permeability through Cl⁻ channels (Hille 1992). Thus, in normal physiological conditions, the reversal potential of GABA_A synaptic responses may be more negative than resting membrane potential

and GABA_A IPSCs may be outward. For all cells, the rise time and decay of GABA_A IPSCs were not different between interneurons and pyramidal cells. The rise time of GABA_A IPSCs (5.0-7.5 ms) was not voltage dependent in the membrane potential range of -60 and 50 mV. Decay time constants of GABA_A IPSCs, however, were sensitive to membrane potential. In all cell types, the decay of GABA_A IPSCs was twofold slower at 50 mV (130-180 ms) than at -60 mV (60-85 ms). Our results of similar GABA_A IPSCs in pyramidal cells and interneurons are somewhat in contrast with previous reports with intracellular recordings in conventional slices. In the latter studies, synaptic responses were predominantly excitatory in interneurons in O/A (Lacaille et al. 1987), PYR (Schwartzkroin and Mathers 1978) and L-M (Lacaille and Schwartzkroin 1988a) but consisted of excitatory and longer inhibitory components in pyramidal cells (Alger and Nicoll 1982). Prominent IPSPs, similar to pyramidal cells responses, have been reported, however, in interneurons in PYR (Lacaille 1991). The present results further confirm the presence of significant GABA_A synaptic responses in interneuron subtypes. The similar time course of GABA_A IPSCs in interneurons and pyramidal cells in the CA1 region was in contrast with the faster decay of spontaneous IPSCs in granule cells compared to hilar neurons in the dentate gyrus (Soltesz and Mody 1994). The similarity of evoked IPSCs in the present experiments may also be due to regional and cellular differences, or to intrinsic differences between evoked and spontaneous synaptic responses (e.g., asynchronous release and postsynaptic summation of a large number of individual homo- or heterogenous events). However, as seen in the present study with the decay of GABA_A IPSCs, the decay of spontaneous IPSCs was voltage dependent in granule

cells (Otis and Mody 1992; Soltesz and Mody 1994). Voltage-dependent decay of GABA_A IPSCs has also been previously reported in CA1 pyramidal cells (Collingridge 1984; Pearce 1993). Although GABA_A receptors display voltage-dependent desensitization (Frosch et al. 1992; Oh and Dichter 1992; Yoon 1994), it is unclear whether such a mechanism is involved in the voltage-dependent decay of GABA_A IPSCs. *In situ* hybridization studies have revealed the presence of diverse GABA_A receptors subunits in the hippocampus (Wisden et al. 1992). Furthermore, the distribution of the $\alpha 1$ subunit of GABA_A receptors may be heterogeneous among subpopulations of hippocampal interneurons (Gao and Fritschy 1994). Although pyramidal cells of the CA1-CA3 region expressed $\alpha 2$, $\beta 3$ and $\gamma 2$ GABA_A subunits, the $\alpha 1$ subunit was mostly observed in interneurons of the str. oriens and pyramidale. Our results suggest that even though the occurrence of $\alpha 1$ subunit may be heterogeneously expressed in interneurons, this difference is not reflected in the time course or voltage sensitivity of GABA_A IPSCs evoked in different interneuron subtypes or pyramidal cells.

Functional implications

The present results suggest that in young rats, different subtypes of interneurons located in O/A, near PYR, and in L-M display membrane properties that are distinguishable from those of pyramidal cells: short-duration and smaller-amplitude action potentials, higher cell input resistance, faster membrane time constant, prominent *f*AHPs and *m*AHPs, and sustained firing during depolarizing

current pulses. Two important points arise from these results. First, these properties in general agree well with the properties of interneurons in str. oriens and PYR, which have been described as fast-spiking cells in conventional slices (Kawaguchi and Hama 1987; Lacaille et al. 1987; Schwartzkroin and Mathers 1978). Second, however, the properties of stellate cells in L-M in slices of young rats were not different from other subtypes of interneurons, which is in contrast to what has been reported in conventional recordings from mature rats (Kawaguchi and Hama 1987; Lacaille and Schwartzkroin 1988a). The homogeneous properties of interneurons in L-M are unlikely to result from the utilization of whole cell recording techniques, because the properties of fast-spiking cells in whole cell recordings were generally similar to those obtained with intracellular recordings, when taking into account known differences arising from whole cell recordings (Staley et al. 1992; Spruston and Johnston 1992). These homogeneous properties may be due, however, to the difference in age of the animals studied (young vs adult). Thus the maturation of membrane properties may differ between interneurons: in young animals, interneurons in O/A, PYR and L-M may express distinct nonpyramidal cell properties (i.e. fast spiking cells), but later during development the properties of interneurons in L-M may further change so that, in adult animals, their properties differ from those of fast-spiking cells (Kawaguchi and Hama 1987; Lacaille and Schwartzkroin 1988a). Therefore the maturation of inhibitory circuits may be achieved to a large degree in young rats, but it may not be fully completed until a later age.

In contrast to their membrane properties, distinctly different from pyramidal cells, the interneuron subtypes examined generally displayed non-NMDA, NMDA,

and GABA_A postsynaptic currents that were similar to those of pyramidal cells, except for NMDA EPSC rise times, which were slower in O/A interneurons. Although stimulating electrodes were similarly positioned near the soma of respective interneurons and the synaptic responses consisted of a large population of individual synapses, the electrotonic locations of the stimulated synapses were not known and could have differed between cell types. Thus more discrete stimulation procedures that could selectively activate subsets of afferents fibers may uncover some more subtle differences in synaptic responses. Nonetheless, the similarity of synaptic currents and the differences in intrinsic membrane properties between principal and nonprincipal cells suggest that interneurons may integrate synaptic information differently than pyramidal cells. Globally, their intrinsic properties endow interneurons with a capacity to respond to identical synaptic currents with greater and faster potential differences, subject to less temporal and more spatial integration, and to generate sustained and more rapid trains of spikes in response to excitatory inputs than pyramidal cells. Indeed, EPSPs recorded simultaneously in interneurons and pyramidal cells displayed a faster rise time, as well as a larger amplitude, in interneurons (Lacaille and Schwartzkroin 1988b; Lacaille et al. 1987).

Finally, the similarity between non-NMDA, NMDA, and GABA_A postsynaptic currents in interneurons in O/A and in L-M is in contrast to the heterogeneous capacity of their EPSCs to undergo long-term potentiation (Ouardouz and Lacaille 1995). Thus differences in non-NMDA and GABA_A synaptic currents are unlikely to underlie the differential sensitivity of their EPSCs to show long-term potentiation. Similarly, the slower kinetics of NMDA currents in interneurons of str.

oriens may not be a critical factor in producing long-term potentiation, because similar NMDA EPSCs with fast rise times were observed in both L-M and pyramidal cells, and only pyramidal cells showed robust long-term potentiation at their excitatory synapses (Ouardouz and Lacaille 1995). Thus factors other than differences in non-NMDA, NMDA, and GABA_A postsynaptic currents may underlie the heterogenous expression of long-term potentiation in interneurons.

Acknowledgements

This research was supported by operating grants from the Medical Research Council of Canada (MRCC) to J.-C. Lacaille (MT-10848) and C. Beaulieu (MT-11368), a Research Center grant from the Fonds pour la Formation de Chercheurs et l'Aide à la Recherche (FCAR) to the Groupe de Recherche sur le Système Nerveux Central, and an Équipe de Recherche grant from the FCAR to J.-C. Lacaille. J.-C. Lacaille is a Senior Scholar of the Fonds de la Recherche en Santé du Québec (FRSQ) and C. Beaulieu is a MRCC Scholar. F. Morin was supported by a studentship from the Savoy Foundation.

BIBLIOGRAPHY

- Alger, B.E. and Nicoll, R.A. Feed-forward dendritic inhibition in rat hippocampal pyramidal cells studied in vitro. *J. Physiol. (Lond.)* 328: 105-123, 1982.
- Amaral, D.G A golgi study of cell types in the hilar region of the hippocampus in the rat. *J. Comp. Neurol.* 182: 851-914, 1978.
- Babb, T.L., Pretorius, J.K., Kupfer, W.R. and Brown, W.J. Distribution of glutamate-decarboxylase-immunoreactive neurons and synapses in the rat and monkey hippocampus: light and electron microscopy. *J. Comp. Neurol.* 278:121-138, 1988.
- Best, N., Mitchell, J., Baimbridge, K.G., and Wheal, H.V. Changes in parvalbumin-immunoreactive neurons in the rat hippocampus following a kainic acid lesion. *Neurosci. Lett.* 155: 1-6, 1993.
- Buhl, E.H., Halasy, K. and Somogyi, P. Diverse sources of hippocampal unitary inhibitory postsynaptic potentials and the number of synaptic release sites. *Nature* 368:823-828, 1994a.
- Buhl, E.H., Han, Z.-S., Lorinczi, Z., Stezhka, V.V., Karnup, S.V., and Somogyi, P. Physiological properties of anatomically identified axo-axonic cells in the rat hippocampus. *J. Neurophysiol.* 71:1289-1307, 1994b.
- Collingridge, G.L. Inhibitory post-synaptic currents in rat hippocampal CA1 neurons. *J. Physiol. (Lond.)* 356: 551-564, 1984.

- Edwards, F.A., Konnerth, A., Sakmann, B., and Takahashi, T. A thin slice preparation for patch clamp recordings from neurones of the mammalian nervous system. *Pfluegers Arch.* 414:600-612, 1989.
- Frosch, M.P., Lipton, S.A. and Dichter, M.A. Desensitization of GABA-activated currents and channels in cultured cortical neurons. *J. Neurosci.* 12:3042-3053, 1992.
- Gao, B. and Fritschy, J.M. Selective allocation of GABA_A receptors containing the α1 subunit to neurochemically distinct subpopulations of rat hippocampal interneurons. *Eur. J. Neurosci.* 6:837-853, 1994.
- Gulyas, A.I., Gorcs, T.J. and Freund, T.F. Innervation of different peptide-containing neurons in the hippocampus by GABAergic septal afferents. *Neuroscience* 37:31-44, 1991.
- Hamill, O.P., Huguenard, J.R. and Prince, D.A. Patch-clamp studies of voltage-gated currents in identified neurons of the rat cerebral cortex. *Cereb Cortex* 1:48-61, 1991.
- Hamill, O.P., Marty, A., Neher, E., Sakmann, B., and Sigworth, F.J. Improved patch-clamp techniques for high resolution current recording from cells and cell-free membrane patches. *Pfluegers Arch.* 391:85-100, 1981.
- Hestrin, S., Nicoll, R.A., Perkel, D.J. and Sah, P. Analysis of excitatory synaptic action in pyramidal cells using whole-cell recording from rat hippocampal slices. *J. Physiol. (Lond.)* 422:203-225, 1990.

- Hestrin, S. Different glutamate receptor channels mediate fast excitatory synaptic currents in inhibitory and excitatory cortical neurons. *Neuron* 11: 1083-1091, 1993.
- Hille, B. *Ionic Channels of Excitable Membranes*. Sunderland, MA: Sinauer, 1992.
- Kawaguchi, Y. and Hama, K. Two subtypes of non-pyramidal cells in rat hippocampal formation identified by intracellular recording and HRP injection. *Brain Res.* 411:190-195, 1987.
- Kawaguchi, Y. and Hama, K. Physiological heterogeneity of nonpyramidal cells in rat hippocampal CA1 region. *Exp. Brain Res.* 72:494-502, 1988.
- Kawaguchi, Y. Groupings of nonpyramidal and pyramidal cells with specific physiological and morphological characteristics in rat frontal cortex. *J. Neurophysiol.* 69: 416-431, 1993.
- Keller, B.U., Konnerth, A. and Yaari, Y. Patch clamp analysis of excitatory synaptic currents in granule cells of rat hippocampus. *J. Physiol. (Lond.)* 435:275-293, 1991.
- Knowles, W.D. and Schwartzkroin, P.A. Local circuit synaptic interactions in hippocampal brain slices. *J. Neurosci.* 1:318-322, 1981.
- Konnerth, A., Keller, B.U., Ballanyi, K. and Yaari, Y. Voltage sensitivity of NMDA-receptor mediated postsynaptic currents. *Exp. Brain Res.* 81:209-212, 1990.
- Lacaille, J.-C. Postsynaptic potentials mediated by excitatory and inhibitory amino acids in interneurons of stratum pyramidale of the CA1 region of rat hippocampal slices in vitro. *J. Neurophysiol.* 66:1441-1454, 1991.

- Lacaille, J.-C., Kunkel, D.D. and Schwartzkroin, P.A. Electrophysiological and morphological characterization of hippocampal interneurons. In: *The Hippocampus- New Vistas*, edited by V. Chan-Palay and C. Kohler. New York: Liss, 1989, p.287-305.
- Lacaille, J.-C., Mueller, A.L., Kunkel, D.D. and Schwartzkroin, P.A. Local circuit interactions between oriens-alveus interneurons and CA1 pyramidal cells in hippocampal slices: electrophysiology and morphology. *J. Neurosci.* 7:1979-1993, 1987.
- Lacaille, J.-C. and Schwartzkroin, P.A. Stratum lacunosum-moleculare interneurons of hippocampal CA1 region. I. Intracellular response characteristics, synaptic responses, and morphology. *J. Neurosci.* 8:1400-1410, 1988a.
- Lacaille, J.-C. and Schwartzkroin, P.A. Stratum lacunosum-moleculare interneurons of hippocampal CA1 region. II. Intrasomatic and intradendritic recordings of local circuit synaptic interactions. *J. Neurosci.* 8:1411-1424, 1988b.
- Lacaille, J.-C. and Williams, S. Membrane properties of interneurons in stratum oriens-alveus of the CA1 region of rat hippocampus in vitro. *Neuroscience* 36:349-359, 1990.
- Lambert, N.A. and Wilson, W.A. Heterogeneity in presynaptic regulation of GABA release from hippocampal inhibitory neurons. *Neuron* 11:1057-1067, 1993.
- Livsey, C.T. and Vicini, S. Slower spontaneous excitatory postsynaptic currents in spiny versus aspiny hilar neurons. *Neuron* 8:745-755, 1992.
- Llewellyn-Smith, I.J., Pilowsky, P. and Minson, J.B. The tungstate-stabilized tetramethylbenzidine reaction for light and electron microscopic

- immunocytochemistry and for revealing biocytin-filled neurons. *J. Neurosci. Meth.* 46:27-40, 1993.
- Lorento De No, R. Studies of the structure of the cerebral cortex. II. Continuation of the study of the ammonic system. *J. Psychol. Neurol. Lpz.* 46:113-177, 1934.
- Maccaferri, G. and McBain, C. J. Hyperpolarization-activated current (I_h) in rat hippocampal st. oriens-alveus inhibitory neurons. *Soc. Neurosci. Abstr.* 21: 62, 1995.
- McBain, C.J. and Dingledine, R. Heterogeneity of synaptic glutamate receptors on CA3 stratum radiatum interneurones of rat hippocampus. *J. Physiol. (Lond.)* 462:373-392, 1993.
- McBain, C.J., Dichiara, T.J. and Kauer, J.A. Activation of metabotropic glutamate receptors differentially affects two classes of hippocampal interneurons and potentiates excitatory synaptic transmission. *J. Neurosci.* 14:4433-4445, 1994.
- Misgeld, U. and Frotscher, M. Postsynaptic GABAergic inhibition of non-pyramidal neurons in the guinea pig hippocampus. *Neuroscience* 19:193-206, 1986.
- Morin, F., Beaulieu, C., and Lacaille, J.-C. Membrane properties of interneuron subtypes and pyramidal cells using whole cell recordings in rat hippocampal slices. *Canad. Physiol. Society* 25: 121, 1995.
- Nathan, T., Jensen, M.S., and Lambert, J.D.C. The slow inhibitory postsynaptic potential in rat hippocampal CA1 neurones is blocked by intracellular injection of QX-314. *Neurosci. Lett.* 110:309-313, 1990.
- Oh, D.J. and Dichter, M.A. Desensitization of GABA-induced currents in cultured rat hippocampal neurons, *Neuroscience* 49:571-576, 1992.

- Otis, T.S. and Mody, I. Modulation of decay kinetics and frequency of GABA_A receptor-mediated spontaneous inhibitory postsynaptic currents in hippocampal neurons, *Neuroscience* 49: 13-32, 1992.
- Ouardouz, M. and Lacaille, J.-C. Mechanisms of selective long-term potentiation of excitatory synapses in stratum oriens/alveus interneurons of rat hippocampal slices. *J. Neurophysiol.* 73: 810-819, 1995.
- Pearce, R.A. Physiological evidence of two distinct GABA_A responses in rat hippocampus. *Neuron* 10:189-200, 1993.
- Perouansky, M. and Yaari, Y. Kinetic properties of NMDA receptor-mediated synaptic currents in rat hippocampal pyramidal cells versus interneurons. *J. Physiol. (Lond.)* 465:223-244, 1993.
- Ramon Y Cajal, S. *Histologie du Système Nerveux de l'Homme et des Vertébrés*. Paris: Maloine, 1911.
- Ribak, C.E., Vaughn, J.E. and Saito, K. Immunocytochemical localization of glutamic acid decarboxylase in neuronal somata following colchicine inhibition of axonal transport. *Brain Res.* 140:315-332, 1978.
- Sah, P., Hestrin, S. and Nicoll, R.A. Properties of excitatory postsynaptic currents recorded in vitro from rat hippocampal interneurons. *J. Physiol. (Lond.)* 430:605-616, 1990.
- Schwartzkroin, P.A. and Kunkel, D.D. Morphology of identified interneurons in the CA1 region of guinea pig hippocampus. *J. Comp. Neurol.* 232:205-218, 1985.

- Schwartzkroin, P.A. and Mathers, L.H. Physiological and morphological identification of a nonpyramidal hippocampal cell type. *Brain Res.* 157:1-10, 1978.
- Schwartzkroin, P.A. and Prince, D.A. Changes in excitatory and inhibitory synaptic potentials leading to epileptogenic activity. *Brain Res.* 183:61-76, 1980.
- Shen, K. and Schwartzkroin, P.A. Effects of temperature alterations on population and cellular activities in hippocampal slices from mature and immature rabbit. *Brain Res.* 475:305-316, 1988.
- Soltesz, I. and Mody, I. Patch-clamp recordings reveal powerful GABAergic inhibition in dentate hilar neurons. *J. Neurosci.* 14:2365-2376, 1994.
- Somogyi, P., Hodgson, A.J., Smith, A.D., Nunzi, M.G., Gorio, A., and Wu, J.-Y. Different populations of GABAergic neurons in the visual cortex and hippocampus of cat contain somatostatin- or cholecystokinin-immunoreactive material. *J. Neurosci.* 4: 2590-2603, 1984.
- Spigelman, I., Zhang, L. and Carlen, P.L. Patch-clamp study of post-natal development of CA1 neurons in rat hippocampal slices: membrane excitability and K^+ currents. *J. Neurophysiol.* 68:55-69, 1992.
- Spruston, N. and Johnson, D. Perforated patch-clamp analysis of the passive membrane properties of three classes of hippocampal neurons. *J. Neurophysiol.* 67: 508-529, 1992.
- Staley, K.J., Otis, T.S. and Mody, I. Membrane properties of dentate gyrus granule cells: comparison of sharp microelectrode and whole-cell recordings. *J. Neurophysiol.* 67: 1346-1358, 1992.

- Storm, J.F. An afterhyperpolarization of medium duration in rat hippocampal pyramidal cells. *J. Physiol. (Lond.)* 409:171-190, 1989.
- Storm, J.F. Potassium currents in hippocampal pyramidal cells. In: *Understanding the Brain Through the Hippocampus*, edited by J. Storm-Mathisen, J. Zimmer, and O. P. Ottersen. New York: Elsevier, 1990, p.161-188.
- Thompson, S.M., Masukawa, L.M. and Prince, D.A. Temperature dependence of intrinsic membrane properties and synaptic potentials in hippocampal CA1 neurons in vitro. *J. Neurosci.* 5:817-824, 1985.
- Traub, R.D., Miles, R. and Wong, R.K.S. Models of synchronized hippocampal bursts in the presence of inhibition. I. Single population events. *J. Neurophysiol.* 58:739-751, 1987.
- Williams, S., Samulack, D.D., Beaulieu, C. and Lacaille, J.-C. Membrane properties and synaptic responses of interneurons located near the stratum lacunosum-moleculare/radiatum border of area CA1 in whole-cell recordings from rat hippocampal slices. *J. Neurophysiol.* 71:2217-2235, 1994.
- Wisden, W., Laurie, D.J., Monyer, H. and Seburg, P.H. The distribution of 13 GABA_A subunit mRNAs in the rat brain. I. Telencephalon, diencephalon, mesencephalon. *J. Neurosci.* 12:1040-1062, 1992.
- Woodson, W.L., Nitecka, L. and Ben-Ari, Y. Organization of the GABAergic system in the rat hippocampal formation: a quantitative immunocytochemical study. *J. Comp. Neurol.* 280:254-271, 1989.

Yoon, K.-W. Voltage-dependent modulation of GABA_A receptor channel desensitization in rat hippocampal neurons. *J. Neurophysiol.* 71:2151-2160, 1994.

Zhang, L. and McBain, C.J. Potassium conductances underlying action potential repolarization and afterhyperpolarization in rat CA1 hippocampal interneurones, *J. Physiol. (Lond.)* 488: 661-672, 1995.

Figure Legends

Figure 1: Camera lucida drawings of biocytin-filled interneurons and pyramidal cells. Representative examples of subtypes of interneurons labeled intracellularly with somata located in stratum (str.) oriens near the alveus (O/A; A), near str. pyramidale (PYR; B) and near the str. lacunosum-moleculare/radiatum border (L-M; C). Arrows point to axonal processes. The morphology was very distinct between each type of interneuron and pyramidal cells (D).

Figure 2: Membrane and firing properties of interneurons (INT: A, C, E) and pyramidal cells (PC: B, D, F). A-B: Single action potentials elicited in an interneuron in L-M (A) and a pyramidal cell (B). The action potential duration (measured at the base) was shorter in the interneuron. Both *f*AHPs (single arrow) and *m*AHPs (double arrows) were larger in amplitude in interneurons. The membrane potential was -52 mV and -45 mV in A and B, respectively. C-D: Responses to current injection. A depolarizing current pulse elicited a regular train of action potentials in interneurons (C). Burst firing followed by a period of accomodation was evoked in the pyramidal cell (D). In both cell types, during large-amplitude hyperpolarizing pulses membrane potential reached an initial peak value (open circles), which was followed by a sag to a steady level (filled squares). E-F: Graph of membrane potential changes, at the peak (open circles) and at the end of the pulse (filled squares), vs current injected, with their respective linear regression, for the cells shown in C and D. In all cell types, with large current injection membrane responses were clearly smaller at the

end of the pulse than at the peak. Cell input resistance was obtained from the slope of the regression lines, at the peak and at the end of the pulse. In both interneurons and pyramidal cells there was a significant reduction in R_{in} at the end of the pulse.

Figure 3: Postsynaptic potentials evoked in interneurons (INT: A-B) and pyramidal cells (PC: C-D) by stimulation of nearby afferent fibers. A: Near resting membrane potential, stimulation with increasing intensities (indicated at left of the traces) elicited an EPSP followed by a longer duration IPSP in an interneuron in L-M. At higher stimulation intensities, EPSPs triggered action potentials. B: In the same interneuron, non-NMDA and NMDA antagonists (20 μ M CNQX and 50 μ M AP5) blocked EPSPs and uncovered IPSPs. C-D: In a pyramidal cell, similar EPSPs and IPSPs were elicited by stimulation of str. radiatum (C), and monosynaptic IPSPs were evoked in the presence of CNQX and AP5.

Figure 4: Pharmacologically isolated non-NMDA EPSCs evoked in interneurons in the presence of AP5 and BIC. A: Averaged non-NMDA EPSCs evoked in a representative L-M interneuron at different membrane potentials (indicated at left of traces). Non-NMDA EPSCs were inward at negative potentials and outward at potentials more positive than 10 mV. B: I-V relation of peak non-NMDA EPSCs for the cell shown in A. A conductance of 4.4 nS was obtained for these non-NMDA EPSCs from the slope of the linear portion of the I-V relationship (line). C: Reversible block of non-NMDA EPSCs by 20 μ M CNQX. Control non-NMDA

EPSCs were evoked at -87 mV in AP5 and BIC (left trace). After the addition of CNQX to the perfusion medium, EPSCs were almost completely blocked (amplitude 95.4% of control). After washout of the antagonist (15-20 min), the EPSC amplitude partially recovered to 27.2% of control.

Figure 5: Decay of non-NMDA EPSCs in interneurons. A: Averaged non-NMDA EPSCs evoked at -87 mV (A) in a representative cell. B: Decay phase of non-NMDA EPSCs was fitted with a single exponential function with time constants of 96.7 ms. C: Graph of decay time constant as a function of rise time of non-NMDA EPSCs evoked at negative membrane potentials (near -80 mV) for different interneuron subtypes (O/A, circle; PYR, square; L-M, triangle).

Figure 6: NMDA EPSCs isolated pharmacologically in 25 μ M BIC and 20 μ M CNQX in a representative O/A interneuron. A: Averaged NMDA EPSCs were outward at positive membrane potentials (37 mV and 55 mV) and inward at 0 and -19 mV. NMDA EPSCs were also inward but almost null at -37 mV. B: Graph of the peak NMDA EPSCs vs membrane potential for the cell shown in A. The I-V relationship of the NMDA EPSC shows a negative slope area between -80 mV and -20 mV. The slope of the linear portion of the I-V relation (filled line) was taken as a measure of NMDA EPSC conductance. C: NMDA EPSCs were blocked by the NMDA antagonist, AP5. NMDA EPSCs evoked at 55 mV (BIC/CNQX, left trace) were reduced by 90.1% with the addition of 50 μ M AP5 (right trace).

Figure 7: Slower rise time of NMDA EPSCs in O/A interneurons. A-B: Averaged NMDA EPSCs in representative interneurons in O/A (A) and PYR (B) evoked at depolarized membrane potentials (indicated at left of trace). Broken lines indicate the onset and peak of NMDA EPSCs. The 10-90% rise time was much slower in the interneuron in O/A (32.0 ms) than in PYR (8.8 ms).

Figure 8: Decay time constant of NMDA EPSCs in a representative O/A interneuron. A: Averaged NMDA EPSCs evoked at 55 mV. B: Decay time constant (137.3 ms) was obtained by fitting the decaying phase of NMDA EPSCs with a single exponential function. C: Graph of decay time constants of NMDA EPSCs in interneurons (O/A, circle; PYR, square; L-M, triangle) plotted against their rise time for responses evoked near 50 mV.

Figure 9: GABA_A IPSCs recorded in an O/A interneuron and isolated in the presence of 20 μ M CNQX and 50 μ M AP5. A: Averaged GABA_A IPSCs were inward at holding potentials of -45 mV and were outward at potentials more positive than -27 mV. B: Graph of the I-V relation of peak GABA_A IPSCs for the cell shown in A. The I-V relationship was mostly linear except at most extreme potentials. GABA_A IPSCs reversed at -38.3 mV in this cell. The conductance of GABA_A IPSCs estimated from the slope of the linear portion of the I-V plot (line), was 6.7 nS in this cell. C: Pharmacological block of GABA_A IPSCs by 25 μ M bicuculline (BIC). Averaged GABA_A IPSCs (left trace, control) were reduced by 89.8% in BIC (middle

trace). IPSC amplitude recovered to 78.7% of control after wash out of BIC (right trace).

Figure 10: Voltage sensitivity of the decay of GABA_A IPSCs in a representative O/A interneuron. A-B: Averaged GABA_A IPSCs, evoked at depolarized (A; 47 mV) and hyperpolarized (B; -63 mV) holding potentials, decayed at different rates. C-D: The decay time constant, obtained by fitting the decaying phase with a single exponential function, was slower at a holding potential of 47 mV (C; 168 ms) than at -63 mV (D; 76 ms). E: Graph of decay time constant of GABA_A IPSCs evoked at depolarized holding potentials plotted against their rise time for O/A (circle), PYR (square) and L-M (triangle) interneurons.

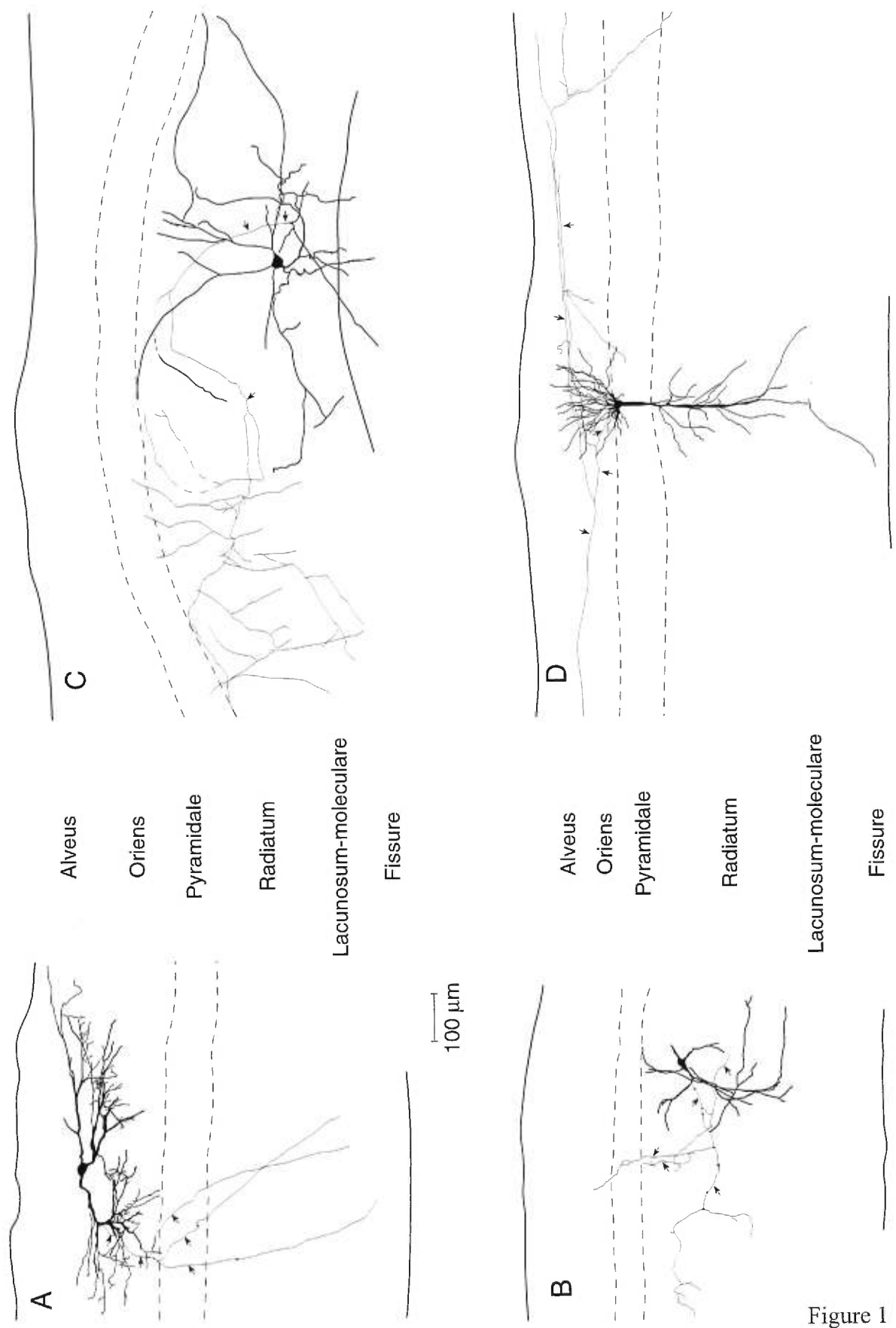


Figure 1

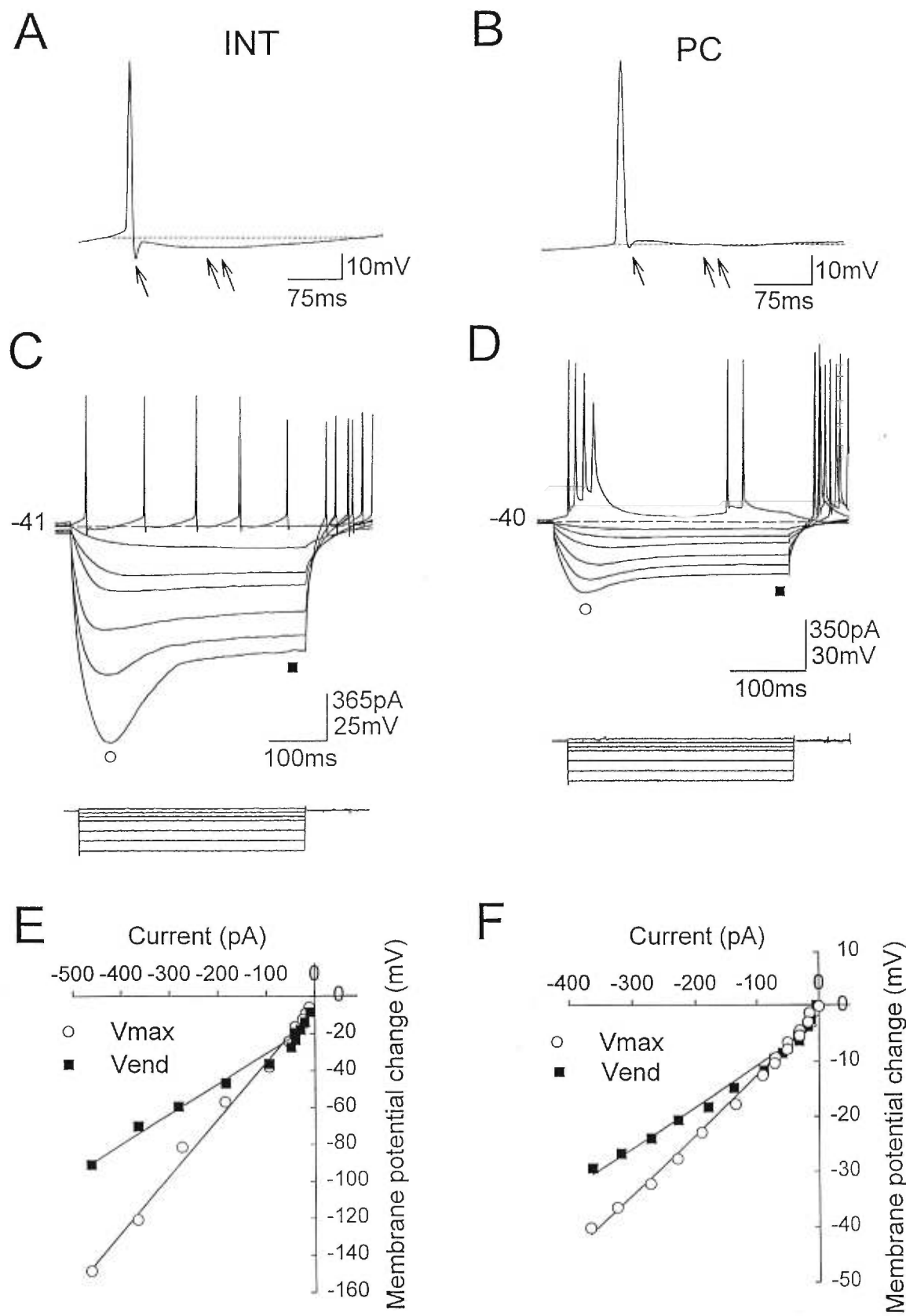


Figure 2

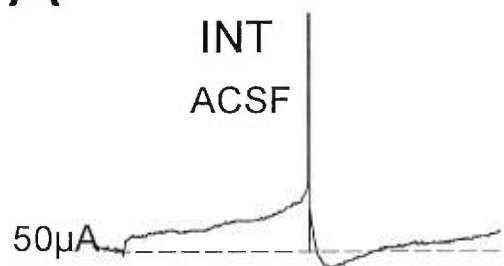
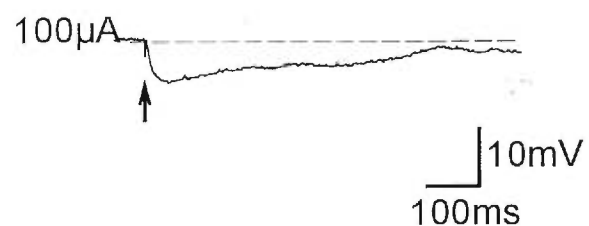
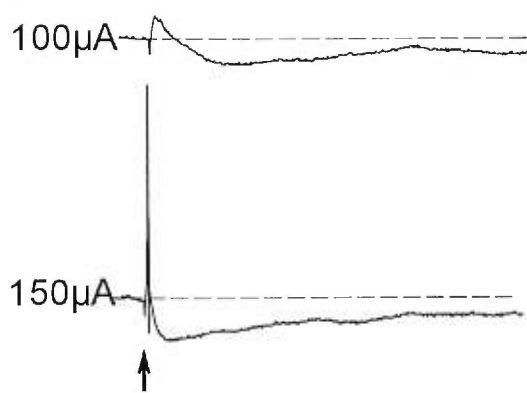
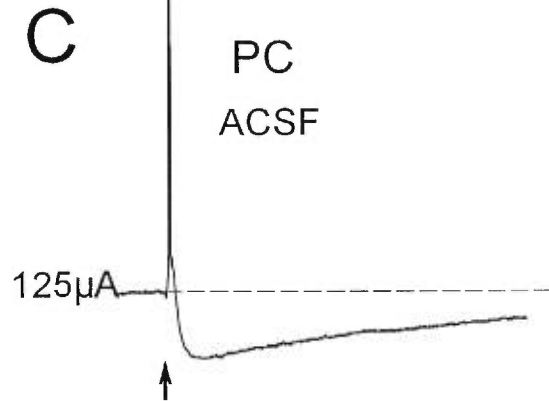
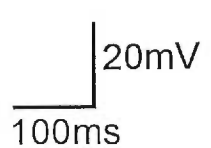
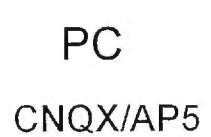
A**B****C****D**

Figure 3

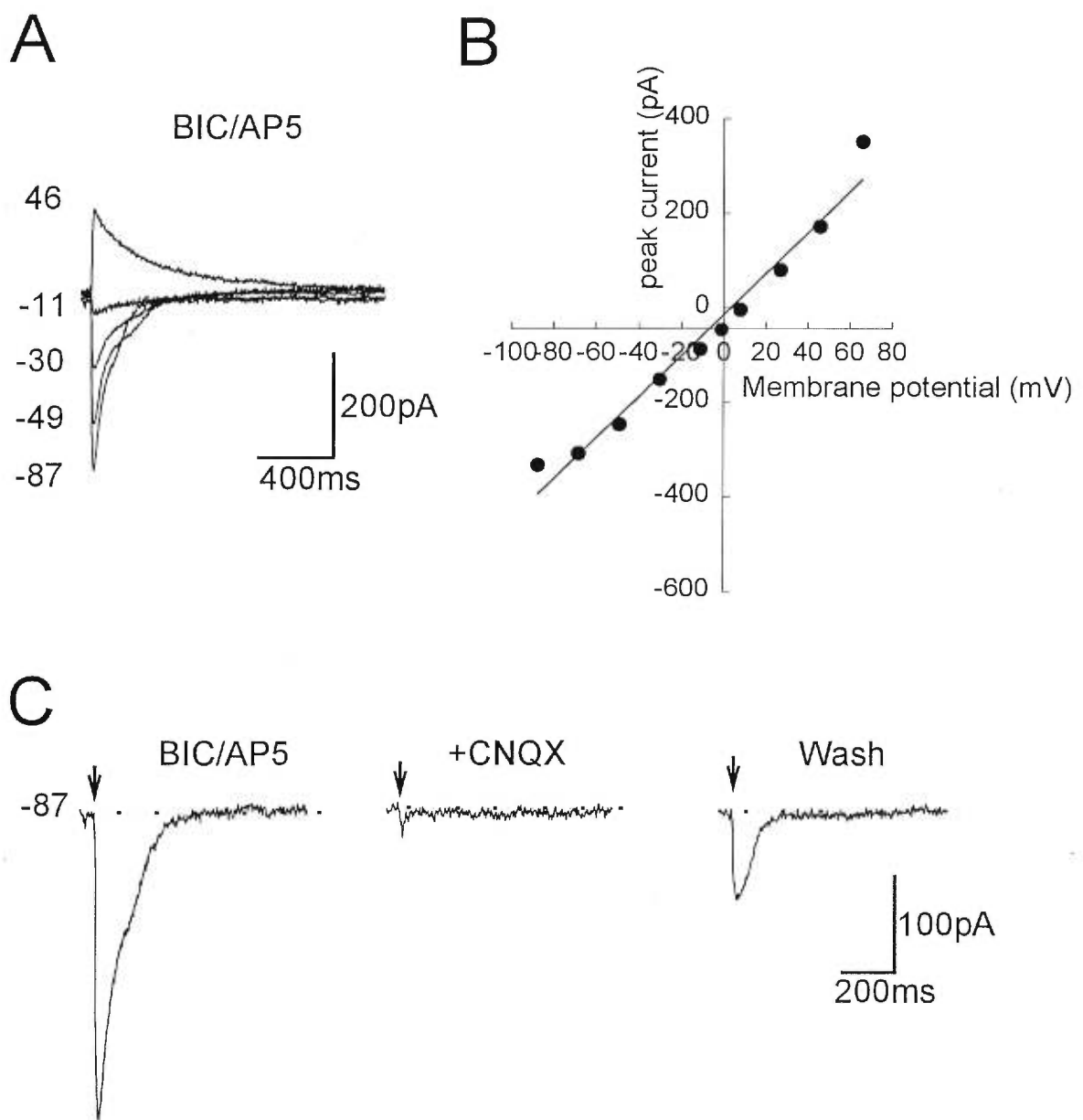


Figure 4

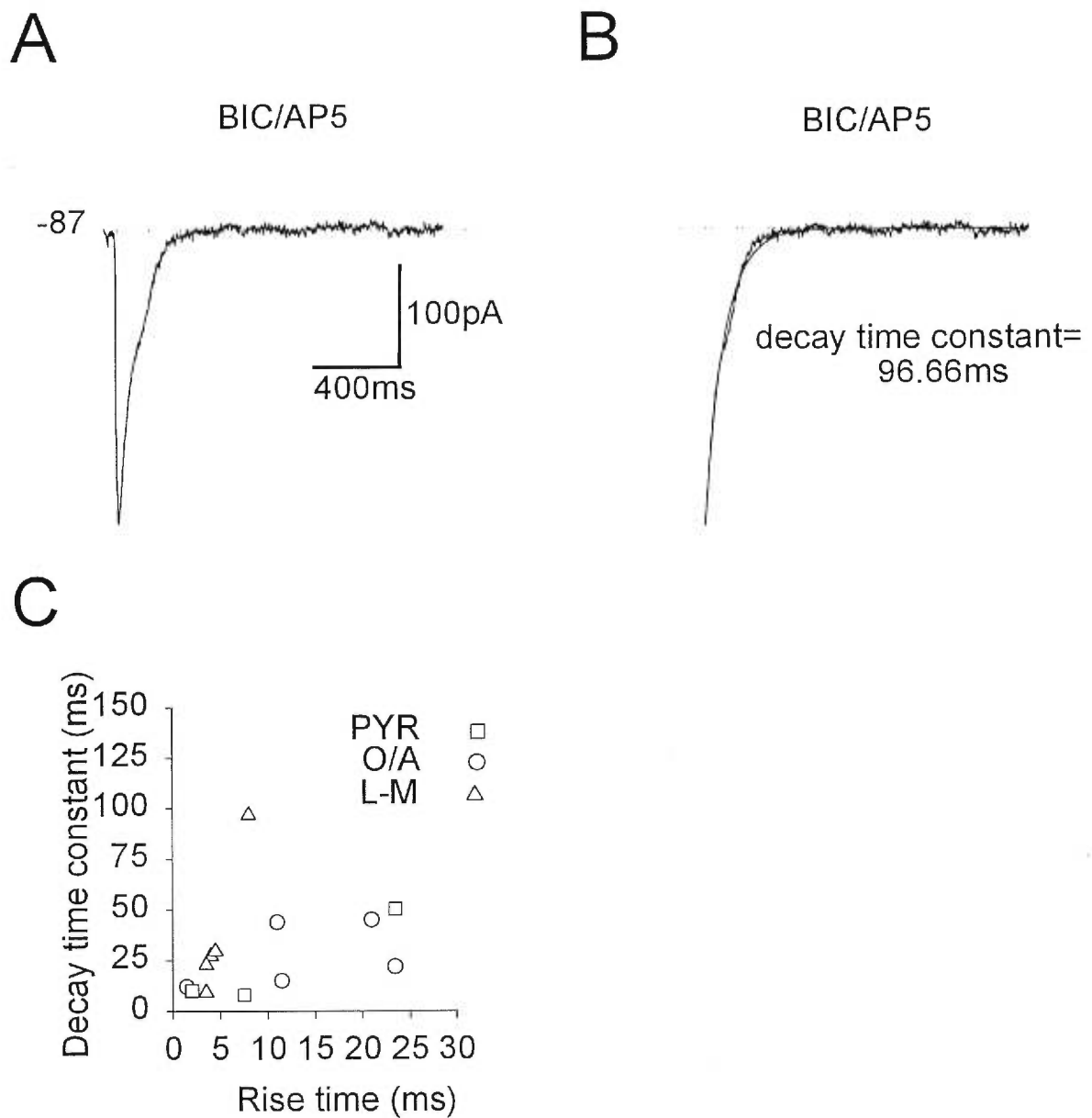


Figure 5

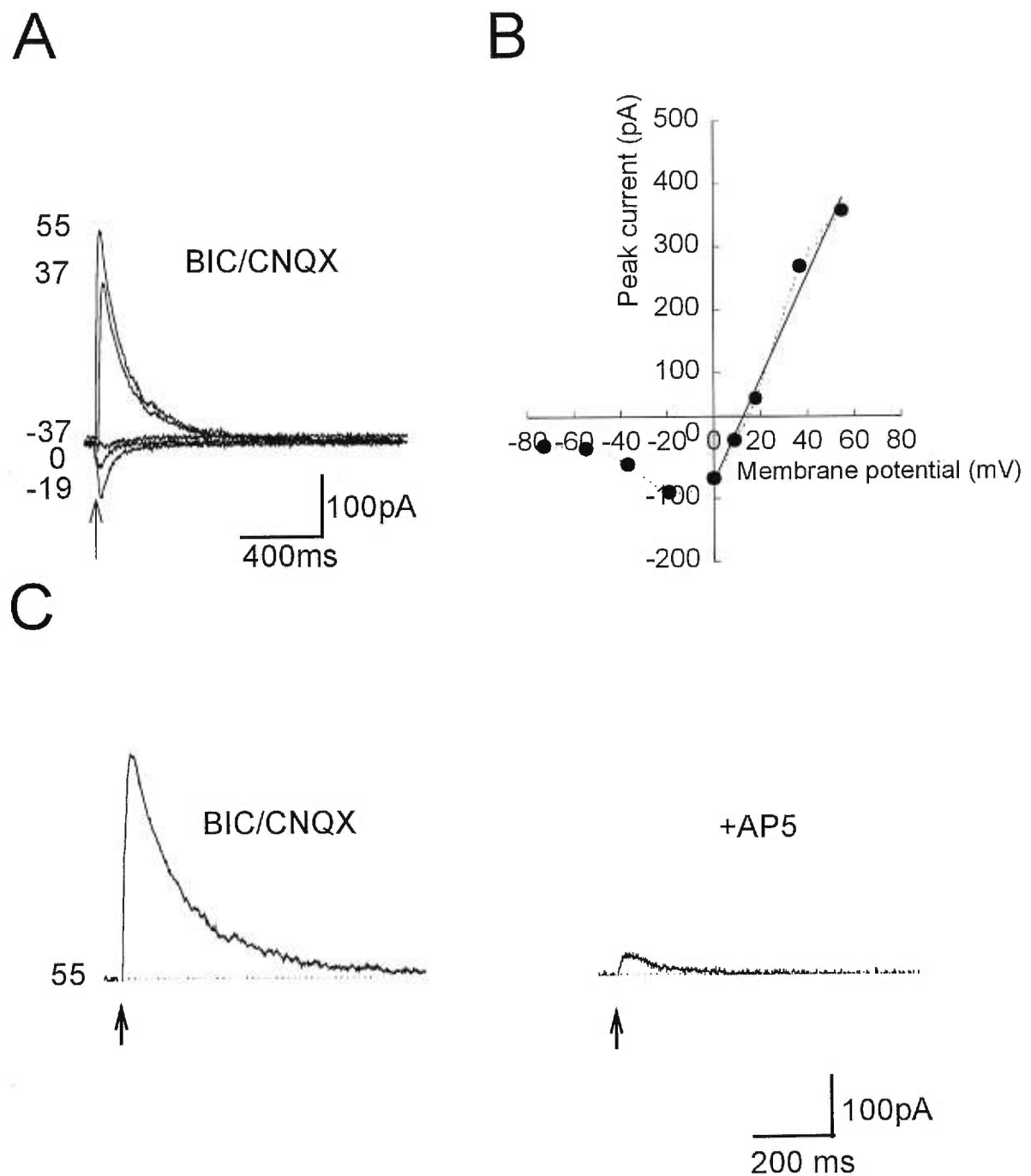


Figure 6

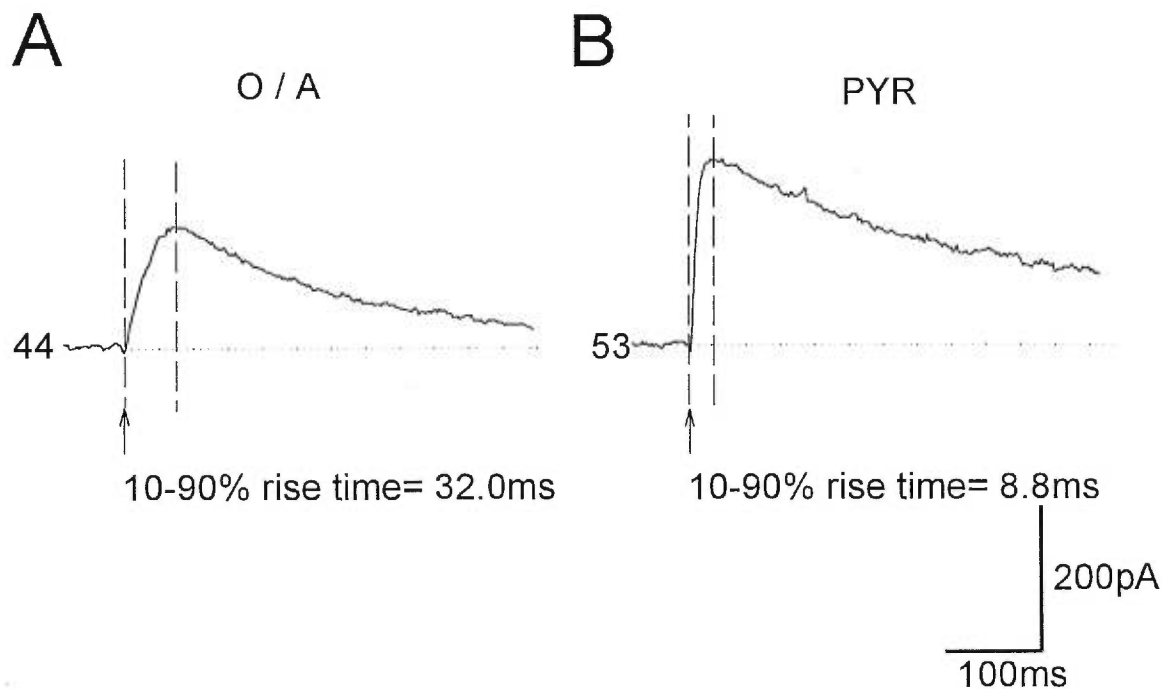


Figure 7

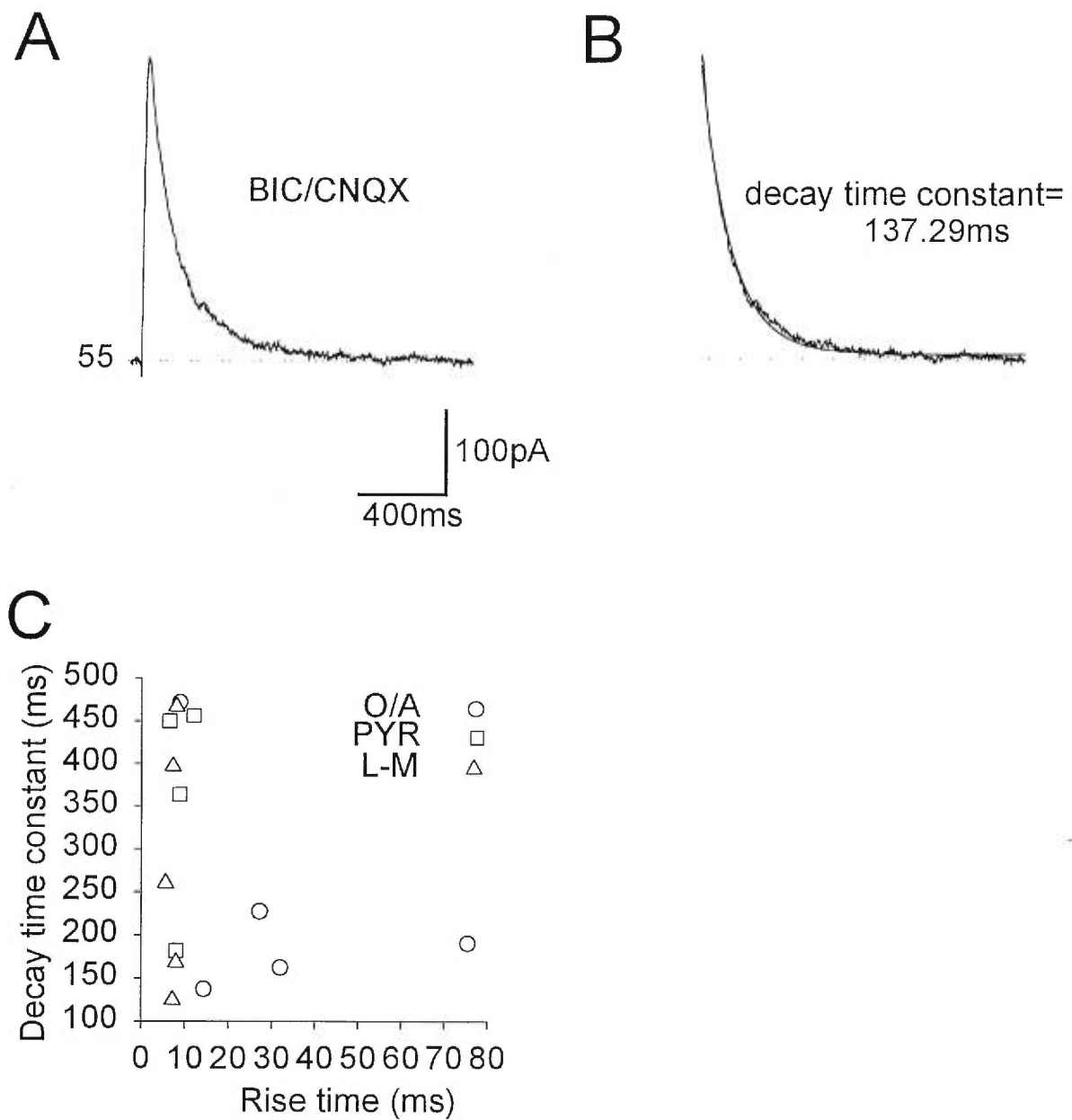


Figure 8

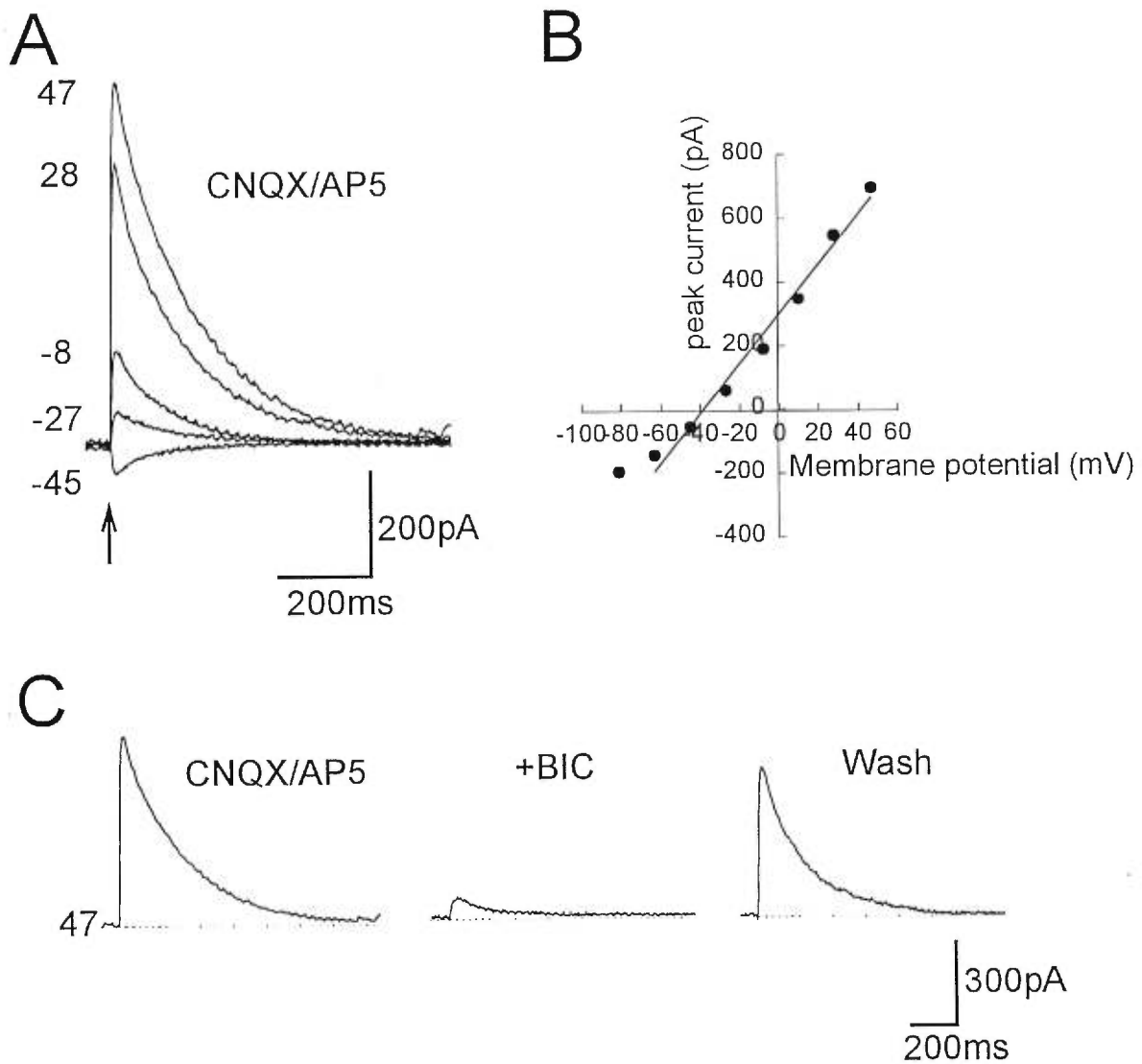


Figure 9

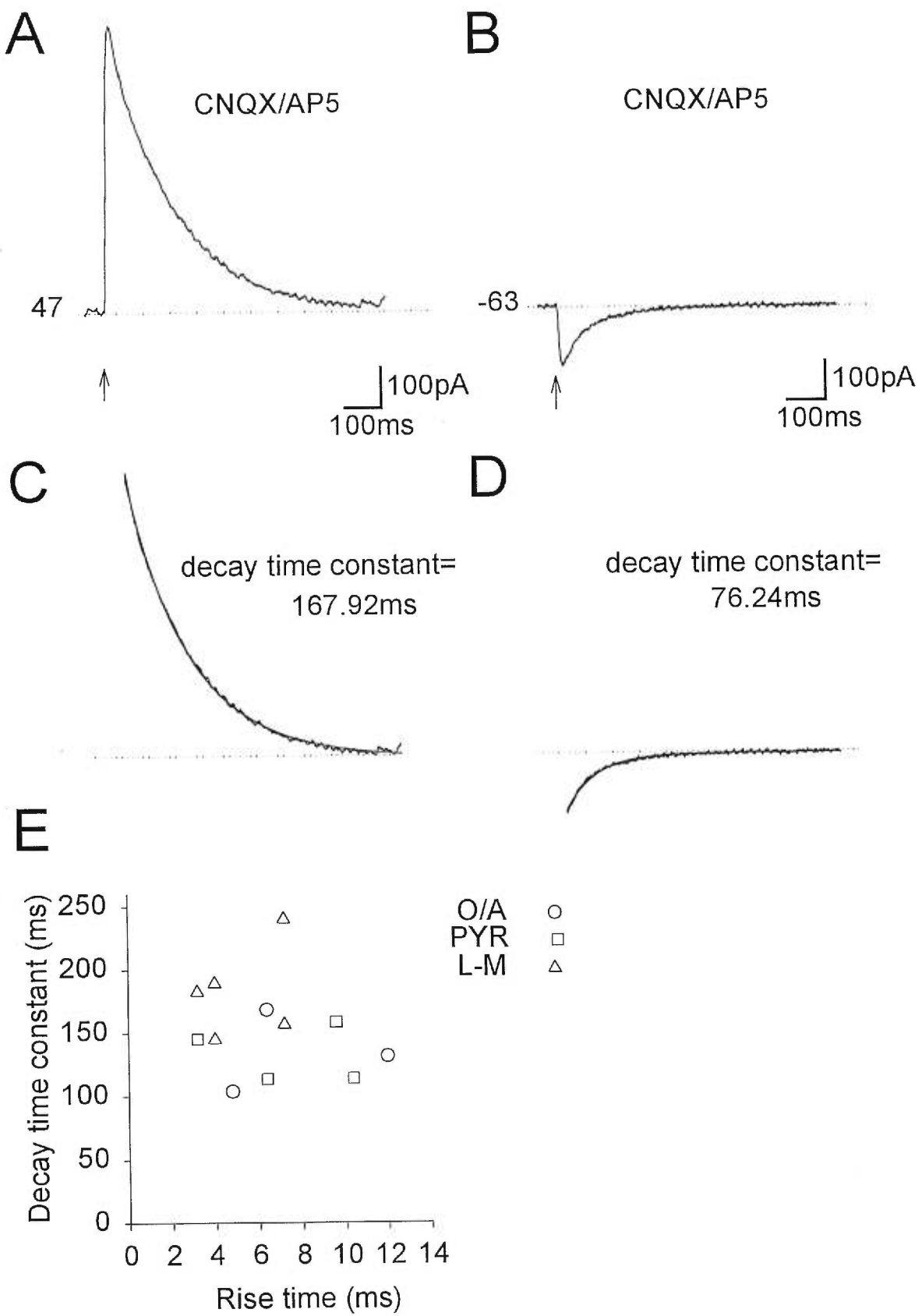


Figure 10

Table 1. Summary table of membrane properties of interneuron subtypes and pyramidal cells (mean±sem).

Cell properties	Interneurons			Pyramidal cells
	O/A (n=5)	PYR (n=5)	L-M (n=5)	(n)
Resting membrane potential (mV)	-51.4±3.9	-55.2±2.9	-55.4±4.6	-48.6±1.7 (9)
Action potential amplitude (mV)	76.5±4.9	85.8±5.5	83.2±3.7	95.4±4.7 (9)*
Action potential duration (ms)	2.1±0.2	1.8±0.1	1.8±0.2	3.0±0.2 (9)*
fAHP amplitude (mV)	-13.7±3.2	-14.8±2.2	-11.0±1.6	-0.1±1.0 (4)*
fAHP latency (ms)	3.0±0.1	2.8±0.3	2.8±0.2	3.6±0.3 (4)*
fAHP recovery (ms)	1.7±0.1	1.6±0.2	1.9±0.2	1.3±0.1 (4)*
mAHP amplitude (mV)	-6.7±1.9	-6.6±1.4	-2.7±0.8	1.1±1.5 (5)*
mAHP latency (ms)	4.9±3.5	2.6±1.3	11.3±1.0 [#]	8.5±3.6 (5)
mAHP recovery (ms)	41.1±10.0	54.6±1.5	34.5±6.1	43.5±11.9 (5)
Time constant (ms)	31.9±9.2	25.5±4.2	29.3±8.0	46.0±5.0 (9)*
R _{in} peak (MΩ)	227.6±54.0	252.0±53.5	228.6±41.3	135.6±12.2 (9)*
R _{in} end (MΩ)	167.6±45.5	194.4±45.5	177.0±38.3	96.7±7.2 (9)*
Rectification ratio	1.4±0.2	1.4±0.1	1.3±0.2	1.4±0.1 (9)
Evoked firing	regular	regular	regular	regular (5/9) burst (4/9)
Polysynaptic EPSPs	4/4	5/5	5/5	8/8
Isolated IPSPs	1/3	3/3	3/5	6/7

* significantly different from interneurons (p<0.05).

[#] significantly different from PYR interneurons (p<0.05).

Table 2. Summary table of properties (mean \pm sem) of pharmacologically isolated synaptic currents in interneuron subtypes and pyramidal cells. N=5 cells unless stated otherwise in parentheses.

Synaptic current	Interneurons			Pyramidal cells
	O/A (n)	PYR (n)	LM (n)	(n)
non-NMDA				
conductance (nS)	5.2 \pm 0.7 (6)	2.8 \pm 0.8	3.8 \pm 0.9 (6)	4.9 \pm 1.7 (6)
E _{rev} (mV)	8.6 \pm 3.9 (6)	-1.2 \pm 3.7	6.5 \pm 3.2 (6)	2.5 \pm 1.2 (6)
rise time (ms) V _m -80 mV	13.2 \pm 3.3 (6)§	7.7 \pm 4.1 §	4.2 \pm 0.9 (6)§	8.4 \pm 1.1 (6)†
decay time constant (ms) V _m -80 mV	27.4 \pm 7.1 §	22.7 \pm 13.7 §	37.1 \pm 15.3 §	32.2 \pm 3.4 (6)†
NMDA				
conductance	5.5 \pm 1.2	4.6 \pm 1.8	5.4 \pm 1.5	5.1 \pm 0.4
E _{rev} (mV)	9.3 \pm 1.9	2.4 \pm 3.8	8.3 \pm 1.2	11.8 \pm 1.7
rise time (ms) V _m 50 mV	31.6 \pm 11.8*§	8.2 \pm 1.1 §	7.2 \pm 0.4 §	10.4 \pm 0.6 †
decay time constant (ms) V _m 50 mV	237.8 \pm 60.4 §	363.0 \pm 63.9 (4)§	283.4 \pm 65.4 §	387.9 \pm 30.0 †
GABA_A				
conductance (nS)	8.3 \pm 3.2	6.3 \pm 2.5	5.4 \pm 1.0	11.3 \pm 2.8
E _{rev} (mV)	-33.0 \pm 2.2	-28.6 \pm 1.6	-34.3 \pm 2.0	-31.1 \pm 1.9
rise time (ms) V _m -60 mV	7.4 \pm 1.3	5.4 \pm 1.7	6.1 \pm 1.0	7.0 \pm 0.7
V _m 50 mV	6.1 \pm 1.6	6.6 \pm 1.5	5.1 \pm 0.9	6.9 \pm 0.9
decay time constant (ms) V _m -60 mV	59.1 \pm 10.9 (4)§	60.4 \pm 6.1 (4)§	83.9 \pm 6.0 §	78.4 \pm 6.8 †
V _m 50 mV	134.1 \pm 18.7 (3)§	132.7 \pm 11.3 (4)§	182.4 \pm 16.5 §	164.5 \pm 9.8 (4)†

*Significantly different from other types of cells (p<0.05).

†Significant difference between values at both membrane potentials (p<0.05).

§Significant difference between pooled interneuron values at both membrane potentials (p<0.001)

CHAPITRE TROISIÈME

**PERTE SÉLECTIVE DES NEURONES GABA DANS LA RÉGION CA1 DE
L'HIPPOCAMPE CHEZ LE RAT APRÈS INJECTION
INTRAVENTRICULAIRE DE L'ACIDE KAÏNIQUE**

**Selective loss of GABA neurons in area CA1 of the rat hippocampus
after intraventricular kainate**

France Morin^{1,2}, Clermont Beaulieu² and Jean-Claude Lacaille*¹

Centre de recherche en sciences neurologiques and Départements de physiologie^{1*} et
de pathologie², Université de Montréal, C.P. 6128, Succursale Centre-ville, Montréal,
Québec, Canada, H3C 3J7.

publié dans

Epilepsy Research, 32: 363-369, 1998.

Abstract

The intraventricular injection of kainic acid (KA) in rats produces a loss of dentate hilar neurons and hippocampal CA3 pyramidal cells, and renders the dentate granule cells and the CA1 pyramidal cells hyperexcitable. We have used immunocytochemical detection of glutamic acid decarboxylase (GAD), a marker of GABA cells, as well as stereological cell counting techniques, to determine whether inhibitory cell loss was present two weeks after KA treatment. In area CA1, we found that the density of GAD-positive cells was reduced by KA, but only in stratum oriens and the alveus. Counts of Nissl-stained neurons were also significantly reduced in this layer. These results demonstrate a loss of GABA cells in the basal dendritic layer of the CA1 region, which may underlie the hyperexcitability of CA1 pyramidal cells following KA treatment.

Key words: Hippocampus, inhibition, interneurons, GABA, temporal lobe epilepsy

Introduction

The kainic acid (KA) model is widely used as an experimental model of human temporal lobe epilepsy because intracerebroventricular injection of KA produces a loss of dentate hilar cells and hippocampal CA3 pyramidal cells similar to that observed in the human epileptic hippocampus [3]. In rats, surviving CA1 pyramidal cells become hyperexcitable [3, 17, 20, 24]. This pyramidal cell hyperexcitability may be due to increased N-methyl-D-aspartate (NMDA) excitatory synaptic transmission [23], and to diminished polysynaptic γ -aminobutyric acid (GABA)-mediated inhibitory synaptic transmission [8, 20, 24]. A selective loss of somatostatin- and parvalbumin-like immunoreactivity has also been seen after KA [4, 5] and in other models of epilepsy [9, 21, 22]. However, immunohistochemical studies have reported that GABAergic inhibitory cells are not lost after KA treatment [6, 8], as well as in human temporal lobe epilepsy [2].

To determine whether GABAergic cells were lost in area CA1 after KA treatment, we counted the number of interneurons immunostained for the GABA synthesizing enzyme, glutamic acid decarboxylase (GAD), in different layers of the CA1 area: (1) in stratum oriens and the alveus (O/A), (2) in stratum pyramidale (PYR) and (3) in strata radiatum and lacunosum-moleculare (R/LM), in control and KA-treated rats. Our results indicate that some GABAergic interneurons located in O/A are vulnerable to KA.

Methods

Three control and six KA-treated animals were used for GAD immunocytochemistry. Adult male Sprague-Dawley rats (150-160 g; Charles River Co.) were administered KA intracerebroventricularly as described previously [8, 20, 24]. All animals showed behavioral evidence of seizures (whisker and facial tremors) during kainic acid injection. Control animals were weight-matched, unoperated rats.

GAD immunostaining

Rats were deeply anesthetized (sodium pentobarbital, 65 mg/kg i.p.) two weeks after KA injections and perfused through the aorta first with phosphate buffered saline (PBS, 0.1 M, pH 7.4) followed by 1.75% glutaraldehyde in 0.1 M phosphate buffer (PB, pH 7.4, 25 min). In addition to providing good tissue preservation, the fixative solution consisting of 1.75% glutaraldehyde in PB yielded a greater intensity of labeled neurons than the fixative solution with 4% paraformaldehyde in PB (with no apparent change in cell number labeled). In addition, it was shown that the immunodetection of many antigenic sites (even of sensitive antigens) was possible after a fixation with 3.5% glutaraldehyde [16]. A tissue block containing the hippocampus was trimmed, and transverse sections were cut along the septo-temporal axis on a Vibratome. For each animal, starting at the level of the hippocampus proper (with CA3-CA1 areas clearly delimited), three series of 15 consecutive sections (60 μ m-thick) were taken at 100 μ m intervals, and were processed for GAD immunocytochemistry [15]. Sections were first rinsed in PB (4x5 min) and treated with 1% sodium borohydride in PB (15 min). Sections were washed in PB (1 hr), PBS (4x5 min) and incubated for 30 min in 10% normal goat serum

(NGS, Vector Labs) in PBS. Following rinses in 1% NGS-PBS, sections were then incubated in a rabbit polyclonal antiserum against glutamic acid decarboxylase (GAD; Chemicon AB108), 1:500, 24-48 hrs at 4° C, in 1% NGS-PBS. This antiserum recognizes the GAD67 enzyme [10] and has been shown to label optimally cell bodies of GABA neurons [7]. Sections were rinsed in PBS (4x5 min) and incubated in biotinylated goat anti-rabbit IgGs (1:1000, 4 hours, Vector Labs) in 1% NGS-PBS. Sections were washed in PBS and incubated in the avidin-biotin complex (1:250, 2 hours, ABC kit Vectastain Elite; Vector Labs) in PBS. After washes in PBS (4x5 min) and Tris buffer (0.05 M, pH 7.6, 2x5 min), the reaction product was visualized by adding 0.001% H₂O₂ to a solution containing 0.05% 3'3'-diaminobenzidine tetrahydrochloride (Sigma), 0.2% nickel-ammonium sulphate (Sigma) and 0.1 M imidazole (Sigma) in Tris buffer. Sections were thoroughly rinsed in Tris buffer and mounted for light microscopy. Tissue sections from control rats were processed for GAD immunostaining simultaneously with tissue sections from kainate-treated rats.

Quantification of GAD-immunopositive cells

The numerical density (neurons per mm³ of tissue, N_V) of GAD-immunopositive cells was estimated using the formula, $N_V = N_A / (t \cdot D)$, where N_A is the number of neurons per mm² of tissue, t is the section thickness, and D is the neuron diameter [1]. For each control (n=3) and KA-treated (n=6) animal, 20 sections were sampled at the same regular intervals from the original set of 45 sections, and drawn using a camera lucida (final magnification of 40X). The

boundaries of area CA1 were determined according to Paxinos and Watson [19], and GAD-positive cells were counted in all 20 sections (final magnification of 400X). GAD-positive cells were considered to be within stratum pyramidale when the soma was located within 20 μm of the principal cell layer. Mean diameter of cells in O/A, PYR and R/LM was obtained from randomly selected cells in each section ($n=20$ cells in each group). The area of O/A and R/LM was measured for each section using a digitizing image analysis system (Image 1.38).

Quantification of Nissl-stained cells

For Nissl-stained sections, two control and two KA-treated rats were deeply anesthetized with sodium pentobarbital (65 mg/kg i.p.) two weeks after KA injection and perfused through the ascending aorta with 2% paraformaldehyde, 2.5% glutaraldehyde, 3.0 mM CaCl₂ in 0.1 M cacodylate buffer (CB, pH 7.4, room temperature). Tissue blocks containing the hippocampus were trimmed as in the previous section for GAD immunocytochemistry, embedded in paraffin, and cut in five μm -thick sections on a Microtome. Sections from the complete hippocampus were processed for conventional Nissl-stains. Briefly, tissue sections were dehydrated in 100% alcohol (2 hours) and incubated in a 0.02% solution of cresyl violet (1 hour). Sections were then washed in 100% alcohol, cleared in xylene, and mounted on gelatin-coated slides with DPX. The Ny of cells in O/A and R/LM was estimated in a sample of 24 sections, taken at regular intervals (equivalent to GAD-labeled sections), for each control and KA-treated rats, as was described for the quantification of GAD positive cells. Neurons were differentiated from glial cells by

their larger cell body and cytoplasmic volume.

Statistical Analysis

The N_v of GAD-immunopositive and Nissl-stained cells was compared between control and KA-treated rats using Student's t-tests (t-test, p<0.05). All data are given as means ± standard errors.

Results and Discussion

Loss of a subpopulation of GAD-positive cells in the CA1 region

Using GAD immunocytochemistry, GAD-positive cells were found in all CA1 layers after KA treatment. However, fewer cells were labeled in O/A and PYR in KA-treated rats compared to control (Fig. 1 A, B). The gross morphology of the KA-resistant GAD-positive cells in O/A and R/LM did not appear obviously altered after KA treatment (Fig. 1 C, D). The quantification of GAD-positive cells in O/A, PYR and R/LM demonstrated that the mean numerical density of GAD-positive cells in O/A was significantly decreased in KA-treated rats to 51% of control (33.8 ± 7.9 vs 65.9 ± 5.2 cells/mm³ in control; p<0.05). In individual rats, the density of GAD-positive cells in O/A was reduced in 6 of 6 KA-treated rats relative to the mean density in control animals, and the range of GAD-positive cell loss in O/A was 19 - 88%. The mean N_v of GAD-positive cells in PYR was 79% of control in KA-treated rats (243.9 ± 38.8 vs 310.4 ± 23.0 cells/mm³ in control), but this was not statistically significant. In addition, the mean N_v of GAD-positive cells in R/LM was not

significantly different in KA-treated rats (60.2 ± 6.0 vs 56.2 ± 11.2 cells/mm³ in control; $p < 0.05$). The selective reduction of GAD-immunopositive cells in O/A, the possible loss of cells in PYR, and the absence of cell loss in R/LM, indicate that the reduced GAD labelling was not due to a general decrease in GAD levels, but rather reflected an apparent loss of particular populations of interneurons.

Selective loss of Nissl-stained cells in the CA1 region

Nissl-stained sections of the hippocampus were examined in naive and KA-treated rats, which confirmed that dentate hilar cells and hippocampal CA3 pyramidal cells were lesioned in all KA-treated animals (Fig. 2 A, B). To verify that the reduction of GAD-immunopositive cells was due to a selective loss of interneurons and not a general reduction of GAD levels, we estimated the density of Nissl-stained cells in O/A and R/LM of naive (Fig. 2 C1 and C2, respectively) and KA-treated (Fig. 2 D1 and D2, respectively) rats. We found that the mean N_V of cells located in O/A was significantly diminished in KA-treated animals to 77% of control (2298.7 ± 36.2 vs 2980.0 ± 97.5 cells/mm³ in control, $p < 0.05$). In contrast, the density of cells in R/LM was not significantly different in control and KA rats (2027.5 ± 195.4 vs 2053.7 ± 336.8 cells/mm³, respectively). The density of Nissl-stained cells was not measured in PYR since GABA interneurons and pyramidal cells cannot be reliably differentiated in the pyramidal cell layer. The difference in the mean density of GAD-positive and Nissl-stained cells in the O/A and R/LM layers of naive rats may be due to multiple factors such as differences in tissue shrinkage [18] and in

histological procedures, an underestimation of GAD-positive cells with immunocytochemical detection, and the inclusion of some glial cells in cell counts in Nissl-stained material. Regardless, the observed reduction of Nissl-stained cells in O/A paralleled the reduction of GAD-positive cells in the same layer after KA treatment. This suggests that there is an actual loss of GAD-immunopositive interneurons in the O/A region after KA lesions.

Overall, the results indicate that a subpopulation of GABA interneurons is selectively vulnerable to KA treatment. These results are consistent with previous findings that some somatostatin- and parvalbumin-immunoreactive cells in stratum oriens of the CA1 region are lost after KA [4, 5]. Our data indicate that this deficit results in a 50% loss of GABA interneurons in these layers. These results appear contradictory to previous reports of preserved GABA neurons after KA [6, 8]. However, these previous studies used a different GAD antibody [6, 8] which has been shown to label terminals better than cell bodies [7]. Our results are consistent with such a presence of KA-resistant GABA cells, but additionally point to a selective loss of subtypes of interneurons in stratum oriens and alveus after KA treatment. This loss of inhibitory interneurons may therefore contribute to a reduction of inhibition in pyramidal cells after KA treatment since interneurons in these layers are involved in feedback inhibition of pyramidal cells [11, 14]. In contrast, the density of GAD-positive cells in R/LM was not altered following KA treatment. Since some inhibitory cells in these layers are involved in feedforward inhibition of pyramidal cells [12, 13], our results suggest that distinct components of inhibitory circuits may be differentially affected by KA-induced cell loss. A selective vulnerability of

GABA- and somatostatin-positive interneurons has also been found in other models [9, 22], and in the human epileptic hippocampus [21]. This selective loss of GABAergic CA1 interneurons after KA appears contradictory to lack of change in monosynaptic inhibitory synaptic responses evoked in CA1 pyramidal cells by direct electrical stimulation of GABA cells in KA-treated animals [24]. However, since these physiological experiments were conducted 2-4 weeks post-lesion, the lack of deficit in monosynaptic inhibition may reflect the involvement of compensatory mechanism in the KA-resistant GABAergic cells or synapses.

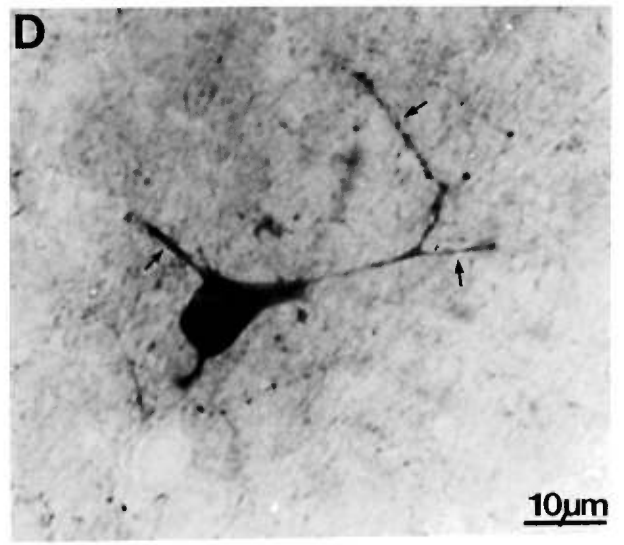
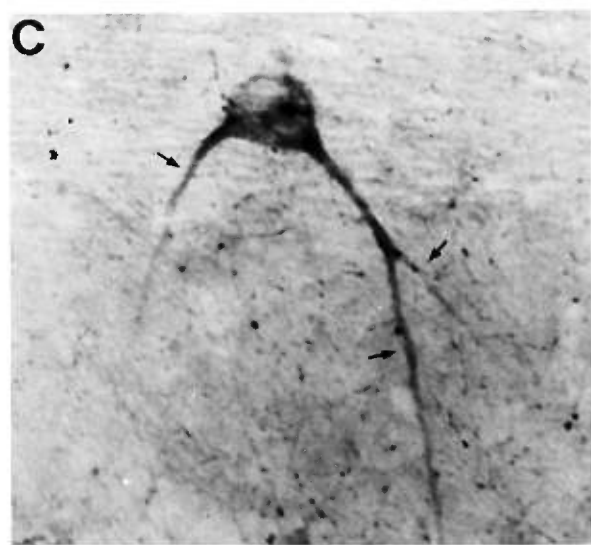
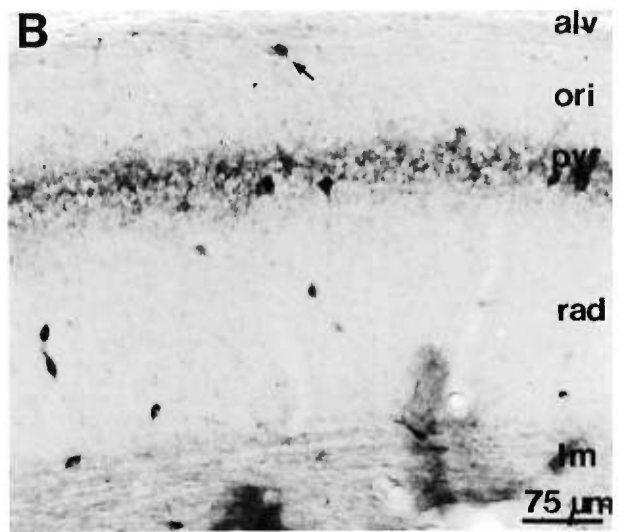
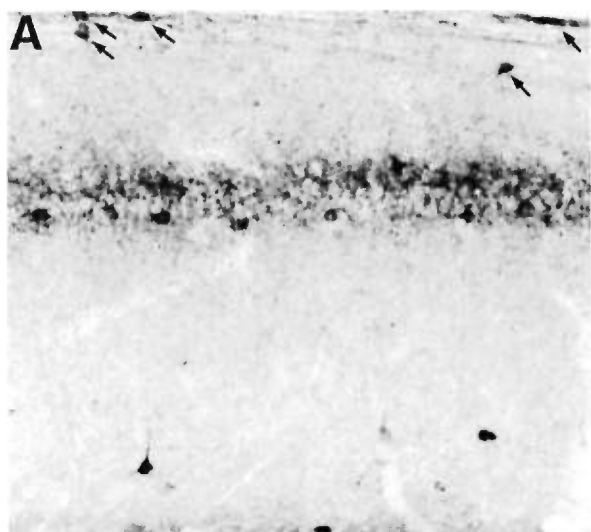
Acknowledgements

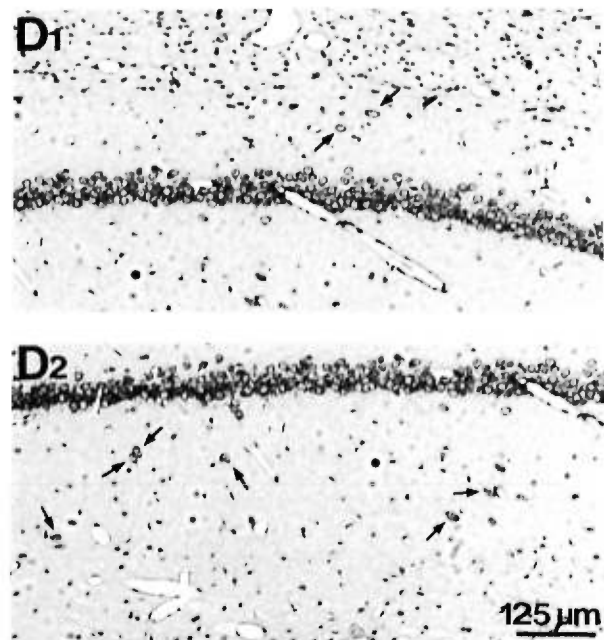
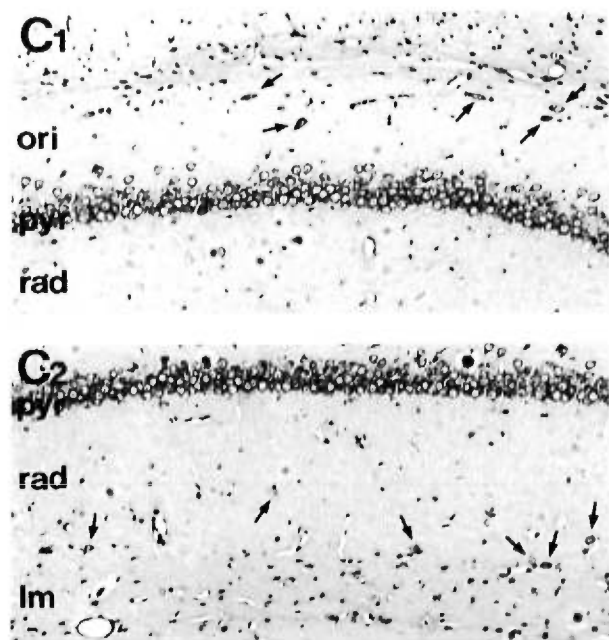
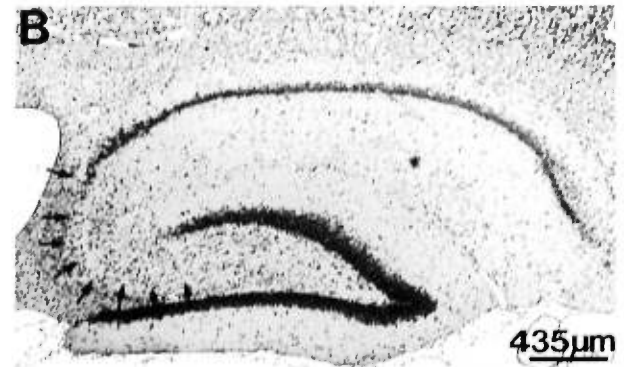
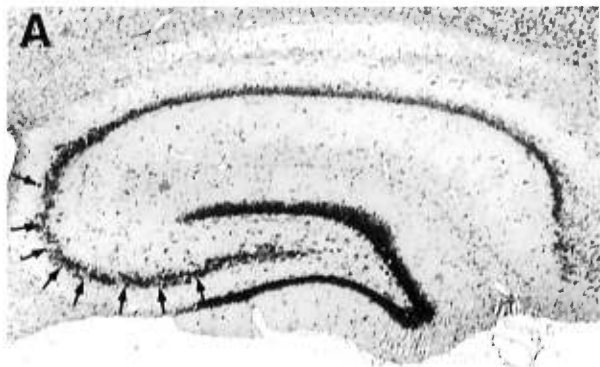
This work was supported by the Fonds de la Recherche en Santé du Québec (FRSQ; J.-C. L.), the Medical Research Council of Canada (MRCC; J.-C. L. and C.B.), the Savoy Foundation for Epilepsy (F.M.), a Research Center grant from the Fonds pour la Formation de Chercheurs et l'Aide à la Recherche (FCAR) to the Groupe de Recherche sur le Système Nerveux Central, and a FCAR group grant (Equipe, J.-C. L.). We also thank I. Jutras for assistance with the kainic acid lesions, G. Lambert with photographic work, and Y. Lepage with statistical analyses.

Figure Legends

Figure 1: (A-B) Light photomicrographs showing the distribution of GAD-immunopositive cells (arrows) in stratum oriens (ori) and alveus (alv) and in strata radiatum (rad) and lacunosum-moleculare (lm) of control (A) and KA-treated (B) rats. GAD-positive cells are found in all area CA1 layers of KA-treated rats, but are less numerous in stratum oriens. (C-D) Higher-power light photomicrographs showing intact gross morphology of representative KA-resistant GAD-positive interneurons in stratum oriens (C) and radiatum (D) from KA-treated rats. Scale bars = 75 μm in A, B; 10 μm in C, D.

Figure 2: (A-B) Nissl-stained sections showing extensive lesion of dentate hilar neurons and CA3 pyramidal cells (arrows) in the KA-treated animal (B), relative to control (A). Principal cells in area CA1 and dentate gyrus were relatively normal after KA treatment. (C-D) Higher-power light photomicrographs from control (C) and KA-treated (D) rats showing the distribution of Nissl-stained cells in O/A (C1, D1) and R/LM (C2, D2) regions. Scale bars = 435 μm in A, B; 125 μm in C, D.





References

1. Abercrombie, M. Estimation of nuclear population from microtome sections, *Anat. Rec.* 94 (1946) 239-247.
2. Babb, T.L., Pretorius, J.K., Kupfer, W.R. and Crandall, R.H., Glutamate decarboxylase-immunoreactive neurons are preserved in human epileptic hippocampus, *J. Neurosci.*, 9 (1989) 2563-2574.
3. Ben-Ari Y., Limbic seizure and brain damage produced by kainic acid: mechanisms and relevance to human temporal lobe epilepsy, *Neuroscience*, 14 (1985) 375-403.
4. Best, N., Mitchell, J., Bainbridge, K.G. and Wheal, H.V., Changes in parvalbumin-immunoreactive neurons in the rat hippocampus following a kainic acid lesion, *Neurosci. Lett.*, 155 (1993) 1-6.
5. Best, N., Mitchell, J. and Wheal, H. V., Ultrastructure of parvalbumin-immunoreactive neurons in the CA1 area of the rat hippocampus following a kainic acid injection, *Acta Neuropathol.*, 87 (1994) 187-195.
6. Davenport, C.J., Brown, W.J. and Babb, T.L., GABAergic neurons are spared after intrahippocampal kainate in the rat, *Epilepsy Res.*, 5 (1990) 28-42.
7. Esclapez, M., Tillakaratne, N.J.K., Kaufman, D.L., Tobin, A.J. and Houser, C.R., Comparative localization of two forms of glutamic acid decarboxylase and their mRNAs in rat brain supports the concept of functional differences between the forms, *J. Neurosci.*, 14 (1994) 1834-1855.
8. Franck, J.E., Kunkel, D.D., Baskin, D.G. and Schwartzkroin, P.A., Inhibition in kainate-lesioned hyperexcitable hippocampi: physiologic, autoradiographic and

- immunocytochemical observations, *J. Neurosci.*, 8 (1988) 1991-2002.
9. Houser, C.R. and Esclapez, M. Vulnerability and plasticity of the GABA system in the pilocarpine model of spontaneous recurrent seizures, *Epilepsy Res.*, 26 (1996) 207-218.
 10. Kaufman, D.L., Houser, C.R. and Tobin, A.J., Two forms of the gamma-aminobutyric acid synthetic enzyme glutamate decarboxylase have distinct intraneuronal distributions and cofactor interactions, *J. Neurochem.*, 56 (1991) 720-723.
 11. Lacaille, J.-C., Mueller, A.L., Kunkel, D.D. and Schwartzkroin, P.A., Local circuit interactions between oriens-alveus interneurons and CA1 pyramidal cells in hippocampal slices: electrophysiology and morphology, *J. Neurosci.*, 7 (1987) 1979-1993.
 12. Lacaille, J.-C. and Schwartzkroin, P.A., Stratum lacunosum-moleculare interneurons of hippocampal CA1 region: I. Intracellular response characteristics, synaptic responses, and morphology, *J. Neurosci.*, 8 (1988) 1400-1410.
 13. Lacaille, J.-C. and Schwartzkroin, P.A., Stratum lacunosum-moleculare interneurons of hippocampal CA1 region: II. Intrasomatic and intradendritic recording of local circuit synaptic interactions, *J. Neurosci.*, 8 (1988) 1411-1424.
 14. Maccaferri, G. and McBain, C.J., Passive propagation of LTD to stratum oriens-alveus inhibitory neurons modulates the temporoammonic input to the hippocampal CA1 region, *Neuron*, 15 (1995) 137-145.
 15. Micheva, K.D. and Beaulieu, C., Neonatal sensory deprivation induces selective changes in the quantitative distribution of GABA-immunoreactive neurons in the

- rat barrel field cortex, *J. Comp. Neurol.*, 361 (1995) 574-584.
16. Mrini, A., Moukles, H., Jacomy, H., Bosler, O. and Doucet, G., Efficient immunodetection of various protein antigens in glutaraldehyde-fixed brain tissue. *J. Histochem. Cytochem.*, 43 (1995) 1285-1291.
17. Nadler, J.V. Kainic acid as a tool for the study of temporal lobe epilepsy, *Life Sci.*, 29 (1981) 2031-2042.
18. O'Kusky, J. and Colonnier, M., A laminar analysis of the number of neurons, glia, and synapses in the visual cortex (area 17) of adult macaque monkeys, *J. Comp. Neurol.*, 210 (1982) 278-290.
19. Paxinos, G. and Watson, C., *The Rat Brain in Stereotaxic Coordinates*, Academic Press, New York, 1986.
20. Perez, Y., Morin, F., Beaulieu, C. and Lacaille, J.-C., Axonal sprouting of CA1 pyramidal cells in hyperexcitable hippocampal slices of kainate-treated rats, *Eur. J. Neurosci.*, 8 (1996) 736-748.
21. Robbins, R.J., Brines, M.L., Kim, J.H., Adrian, T., deLanerolle, N., Welsh, S. and Spencer, D.D., A selective loss of somatostatin in the hippocampus of patients with temporal lobe epilepsy, *Ann. Neurol.*, 29 (1991) 325-332.
22. Sloviter, R., Decreased hippocampal inhibition and a selective loss of interneurons in experimental epilepsy, *Science*, 235 (1987) 73-76.
23. Turner, D.A. and Wheal, H.V., Excitatory synaptic potentials in kainic acid-denervated rat CA1 pyramidal neurons, *J. Neurosci.*, 11 (1991) 2786-2794.
24. Williams, S., Vachon, P. and Lacaille, J.-C., Monosynaptic GABA-mediated inhibitory postsynaptic potentials in CA1 pyramidal cells of hyperexcitable

hippocampal slices from kainic acid-treated rats, *Neuroscience*, 52 (1993) 541-554.

CHAPITRE QUATRIÈME

**ALTERATIONS SPÉCIFIQUES DES PROPRIÉTÉS SYNAPTIQUES DES
INTERNEURONES DE LA RÉGION CA1 DE L'HIPPOCAMPE APRÈS LE
TRAITEMENT À L'ACIDE KAÏNIQUE**

**Cell-specific alterations in synaptic properties of hippocampal CA1 interneurons
after kainate treatment**

F. Morin^{1,2}, C. Beaulieu² and J.-C. Lacaille¹

Centre de recherche en sciences neurologiques et Départements de physiologie¹ et de pathologie², Université de Montréal, Montréal, Québec, Canada, H3C 3J7.

publié dans

Journal of Neurophysiology, 80: 2836-2847, 1998.

Abstract

Hippocampal sclerosis and hyperexcitability are neuropathological features of human temporal lobe epilepsy which are reproduced in the kainic acid (KA) model of epilepsy in rats. To assess directly the role of inhibitory interneurons in the KA model, the membrane and synaptic properties of interneurons located in (1) stratum oriens near the alveus (O/A) and (2) at the border of stratum radiatum and stratum lacunosum-moleculare (LM), as well as those of pyramidal cells, were examined with whole-cell recordings in slices of control and KA-lesioned rats.

In current-clamp recordings, intrinsic cell properties such as action potential amplitude and duration, amplitude of fast and medium duration afterhyperpolarizations, membrane time constant and input resistance were generally unchanged in all cell types after KA treatment. In voltage-clamp recordings, the amplitude and conductance of pharmacologically isolated excitatory postsynaptic currents (EPSCs) were significantly reduced in LM interneurons of KA-treated animals, but were not significantly changed in O/A and pyramidal cells. The rise time of EPSCs was not significantly changed in any cell type after KA treatment. In contrast, the decay time constant of EPSCs was significantly faster in O/A interneurons of KA-treated rats, but was unchanged in LM and pyramidal cells. The amplitude and conductance of pharmacologically isolated GABA_A inhibitory postsynaptic currents (IPSCs) were not significantly changed in any cell type of KA-treated rats. The rise time and decay time constant of GABA_A IPSCs were significantly faster in pyramidal cells of KA-treated rats, but were not significantly changed in O/A and LM interneurons.

These results suggest that complex alterations in synaptic currents occur in specific subpopulations of inhibitory interneurons in the CA1 region following KA lesions. A reduction of evoked excitatory drive onto inhibitory cells located at the border of stratum radiatum and stratum lacunosum-moleculare may contribute to disinhibition and polysynaptic epileptiform activity in the CA1 region. Compensatory changes, involving excitatory synaptic transmission on other interneuron subtypes and inhibitory synaptic transmission on pyramidal cells, may also take place and contribute to the residual, functional monosynaptic inhibition observed in principal cells after KA treatment.

Introduction

Intracerebroventricular injection of kainic acid (KA) in rats produces a selective loss of hippocampal CA3 and hilar cells and renders the surviving CA1 pyramidal cells hyperexcitable (Ben-Ari 1985; Franck and Schwartzkroin 1985; Nadler 1981). Ammon's horn sclerosis and hippocampal hyperexcitability are also major features of human temporal lobe epilepsy (TLE) (Ben-Ari 1985; Lothman et al. 1991), and this makes the KA model useful to investigate the basic mechanisms of human TLE. In the KA model, the hyperexcitability of CA1 pyramidal cells may be due to multiple changes in excitatory and inhibitory synaptic pathways. First, hyperexcitable CA1 pyramidal cells of KA-treated rats show increased *N*-methyl-*D*-aspartate (NMDA) excitatory postsynaptic responses (Turner and Wheal 1991; Williams et al. 1993) that may arise in part from aberrant, newly formed, recurrent excitatory synapses between CA1 pyramidal cells (Meier and Dudek 1996; Nadler et al. 1980a,b; Perez et al. 1996). In addition, polysynaptic γ -aminobutyric acid (GABA)-mediated inhibitory synaptic responses are diminished in CA1 pyramidal cells of KA-treated rats (Ashwood et al. 1986; Franck and Schwartzkroin 1985; Franck et al. 1988). However, direct electrical stimulation of inhibitory cells revealed unimpaired monosynaptic inhibition in hyperexcitable CA1 pyramidal cells (Williams et al. 1993), suggesting that the reduction in polysynaptic inhibition after KA treatment may be due to diminished excitatory drive on inhibitory interneurons. Such reduction of excitatory drive on interneurons is analogous to the dormant cell hypothesis proposed for other models of epilepsy (Bekenstein and Lothman 1993;

Lothman et al. 1995; Sloviter 1991, 1994). Impairment in inhibition may also be due to a selective loss of inhibitory cells after KA since the number of parvalbumin- and somatostatin-containing interneurons in the CA1 region is reduced after KA treatment (Best et al. 1993, 1994). Despite their crucial role in generating inhibition (Lacaille et al. 1989; Freund and Buzsáki 1996), the physiological properties of inhibitory cells still remain ill-defined in the KA model, as well as in human TLE (Isokawa 1996) and other related experimental models (Buhl et al. 1996; Lothman et al. 1995; Mangan et al. 1995; Rice et al. 1996; Sloviter 1994).

GABA inhibition of CA1 pyramidal cells involves multiple subtypes of interneurons which can be differentiated on the basis of their soma location, postsynaptic targets, intrinsic membrane properties, and local circuit connectivity (Buhl et al. 1994; Freund and Buzsáki 1996; Houser 1991; Lacaille et al. 1989; Sik et al. 1995). The present study was undertaken to assess directly if impairment in the physiological properties of inhibitory cells contribute to the generation of epileptiform activity in the CA1 region of the KA model of epilepsy (Franck et al. 1988; Nakajima et al. 1991; Williams et al. 1993). We have taken advantage of the laminar organization of the CA1 region and the known distribution of various subtypes of GABA interneurons (Morin et al. 1996) to examine, using whole-cell recordings, the membrane properties as well as the evoked excitatory and inhibitory postsynaptic currents of inhibitory interneurons in hippocampal slices from KA-treated rats. We have focused on interneurons located 1) in stratum oriens near the alveus (O/A) and 2) at the border of stratum radiatum and stratum lacunosum-moleculare (LM) since these populations of interneurons are differentially involved in

feedback and feedforward inhibition respectively (Blasco-Ibanez and Freund 1995; Lacaille et al. 1987; Lacaille and Schwartzkroin 1988a,b; Maccaferri and McBain 1995). Our results suggest that, in hyperexcitable slices of KA-treated animals, the membrane properties of inhibitory interneurons are generally unimpaired, the excitatory synaptic currents are selectively reduced in certain interneurons, and the inhibitory synaptic currents are not diminished in interneurons or pyramidal cells.

Methods

Kainate lesions

Procedures for kainate lesions were as previously described (Perez et al. 1996). Briefly, adult male Sprague-Dawley rats (150-160 g, n=74; Charles River) were anesthetized with a mixture of ketamine and xylazine (165 and 10 mg/kg i.m., respectively) following pretreatment with atropine (0.27 mg/kg i.p.) to prevent respiratory difficulties during anesthesia. Bilateral intracerebroventricular injections of kainic acid (0.55 µg/µl over 30 min; in 0.9% saline, pH 7.3-7.4) were made using a 10 µl Hamilton syringe at the following stereotaxic coordinates: 0.6 mm posterior to bregma, 2.0 mm lateral to the midline, and 3.5 mm ventral to the dura. Wounds were treated with aerosol antibiotic (Neosporin) and closed with sutures. Animals were returned to their cages and given water and food *ad libitum* for a period of two weeks.

Hippocampal slices

Hippocampal slices were obtained as described previously (Morin et al. 1996). Briefly, KA-treated rats (2 weeks postlesion) and age-matched unoperated

control rats (225-250 g; n=40) were anesthetized with ether and decapitated. The brain was quickly removed from the skull and rinsed in artificial cerebrospinal fluid (ACSF, 4 °C) containing (in mM) 124 NaCl, 5 KCl, 1.25 NaH₂PO₄, 2 MgSO₄, 2 CaCl₂, 26 NaHCO₃ and 10 dextrose. Transverse hippocampal slices (300 µm-thick) were cut from each hemisphere on a Vibratome (Campden Instruments) and transferred to a container filled with oxygenated ACSF at room temperature. After a recovery period of one hour, a slice was positioned in the recording chamber, maintained submerged with a U-shaped platinum wire (Edwards et al. 1989) and continuously perfused with oxygenated ACSF (3-4 ml/min) at room temperature (22-24 °C). The recording chamber was mounted on an upright microscope (Zeiss Axioskop) equipped with a long range water-immersion objective (40X), differential interference contrast (DIC) and an infrared video camera (Cohu 6500), which allowed visual identification of interneurons and pyramidal cells in slices.

Extracellular and whole-cell recordings

Field potentials were recorded with patch electrodes (5-7 MΩ) filled with 2 M NaCl placed in stratum pyramidale, and were evoked by stimulating CA1 afferent fibers in stratum radiatum (bipolar electrode, 0.05 ms, 0-1000 µA). In all experiments, the CA1 and CA3 regions were isolated by a surgical cut. For current-clamp experiments, patch electrodes (5-10 MΩ) were filled with (in mM): 140 K-methanesulfonate, 5 NaCl, 2 MgCl₂, 10 N-2-hydroxyethylpiperazine-N-2-ethanesulfonic acid (HEPES), 0.5 CaCl₂, 0.5 ethylene glycol-bis(β-aminoethyl

ether)-*N,N,N,N*-tetraacetic acid (EGTA), 2 ATP-tris, 0.4 GTP-tris (pH 7.4 adjusted with KOH). For voltage-clamp experiments, the internal solution of the patch electrodes contained (in mM): 120 Cs-methanesulphonate, 20 QX-314, 8 NaCl, 1 MgCl₂, 10 HEPES, 1 EGTA, 2 ATP-tris, 0.4 GTP-tris (pH 7.4 adjusted with CsOH). In these experiments, Cs-methanesulphonate and QX-314 (bromide salt; Research Biochemicals, RBI) were added to the recording solution to improve the space clamp and block K⁺ and Na⁺ currents (Nathan et al. 1990). In all experiments, 0.1% biocytin was added to the internal patch to label cell bodies and processes, and allow their subsequent morphological characterization.

After a tight-seal (>1 GΩ) was formed on the cell body of a neuron, whole-cell recording was obtained by rupturing the cell membrane with negative pressure (Hamill et al. 1981). Extracellular, current- and voltage-clamp recordings were made using an Axopatch 1D amplifier (Axon Instruments) with low-pass filtering at 10 KHz (-3db) and digitized at 22 KHz for storage on a video cassette recorder (Neurocorder DR-886). Recordings were also digitized and analyzed with a microcomputer equipped with a data acquisition system (TL-125 and pClamp, Axon Instruments). Recordings with unstable holding current or with series resistance and capacitance that could not be properly compensated, were discarded. Liquid junction potentials were measured at the end of the experiments after withdrawal from the cell, and membrane potentials were subsequently corrected.

Whole-cell postsynaptic responses were evoked by electrical stimulation (constant current pulses, 0.05 ms, 0-300 μA) of nearby afferent fibers using a

monopolar tungsten microelectrode (Frederick Haer, Co.). For responses evoked in pyramidal cells, the stimulating electrode was positioned in stratum radiatum, whereas for interneurons it was placed 150-250 μm laterally from the soma (within the same layer). In voltage-clamp experiments, the peak amplitude and kinetics (10-90% rise time and decay time constant obtained from a single-exponential fit) of EPSCs and IPSCs were also compared in the different cell types between control and KA-treated rats. The analysis of postsynaptic currents was performed on averaged responses ($n=2$).

Pharmacology

Receptor antagonists were prepared in distilled water and stored frozen in 1 ml aliquots: 6-cyano-7-nitroquinoxaline-2,3-dione (CNQX; 3.1 mM, RBI) for non-*N*-methyl-*D*-aspartate (non-NMDA) receptors, (\pm)-2-amino-5-phosphonopentoanoic acid (AP5; 7.7 mM, Sigma) for NMDA receptors, and bicuculline (BIC; 3.3 mM, Sigma) for GABA_A receptors. Before each experiment, concentrated stock solutions were diluted in ACSF to their final concentration (CNQX, 20 μM ; AP5, 50 μM ; BIC, 25 μM) and bath applied.

Statistical analysis

Group differences between cells in control slices and in hyperexcitable slices from KA-treated animals were analyzed using Student's t-tests. All data are given as mean \pm standard error.

Histology

After completion of physiological recordings, slices were put in a fixative solution containing 4% paraformaldehyde, 1% glutaraldehyde, 2.5% dimethyl sulfoxide (DMSO), 3.0 mM CaCl₂ in 0.1 M cacodylate buffer (CB) for 4 hours. They were then rinsed and left overnight in 0.1 M CB (4 °C). To improve visualization of the axonal and dendritic plexus of cells, slices were embedded in 1% agarose and cut on a vibratome in 60 µm-thick sections. Sections were treated with 1% H₂O₂ for 20 min to eliminate endogenous peroxidases, then washed in phosphate buffer salt (PBS, pH 7.4, 4x5 min) and in PBS containing 2.5% DMSO (4x5 min). Slices were incubated in the avidin biotin complex (ABC kit, Vector Labs) at a concentration of 1:200 for 24 hrs and revealed according to a modified protocol using the tetramethylbenzidine (TMB) product (see Llewellyn-Smith et al. 1993). Slices were incubated for 20 min in a solution of phosphate buffer (PB, 0.1 M, pH 6.0) containing 0.4% ammonium chloride (Sigma) and 0.001% TMB (Sigma). The blue reaction was visualized by adding 0.05% H₂O₂ to the first incubating solution. To stabilize the TMB product, the slices were incubated 15 min in a solution of PB (pH 6.0) containing 0.4% NH₄Cl, 1% cobalt chloride (Sigma), 0.1% DAB and 0.1% H₂O₂. Sections were cleared in xylene and mounted in DPX (Electron Microscopy Sciences) for light microscopy. The dendritic and axonal arborizations of the cells were then drawn and reconstructed using a camera lucida at a final magnification of 400X.

The presence of KA lesions was verified using Nissl staining in three KA-treated rats and compared with two control animals. Rats were anesthetized with

sodium pentobarbital (65 mg/kg i.p.) and perfused through the ascending aorta with 2% paraformaldehyde, 2.5% glutaraldehyde, 3.0 mM CaCl₂ in 0.1 M CB (pH 7.4, room temperature). Coronal sections of the whole hippocampus were taken and processed for conventional Nissl stains.

Results

Kainate lesions and extracellular recordings

Nissl-stained sections from control animals (n=2) showed intact principal cells (Fig. 1 A) in all hippocampal subfields (dentate gyrus, CA3 and CA1). In contrast, extensive lesions of hippocampal CA3 cells were observed (Fig. 1 B, arrows) in KA-treated animals (n=3).

Hyperexcitable slices from KA-treated animals were identified using field potentials evoked by stimulation of stratum radiatum. Slices were considered hyperexcitable if evoked responses consisted of two or more population spikes and were selected for further whole-cell recordings. In slices of control rats, field potentials recorded in stratum pyramidale consisted of a single population spike (mean amplitude of maximal population spike, 2.0±0.2 mV; n=52; Fig. 2 A). In hyperexcitable slices from KA-treated animals (Fig. 2 B), responses were composed of multiple population spikes (amplitude of largest population spike, 2.4±0.2 mV; n=48).

Whole-cell recordings and morphology of biocytin-filled cells

Interneurons and pyramidal cells were visually identified using infrared video microscopy in hyperexcitable slices of KA-treated rats and in slices of control animals. Cells were selected for whole-cell recordings based on their morphology (soma and primary dendrites) and their soma location in specific CA1 layers. Recordings were obtained from interneurons located 1) in stratum oriens near the alveus (O/A, n=17 in control and in KA groups) and 2) at the border of stratum radiatum and stratum lacunosum-moleculare (LM, n=32 and 31 in control and KA groups, respectively), and from pyramidal cells (n=29 and 26 in control and KA groups, respectively).

The morphological profiles of each cell type were generally similar in control and KA-treated rats. The dendritic and axonal arborizations of biocytin-labeled interneurons in O/A (n=6 in control; n=14 in KA-treated group) and in LM (n=18 in control; n=17 in KA-treated group), as well as of pyramidal cells (n=13 in control; n=6 in KA-treated group), were generally as previously described in normal rats (Morin et al. 1996; data not shown).

Membrane properties and postsynaptic potentials

In whole-cell current-clamp recordings, the basic membrane properties of O/A, LM and pyramidal cells were generally not different in control and KA-treated rats (Table 1). The resting membrane potential was near -50 mV for all cells, except for pyramidal cells of KA-treated animals which displayed a significantly more hyperpolarized membrane potential (-58 mV). In O/A cells, the action potential amplitude was significantly greater after KA treatment (106 mV) but it was

unchanged in other cells. Other intrinsic membrane properties (Table 1) were not significantly different in any cell type, and were generally similar to those previously described in normal rats (Morin et al. 1996).

Stimulation of CA1 afferent fibers elicited postsynaptic potentials that were composed of initial excitatory postsynaptic potentials (EPSPs) followed by inhibitory postsynaptic potentials (IPSPs) in all cells. These responses were similar in all cell types of control (O/A: n=4; LM: n=8; pyramidal: n=8) and KA-treated (O/A: n=6; LM: n=11; pyramidal: n=8) animals, except that more action potentials were usually elicited in interneurons of O/A and pyramidal cells after KA.

Excitatory postsynaptic currents

To examine if synaptic currents were altered after KA treatment, compound excitatory and inhibitory postsynaptic currents (PSCs) were evoked by stimulating CA1 afferent fibers in normal ACSF and were recorded in voltage-clamp with the cell held at -80 mV. PSCs were inward and the amplitude increased with stimulation intensity (0-300 μ A) until they reached a maximum. Mean amplitude of PSCs was compared at a stimulation intensity of 200 μ A in O/A, LM and pyramidal cells of control and KA-treated rats. In KA-treated rats, the mean amplitude of PSCs was not significantly different in interneurons of either O/A (655.8 ± 145.9 pA in KA vs 788.7 ± 160.9 pA in control; n=11 in each group) or LM (338.5 ± 63.0 pA in KA vs 465.7 ± 71.4 pA in control; n=20 and 24, respectively). However in pyramidal cells, PSC amplitude was significantly increased in KA-treated animals (655.3 ± 88.5 pA in KA vs 380.8 ± 56.1 pA in control; n=20 in each group; p<0.05; Fig. 3).

To examine individually how excitatory and inhibitory synaptic transmission were affected by KA treatment, glutamate and GABA_A postsynaptic currents were pharmacologically isolated. Excitatory postsynaptic currents (EPSCs) were evoked at different membrane potentials (-80 to 60 mV) in the presence of the GABA_A receptor antagonist bicuculline. As previously described in control animals (Morin et al. 1996; Sah et al. 1990), EPSCs were composed of a fast component mediated by non-NMDA receptors and a slow component mediated by NMDA receptors in interneurons and pyramidal cells (Fig. 4). Latencies for measuring both components were determined in each cell at a membrane potential of -80 mV. The fast EPSC was measured at the initial peak current and the slow EPSC was measured at a latency when the fast EPSC had decayed near baseline (Fig. 4A, B). The mean amplitude of fast EPSCs (measured at -80 mV) was not significantly changed after KA in O/A ($100.9 \pm 30.1\%$ of control) and pyramidal ($101.1 \pm 16.7\%$ of control) cells, but was significantly reduced in LM interneurons ($51.8 \pm 10.8\%$ of control; $p < 0.05$; Table 2). The mean amplitude of slow EPSCs (measured at 60 mV) was not significantly changed after KA in O/A ($223.2 \pm 75.5\%$ of control), LM ($64.5 \pm 13.5\%$ of control) or pyramidal ($221.8 \pm 97.3\%$ of control) cells (Table 2). From the amplitude of both components at various membrane potentials, current-voltage (I-V) relationships of fast and slow EPSCs were determined (Fig. 4C, D). The mean conductance of fast EPSCs, obtained from the slope of the linear portion of the I-V relation, was not significantly different after KA in O/A interneurons ($131.5 \pm 39.1\%$ of control) and pyramidal cells ($117.2 \pm 34.5\%$ of control). In contrast, the mean conductance of fast EPSCs was significantly reduced in LM interneurons of KA-treated rats ($46.9 \pm 8.2\%$

of control; $p<0.05$; Table 2, Fig. 4). The I-V relation of slow EPSCs demonstrated a region of negative slope for membrane potentials between -80 and -30 mV and a linear portion at more depolarized potentials (Fig. 4). The mean conductance of slow EPSCs, obtained from the linear portion of the I-V relation, was not significantly different after KA in O/A ($165.7\pm50.7\%$ of control) and pyramidal ($135.7\pm42.9\%$ of control) cells, but was significantly reduced in LM interneurons ($63.2\pm10.5\%$ of control; $p<0.05$; Table 2, Fig. 4).

To determine if KA treatment caused changes in the kinetics of EPSCs, the rise time and decay time constant of fast EPSCs (at -80 mV) were also compared between cells of control and KA-treated rats. The 10-90% rise time was not significantly different in all cell types after KA (O/A: $67.0\pm40.8\%$ of control; LM: $57.1\pm5.4\%$ of control; pyramidal cells: $88.8\pm15.5\%$ of control; Table 2). The decay time constant of fast EPSCs, obtained from single-exponential fit of the decay phase, was significantly faster in O/A interneurons of KA-treated rats ($29.4\pm7.4\%$ of control; $p<0.05$), but was not significantly changed in LM ($59.9\pm17.1\%$ of control) and pyramidal ($83.6\pm19.3\%$ of control) cells (Table 2, Fig. 4). Therefore, the kinetics of fast EPSCs were in general not significantly changed between control and KA-treated rats, except for a faster decay in O/A interneurons of KA-treated animals.

To verify that fast and slow EPSCs were mediated by non-NMDA and NMDA receptors, their antagonists (CNQX and AP5, respectively) were bath-applied (Fig. 4). Fast EPSCs, recorded at -80 mV, were significantly reduced in all cell types: in O/A cells by $98.3\pm1.8\%$ ($n=6$) and $97.5\pm0.6\%$ ($n=3$), in control and KA groups, respectively; in LM cells by $88.4\pm2.8\%$ ($n=9$) and $92.8\pm2.9\%$ ($n=7$), in

control and KA groups, respectively; in pyramidal cells by $94.9\pm4.3\%$ (n=10) and $93.3\pm4.8\%$ (n=8), in control and KA groups, respectively. Slow EPSCs recorded at positive membrane potentials (60 mV) in the same cells were also significantly reduced during application of these antagonists: in O/A cells by $94.7\pm1.0\%$ (n=5) and $90.6\pm2.1\%$ (n=3), in control and KA groups, respectively; in LM cells by $78.3\pm3.4\%$ (n=9) and $86.1\pm2.3\%$ (n=7), in control and KA groups, respectively; and in pyramidal cells by $75.8\pm5.1\%$ (n=9) and $86.6\pm5.1\%$ (n=7), in control and KA groups, respectively. In all cell types of either control or KA-treated groups, the effects of these antagonists on fast and slow EPSCs were partially reversible after wash out of the antagonists (range 13.0 ± 6.1 to $66.8\pm8.6\%$, data not shown).

Inhibitory postsynaptic currents

To examine GABA synaptic responses in isolation, monosynaptic GABA_A inhibitory postsynaptic currents (IPSCs) were evoked in the presence of non-NMDA and NMDA receptor antagonists (CNQX and AP5, respectively) (Fig. 5). Monosynaptic GABA_A IPSCs, recorded at -80 mV, were inward and their mean peak amplitude was not significantly different after KA in interneurons of O/A ($126.8\pm48.6\%$ of control) and LM ($123.1\pm32.8\%$ of control), or in pyramidal cells ($159.4\pm44.7\%$ of control) (Table 3). The I-V relations of GABA_A IPSCs, obtained from series of responses recorded at different membrane potentials (-80 to 60 mV; Fig. 5), were linear. The mean reversal potentials of GABA_A IPSCs were not significantly different in KA-treated rats for interneurons in O/A ($85.5\pm7.7\%$ of control) and LM ($94.1\pm6.8\%$ of control), and in pyramidal cells ($95.9\pm7.9\%$ of

control) (Table 3). The mean conductance of GABA_A IPSCs, obtained from the slope of the linear I-V relation, was generally increased after KA in interneurons of O/A (113.1±36.5% of control) and LM (123.1±37.4% of control) and in pyramidal cells (152.6±39.1% of control), but this increase was not significant (Table 3, Fig. 5C, F).

The 10-90% rise time and decay time constant of GABA_A IPSCs were also compared in cells of control and KA-treated rats. After KA treatment, the mean rise time of GABA_A IPSCs recorded at -80 mV was not significantly different in interneurons of O/A (108.9±44.4% of control) and LM (113.8±11.7% of control), but was significantly faster in pyramidal cells (69.9±4.9% of control, p<0.05; Table 3, Fig. 5F). The mean decay time constant of GABA_A IPSCs recorded at -80 mV, obtained from a single-exponential fit of the decay phase, was not significantly different in KA-treated rats for interneurons of O/A (74.0±15.3% of control) and LM (103.0±9.7% of control), but was significantly faster for pyramidal cells (68.8±7.4% of control, p<0.05; Table 3, Fig. 5F). These results indicate that the kinetics of monosynaptic GABA_A IPSCs evoked in pyramidal cells were significantly faster after KA treatment. Despite these faster kinetics, the total charge transfer during IPSCs was not significantly changed in CA1 pyramidal cells of KA-treated animals (148.3±26.6% of control).

To verify that monosynaptic IPSCs were GABA_A mediated, the effects of the GABA_A antagonist, bicuculline, were examined (Fig. 5). The mean amplitude of GABA_A IPSCs (recorded at -80 mV) was significantly reduced in cell types: in O/A cells by 60.0±4.9% (n=3) and 95.5±3.7% (n=2), in control and KA groups, respectively; in LM cells by 96.9±1.0% (n=9) and 94.8±2.4% (n=6), in control and

KA groups, respectively; and in pyramidal cells by $62.3\pm7.7\%$ ($n=7$) and $79.9\pm5.2\%$ ($n=5$), in control and KA groups, respectively. The bicuculline effects were reversible with wash out in all cell types of control and KA groups (range 31.4 ± 7.0 to $81.5\pm7.2\%$, eg. Fig. 5).

Discussion

The major findings of this study were that multiple changes take place in inhibitory circuits after KA treatment and that these alterations occur selectively in certain interneuron subtypes. First, morphological characteristics of biocytin-labeled interneurons were similar in control and KA-treated animals. Second, in current-clamp experiments, basic intrinsic membrane properties of interneurons and pyramidal cells were generally not changed following KA treatment, except for action potentials of larger amplitude in O/A interneurons, and more hyperpolarized resting membrane potentials in pyramidal cells. Third, excitatory and inhibitory postsynaptic potentials could be evoked in all cell types of KA-treated rats. Fourth, in voltage-clamp experiments, the amplitude and conductance of pharmacologically isolated excitatory postsynaptic currents (EPSCs) were significantly reduced but specifically in LM interneurons of KA-treated animals. The rise time of EPSCs was unchanged in all cell types, but the decay time constant was significantly faster in O/A interneurons after KA. Fifth, the conductance and amplitude of pharmacologically isolated inhibitory postsynaptic currents (IPSCs) were not significantly changed in any cell type after KA. However, the rise time and decay time constant of IPSCs were significantly faster in pyramidal cells of KA-treated rats.

Morphology of biocytin-filled cells

Overall, the morphology of biocytin-labeled interneurons and pyramidal cells was similar in control and KA-treated groups, indicating that recordings were obtained from similar types of interneurons in both groups. Interneurons in O/A were similar to the previously described vertical (Lacaille et al. 1987; Lacaille and Williams 1990) and horizontal (Maccaferri and McBain 1995; McBain et al. 1994) cells, whereas LM interneurons were like stellate cells (Kawaguchi and Hama 1988; Lacaille and Schwartzkroin 1988a; Williams et al. 1994). A quantitative analysis of GAD-immunostained cells in the CA1 region demonstrated that 50% of interneurons located in stratum oriens and the alveus were lost after KA treatment (Morin et al. 1998). Others have shown that somatostatin- and parvalbumin-immunoreactive cells were lost following KA treatment (Best et al. 1993, 1994). Because of their soma location and axonal arborization patterns, these may correspond to the horizontal interneurons in O/A (Maccaferri and McBain 1995). In the present study, some of our biocytin-labeled O/A interneurons of KA-treated animals displayed axonal projections typical of horizontal cells, which suggests that the loss of these cells may only be partial after KA treatment.

Intrinsic membrane properties

Intrinsic properties were generally unaltered in interneurons and pyramidal cells after KA treatment. Resting membrane potential, membrane time constant, cell input resistance, action potential duration, and amplitude of afterhyperpolarizations

were unchanged. However, in KA-treated animals, action potential amplitude was larger in O/A cells and resting membrane potential was more hyperpolarized in pyramidal cells. Our results indicate that the hyperexcitability in the CA1 region after KA treatment may not be due to an impairment of the basic intrinsic properties of interneurons that could have led to their loss of excitability. This is consistent with a previous report using intracellular recordings with sharp electrodes that the input resistance of interneurons located within stratum pyramidale was not significantly different after KA treatment (Franck et al. 1988). Similarly, in a model of status epilepticus, membrane properties of interneurons located in stratum oriens, stratum radiatum, or stratum lacunosum-moleculare were not significantly altered after chronic seizures (Rempe et al. 1997). As previously found using intracellular recordings (Perez and al. 1996; Williams et al. 1993), our results also suggest that the CA1 hyperexcitability does not arise from alterations in intrinsic properties of pyramidal cells, since these were unchanged after KA treatment. However, we have not observed the increases in input resistance of CA1 pyramidal cells that have been described after KA treatment by others (Franck and Schwartzkroin 1985; Franck et al. 1988; Nakajima et al. 1991). Basic properties of hippocampal CA1 pyramidal cells and dentate gyrus granule cells also appear unchanged in the chronic model of status epilepticus (Bekenstein and Lothman 1993; Rempe et al. 1995), after kindling (Mody et al. 1988; Olivier and Miller 1985) and in human TLE (Isokawa 1996).

Alteration in glutamate synaptic transmission

Current-clamp experiments showed that excitatory and inhibitory postsynaptic potentials were evoked in all cell types in KA-treated rats. However, voltage-clamp analysis of pharmacologically isolated excitatory and inhibitory postsynaptic currents indicated that evoked currents were altered after KA treatment, but only in specific cell types. In interneurons, evoked EPSCs were composed of a fast component mediated by non-NMDA receptors and a slow component mediated by NMDA receptors. Our results demonstrated that the conductance of both non-NMDA and NMDA components of EPSCs were significantly reduced after KA treatment in LM interneurons, but were intact in O/A interneurons and pyramidal cells. These results suggest a reduction of evoked excitatory drive specific to LM interneurons after KA. Since degenerating terminals have been identified on LM interneurons after KA treatment (Kunkel et al. 1988), the decrease in excitatory drive likely reflects the partial deafferentation of LM cells. This observation of a reduced excitatory drive onto some CA1 inhibitory interneurons provides direct support to the dormant cell hypothesis (Sloviter 1991). According to this hypothesis, the disinhibition that contributes to epileptogenesis is due to a loss of afferent excitatory drive onto inhibitory interneurons resulting in a reduction of inhibition of principal cells (Sloviter 1987, 1991). In the CA1 region of the KA model, disinhibition is seen as a decrease in polysynaptic inhibition of pyramidal cells (Franck et al. 1988; Perez et al. 1996; Williams et al. 1993). However, direct electrical stimulation of inhibitory interneurons in slices of KA-treated rats demonstrated that monosynaptic inhibition was still intact in CA1 pyramidal cells after KA treatment (Nakajima et al. 1991; Williams et al. 1993), suggesting that inhibitory circuits are still functional following

KA. Our results are consistent with these findings and further indicate that the reduced excitatory drive on LM interneurons may contribute to the impairment of polysynaptic inhibition in CA1 pyramidal cells and to the development of epileptiform activity in the CA1 area after KA treatment. In a model of chronic epilepsy, whole-cell current-clamp recordings of interneurons in stratum oriens and alveus, in stratum radiatum, and in stratum lacunosum-moleculare have found that the excitatory drive of CA1 interneurons was still functional (Rempe et al. 1997). However, this model of status epilepticus produces a more generalized hippocampal cell loss (Rempe et al. 1997), suggesting that a specific loss of afferents from the CA3 region may be the key factor for the reduction of excitatory drive on LM interneurons after KA.

In the present study, no deficit was observed in the amplitude and conductance of non-NMDA and NMDA EPSCs in O/A interneurons after KA treatment. Thus, this reduction in evoked excitatory drive occurs selectively in some subtypes of interneurons. This loss of excitatory afferents restricted to certain specific types of interneurons may explain why previous investigations did not observe a reduction of excitatory drive in interneurons after KA (Esclapez et al. 1997). Although the amplitude and conductance of evoked responses were unchanged, the faster decay time constant of EPSCs in O/A interneurons after KA treatment suggests that alterations have taken place at excitatory inputs on O/A cells. Indeed, preliminary findings indicated that the kinetics of spontaneous EPSCs in O/A interneurons were modified after KA treatment (Perez and Lacaille 1997). Interneurons in O/A may also become partially deafferented after KA treatment since

they are normally contacted by CA3 afferents (Lacaille et al. 1987). The presence of excitatory synaptic currents with intact conductance but altered kinetics suggests that compensatory changes may have taken place in these interneurons after KA. Thus, the increase in local axonal arborizations of CA1 pyramidal cells after KA (Perez et al. 1996) may have led to the formation of new excitatory synapses onto O/A interneurons to compensate for the KA-induced loss. These new synapses may restore the amplitude and conductance of EPSCs to control levels, but they may have different properties from the original ones, resulting in different kinetics from control EPSCs. These ongoing compensatory changes involving O/A interneurons may contribute to the recovery of polysynaptic IPSPs that has been reported at longer interval (2-4 months) after KA treatment (Franck and Schwartzkroin 1985). Finally, a determinant factor in the interneuron response to KA treatment appears to be its hippocampal connections. LM interneurons, which do not receive excitatory inputs from CA1 pyramidal cells (Lacaille and Schwartzkroin 1988a,b), remain partially deafferented and show reduced excitatory drive after KA treatment. In contrast, O/A interneurons that receive excitatory inputs from CA1 pyramidal cells (Blasco-Ibanez and Freund 1995; Lacaille et al. 1987; Maccaferri and McBain 1995) may undergo compensatory changes and do not show reduced excitatory drive.

Changes at GABAergic synapses

Our results suggest that inhibitory synapses in interneurons and pyramidal cells were unimpaired in KA-treated rats. Inhibitory synaptic responses were recorded in all cell types and the amplitude and conductance of GABA_A IPSCs were

not significantly changed in either interneurons or pyramidal cells after KA treatment. Therefore, in the KA model of epilepsy, increased inhibition of inhibitory interneurons does not appear to be the cause of polysynaptic epileptiform activity in the CA1 region, in contrast to the seizure-sensitive gerbil (Peterson et al. 1985). Moreover, the tendency for the peak conductance of monosynaptic GABA_A IPSCs to be increased in pyramidal cells after KA treatment indicated that a reduction of monosynaptic GABA_A inhibition in pyramidal cells was not responsible for their polysynaptic disinhibition. These results are consistent with previous reports of functional monosynaptic inhibition in the CA1 region of KA (Esclapez et al. 1997; Williams et al. 1993) and other models (Mangan et al. 1995; Mangan and Lothman 1996) of human TLE. However, the faster rise time and decay time constant of evoked monosynaptic GABA_A IPSCs in pyramidal cells after KA would suggest that some alterations have occurred at GABAergic synapses. In addition, the unimpaired synaptic conductance of GABA_A IPSCs in pyramidal cells despite a partial loss of interneurons in the CA1 region after KA treatment (Best et al. 1993, 1994; Morin et al. in press) suggests that compensatory changes have occurred at GABAergic synapses. It remains to be clarified whether these compensatory changes involve the formation of new synapses due to the sprouting of axons of KA-resistant inhibitory interneurons, as found in the dentate gyrus (Davenport et al. 1990), or due to a functional alteration of existing synapses of KA-resistant interneurons. Region-specific alterations in GABA_A receptor function due to changes in receptor subunit expression have been found in other models of human TLE (Gibbs et al. 1997; Kapur and Coulter 1995; Kapur and Macdonald 1997). In the pilocarpine model, the mRNA

expression for $\alpha 2$ and $\alpha 5$ subunits of GABA_A receptors was decreased in CA1 hippocampal cells, while that of the $\alpha 1$, $\beta 2$ or $\gamma 2$ subunits was unchanged (Houser and Esclapez 1996; Rice et al. 1996; Vick et al. 1996). Additionally, complex changes in GABA_A receptor function have been described in the CA1 region after status epilepticus (Gibbs et al. 1997; Kapur and Coulter 1995). The efficacy of GABA in activating GABA currents was decreased in acutely isolated CA1 pyramidal cells, while the potency of GABA was enhanced (Gibbs et al. 1997). Furthermore, the benzodiazepine augmentation of GABA currents was reduced in these neurons (Gibbs et al. 1997). Overall, these data clearly indicate that GABA receptor function may be modified, but remain functional in these experimental models of temporal lobe epilepsy.

Functional implications

Overall, our results suggest that multiple changes occur in hippocampal inhibitory circuits after intraventricular kainate injection, and that these changes do not affect inhibitory interneurons uniformly. In addition, some of these changes may contribute to disinhibition of CA1 pyramidal cells, whereas others may tend to re-establish inhibition. These alterations in CA1 hippocampal circuits are illustrated in Figure 6. In this diagram of the hippocampal CA1 region, the only inhibitory interneurons represented are those which were studied in the present experiments. These are the interneurons located in stratum oriens and the alveus, vertical (Lacaille et al. 1987; Lacaille et Williams 1990) and horizontal (Maccaferri and McBain 1995)

cells, and those found at the border of stratum radiatum and stratum lacunosum-moleculare, stellate cells (Lacaille and Schwartzkroin 1988a,b). The vertical cells are involved in both feedforward and feedback inhibition (Lacaille et al. 1987; Maccaferri and McBain 1996), while the horizontal cells are involved in feedback inhibition (Maccaferri and McBain 1995, 1996). These inhibitory interneurons receive excitatory inputs from CA1 pyramidal cells and in turn make inhibitory contacts onto pyramidal cells. In contrast, interneurons located at the border of stratum radiatum and stratum lacunosum-moleculare (stellate cells) are mostly responsible for feedforward inhibition (Lacaille and Schwartzkroin 1988a,b). These cells receive excitatory inputs from CA3 pyramidal cells and make inhibitory contacts onto dendrites of CA1 pyramidal cells (Kunkel et al. 1988). Two weeks following KA treatment, there is a partial loss of Schaffer collaterals, however excitatory inputs to CA1 pyramidal cells remain unimpaired because of synaptic replacement (Nadler et al. 1980b) due to sprouting of CA1 afferents (spared Schaffer collaterals and commissural fibers) (Nadler et al. 1980b) or local axon collaterals of CA1 pyramidal cells (Perez et al. 1996). In addition, two types of changes in the inhibitory circuitry promote disinhibition and epileptiform activity in the CA1 region. First, there is a significant loss of GABA interneurons in stratum oriens and the alveus (Best et al. 1993; Morin et al. 1998). Since these vulnerable interneurons are immunopositive for parvalbumin and somatostatin (Best et al. 1993, 1994), they may correspond to horizontal cells (Blasco-Ibanez and Freund 1995). Second, a partial deafferentation of interneurons results in a partial loss of evoked excitatory drive in stellate cells that may contribute to the decrease in polysynaptic inhibition of pyramidal cells.

However, other alterations in the circuitry appear compensatory and may restore inhibition. First, since KA-resistant interneurons in O/A have unimpaired excitatory synaptic currents despite their partial deafferentation, axonal sprouting of pyramidal cells may have restored their excitatory inputs. Second, monosynaptic GABA_A IPSCs were unimpaired in pyramidal cells despite a partial loss of interneurons, suggesting that some compensatory changes must have taken place at inhibitory synapses. These latter changes may involve sprouting by KA-resistant interneurons and the formation of new inhibitory terminals, or functional alterations of synapses of KA-resistant interneurons.

Acknowledgements

This work was supported by the Fonds de la Recherche en Santé du Québec (FRSQ; J.-C. L.), the Medical Research Council of Canada (MRCC; J.-C. L. and C.B.), the Savoy Foundation (F.M.), a Research Center grant from the Fonds pour la Formation de Chercheurs et l'Aide à la Recherche (FCAR) to the Groupe de Recherche sur le Système Nerveux Central, and an Équipe de Recherche grant from the FCAR (J.-C. L.). We also thank I. Jutras for assistance with the kainic acid lesions and G. Lambert for photographic work.

References

- Ashwood, T.J., Lancaster, B., and Wheal, H.V. Intracellular electrophysiology of CA1 pyramidal neurons in slices of kainic acid-lesioned hippocampus of the rat. *Exp. Brain Res.* 62: 189-198, 1986.
- Bekenstein, J.W., and Lothman, E.W. Dormancy of inhibitory interneurons in a model of temporal lobe epilepsy. *Science* 259: 97-100, 1993.
- Ben-Ari Y. Limbic seizure and brain damage produced by kainic acid: mechanisms and relevance to human temporal lobe epilepsy. *Neuroscience* 14: 375-403, 1985.
- Best, N., Mitchell, J., Baimbridge, K.G., and Wheal, H.V. Changes in parvalbumin-immunoreactive neurons in the rat hippocampus following a kainic acid lesion. *Neurosci. Lett.* 155: 1-6, 1993.
- Best, N., Mitchell, J., and Wheal, H.V. Ultrastructure of parvalbumin-immunoreactive neurons in the CA1 area of the rat hippocampus following a kainic acid injection. *Acta Neuropathol.* 87: 187-195, 1994.
- Blasco-Ibanez, J.M., and Freund, T.F. Synaptic input of horizontal interneurons in stratum oriens of the hippocampal CA1 subfield: structural basis of feed-back activation. *Eur. J. Neurosci.* 7: 2170-2180, 1995.
- Buhl, E.H., Han, Z.-S., Lorinczi, Z., Stezhka, V.V., Karnup, S.V., and Somogyi, P. Physiological properties of anatomically identified axo-axonic cells in the rat hippocampus. *J. Neurophysiol.* 71: 1289-1307, 1994.
- Buhl, E.H., Otis, T.S., and Mody, I. Zinc-induced collapse of augmented inhibition by GABA in a temporal lobe epilepsy model. *Science* 271: 369-373, 1996.

- Davenport, C.J., Brown, W.J., and Babb, T.L. Sprouting of GABAergic and mossy fiber axons in dentate gyrus following intrahippocampal kainate in the rat. *Exp. Neurol.* 109: 180-190, 1990.
- Edwards, F.A., Konnerth, A., Sakmann, B., and Takahashi, T. A thin slice preparation for patch clamp recordings from neurones of the mammalian nervous system. *Pfluegers Arch.* 414: 600-612, 1989.
- Esclapez, M., Hirsch, J.C., Khazipov, R., Ben-Ari, Y., and Bernard, C. Operative GABAergic inhibition in hippocampal CA1 pyramidal neurons in experimental epilepsy. *Proc. Natl. Acad. Sci. (USA)* 94: 12151-12156, 1997.
- Franck, J.E., and Schwartzkroin, P.A. Do kainate-lesioned hippocampi become epileptogenic? *Brain Res.* 389: 309-313, 1985.
- Franck, J.E., Kunkel, D.D., Baskin, D.G., and Schwartzkroin, P.A. Inhibition in kainate-lesioned hyperexcitable hippocampi: physiologic, autoradiographic and immunocytochemical observations. *J. Neurosci.* 8: 1991-2002, 1988.
- Freund, T.F., and Buzsáki, G. Interneurons of the hippocampus. *Hippocampus* 6: 347-470, 1996.
- Gibbs, J.W., Shumate, M.D., and Coulter, D.A. Differential epilepsy-associated alterations in postsynaptic GABA_A receptor function in dentate granule cells and CA1 neurons. *J. Neurophysiol.* 77: 1924-1938, 1997.
- Hamill, O.P., Marty, A., Neher, E., Sakmann, B., and Sigworth, F.J. Improved patch-clamp techniques for high resolution current recording from cells and cell-free membrane patches. *Pfluegers Arch.* 391: 85-100, 1981.

- Houser, C.R. GABA neurons in seizure disorders: a review of immunocytochemical studies. *Neurochem. Res.* 16: 295-308, 1991.
- Houser, C.R., and Esclapez, M. Vulnerability and plasticity of the GABA system in the pilocarpine model of spontaneous recurrent seizures. *Epilepsy Res.* 26: 207-218, 1996.
- Isokawa, M. Decrement of GABA_A receptor-mediated inhibitory postsynaptic currents in dentate granule cells in epileptic hippocampus. *J. Neurophysiol.* 75: 1901-1908, 1996.
- Kawaguchi, Y., and Hama, K. Physiological heterogeneity of nonpyramidal cells in rat hippocampal CA1 region. *Exp. Brain Res.* 72:494-502, 1988.
- Kapur, J., and Coulter, D.A. Experimental status epilepticus alters γ -aminobutyric acid type A receptor function in CA1 pyramidal neurons. *Ann. Neurol.* 38: 893-900, 1995.
- Kapur, J., and Macdonald, R.L. Rapid seizure-induced reduction of benzodiazepine and Zn²⁺ sensitivity of hippocampal dentate gyrus cell GABA_A receptors. *J. Neurosci.* 17: 7532-7540, 1997.
- Kunkel, D.D., Lacaille, J.-C., and Schwartzkroin, P.A. Ultrastructure of stratum lacunosum-moleculare interneurons of hippocampal CA1 region. *Synapse* 2 : 382-394, 1988.
- Lacaille, J.-C., Mueller, A.L., Kunkel, D.D., and Schwartzkroin, P.A. Local circuit interactions between oriens-alveus interneurons and CA1 pyramidal cells in

- hippocampal slices: electrophysiology and morphology. *J. Neurosci.* 7: 1979-1993, 1987.
- Lacaille, J.-C., and Schwartzkroin, P.A. Stratum lacunosum-moleculare interneurons of hippocampal CA1 region: I. Intracellular response characteristics, synaptic responses, and morphology. *J. Neurosci.* 8: 1400-1410, 1988a.
- Lacaille, J.-C., and Schwartzkroin, P.A. Stratum lacunosum-moleculare interneurons of hippocampal CA1 region: II. Intrasomatic and intradendritic recording of local circuit synaptic interactions. *J. Neurosci.* 8: 1411-1424, 1988b.
- Lacaille, J.-C., Kunkel, D.D., and Schwartzkroin, P.A. Electrophysiological and morphological characterization of hippocampal interneurons. In: *The Hippocampus-New Vistas*, edited by V. Chan-Palay and C. Kohler. New York: Liss, 1989, p.287-305.
- Lacaille, J.-C., and Williams, S. Membrane properties of interneurons in stratum oriens-alveus of the CA1 region of rat hippocampus in vitro. *Neuroscience* 36: 349-359, 1990.
- Llewellyn-Smith, I.J., Pilowsky, P., and Minson, J.B. The tungstate-stabilized tetramethylbenzidine reaction for light and electron microscopic immunocytochemistry and for revealing biocytin-filled neurons. *J. Neurosci. Meth.* 46: 27-40, 1993.
- Lothman, E.W., Bertram III, E.H., and Stringer, J.L. Functional anatomy of hippocampal seizures. *Prog. Neurobiol.* 37: 1-82, 1991.

- Lothman, E.W., Rempe, D.A., and Mangan, P.S. Changes in excitatory neurotransmission in the CA1 region and dentate gyrus in a chronic model of temporal lobe epilepsy. *J. Neurophysiol.* 74: 841-848, 1995.
- Maccaferri, G., and McBain, C.J. Passive propagation of LTD to stratum oriens-alveus inhibitory neurons modulates the temporoammonic input to the hippocampal CA1 region, *Neuron* 15: 137-145, 1995.
- Maccaferri, G., and McBain, C.J. Long-term potentiation in distinct subtypes of hippocampal nonpyramidal neurons. *J. Neurosci.* 16: 5334-5343, 1996.
- Mangan, P.S., Rempe, D.A., and Lothman, E.W. Changes in inhibitory neurotransmission in the CA1 region and dentate gyrus in a chronic model of temporal lobe epilepsy. *J. Neurophysiol.* 74: 829-840, 1995.
- Mangan, P.S., and Lothman, E.W. Profound disturbances of pre- and postsynaptic GABA_B receptor-mediated processes in region CA1 in a chronic model of temporal lobe epilepsy. *J. Neurophysiol.* 76: 1282-1296, 1996.
- McBain, C.J., Dichiara, T.J., and Kauer, J.A. Activation of metabotropic glutamate receptors differentially affects two classes of hippocampal interneurons and potentiates excitatory synaptic transmission. *J. Neurosci.* 14: 4433-4445, 1994.
- Meier, C.L., and Dudek, F.E. Spontaneous and stimulation-induced synchronized burst afterdischarges in the isolated CA1 of kainate-treated rats. *J. Neurophysiol.* 76: 2231-2239, 1996.
- Mody, I., Stanton, P.K., and Heinemann, U. Activation of *N*-methyl-*D*-aspartate receptors parallels changes in cellular and synaptic properties of dentate gyrus granule cells after kindling. *J. Neurophysiol.* 50: 1033-1054, 1988.

- Morin, F., Beaulieu, C., and Lacaille, J.-C. Membrane properties and synaptic currents evoked in CA1 interneuron subtypes in rat hippocampal slices. *J. Neurophysiol.* 76: 1-16, 1996.
- Morin, F., Beaulieu, C., and Lacaille, J.-C. Selective loss of GABA neurons in area CA1 of the rat hippocampus after intraventricular kainate. *Epilepsy Res.*, 32: 363-369, 1998.
- Nadler, J.V., Perry, B.W., and Cotman, C.W. Selective reinnervation of hippocampal area CA1 and the fascia dentata after destruction of CA3-CA4 afferents with kainic acid. *Brain Res.* 182: 1-9, 1980a.
- Nadler, J.V., Perry, B.W., Gentry, C., and Cotman, C.W. Loss and reacquisition of hippocampal synapses after selective destruction of CA3-CA4 afferents with kainic acid. *Brain Res.* 191: 387-403, 1980b.
- Nadler, J.V. Kainic acid as a tool for the study of temporal lobe epilepsy. *Life Sci.* 29: 2031-2042, 1981.
- Nakajima, S., Franck, J.E., Bilkey, D., and Schwartzkroin, P.A. Local circuit synaptic interactions between CA1 pyramidal cells and interneurons in the kainate-lesioned hyperexcitable hippocampus. *Hippocampus* 1: 67-78, 1991.
- Nathan, T., Jensen, M.S., and Lambert, J.D.C. The slow inhibitory postsynaptic potential in rat hippocampal CA1 neurones is blocked by intracellular injection of QX-314. *Neurosci. Lett.* 110: 309-313, 1990.
- Olivier, M.W., and Miller, J.J. Inhibitory processes of hippocampal CA1 pyramidal neurons following kindling-induced epilepsy in the rat. *Can. J. Physiol. Pharmacol.* 63: 872-878, 1985.

- Perez, Y., Morin, F., Beaulieu, C., and Lacaille, J.-C. Axonal sprouting of CA1 pyramidal cells in hyperexcitable hippocampal slices of kainate-treated rats. *Eur. J. Neurosci.* 8: 736-748, 1996.
- Perez, Y., and Lacaille, J.-C. Spontaneous excitatory postsynaptic currents in hippocampal CA1 interneurons in the kainate model of epilepsy. *Soc. Neurosci. Abstr.* 23: 2153, 1997.
- Peterson, G.M., Ribak, C.E., and Oertel, W.H. A regional increase in the number of hippocampal GABAergic neurons and terminals in the seizure-sensitive gerbil. *Brain Res.* 340: 384-389, 1985.
- Pyapali, G.K., and Turner, D.A. Denervation-induced dendritic alterations in CA1 pyramidal cells following kainic acid hippocampal lesions in rats. *Brain Res.* 652: 279-290, 1994.
- Rempe, D.A., Mangan, P.S., and Lothman, E.W. Regional heterogeneity of pathophysiological alterations in CA1 and dentate gyrus in a chronic model of temporal lobe epilepsy. *J. Neurophysiol.* 74: 816-828, 1995.
- Rempe, D.A., Bertram, E.H., Williamson, J.M., and Lothman, E.W. Interneurons in area CA1 stratum radiatum and stratum oriens remain functionally connected to excitatory synaptic input in chronically epileptic animals. *J. Neurophysiol.* 78: 1504-1515, 1997.
- Rice, A., Rafiq, A., Shapiro, S.M., Jakoi, E.R., Coulter, D.A., and DeLorenzo, R.J. Long-lasting reduction of inhibitory function and γ -aminobutyric acid type A

- receptor subunit mRNA expression in a model of temporal lobe epilepsy. Proc. Natl. Acad. Sci. (USA) 93: 9665-9669, 1996.
- Sah, P., Hestrin, S., and Nicoll, R.A. Properties of excitatory postsynaptic currents recorded in vitro from rat hippocampal interneurons. J. Physiol. (Lond.) 430:605-616, 1990.
- Sik, A., Penttonen, M., Ylinen, A., and Buzsáki, G. Hippocampal CA1 interneurons: an *in vivo* intracellular labeling study. J. Neurosci. 15: 6651-6665, 1995.
- Sloviter, R.S. Decreased hippocampal inhibition and a selective loss of interneurons in experimental epilepsy. Science 235: 73-76, 1987.
- Sloviter, R.S. Permanently altered structure, excitability, and inhibition after experimental status epilepticus in the rat: the “dormant basket cell” hypothesis and its possible relevance to temporal lobe epilepsy. Hippocampus 1: 41-66, 1991.
- Sloviter, R.S. The functional organization of the hippocampal dentate gyrus and its relevance to the pathogenesis of temporal lobe epilepsy. Ann. Neurol. 35: 640-654, 1994.
- Turner, D.A., and Wheal, H.V. Excitatory synaptic potentials in kainic acid-denervated rat CA1 pyramidal neurons. J. Neurosci. 11: 2786-2794, 1991.
- Vick, R.S., Rafiq, A., Coulter, D.A., Jakoi, E.R., and DeLorenzo, R.J. GABA_A $\alpha 2$ mRNA levels are decreased following induction of spontaneous epileptiform discharges in hippocampal-entorhinal cortical slices. Brain Res. 721: 111-119, 1996.

Williams, S., Vachon, P., and Lacaille, J.-C. Monosynaptic GABA-mediated inhibitory postsynaptic potentials in CA1 pyramidal cells of hyperexcitable hippocampal slices from kainic acid-treated rats. *Neuroscience* 52: 541-554, 1993.

Williams, S., Samulack, D.D., Beaulieu, C., and Lacaille, J.-C. Membrane properties and synaptic responses of interneurons located near the stratum lacunosum-moleculare/radiatum border of area CA1 in whole-cell recordings from rat hippocampal slices. *J. Neurophysiol.* 71: 2217-2235, 1994.

Table 1. Membrane properties of interneurons and pyramidal cells from control and KA-treated rats

	Interneurons			Pyramidal cells		
	O/A	LM	Kainate (n=8)	Control (n=11)	Control (n=10)	Kainate (n=8)
Control (n=5)						
RMP (mV)	-46.8±0.9(4)	-51.3±1.8	-52.3±1.5	-49.7±1.3	-53.5±1.3	-58.4±1.0*
Action potential amplitude (mV)	81.2±6.2	106.0±3.4*	92.0±4.6	82.5±4.7	103.0±3.5	114.2±7.8
Action potential duration (ms)	2.2±0.3	2.0±0.1	2.3±0.2	2.6±0.2	2.8±0.2	2.5±0.2
fAHP amplitude (mV)	12.8±2.3	8.0±3.0	9.0±1.4	15.0±3.6	3.2±1.0	4.9±0.8
mAHP amplitude (mV)	3.8±2.7	5.9±1.8	7.0±1.1	9.4±1.2	2.9±0.7	2.5±0.7
Time constant (ms)	28.2±3.4	35.2±4.5	32.3±6.4	34.2±5.9	42.0±4.5	49.2±2.7
R _{in} peak (MΩ)	188.0±26.3	185.0±29.6	150.0±25.1	198.0±17.1	103.9±10.4	99.4±8.3
R _{in} end (MΩ)	136.0±19.3	107.0±20.4	124.0±14.0	150.0±8.8	83.6±9.5	78.1±6.7
Rectification ratio #	1.4±0.1	1.8±0.2	1.2±0.1	1.3±0.1	1.1±0.1	1.4±0.03

Data are expressed as mean ± sem

* Significantly different from controls (t-test, p<0.05).

rectification ratio (R_{in} peak/R_{in} end)

Table 2. Properties of evoked excitatory postsynaptic currents in interneurons and pyramidal cells from control and KA-treated rats

EPSCs	Interneurons			Pyramidal cells		
	O/A	LM	Kainate (n=5)	Control (n=13)	Kainate (n=10)	Control (n=10)
Conductance of fast EPSCs (nS)	9.2±2.2	12.1±3.6	4.9±0.9	2.3±0.4*	8.7±2.0	10.2±3.0
Conductance of slow EPSCs (nS)	6.7±1.9	11.1±3.4	3.8±0.5	2.4±0.4*	4.2±1.0	5.7±1.8
Amplitude of fast EPSCs (pA) #	748.5±159.7	755.0±225.4	277.5±50.2	143.7±30.1(11)*	737.9±171.2(11)	746.0±123.2
Amplitude of slow EPSCs (pA) ‡	265.0±89.0	591.6±200.1	181.0±50.2(7)	116.7±24.5(9)	110.0±29.8	244.0±107.0(9)
Rise time of fast EPSCs (ms) #	10.3±3.4	6.9±4.2	5.6±1.5	3.2±0.3(9)	11.6±1.0	10.3±1.8
Decay time constant of fast EPSCs (ms) #	82.4±12.0	24.2±6.1*	37.4±8.0	22.4±6.4(9)	172.9±40.7	144.5±33.3(9)

Data are expressed as mean ± sem.

* Significantly different from controls (t-test, p<0.05).

measured at holding potential near -80 mV.

‡ measured at holding potential near 60 mV.

Table 3. Properties of evoked inhibitory postsynaptic currents in interneurons and pyramidal cells of control and KA-treated rats

IPSCs	Interneurons			Pyramidal cells		
	O/A	LM	Kainate (n=10)	Control (n=11)	Kainate (n=10)	Control (n=10)
Conductance (nS)	13.7±5.1	15.5±5.0	9.1±1.7	11.2±3.4	15.6±3.8	23.8±6.1
E_{rev} (mV)	-44.2±5.8	-37.8±3.4	-35.3±3.6	-33.2±2.4	-49.1±3.9	-47.1±3.9
Amplitude (pA) #	221.0±117.6	280.2±107.4	166.9±38.6	205.4±54.7	317.8±65.7	506.5±141.9
Rise time (ms) #	9.0±1.5(4)	9.8±4.0	9.4±1.6	10.7±1.1	12.3±1.0(7)	8.6±0.6*
Decay time constant (ms) #	61.5±5.8	45.5±9.4	74.4±9.1	76.6±7.2	135.4±15.7	93.2±10.0*

Data are expressed as mean ± sem.

* Significantly different from controls (t-test, p<0.05).

measured at holding potential near -80 mV.

Figure Legends

Figure 1: (A-B) Light photomicrographs of Nissl-stained sections of the hippocampus showing cells located in dentate gyrus, CA3 and CA1 regions. Principal cells of the dentate gyrus and CA3-CA1 areas were intact in control rats (A; CA3 indicated by arrows). In contrast, cells of the CA3 area (B; indicated by arrows) were selectively lost after bilateral intracerebroventricular injections of kainic acid, while principal cells of the CA1 area and dentate gyrus were undamaged.

Figure 2: (A-B) Schematic drawings of hippocampal slices (left) showing the placement of electrodes for extracellular stimulation and field potentials recordings in slices from control (A) and KA-treated (B) rats. Field potentials were recorded in stratum pyramidale and evoked by stimulation of afferent fibers in stratum radiatum. Representative examples of field responses (right) from a slice of a control rat (A) showing a single population spike, and a hyperexcitable slice of a KA-treated rat (B) consisting of multiple population spikes (stimulation indicated by arrow).

Figure 3: Compound excitatory and inhibitory postsynaptic currents (PSCs) recorded in representative LM (A) and pyramidal (B) cells of control and KA-treated rats. PSCs evoked by stimulation of afferent fibers (200 μ A intensity) were inward at a membrane potential of -80 mV. PSCs were smaller in amplitude in LM interneurons (A) of KA-treated rats (right trace) relative to control (left trace). In pyramidal cells (B) of KA-treated rats (right trace), responses were increased in amplitude relative to

control animals (left trace). (C) Summary histogram of mean values of peak amplitude of PSCs evoked in interneurons in O/A, LM and pyramidal cells of control (open bars) and KA-treated (filled bars) rats. Mean amplitude of PSCs was not significantly different in O/A and LM interneurons of KA-treated rats. In contrast, mean amplitude of PSCs was significantly increased in pyramidal cells of KA-treated animals (*, p<0.05).

Figure 4: Changes in pharmacologically isolated EPSCs after KA treatment. (A) Averaged fast (open circle) and slow (open square) EPSCs evoked in the presence of 25 μ M bicuculline in a representative LM interneuron from a control rat, at different membrane potentials (-108 to 32 mV). (B) In a LM cell of a KA-treated rat, the amplitude of both components of EPSCs (filled circles and squares) evoked in similar conditions were reduced. (C-D) Current-voltage (I-V) relationships of fast (C) and slow (D) components of EPSCs for the cells shown in A and B. Slope conductance, obtained from the linear portion (dotted lines) of each I-V relation, was reduced in the cell of the KA-treated rat (filled symbols) relative to the control cell (open symbols). (E-F) EPSCs were antagonized by non-NMDA and NMDA receptor antagonists (20 μ M CNQX and 50 μ M AP5, respectively). Fast and slow EPSCs from representative LM interneurons were significantly reduced by 92 and 68%, respectively in the control rat (E), and by 69 and 77%, respectively in the KA-treated animal (F) (note the difference in calibration bars in E and F). (G) Summary histogram of mean values for all cells (expressed as fraction of control). In KA-treated rats, the conductance of fast and slow EPSCs (g_{fast} and g_{slow} , respectively) were significantly

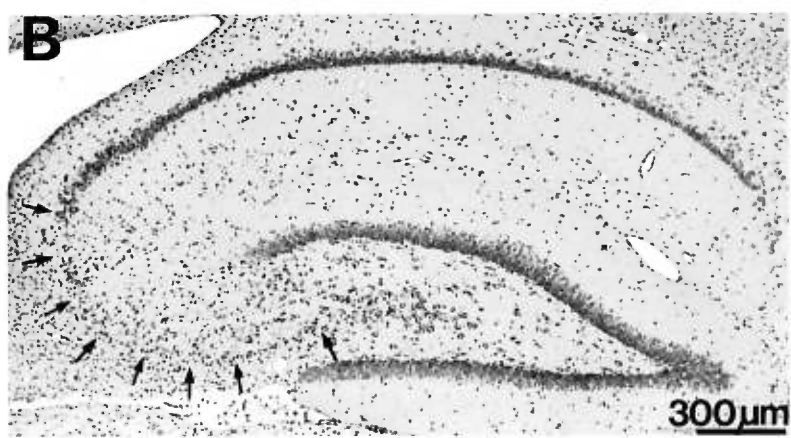
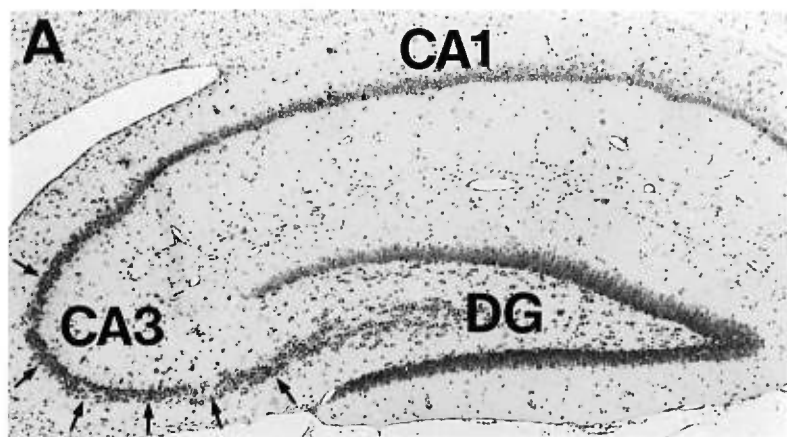
reduced in LM cells (filled bars), but not in O/A (open bars) or pyramidal (hatched bars) cells. The EPSC decay time constant, obtained from single-exponential fitting of the decay phase, was reduced in all cell types, but this was significant only for O/A cells (*, p<0.05).

Figure 5: Changes in monosynaptic GABA_A IPSCs after KA treatment. (A-B) Series of averaged IPSCs recorded at different membrane potentials (-80 to 60 mV) from representative pyramidal cells of control (A) and KA-treated (B) rats in the presence of non-NMDA and NMDA antagonists (20 μM CNQX and 50 μM AP5, respectively). The peak IPSC amplitude was larger in the cell of KA-treated rats (filled circle; B) relative to control (open circle; A). (C) I-V relations of IPSCs shown in A and B. The IPSC conductance, obtained from the slope of the linear regression (dotted lines), was larger in the cell from the KA-treated animal. (D-E) Reversible antagonism of IPSCs by the GABA_A antagonist, bicuculline in representative LM interneurons from control (D) and KA-treated (E) rats. After bath application of 25 μM bicuculline, IPSCs were reduced by 88% and 93% in the LM cell of control and KA-treated rats respectively (+BIC, middle trace). After the washout of the antagonist (CNQX/AP5, right traces), IPSC amplitude partially recovered in both cells. (F) Summary histogram of conductance (g_{IPSC}), rise time and decay time constant of GABA_A IPSCs in cells of KA-treated rats, expressed as fraction of control, for all cell types (O/A: open bars; LM: filled bars; pyramidal cells: oblique bars). The IPSC conductance was not significantly different in any cell type

after KA treatment. The IPSC rise time and decay time constant were significantly faster in pyramidal cells of KA-treated rats (*, p<0.05).

Figure 6: Schematic diagram of alterations in hippocampal CA1 inhibitory circuits after KA treatment. (A) In the normal hippocampus, two types of inhibitory interneurons are represented in stratum oriens near the alveus, the vertical (V) and the horizontal (H) cells. Both cell types receive an excitatory input (open terminals) from pyramidal cells (P) and subsequently make inhibitory contacts (filled terminals) onto the principal cells, thus mediating feedback inhibition. The axonal projections of CA3 pyramidal cells, the Schaffer collaterals (Sch), make excitatory connections onto CA1 pyramidal cells, but also on vertical cells and on other interneurons located at the border of stratum radiatum and stratum lacunosum-moleculare (LM), the stellate cells (S). Through these pathways, these interneurons mediate feedforward inhibition. (B) Two weeks after KA treatment, there is a partial loss of CA3 afferents to CA1 (broken lines), and consequently a decrease of excitatory drive from CA3 onto interneurons involved in feedforward inhibition (V and S cells). However, only stellate cells remain partially deafferented and have reduced excitatory drive. Sprouting of CA1 pyramidal cell axons takes place and new excitatory terminals (marked by asterisks) may be formed onto neighboring pyramidal cells and onto interneurons. These latter contacts may compensate for the partial deafferentation of interneurons in stratum oriens induced by KA. A partial loss of somatostatin- and parvalbumin-immunopositive interneurons (H cells) is also observed after KA treatment (broken outline). Since no decrease in monosynaptic inhibition of

pyramidal cells was observed, compensatory mechanisms such as axonal sprouting of inhibitory inputs from KA-resistant interneurons may take place (inhibitory terminals marked by question marks and asterisks), or other functional changes may occur at inhibitory synapses of KA-resistant interneurons.



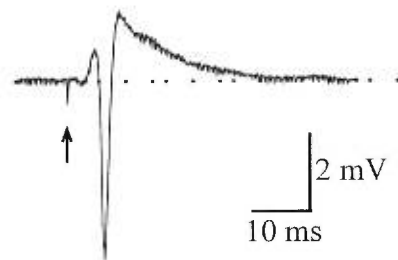
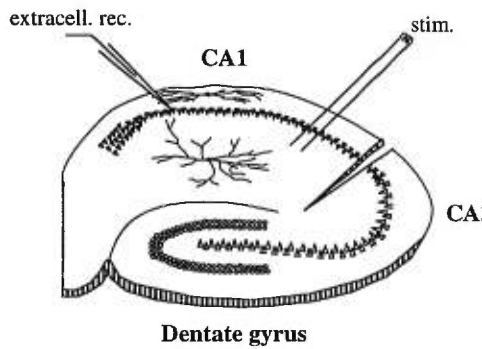
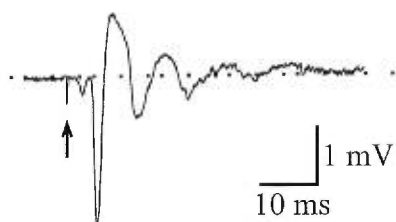
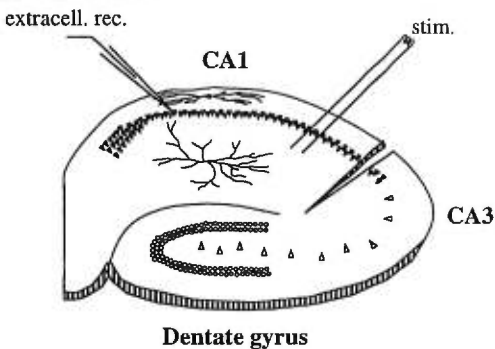
A Control**B Kainate**

Figure 2

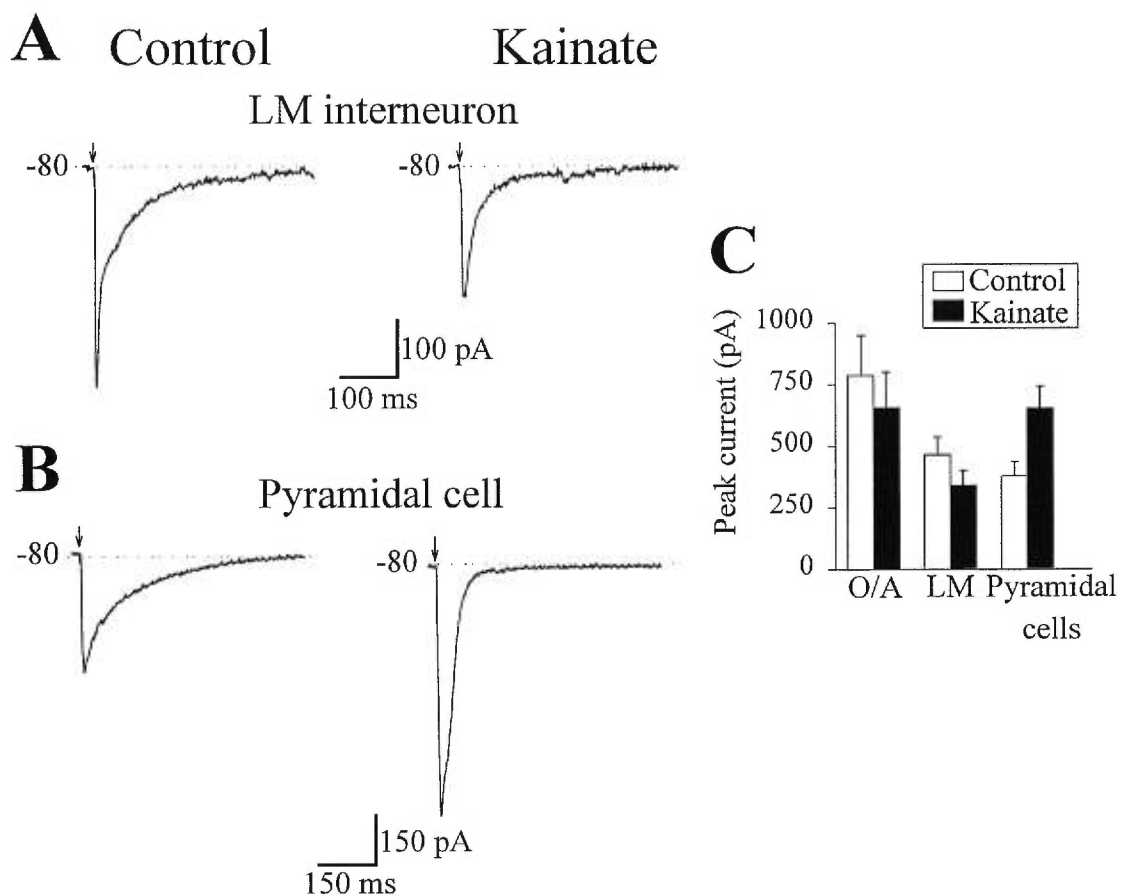


Figure 3

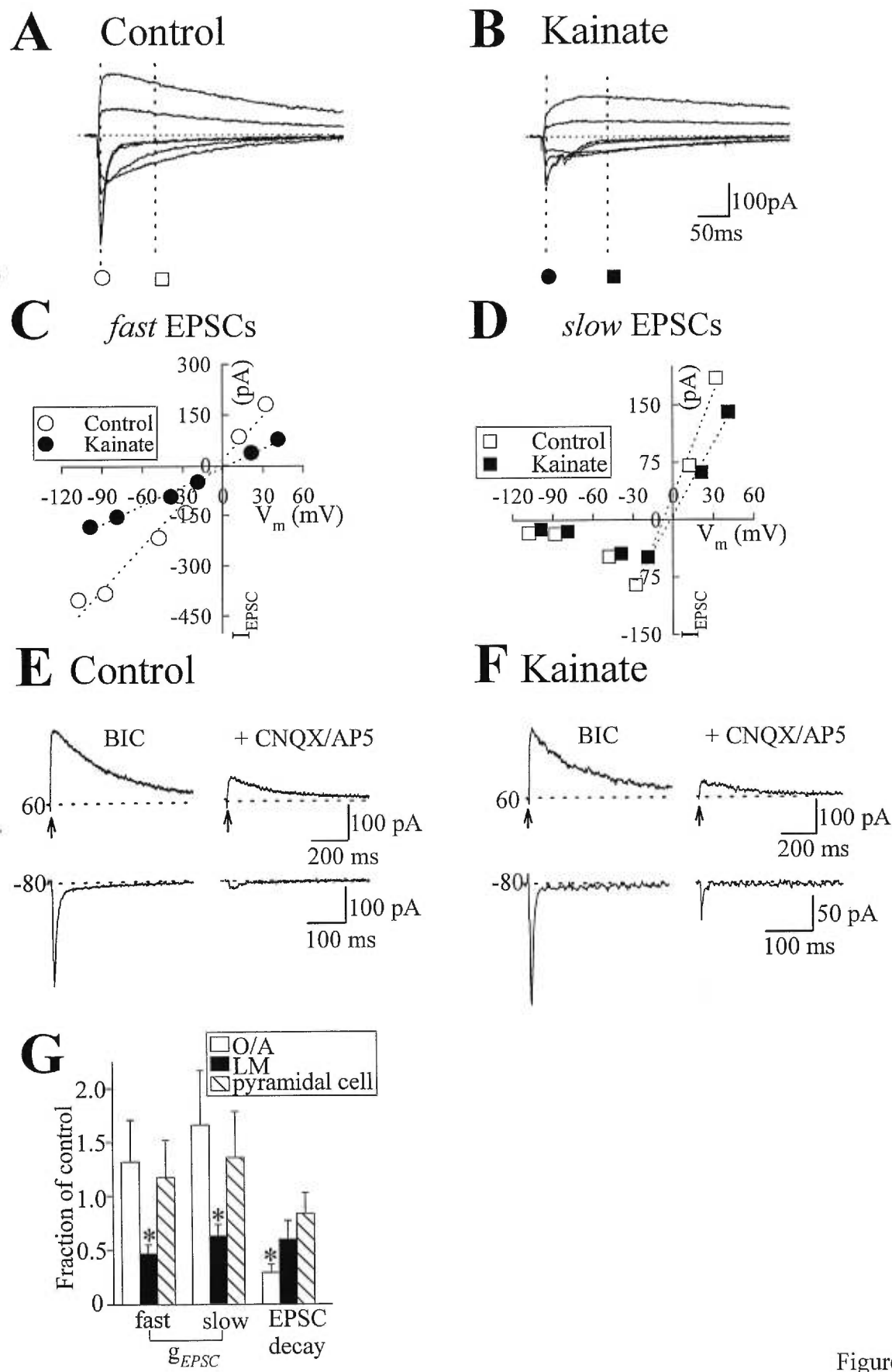


Figure 4

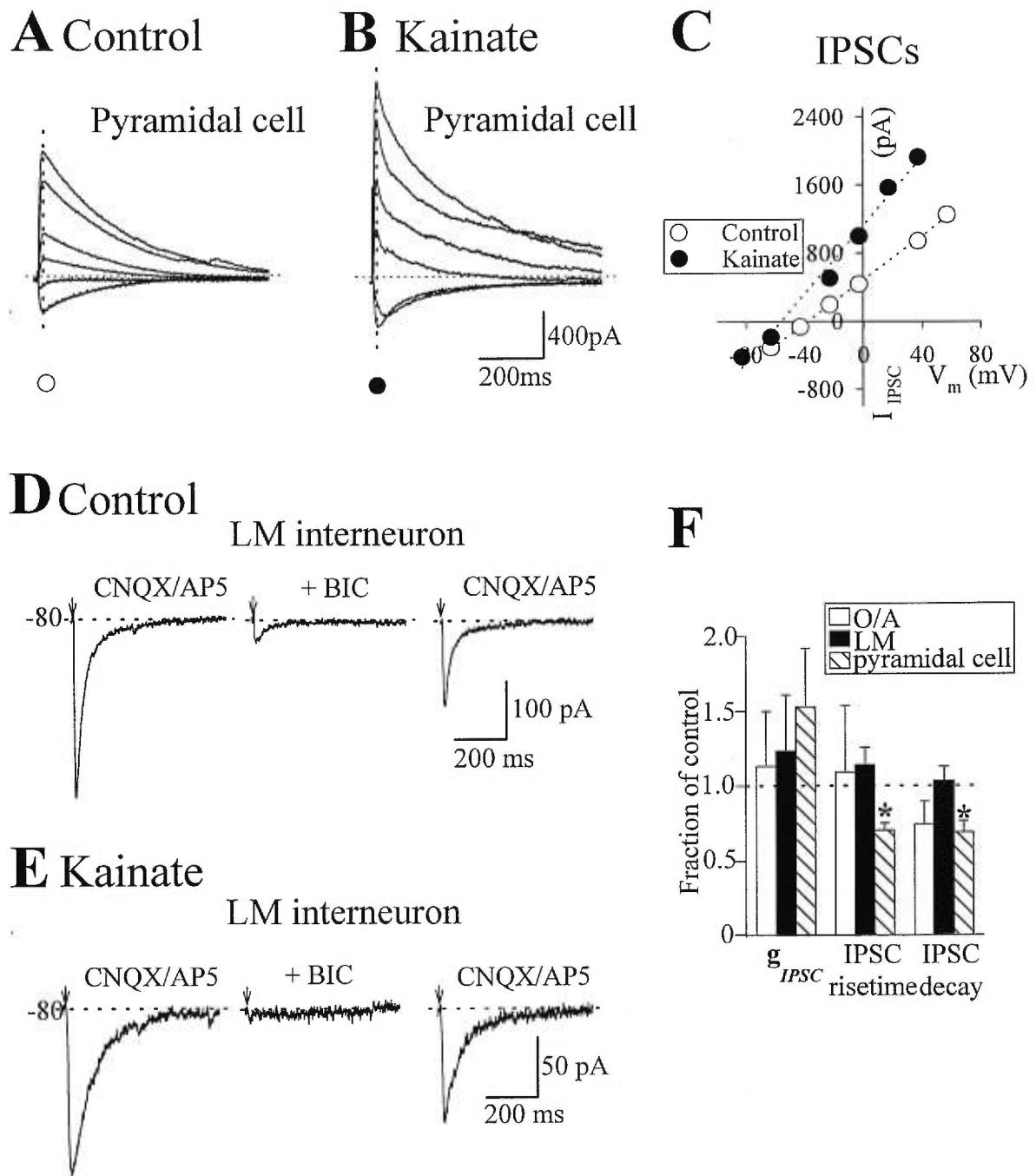


Figure 5

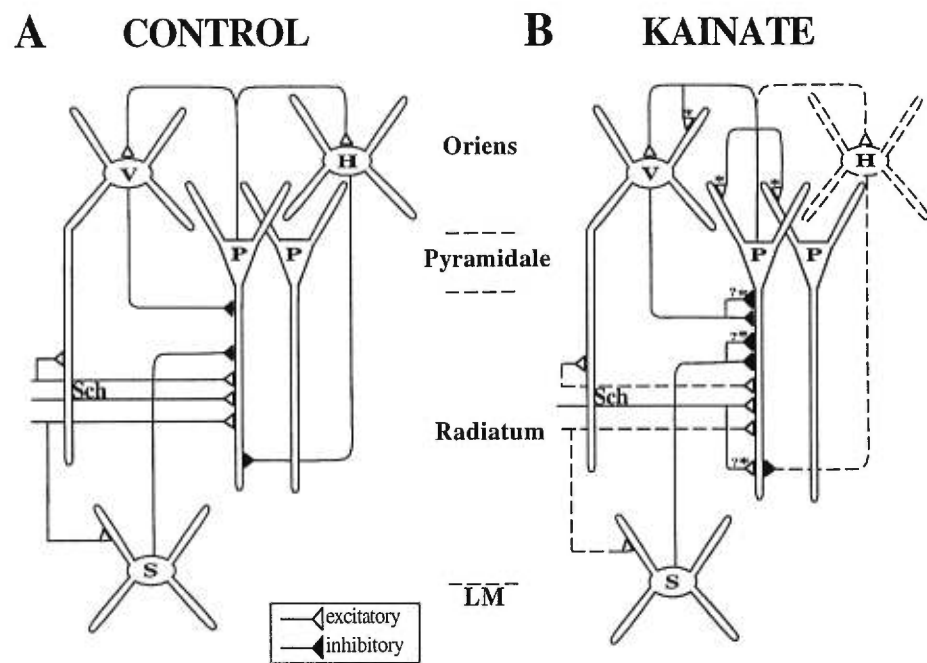


Figure 6

CHAPITRE CINQUIÈME

**ALTÉRATIONS DES SYNAPSES PÉRISOMATIQUES GABA DANS LES
INTERNEURONES INHIBITEURS ET LES CELLULES PYRAMIDALES DE
LA RÉGION CA1 DE L'HIPPOCAMPE DANS LE MODÈLE
D'ÉPILEPSIE DE L'ACIDE KAÏNIQUE**

**Alterations of perisomatic GABA synapses on hippocampal CA1 inhibitory
interneurons and pyramidal cells in the kainate model of epilepsy**

F. Morin, C. Beaulieu and J.-C. Lacaille

Centre de recherche en sciences neurologiques and Département de physiologie,
Université de Montréal, Montréal, Québec, CANADA, H3C 3J7

sous presse dans Neuroscience

Abstract

In the kainic acid model of epilepsy, electrophysiological and anatomical modifications occur in inhibitory circuits of the CA1 region of rat hippocampus. Using postembedding GABA immunocytochemistry and electron microscopy, we characterized perisomatic GABA and non-GABA synaptic contacts in CA1 pyramidal cells and GABAergic interneurons of stratum oriens/alveus (O/A) and stratum lacunosum-moleculare (LM), and examined if changes occurred at these synapses at two weeks post-kainic acid treatment. We found that in control rats the number and total length of perisomatic *GABA* synapses were significantly smaller (approximately by 40-50%) in LM interneurons than in O/A interneurons and pyramidal cells. Additionally, the number and total length of perisomatic *non-GABA* synapses were different among all cell types, with these parameters significantly increasing in the following order: pyramidal cells << LM interneurons < O/A interneurons. Following kainic acid treatment, we found that the number and total length of GABA synapses were significantly increased in LM interneurons (by 76 and 100%, respectively), but were unchanged in pyramidal cells and O/A interneurons. In addition, the mean length of individual GABA synapses was significantly increased (by 17%) in pyramidal cells after KA treatment. In contrast, no changes were observed at non-GABA synapses in any cell type examined after kainic acid treatment.

These results indicate that in control animals the ultrastructural correlates of perisomatic GABA inhibition are less pronounced in LM than O/A interneurons or pyramidal cells, whereas those of perisomatic excitation are more prominent in O/A

than LM interneurons, and much less present in pyramidal cells. In addition, our results with kainic acid-treated animals suggest that cell-specific changes in perisomatic inhibition may occur in CA1 inhibitory interneurons in the chronically hyperexcitable hippocampus. The ultrastructural correlates of perisomatic inhibition were increased in LM interneurons, which may thus suggest some disinhibition of pyramidal cells. However, the ultrastructural correlates of perisomatic inhibition were increased in pyramidal cells, implying some enhancement of perisomatic inhibition of principal cells in the hyperexcitable hippocampus.

Key words: interneurons, GABA, hippocampus, electron microscopy, immunocytochemistry, epilepsy

Intracerebroventricular injections of kainic acid (KA) in rats is an animal model of epilepsy which has been useful to study the basic mechanisms involved in the generation of epileptiform activity.^{6,40} In this model, there is a selective loss of dentate hilar cells, hippocampal CA3 pyramidal cells and specific CA1 interneuron subtypes, while surviving CA1 pyramidal neurons become hyperexcitable, features which are common to some human temporal lobe epilepsies.^{6,7,37,40,41,56} The hyperexcitability of CA1 pyramidal cells is due to multiple factors including an increase in *N*-methyl-*D*-aspartate (NMDA) excitatory synaptic transmission⁵⁴ and a decrease in polysynaptic γ -aminobutyric acid (GABA)-mediated inhibitory synaptic transmission.^{18,56} Intracellular and whole-cell recordings have demonstrated that monosynaptic inhibitory postsynaptic responses appear intact in hyperexcitable CA1 pyramidal cells after KA treatment^{38,56}, suggesting that the reduction in polysynaptic inhibition may be due to a decrease in excitatory drive on inhibitory interneurons. In support of this, a cell-specific reduction of evoked excitatory postsynaptic currents (EPSCs) has been observed in interneurons of stratum lacunosum-moleculare (LM) in KA-treated rats.³⁸ Therefore, a partial deafferentation of certain inhibitory subtypes of interneurons and a specific loss of other subtypes may contribute to the polysynaptic epileptiform activity in the chronically hyperexcitable CA1 region after KA treatment.

In the alumina gel model of epilepsy, a significant decrease of GABA-immunopositive punctate profiles and synapses was reported in epileptic foci.^{25,44,45} In epileptic patients, a loss of inhibitory synapses on the soma and axon initial

segment of pyramidal cells was found in epileptic peritumoural neocortex.³³ In contrast, an immunocytochemical study has shown that glutamic acid decarboxylase-immunoreactive neurons and punctate profiles were preserved in hippocampal foci.⁴ In KA-treated animals, a significant reduction of parvalbumin-immunoreactive terminals was observed at the soma and proximal dendrites of CA1 pyramidal cells.⁸ Since parvalbumin-immunoreactive cells are GABAergic, such loss was proposed to contribute to the hyperexcitability of CA1 pyramidal cells.⁸ However, it remains undetermined if perisomatic *GABAergic* synaptic terminals are lost on CA1 pyramidal cells after KA treatment.

The aim of the present study was to characterize perisomatic GABA synaptic contacts using postembedding GABA immunocytochemistry and electron microscopy in CA1 pyramidal cells and in inhibitory interneurons of stratum oriens/alveus (O/A) and stratum lacunosum-moleculare (LM) in normal animals, and then examine how these synaptic contacts change at two weeks post-KA treatment. Since previous physiological findings suggested a cell-specific reduction of excitatory inputs of LM interneurons after KA treatment³⁸, we also investigated perisomatic non-GABA synaptic contacts in normal animals and after KA treatment. Our results suggest ultrastructural differences in perisomatic GABA and non-GABA synapses between these cell types in normal animals. In addition, following KA treatment, changes at GABA synaptic contacts were indicative of cell-specific increases in the ultrastructural correlates of perisomatic inhibition.

Experimental Procedures

For KA lesions, male Sprague-Dawley rats (Charles River, n=4) were injected intracerebroventricularly with kainic acid.^{38,41} Briefly, adult rats (150-160 g) were anesthetized with ketamine (165 mg/kg i.m.), xylazine (10 mg/kg i.m.) and atropine (0.27 mg/kg i.p.). Rats were positioned in a stereotaxic apparatus and bilateral intracerebroventricular injections of kainic acid (0.55 µg/µl, 0.9% saline, pH 7.3-7.4) were made using a 10 µl Hamilton syringe. Stereotaxic coordinates of the injection site were 0.6 mm posterior to bregma, 2.0 mm lateral to the midline, and 3.5 mm ventral to the dura. Each KA injection lasted 30 minutes. The wound was then treated with an aerosol antibiotic (Neosporin) and closed with sutures. The animals were returned to their cages and given water and food *ad libitum* for a period of two weeks. All efforts were made to minimize animal suffering, to reduce the number of animals used, and to utilize alternatives to *in vivo* techniques. This protocol conforms to the guidelines of the Canadian Council for the Protection of Animals (Comité de déontologie de l'expérimentation sur les animaux de l'Université de Montréal).

Tissue processing

Chemicals were obtained from Sigma (St. Louis, MO) unless otherwise stated. KA-treated and control (weight-matched unoperated rats, 225-250 g, n=4) animals were deeply anesthetized with sodium pentobarbital (65mg/kg i.p.) and perfused through the aorta with 0.1 M cacodylate buffer (CB, pH 7.4; room temperature) followed by a solution containing 2% paraformaldehyde (Fisher, Fair

Lawn, NJ), 2.5% glutaraldehyde (J.B.EM, St-Laurent, Qc), 3.0 mM calcium chloride in CB. The brain was removed and postfixed in the same fixative for 1 hour at room temperature and then rinsed in 0.1 M CB. For each hemisphere, a block of tissue containing the hippocampus was trimmed. Transverse sections (100 μ m-thick) of the hippocampus were cut on a Vibratome and processed for electron microscopy. Sections were postfixed in 1% osmium tetroxide (J.B.EM, St-Laurent, Qc) in 0.1 M CB for 30 minutes, and then in 1% osmium tetroxide and 1.5% potassium ferrocyanide in CB for 10 minutes. Following many washes in 0.1 M phosphate buffer (PB, pH 7.4), sections were dehydrated in graded alcohols and propylene oxide, and then embedded in Durcupan ACM resin (Fluka). Tissue blocks containing the CA1 area were cut and re-embedded in resin for electron microscopic examination. Series of ultrathin (50 nm-thick) sections were cut on an ultramicrotome (Ultracut S, Reichert) and placed on single slot nickel grids coated with Pioloform.

GABA postembedding immunocytochemistry

Ultrathin sections were processed for GABA immunocytochemistry as in previous studies^{5,34,35} according to a modified protocol of Somogyi et al.⁵³ and Beaulieu et al.⁵ Briefly, sections were treated with 1% periodic acid (5 min) and then in 1% sodium borohydride in Tris-buffered saline (TBS, 0.05 M Tris buffer and 0.9% NaCl, pH 7.4, 5 min). Sections were placed in 1% ovalbumin in TBS (30 min) and then incubated in rabbit anti-GABA antiserum⁵ diluted 1:3,000 in a solution of 1% normal goat serum in TBS (90 min). Sections were treated with 1% bovine serum

albumin and 0.5% Tween in Tris buffer (pH 7.6, 2x5 min), and then incubated in goat anti-rabbit IgG-coated colloidal gold (15 nm, Janssen) diluted 1:25 in the previous solution (2 hrs). Between the different steps, grids were rinsed in TBS. Finally, sections were treated with 1% glutaraldehyde (1 min), washed in distilled water and stained with uranyl acetate (2 min) and lead citrate (2 min).

Electron microscopic analysis of GABA and non-GABA synapses

The alveus, stratum pyramidale and stratum lacunosum-moleculare were first delimited in the hippocampal CA1 area at low magnification. Somata were identified by the presence of a nucleus, endoplasmic reticulum and Golgi apparatus. GABA-immunopositive interneurons located (1) in stratum oriens/alveus (O/A), or (2) in stratum lacunosum-moleculare (LM) were identified in single sections and selected for study. Due to the low density of interneurons in ultrathin sections, cells were sampled in multiple blocks of tissue. Cells selected from the same tissue block were sampled in sections with a distance interval >50 μm . GABA-immunonegative pyramidal cells in stratum pyramidale were selected randomly in sections where interneurons were found and usually 2-3 pyramidal cells were selected in a section. Using a computerized image analysis system, the perimeter of the soma and proximal dendrites of a selected neuron was determined on individual ultrathin sections (magnification 3,900-5,200X). Synaptic contacts (synapses) were examined at a magnification of 34,000X and defined as closely apposed presynaptic and postsynaptic membrane profiles, separated by a synaptic cleft, and a presynaptic profile containing at least three synaptic vesicles. A profile was considered

immunopositive for GABA when its density of gold particles was several times higher than that of the background. The density of gold particles was variable but was usually clearly differentiable between GABA-immunopositive (GABA) and GABA-immunonegative (non-GABA) elements. In occasional ambiguous cases (eg. Figure 3C), the presence of symmetric or asymmetric pre- and postsynaptic densities was also used to classify uncertain GABA-positive and -negative terminals, respectively. To obtain a quantitative estimate of the difference in immunogold labeling, we measured the density of gold particles in a subset of our sample of GABA and non-GABA boutons and cells. Particle density was significantly higher in these GABA (34.1 ± 8.0 particles/bouton) than non-GABA (0.7 ± 0.3 particles/boutons) boutons ($n=10$ each; $p<0.0005$). Particle density in a $0.5 \mu\text{m}^2$ postsynaptic area adjacent to the synaptic boutons was significantly greater in O/A (13.0 ± 5.1 particles/ $0.5 \mu\text{m}^2$, $n=6$) and LM (11.1 ± 2.1 particles/ $0.5 \mu\text{m}^2$, $n=9$) interneurons than in pyramidal cells (1.2 ± 0.5 particles/ $0.5 \mu\text{m}^2$, $n=5$) or background (1.1 ± 0.4 particles/ $0.5 \mu\text{m}^2$, $n=20$; ANOVA and Student-Newman-Keuls pairwise tests, $p<0.05$). The number and total length of GABA and non-GABA synaptic contacts were calculated and normalized to the perimeter of the soma and proximal dendrites sampled for each cell to avoid the likelihood of significant differences in these parameters due to variations in cell perimeter sampled.⁴⁵ In addition, the length of synaptic contacts was measured at individual GABA and non-GABA cell types.

Statistics

Statistical differences between the different cell types were examined using an analysis of variance (ANOVA, $p<0.05$) and post-hoc differences detected using the Student-Newman-Keuls test. The significance of differences between control and KA-treated animals was statistically assessed using unpaired t-tests ($p<0.05$). All data are given as mean \pm standard error.

Results

GABA and non-GABA synaptic contacts on interneurons and pyramidal cells

Postembedding GABA immunogold labeling was used to identify pyramidal cells and interneurons in the hippocampal CA1 region. GABA-immunonegative cells with a pyramidal-shaped soma located in stratum pyramidale were identified as pyramidal cells, whereas GABA-immunopositive cells with a soma located either in stratum oriens/alveus (O/A) or in stratum lacunosum-moleculare (LM) were selected as two groups of interneurons. In general, cells found in O/A and LM were GABA-immunopositive. GABA-immunonegative neurons in O/A or LM were not included in the study. Non-GABAergic neurons have been reported outside the CA1 pyramidal cell layer (e.g. displaced pyramidal cells⁴³ and giant cells²⁴).

We first examined the ultrastructure of interneurons and pyramidal cells, as well as their synaptic contacts in normal animals. The ultrastructural features of O/A and LM interneurons were similar, but were clearly different from those of pyramidal cells. The soma of GABA-immunopositive cells in O/A and LM were ovoid (Fig. 1A,

2A). As previously described for other hippocampal interneurons^{3,48}, the nuclear membrane of O/A and LM interneurons demonstrated invaginations, and the cytoplasm contained a high density of mitochondria, endoplasmic reticulum and Golgi apparatus (Fig. 1A, 2A). In contrast, the soma of the GABA-immunonegative pyramidal cells was pyramidal-shaped and was occupied to a larger extent by their nucleus⁴⁸ (Fig. 3A).

All three groups of cells received GABA and non-GABA synaptic contacts on their soma and proximal dendrites. At high magnification (34,000X), both GABA-immunonegative and GABA-immunopositive synaptic contacts were readily found on the soma and proximal dendrites of the GABA-immunopositive interneurons of O/A and LM (Fig. 1 and 2). Interestingly, a GABA-immunonegative synaptic contact was found on a GABA-immunopositive somatic spine on the LM interneuron illustrated (Fig. 2C). Both GABA-immunopositive and GABA-immunonegative synaptic contacts were also observed on the soma and proximal dendrites of pyramidal cells, but GABA-immunopositive terminals were much more frequent (Fig. 3B, C, D).

Quantitative analysis of synaptic contacts on interneurons and pyramidal cells in control animals

Since our qualitative assessment of synaptic contacts suggested differences between the three cell types examined, a more detailed analysis of the synaptic contacts was made in control animals. Significant differences were found in the incidence and total length of GABA and non-GABA synapses between cell types.

The number of GABA-immunopositive synaptic contacts, normalized to the cell perimeter sampled (number per 100 μm of membrane, $N_{L\text{-GABA}}$) was significantly smaller in LM interneurons than in O/A interneurons ($38.7\pm10.6\%$) and pyramidal cells ($40.9\pm10.0\%$) ($p<0.05$; Table 1). Similarly, the total length of GABA-immunopositive synaptic contacts, normalized to the cell perimeter sampled ($L_{L\text{-GABA}}$), was significantly smaller in LM interneurons than in O/A and pyramidal cells ($43.8\pm8.1\%$ and $51.3\pm7.0\%$, respectively; $p<0.05$; Table 1). Thus, LM interneurons have significantly less GABA synaptic contacts on their soma and proximal dendrites than O/A and pyramidal cells.

The number of GABA-immunonegative synaptic contacts ($N_{L\text{-non-GABA}}$) was significantly different between each cell group (Table 1). LM interneurons and pyramidal cells received significantly less GABA-immunonegative synaptic contacts than O/A interneurons ($47.0\pm10.3\%$ and $92.8\pm3.6\%$, respectively; $p<0.05$; Table 1). Similarly, the total length of GABA-immunonegative synaptic contacts ($L_{L\text{-non-GABA}}$) was significantly different between each cell group and was significantly smaller in LM interneurons and pyramidal cells than in O/A interneurons ($54.3\pm10.4\%$ and $81.7\pm5.1\%$, respectively; $p<0.05$; Table 1). Thus, O/A interneurons receive significantly more, pyramidal cells receive significantly less, and LM interneurons have an intermediate number of non-GABA synaptic contacts on their soma and proximal dendrites.

In contrast, the mean length of individual GABA and non-GABA synaptic contacts (not normalized to the cell perimeter) was not significantly different between cell groups (Table 1). Finally, our results also indicate that for both O/A and LM

interneurons, an equal proportion of GABA and non-GABA synaptic contacts was found on their soma and proximal dendrites, whereas pyramidal cells receive much greater GABA than non-GABA synaptic contacts (Table 1).

Changes in GABA synaptic contacts in interneurons and pyramidal cells after KA treatment

In KA-treated rats, the presence of hippocampal lesions was verified in osmicated 100 μm -thick tissue sections prior to tissue re-embedding for electron microscopy. Hippocampal sections of KA-treated animals demonstrated a loss of dentate hilar cells and CA3 pyramidal neurons, whereas these cell populations were intact in all control animals (data not shown; see³⁷). In KA-treated animals, blocks of the CA1 area were cut from hippocampal sections that demonstrated such lesions and re-embedded for electron microscopy. All KA-treated rats exhibited behavioral signs of seizures immediately following intracerebroventricular injection of KA. However, in the present study, no further behavioral monitoring or EEG recording were obtained in the two week period after KA treatment. Previous studies have documented behavioral and electrographic seizures using surface or depth electrodes in such KA-treated rats⁴⁰. Additionally, many other reports have shown that hippocampal slices of kainate-treated rats are hyperexcitable 2 weeks following such KA treatment^{18,38,41,54,56}.

At the ultrastructural level, interneurons and pyramidal cells from KA-treated rats were similar to their counterparts in control animals. An example of a GABA-immunopositive LM interneuron from a KA-treated rat is shown in Figure 4 with its

characteristic ovoid soma, nuclear invaginations and cytoplasm containing a high number of mitochondria, endoplasmic reticulum and Golgi apparatus. GABA-immunopositive and GABA-immunonegative synaptic contacts were also found on the soma and proximal dendrites of pyramidal cells and interneurons of O/A and LM in KA-treated animals (eg. Fig. 4B-D).

After KA treatment, cell-specific ultrastructural changes were observed at GABA synaptic contacts of interneurons and pyramidal cells. There was a tendency for the number of GABA-immunopositive synapses ($N_{L\text{-GABA}}$) to be increased in all cell types relative to control (O/A: $123.7 \pm 32.2\%$ of control; pyramidal cells: $111.2 \pm 19.9\%$ of control), however this increase was significant only for LM interneurons ($175.6 \pm 30.7\%$ of control) (Table 1). Similarly, the total length of GABA-immunopositive synaptic contacts ($L_{L\text{-GABA}}$) was significantly longer only in LM interneurons of KA-treated rats ($200.0 \pm 37.3\%$ of control) (Table 1), whereas a tendency for a longer total length was observed in O/A interneurons ($115.6 \pm 41.0\%$ of control) and pyramidal cells ($127.1 \pm 20.4\%$ of control) (Table 1). Since KA-treated rats were compared with unoperated controls, the alterations observed at GABA synaptic contacts could be due to non-specific changes caused by the intracerebroventricular injection procedure. However, the changes were specifically observed in certain cell types and not in others, indicating that these modifications were not likely due to non-specific effects at GABA synaptic contacts in KA-treated rats.

Changes after KA treatment were specific to GABA synapses since no ultrastructural changes were observed at non-GABA synapses in the same groups.

Both the number and total length of GABA-immunonegative synaptic contacts were not significantly altered in pyramidal cells and interneurons of O/A and LM after KA treatment (Table 1).

To examine if the size of individual synaptic contacts were altered after KA treatment, the mean length of GABA-immunopositive and GABA-immunonegative synaptic contacts was calculated in each cell type. The mean length of GABA-immunopositive synaptic contacts was not significantly changed after KA treatment in interneurons of O/A ($90.5\pm9.5\%$ of control) or LM ($110.5\pm5.3\%$ of control) but was significantly increased in pyramidal cells ($117.4\pm4.3\%$ of control) (Table 1, Fig. 5). Analysis of the frequency distribution of synaptic contact length indicated that, after KA treatment, there was a decrease in the number of GABA-immunopositive synaptic contacts in pyramidal cells with a length $< 0.25 \mu\text{m}$ and an increase in the number of contacts with a length $> 0.25 \mu\text{m}$ (Fig. 5). These changes in mean length of synaptic contacts were limited to GABA synapses, since the mean length of GABA-immunonegative synaptic contacts was not significantly altered in any cell type after KA: interneurons of O/A ($100.0\pm14.3\%$ of control) or LM ($116.7\pm22.2\%$ of control) and pyramidal cells ($78.9\pm31.6\%$ of control) (Table 1, Fig. 5).

Discussion

Electron microscopy and postembedding immunogold staining for GABA were used (1) to characterize perisomatic GABA and non-GABA synaptic contacts on CA1 pyramidal cells and inhibitory interneurons located in stratum oriens/alveus

and stratum lacunosum-moleculare of normal rats, and (2) to examine if these synaptic contacts were altered in the chronic hyperexcitable hippocampus following KA treatment. In normal animals, our main findings were that the number and total length of perisomatic GABA synapses were significantly smaller in LM interneurons than in O/A interneurons and pyramidal cells. In addition, the number and total length of perisomatic non-GABA synapses were different among all cell types, with these parameters increasing significantly in the following order, pyramidal cells << LM interneurons < O/A interneurons. Thus, the ultrastructural correlates of perisomatic GABA inhibition may be less pronounced in LM interneurons than in O/A interneurons and pyramidal cells, whereas those of perisomatic non-GABA, likely glutamate, synaptic inputs may be more prominent in O/A interneurons than in LM interneurons and pyramidal cells. Finally, both types of interneurons received equal proportion of GABA and non-GABA perisomatic synapses, whereas pyramidal cells received a much greater proportion of perisomatic GABA than non-GABA synapses, suggesting a predominance of perisomatic inhibition over excitation only in pyramidal cells. In the chronically hyperexcitable hippocampus following KA treatment, the number and total length of GABA synapses were significantly increased in LM interneurons, but were not changed in pyramidal cells and O/A interneurons. In addition, the mean length of GABA synapses was significantly increased in pyramidal cells. In contrast, no changes were observed at non-GABA synapses on any cell type after KA treatment. Therefore, following KA treatment cell-specific changes in the ultrastructural correlates of perisomatic inhibition occur in CA1 inhibitory interneurons, and these modifications appear consistent with an

increase in perisomatic inhibition of LM interneurons, which could lead to some disinhibition of pyramidal cells. However, the ultrastructural correlates of perisomatic inhibition of pyramidal cells also appear increased, which could imply an enhancement of perisomatic inhibition of pyramidal cells.

Inhibitory inputs on GABAergic interneurons and pyramidal cells of normal rats

Our results indicated that perisomatic GABA synaptic contacts were just as numerous on pyramidal cells and O/A interneurons, but less on LM interneurons. GABA synaptic contacts located on the soma and proximal dendrites of pyramidal cells arise mostly from basket cells^{10,32,43,47,48} and trilaminar interneurons.⁵¹ It has been suggested that the functional role of this perisomatic inhibition may be to control the generation of somatic action potentials in principal cells.³⁶ Our results suggest that a similar function of perisomatic inhibition may be prominent in O/A interneurons but less pronounced in LM interneurons. The exact reason for the reduction in the ultrastructural correlates of perisomatic inhibition in LM interneurons relative to O/A interneurons remains unclear, but it may be due to a preferential perisomatic innervation of O/A interneurons by some afferents. Basket cells have been shown to preferentially make perisomatic synapses on both pyramidal cells and other interneurons¹³, however given that their axon arborizes mostly in or near stratum pyramidale, they are unlikely to provide such specific perisomatic input to O/A interneurons. Other subtypes of interneurons, immunoreactive to vasoactive intestinal polypeptide, specifically contact interneurons in stratum oriens/alveus, however their synaptic contacts are largely made on dendrites.^{1,2}

Septohippocampal GABAergic afferents have also been shown to contact the soma and dendrites of many types of inhibitory interneurons immunoreactive to various calcium binding proteins and neuropeptides.^{19,20,21} These septohippocampal GABA afferents may thus account for some of the perisomatic GABA contacts of O/A and LM interneurons since these interneurons have been shown to contain these peptides and calcium binding proteins.^{9,21,23,26} However, it remains unknown whether septohippocampal GABAergic afferents preferentially target interneurons located in stratum oriens/alveus versus those found in stratum lacunosum-moleculare.

Non-GABA synaptic inputs on GABA interneurons and pyramidal cells of normal rats

Glutamate is the neurotransmitter at excitatory synapses on hippocampal CA1 pyramidal cells and interneurons.^{15,46} Other types of synaptic terminals containing acetylcholine, noradrenaline or serotonin only account for 1% of synaptic terminals in CA1 stratum radiatum.⁵⁵ If the incidence of these terminals is similar in the layers sampled in the present study, the majority of non-GABA synaptic contacts found on CA1 interneurons are likely glutamatergic.

Our results indicated that perisomatic non-GABA synaptic contacts were more numerous on O/A than LM interneurons. The predominance of non-GABA synaptic contacts on O/A interneurons may be due to the presence of specific excitatory afferents impinging on them. Inhibitory interneurons located in stratum oriens/alveus, either vertical^{28,31} or horizontal⁹ interneurons receive major excitatory inputs from CA1 pyramidal cells. In contrast, interneurons located at the border of stratum radiatum and stratum lacunosum-moleculare receive their excitatory inputs

from Schaffer collaterals and entorhinal afferents, but not from CA1 pyramidal cells.^{27,30} Thus, the predominance of perisomatic non-GABA contacts on O/A interneurons may be due to an excitatory input originating from CA1 pyramidal cell collaterals.⁹ It is interesting to note that spontaneous excitatory synaptic activity is more marked in O/A than LM interneurons^{29,31}, which may be related to the increased incidence of perisomatic non-GABA synapses on O/A cells.

Our results also indicated that perisomatic non-GABA synaptic contacts were significantly less frequent in pyramidal cells than in interneurons. Electrical stimulation of excitatory afferents elicited EPSPs with faster risetime and which reached threshold at lower stimulation intensities in interneurons than pyramidal cells.^{28,30} Although inhibitory interneurons and pyramidal cells have distinct glutamate receptor mechanisms²² which likely contribute to differences in EPSP time course, the predominance of perisomatic non-GABA synapses in interneurons versus pyramidal cells suggest that the proximal location of excitatory synapses on interneurons may also favor excitatory synaptic efficacy in these cells.

Changes at GABA synaptic contacts following KA treatment

In the present study, ultrastructural changes were examined at two weeks after KA treatment. In this chronic state, CA3 pyramidal cells as well as subsets of dentate hilar neurons and CA1 inhibitory interneurons are lost, and CA1 pyramidal cells have become hyperexcitable.^{6,7,37,40} Our present results showed that the number and total length of GABA synapses were significantly increased in LM interneurons after KA treatment but were not altered in pyramidal cells and O/A interneurons. In addition,

the mean length of individual GABA synapses was significantly increased in pyramidal cells. These results are suggestive of an increased perisomatic inhibition in LM interneurons and pyramidal cells of KA-treated rats.

The increase in perisomatic GABA synapses in LM interneurons of KA-treated rats is consistent with the disinhibition hypothesis proposed in seizure-sensitive gerbils, which suggests that epileptiform activity may arise because of increased inhibitory inputs on inhibitory neurons.^{17,42} Our ultrastructural results appear contradictory to previous electrophysiological findings of unchanged evoked inhibitory postsynaptic currents (IPSCs) in LM interneurons of KA-treated rats.³⁸ However, the increase in the ultrastructural correlates of perisomatic inhibition and the intact evoked IPSCs would not be incompatible if there was an additional loss of dendritic inhibitory synapses in LM interneurons after KA treatment. Indeed, somatostatin-immunoreactive horizontal interneurons of stratum oriens, which make inhibitory dendritic contacts with pyramidal cells in stratum lacunosum-moleculare⁹, are lost after KA treatment.⁷ If these interneurons also make synaptic contacts with inhibitory interneurons, they could contribute to such a decrease in dendritic inhibitory synapses.

Our observed increase in length of individual perisomatic GABA synapses in pyramidal cells following KA treatment is inconsistent with the reported loss of parvalbumin (PV)-immunoreactive perisomatic inhibitory contacts of CA1 pyramidal cells.⁸ However, it has recently been demonstrated that while the density of PV-immunopositive interneurons was significantly reduced in seizure-sensitive gerbils, GABA-immunopositive neurons were intact.⁴⁹ Therefore, seizure activity may alter

the level of immunoreactive labeling for parvalbumin without necessarily causing the loss of PV-immunopositive neurons.⁴⁹ The level of GABA immunoreactivity has been reported to change in the dentate gyrus after seizure activity, but not in the CA1 region.⁵² The level of immunoreactive labeling for GABA in our study was unchanged after seizures since the density of gold particles in a subset of our GABA synaptic boutons was not significantly different between control and KA-treated animals (34.1 ± 8.0 vs 27.5 ± 5.8 particles/bouton, respectively; $n=10$ in each group). The hyperexcitability of CA1 pyramidal cells following KA treatment also appears paradoxical with the increase in the ultrastructural correlates of perisomatic inhibition observed in the present study. Furthermore, our recent electrophysiological evidence suggested that monosynaptic IPSCs were unchanged in CA1 pyramidal cells after KA treatment.³⁸ Again, the evidence of functionally unchanged inhibition in the presence of increased ultrastructural correlates of perisomatic inhibition of CA1 pyramidal cells suggest an additional loss of dendritic inhibitory synapses on pyramidal cells. In agreement with this suggestion, a specific subset of GABA interneurons immunoreactive to somatostatin located in stratum oriens, and which target dendritic portions of CA1 pyramidal cells appear lost following KA treatment.^{7,37} In addition, as previously suggested in the dentate gyrus¹⁴, the sprouting of axonal collaterals of inhibitory interneurons may lead to the formation of new GABA synaptic terminals on pyramidal cells and contribute to the increase of perisomatic inhibition in these cells. However, further experiments investigating morphological changes at earlier times after KA treatment will be useful in delineating the different compensatory changes that develop after KA lesions.

Non-GABA synaptic contacts are unaltered after KA treatment

Following KA treatment, a large number of excitatory CA3 afferents normally innervating CA1 pyramidal cells degenerate.⁴⁰ However, electron microscopic studies have suggested that newly formed excitatory synaptic terminals arising from KA-resistant CA3 afferents replace these lost synaptic contacts.³⁹ Sprouting of CA1 pyramidal cells axon collaterals takes place in KA-treated rats and this may contribute in part to the formation of new excitatory terminals on pyramidal cells and interneurons.⁴¹ In the present study, no significant change was observed at perisomatic non-GABA synaptic contacts on interneurons or pyramidal cells two weeks after KA treatment. Thus, we cannot determine if there was no change at all at perisomatic synapses, or whether there was a loss followed by a replacement of perisomatic non-GABA synapses.

These morphological results are consistent with electrophysiological evidence of intact amplitude and conductance of evoked excitatory postsynaptic currents (EPSCs) in pyramidal cells and O/A interneurons³⁸, as well as functional synaptic activation of CA1 interneurons¹⁶, after KA treatment. However, since the time course of EPSCs were altered in O/A interneurons after KA treatment, some changes may have occurred at their excitatory synapses.³⁸ Our results suggest that if these physiological changes are accompanied by ultrastructural changes, they may take place at dendritic, and not perisomatic, non-GABA synapses. Finally, the unchanged number of non-GABA synaptic terminals on LM interneurons of KA-treated rats appears inconsistent with our previous electrophysiological finding of reduced

amplitude and conductance of evoked EPSCs in LM interneurons after KA treatment.³⁸ However, an unchanged number of perisomatic non-GABA synaptic terminals on LM interneurons may still be compatible with a reduced excitatory drive in these interneurons, if a reduction of non-GABA synapses took place at dendritic locations.

Conclusions

Using postembedding immunogold labeling for GABA and electron microscopy, we found that the number and total length of perisomatic GABA and non-GABA synaptic contacts were significantly different between O/A, LM and pyramidal cells in normal animals. Our results suggest that LM interneurons receive less perisomatic GABAergic innervation than O/A interneurons and pyramidal cells. In addition, O/A interneurons were preferentially innervated by perisomatic non-GABA inputs compared to LM interneurons, whereas pyramidal cells received much less. The present study also indicated that in the chronically hyperexcitable hippocampus induced by KA treatment, cell-specific alterations take place at GABA synaptic contacts that are suggestive of an increase in perisomatic inhibition of LM interneurons and pyramidal cells.

Acknowledgements

This work was supported by the Fonds de la Recherche en Santé du Québec (FRSQ; J.-C. L.), the Medical Research Council of Canada (MRCC; J.-C. L. and C.B.), the Savoy Foundation (F.M.), a Research Center grant from the Fonds pour la Formation de Chercheurs et l'Aide à la Recherche (FCAR) to the Groupe de Recherche sur le Système Nerveux Central and an Équipe de Recherche grant from the FCAR (J.-C. L.).

References

1. Acsady L., Arabadzisz D. and Freund T. F. (1996a) Correlated morphological and neurochemical features identify different subsets of vasoactive intestinal polypeptide-immunoreactive interneurons in rat hippocampus. *Neuroscience* **73**, 299-315.
2. Acsady L., Arabadzisz D. and Freund T. F. (1996b) Different populations of vasoactive intestinal polypeptide-immunoreactive interneurons are specialized to control pyramidal cells or interneurons in the hippocampus. *Neuroscience* **73**, 317-334.
3. Babb T. L., Pretorius J. K., Kupfer W. R. and Brown W. J. (1988) Distribution of glutamate-decarboxylase-immunoreactive neurons and synapses in the rat and monkey hippocampus: Light and electron microscopy. *J. Comp. Neurol.* **278**, 121-138.
4. Babb T. L., Pretorius J. K., Kupfer W. R. and Crandall R. H. (1989) Glutamate decarboxylase-immunoreactive neurons are preserved in human epileptic hippocampus. *J. Neurosci.* **9**, 2563-2574.
5. Beaulieu C., Campistron G. and Crevier C. (1994) Quantitative aspects of the GABA circuitry in the primary visual cortex of the adult rat, *J. Comp. Neurol.* **339**, 559-572.
6. Ben-Ari Y. (1985) Limbic seizure and brain damage produced by kainic acid: mechanisms and relevance to human temporal lobe epilepsy, *Neuroscience* **14**, 375-403.

7. Best N., Mitchell J., Baimbridge K. G. and Wheal H. V. (1993) Changes in parvalbumin-immunoreactive neurons in the rat hippocampus following a kainic acid lesion. *Neurosci. Lett.* **155**, 1-6.
8. Best N., Mitchell J., and Wheal H. V. (1994) Ultrastructure of parvalbumin-immunoreactive neurons in the CA1 area of the rat hippocampus following a kainic acid injection. *Acta Neuropathol.* **87**, 187-195.
9. Blasco-Ibanez J. M. and Freund T. F. (1995) Synaptic input of horizontal interneurons in stratum oriens of the hippocampal CA1 subfield: structural basis of feed-back activation. *Eur. J. Neurosci.* **7**, 2170-2180.
10. Buhl E. H., Cobb S. R., Halasy K. and Somogyi P. (1995) Properties of unitary IPSPs evoked by anatomically identified basket cells in the rat hippocampus. *Eur. J. Neurosci.* **7**, 1989-2004.
11. Bundman M. C., Pico R. M. and Gall C. M. (1994a) Ultrastructural plasticity of the dentate gyrus granule cells following recurrent limbic seizures: I. Increase in somatic spines. *Hippocampus* **4**, 601-610.
12. Bundman M. C. and Gall C. M. (1994b) Ultrastructural plasticity of the dentate gyrus granule cells following recurrent limbic seizures: II. Alterations in somatic synapses. *Hippocampus* **4**, 611-622.
13. Cobb S. R., Halasy K., Vida I., Nyiri G., Tamas G., Buhl E. H. and Somogyi P. (1997) Synaptic effects of identified interneurons innervating both interneurons and pyramidal cells in the rat hippocampus. *Neuroscience* **79**, 629-648.

14. Davenport C. J., Brown W. J. and Babb T. L. (1990) Sprouting of GABAergic and mossy fiber axons in dentate gyrus following intrahippocampal kainate in the rat. *Exp. Neurol.* **109**, 180-190.
15. Davies S. N. and Collingridge G. L. (1989) Role of excitatory amino acid receptors in synaptic transmission in area CA1 of rat hippocampus. *Proc. R. Soc. of Lond.-B.* **236**, 373-384.
16. Esclapez M., Hirsch J.C., Khazipov R., Ben-Ari Y. and Bernard C. (1997) Operative GABAergic inhibition in hippocampal CA1 pyramidal neurons in experimental epilepsy. *Proc. Natl. Acad. Sci. (USA)* **94**, 12151-12156.
17. Farias P. A., Low S. Q., Peterson G. M. and Ribak C. E. (1992) Morphological evidence for altered synaptic organization and structure in the hippocampal formation of seizure-sensitive gerbils. *Hippocampus* **2**, 229-245.
18. Franck J. E., Kunkel D. D., Baskin D. G. and Schwartzkroin P. A. (1988) Inhibition in kainate-lesioned hyperexcitable hippocampi: physiologic, autoradiographic and immunocytochemical observations. *J. Neurosci.* **8**, 1991-2002.
19. Freund T. F. and Antal M. (1988) GABA-containing neurons in the septum control inhibitory interneurons in the hippocampus. *Nature* **336**, 170-173.
20. Freund T. F. (1992) GABAergic septal and serotonergic median raphe afferents preferentially innervate inhibitory interneurons in the hippocampus and dentate gyrus. *Epilepsy Res. (Suppl.)* **7**, 79-91.
21. Freund T. F. and Buzsaki G. (1996) Interneurons of the hippocampus. *Hippocampus* **6**, 347-470.

22. Geiger J. R. P., Melcher T., Koh D.-S., Sakmann B., Seeburg P. H., Jonas P. and Monyer H. (1995) Relative abundance of subunit mRNAs determines gating and Ca^{2+} permeability of AMPA receptors in principal neurons and interneurons in rat CNS. *Neuron* **15**, 193-204.
23. Gulyas A. I., Toth K., Danos P. and Freund T. F. (1991) Subpopulations of GABAergic neurons containing parvalbumin, calbindin D-28k, and cholecystokinin in the rat hippocampus. *J. Comp. Neurol.* **312**, 371-378.
24. Gulyas A. I., Toth K., McBain C. J. and Freund T. F. (1998) Stratum radiatum giant cells: a type of principal cell in rat hippocampus. *Eur. J. Neurosci.* **10**, 3813-3822.
25. Houser C. R., Harris A. B. and Vaughn J. E. (1986) Time course of the reduction of GABA terminals in a model of focal epilepsy: a glutamic acid decarboxylase immunocytochemical study. *Brain Res.* **383**, 129-145.
26. Kosaka T., Katsumaru H., Hama K., Wu J.-Y. and Heizmann C. W. (1987) GABAergic neurons containing the Ca^{2+} -binding protein parvalbumin in the rat hippocampus and dentate gyrus. *Brain Res.* **419**, 119-130.
27. Kunkel D. D., Lacaille J.-C. and Schwartzkroin P. A. (1988) Ultrastructure of stratum lacunosum-moleculare interneurons of hippocampal CA1 region. *Synapse* **2**, 382-394.
28. Lacaille J.-C., Mueller A. L, Kunkel D. D. and Schwartzkroin P. A. (1987) Local circuit interactions between oriens-alveus interneurons and CA1 pyramidal cells in hippocampal slices: electrophysiology and morphology. *J. Neurosci.* **7**, 1979-1993.

29. Lacaille J.-C. and Schwartzkroin P. A. (1988a) Stratum lacunosum-moleculare interneurons of hippocampal CA1 region: I. Intracellular response characteristics, synaptic responses, and morphology. *J. Neurosci.* **8**, 1400-1410.
30. Lacaille J.-C. and Schwartzkroin P. A. (1988b) Stratum lacunosum-moleculare interneurons of hippocampal CA1 region: II. Intrasomatic and intradendritic recording of local circuit synaptic interactions. *J. Neurosci.* **8**, 1411-1424.
31. Lacaille J.-C. and Williams S. (1990) Membrane properties of interneurons in stratum oriens-alveus of the CA1 region of rat hippocampus in vitro. *Neuroscience* **36**, 349-359.
32. Lorente de Nò R. (1934) Studies on the structure of the cerebral cortex II. Continuation of the study of the ammonic system. *J. Psychol. Neurol. (Lpz)* **46**, 113-177.
33. Marco P., Sola R. G., Ramon y Cajal S. and DeFelipe J. (1997) Loss of inhibitory synapses on the soma and axon initial segment of pyramidal cells in human epileptic peritumoural neocortex: implications for epilepsy. *Brain Res. Bull.* **44**, 47-66.
34. Micheva K. D. and Beaulieu C. (1995) An anatomical substrate for experience-dependent plasticity of the rat barrel field cortex. *Proc. Natl. Acad. Sci. USA* **92**, 11834-11838.
35. Micheva K. D. and Beaulieu C. (1996) Quantitative aspects of synaptogenesis in the rat barrel field cortex with special reference to GABA circuitry. *J. Comp. Neurol.* **373**, 340-354.

36. Miles R., Toth K., Gulyas, A. I., Hajos N. and Freund T. F. (1996) Differences between somatic and dendritic inhibition in the hippocampus. *Neuron* **16**, 815-823.
37. Morin F., Beaulieu C. and Lacaille J.-C. (1998a) Selective loss of GABA neurons in area CA1 of the rat hippocampus after intraventricular kainate. *Epilepsy. Res.* **32**, 363-369.
38. Morin F., Beaulieu C. and Lacaille J.-C. (1998b) Cell-specific alterations in synaptic properties of hippocampal CA1 interneurons after kainate treatment. *J. Neurophysiol.* **80**, 2836-2847.
39. Nadler J. V., Perry B. W., Gentry C. and Cotman C. W. (1980) Loss and reacquisition of hippocampal synapses after selective destruction of CA3-CA4 afferents with kainic acid. *Brain Res.* **191**, 387-403.
40. Nadler J. V. (1981) Kainic acid as a tool for the study of temporal lobe epilepsy. *Life Sci.* **29**, 2031-2042.
41. Perez Y., Morin F., Beaulieu C. and Lacaille J.-C. (1996) Axonal sprouting of CA1 pyramidal cells in hyperexcitable hippocampal slices of kainate-treated rats, *Eur. J. Neurosci.* **8**, 736-748.
42. Peterson G. M., Ribak C. E. and Oertel W. H. (1985) A regional increase in the number of hippocampal GABAergic neurons and terminals in the seizure-sensitive gerbil. *Brain Res.* **340**, 384-389.
43. Ramon y Cajal S. (1911) Histologie du système nerveux de l'homme et des vertébrés. Maloine, Paris.

44. Ribak C. E., Harris A. B., Vaughn J. E. and Roberts E. (1979) Inhibitory, GABAergic nerve terminals decrease at sites of focal epilepsy. *Science* **205**, 211-214.
45. Ribak C. E., Bradburne R. M. and Harris A. B. (1982) A preferential loss of GABAergic, symmetric synapses in epileptic foci: A quantitative ultrastructural analysis of monkey neocortex. *J. Neurosci.* **2**, 1725-1735.
46. Sah P., Hestrin S. and Nicoll R.A (1990) Properties of excitatory postsynaptic currents recorded in vitro from rat hippocampal interneurons. *J. Physiol (Lond.)* **430**, 605-616.
47. Schwartzkroin P. A. and Mathers L. H. (1978) Physiological and morphological identification of a nonpyramidal hippocampal cell type. *Brain Res.* **157**, 1-10.
48. Schwartzkroin P. A. and Kunkel D. D. (1985) Morphology of identified interneurons in the CA1 regions of guinea pig hippocampus. *J. Comp. Neurol.* **232**, 205-218.
49. Scotti A. L., Kalt G., Bollag O. and Nitsch C. (1997) Parvalbumin disappears from GABAergic CA1 neurons of the gerbil hippocampus with seizure onset while its presence persists in the perforant path. *Brain Res.* **760**, 109-117.
50. Seress L. and Ribak C. E. (1992) Ultrastructural features of primate granule cell bodies show important differences from those of rats - axosomatic synapses, somatic spines and infolded nuclei. *Brain Res.* **569**, 353-357.
51. Sik A., Penttonen M., Ylinen A. and Buzsaki G. (1995) Hippocampal CA1 interneurons: an *in vivo* intracellular labeling study. *J. Neurosci.* **15**, 6651-6665.

52. Sloviter R. S., Dichter M. A., Rachinsky T. L., Dean E., Goodman J. H., Sollas A. L. and Martin D. L. (1996) Basal expression and induction of glutamate decarboxylase and GABA in excitatory granule cells of the rat and monkey hippocampal dentate gyrus. *J. Comp. Neurol.* **373**, 593-618.
53. Somogyi P. and Hodgson A. J. (1985) Antisera to γ -aminobutyric acid. III. Demonstration of GABA in Golgi-impregnated neurons and in conventional electron microscopic sections of cat striate cortex. *J. Histochem. Cytochem.* **33**, 249-257.
54. Turner D. A. and Wheal H. V. (1991) Excitatory synaptic potentials in kainic acid-denervated rat CA1 pyramidal neurons. *J. Neurosci.* **11**, 2786-2794.
55. Umbriaco D., Garcia S., Beaulieu C. and Descarries L. (1995) Relational features of acetylcholine, noradrenaline, serotonin and GABA axon terminals in the stratum radiatum of adult rat hippocampus (CA1). *Hippocampus* **5**, 605-620.
56. Williams S., Vachon P. and Lacaille J.-C. (1993) Monosynaptic GABA-mediated inhibitory postsynaptic potentials in CA1 pyramidal cells of hyperexcitable hippocampal slices from kainic acid-treated rats, *Neuroscience* **52**, 541-554.

Figure Legends

Figure 1: Ultrastructure of an interneuron in stratum oriens/alveus (O/A) of the hippocampal CA1 region from a normal rat. (A) Low power (3,900X) electron micrograph showing the ovoid soma and the invaginated nucleus characteristic of hippocampal interneurons. The cytoplasm contained a high number of mitochondria, endoplasmic reticulum and Golgi apparatus. Arrows point to synaptic contacts found on the soma and shown at higher magnification in B, C and D. Arrowheads point to nuclear invaginations. (B-D) Higher power (34,000X) electron micrographs of axon terminals (t) that are GABA-immunonegative (B, D) or GABA-immunopositive (C), and contact the interneuron soma (S) containing gold particles. The synaptic contacts were characterized by closely apposed membranes with cleft material, and the presence of synaptic vesicles associated with presynaptic membrane specializations. The length of synaptic contacts was measured for each synapse (distance between small arrows). Scale bars: (A) 2 μ m, (B-D) 0.25 μ m.

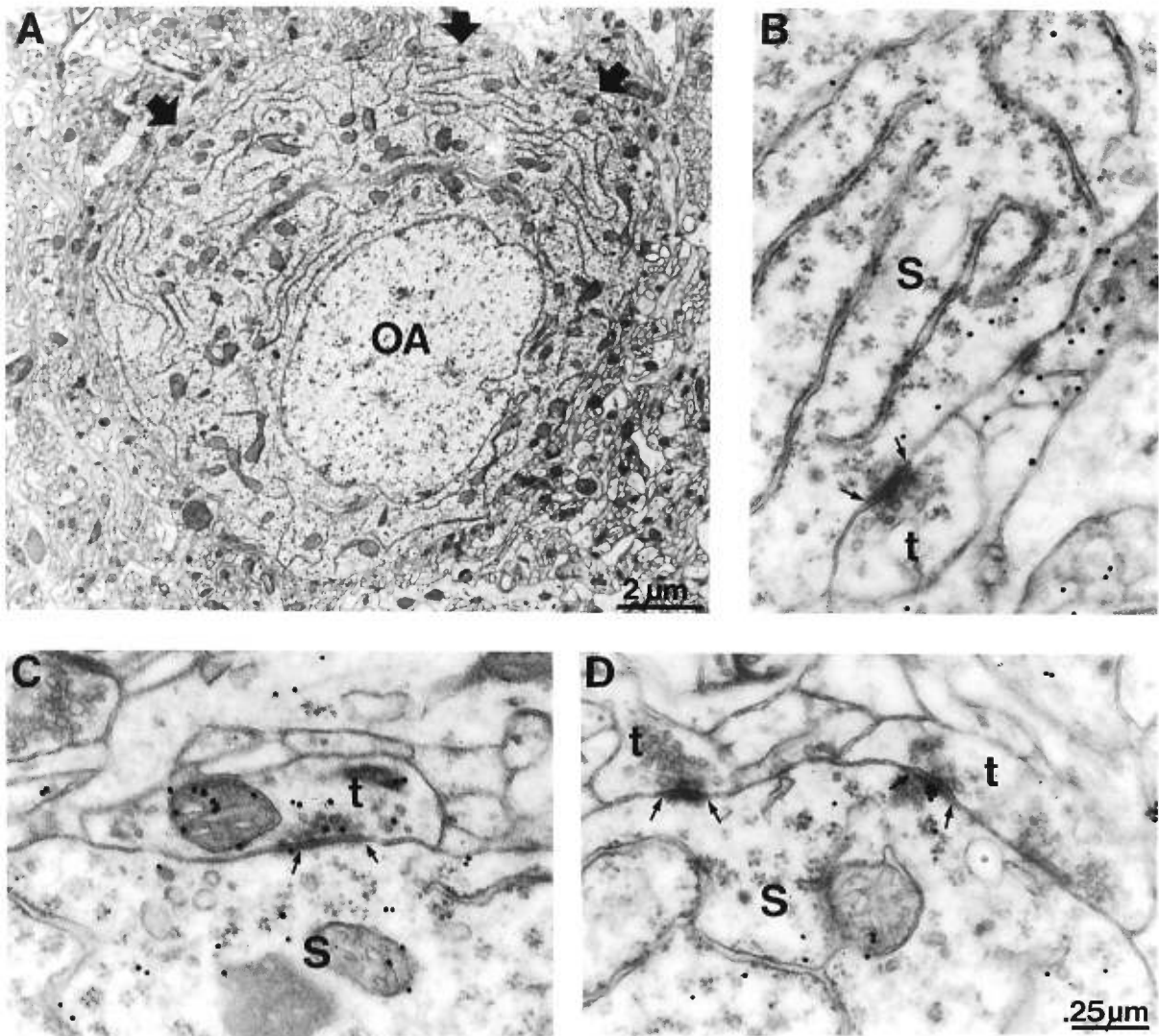
Figure 2: Ultrastructure of an interneuron in stratum lacunosum-moleculare (LM) of the hippocampal CA1 region from a normal rat. (A) Low power (3,900X) electron micrograph showing the ovoid soma and the nuclear membrane with invaginations. Arrows indicate synaptic contacts found on the soma, and shown at higher magnification in B, C and D. (B-D) Higher power (34,000X) electron micrographs of GABA-immunonegative (B-C) and GABA-immunopositive (D) terminals (t) making synaptic contacts (small arrows) on the GABA-immunopositive soma (S) of the

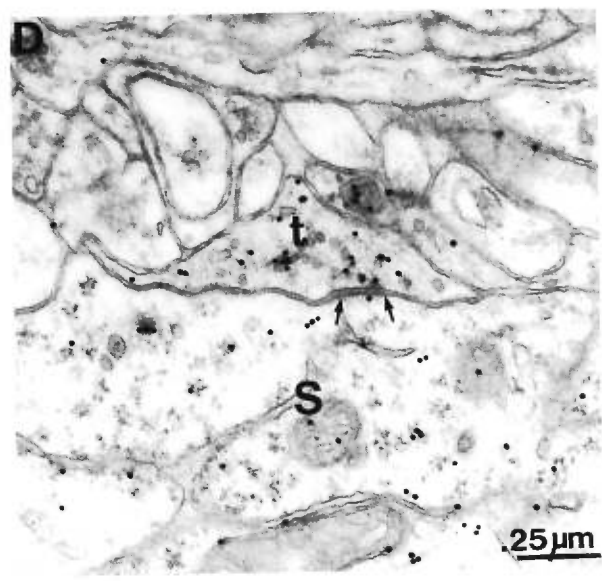
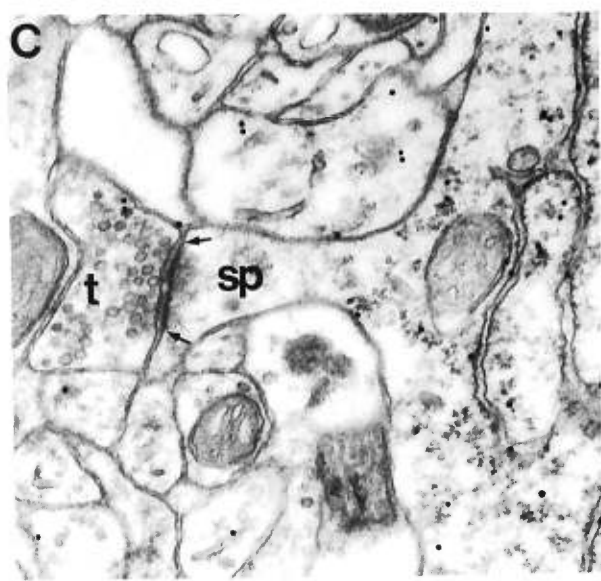
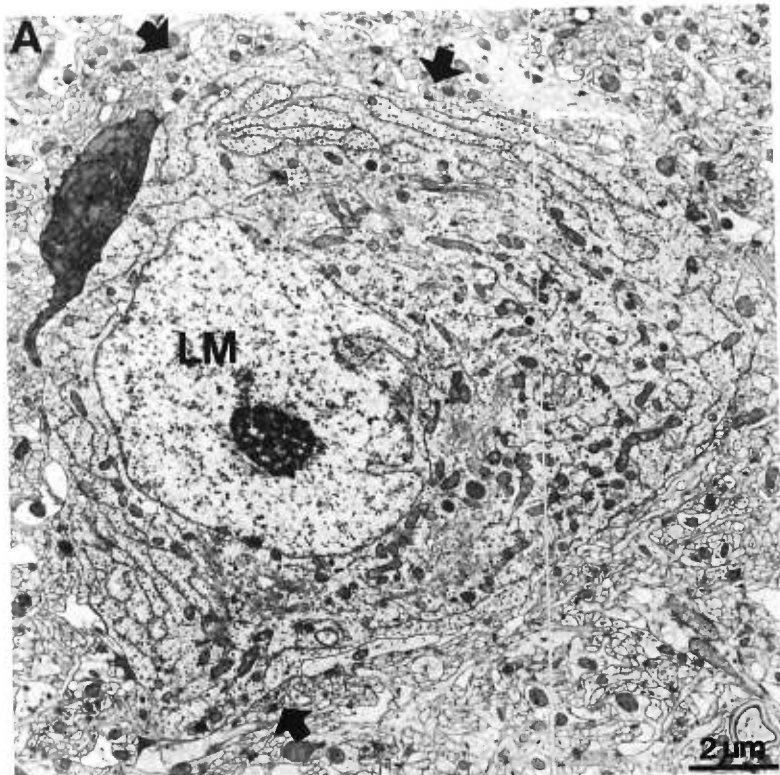
interneuron. Note in C that the GABA-immunonegative terminal is making a synaptic contact with a spine (sp) emerging from the GABA-immunopositive soma. Scale bars: (A) 2 μm , (B-D) 0.25 μm .

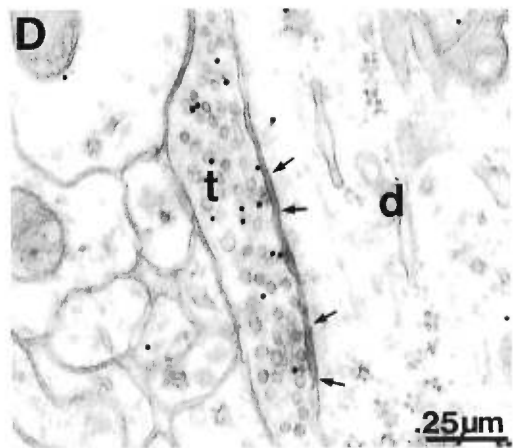
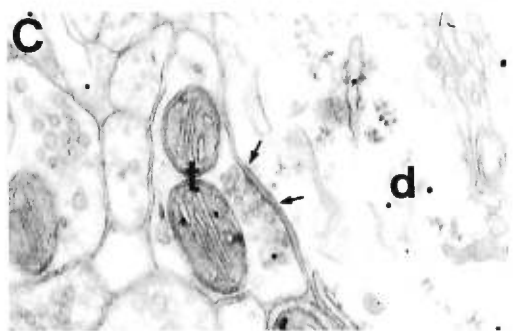
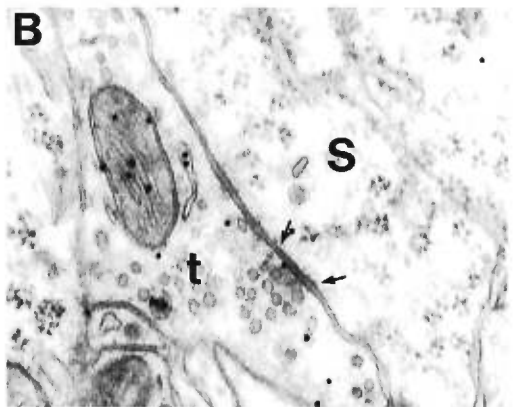
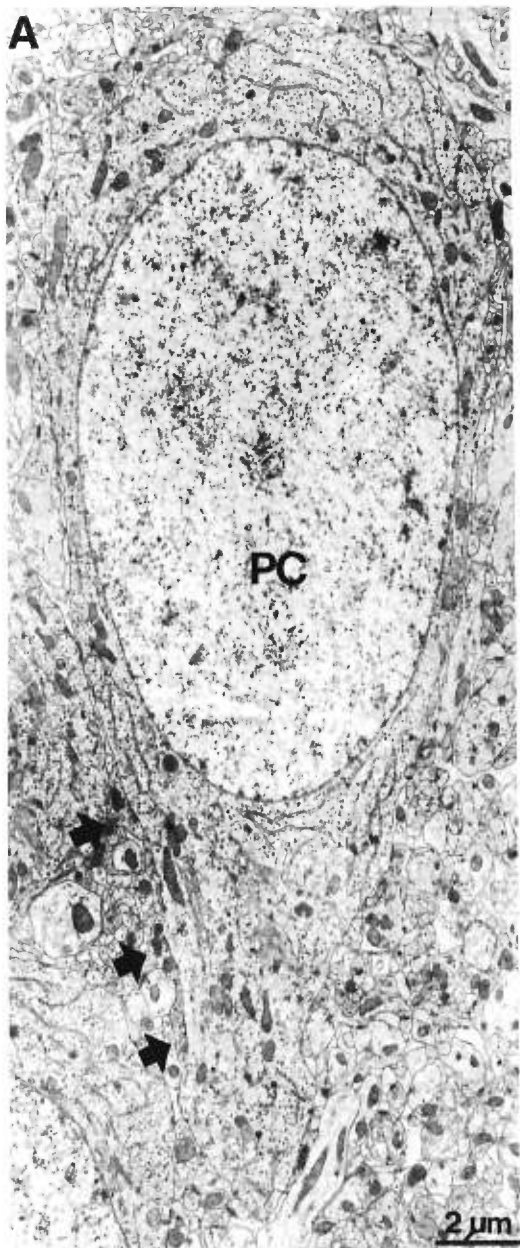
Figure 3: Ultrastructure of a CA1 pyramidal cell from a normal rat. (A) Low power (3,900X) electron micrograph showing the pyramidal-shaped soma and the nucleus with no membrane invaginations. The nucleus occupied a larger proportion of the soma in pyramidal cells than in interneurons (see Fig. 1 and 2). Arrows indicate synaptic contacts found on the soma and proximal dendrite of the pyramidal cell and are shown at higher magnification in B, C and D. (B-D) Higher power (34,000X) electron micrographs of GABA-immunopositive terminals (t) making synaptic contacts (small arrows) on the GABA-immunonegative soma (S) and proximal dendrite (d) of the pyramidal cell. Scale bars: (A) 2 μm , (B-D) 0.25 μm .

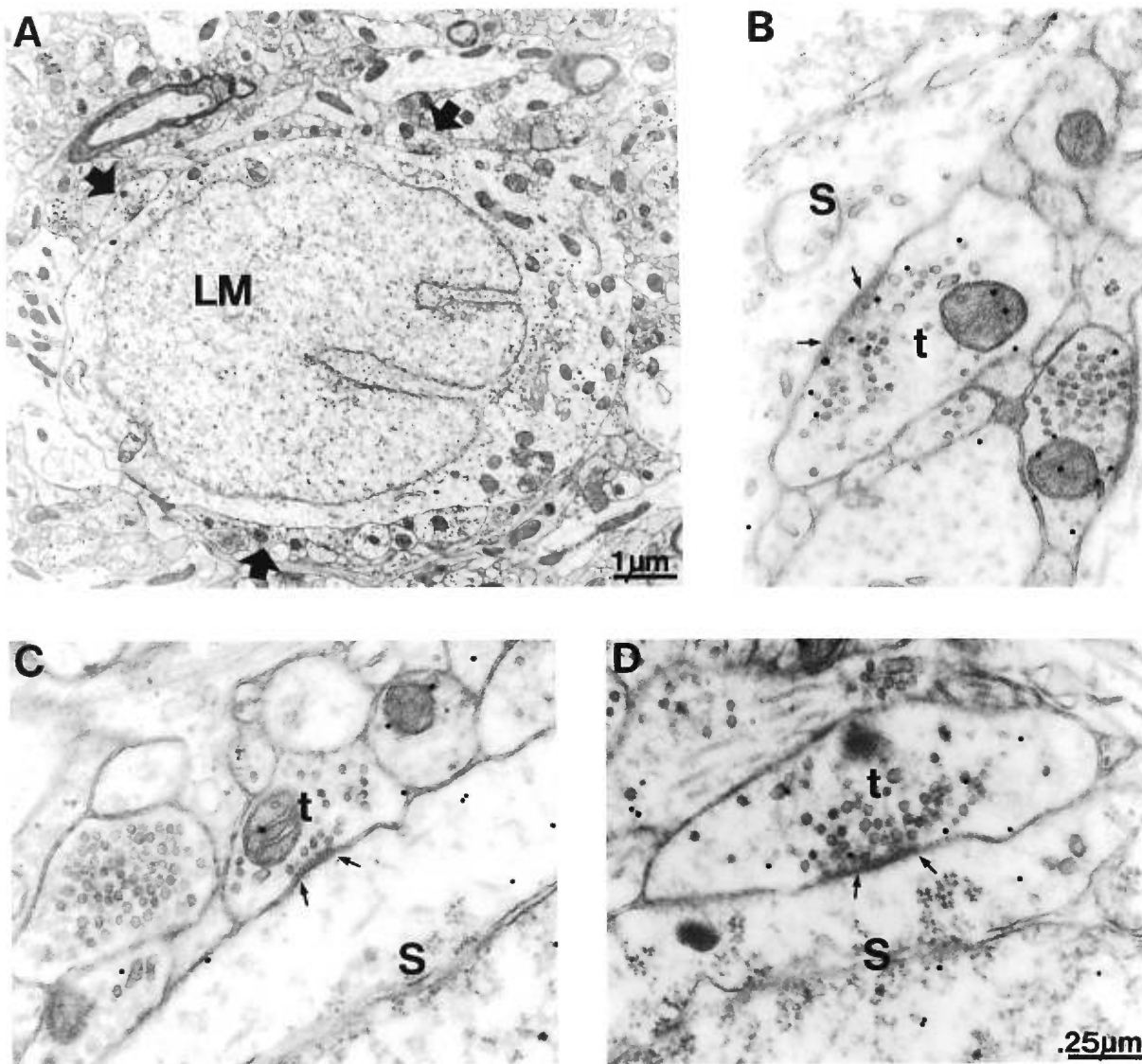
Figure 4: Ultrastructure of a CA1 interneuron in stratum lacunosum-moleculare (LM) of a KA-treated rat. (A) Low power (5,200X) electron micrograph showing the ovoid soma, nucleus with invaginations, and cytoplasm with numerous mitochondria, endoplasmic reticulum and Golgi apparatus. Black arrows indicate synaptic contacts found on the soma and shown at higher magnification in B, C and D. (B-D) Higher power (34,000X) electron micrographs of GABA-immunopositive terminals (t) making synaptic contact (indicated by small arrows) on the GABA-immunopositive soma (S) of the LM interneuron. Scale bars: (A) 1 μm , (B-D) 0.25 μm .

Figure 5: Histograms of the frequency distribution of synaptic contact length (μm) of GABA-immunopositive (A-C) and GABA-immunonegative (D-F) synaptic contacts for each cell type pooled for control (open bars) and KA-treated (filled bars) rats. (A-C) The mean length of GABA-immunopositive synaptic contacts was unchanged in interneurons of O/A and LM of KA-treated rats, but was significantly increased in pyramidal cells. After KA treatment, the number of synaptic contacts in pyramidal cells $< 0.25 \mu\text{m}$ was reduced, whereas the number of these $> 0.25 \mu\text{m}$ was increased. (D-F) The change in synaptic contact was specific to GABA synapses. The mean length of GABA-immunonegative synaptic contacts was not significantly different in any cell type of KA-treated rats. Values are pooled number of observations in four rats per group.









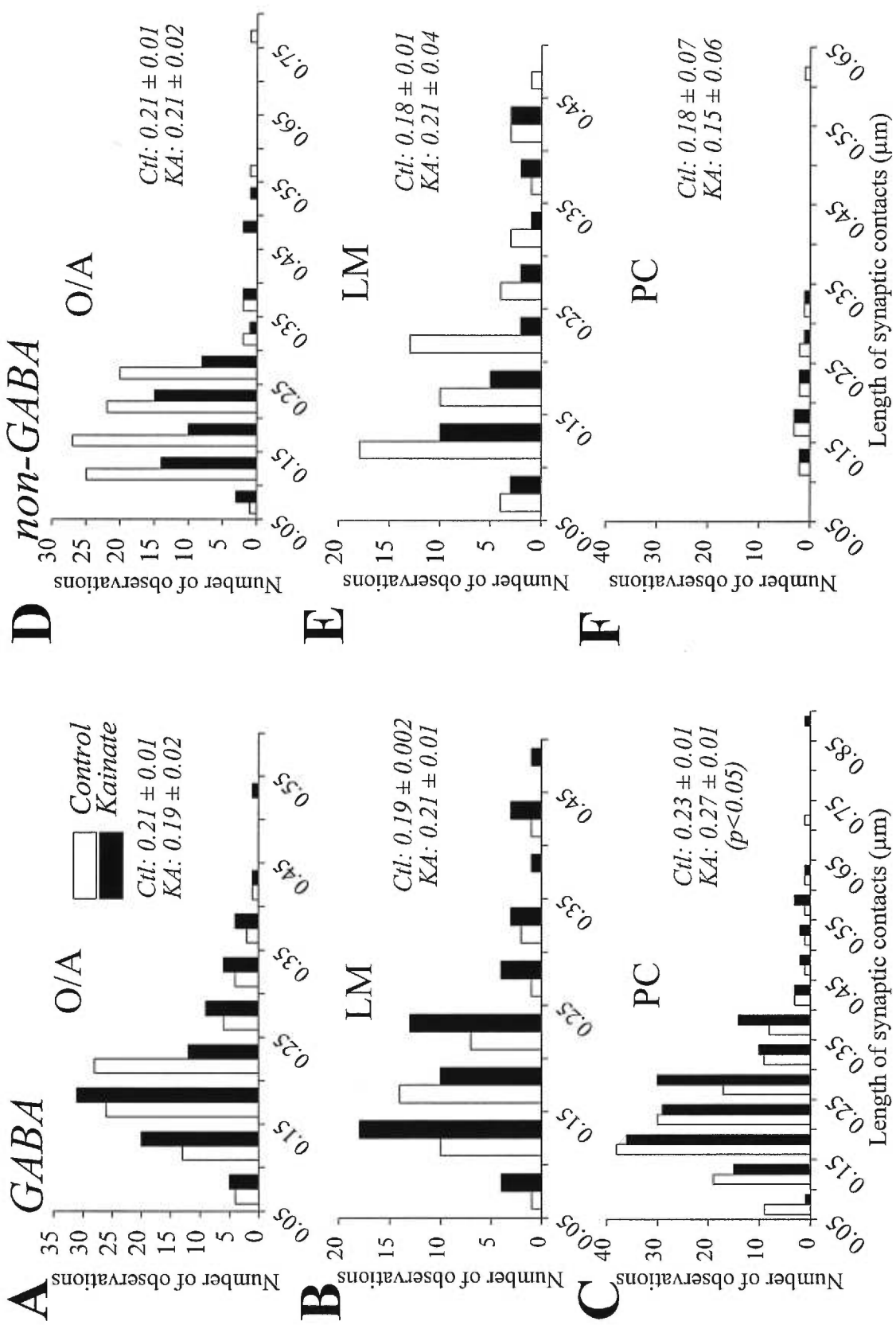


Table 1. Perisomatic synaptic contacts of interneurons and pyramidal cells in control and KA-treated rats

	INTERNEURONS			PYRAMIDAL CELLS			
	Oriens/Alveus		Lacunosum-moleculare	Control		Kainate	
	Control	Kainate		Control	Kainate	Control	Kainate
Number of cells	34	29	30	31	31	58	62
Number of synaptic contacts	185	145	69	85	149	149	152
Perimeter (μm)	57.2±5.4	55.3±4.1	51.6±1.7	46.5±2.7	58.0±2.9	53.5±0.9	53.5±0.9
$N_L GABA$ ($\times 10^{-2}/\mu\text{m}$)	3.88±0.57	4.80±1.25	2.38±0.41†	4.18±0.73*	4.03±0.21	4.03±0.21	4.48±0.80
$N_L non-GABA$ ($\times 10^{-2}/\mu\text{m}$)	4.15±0.61‡	2.63±0.91	2.20±0.43‡	2.00±0.59	0.30±0.15‡	0.30±0.15‡	0.55±0.36
$L_L GABA$ ($\text{nm}/\mu\text{m}$)	8.00±1.22	9.25±3.33	4.50±0.64†	9.00±1.68**	9.25±0.48	9.25±0.48	11.75±1.89
$L_L non-GABA$ ($\text{nm}/\mu\text{m}$)	8.75±1.31‡	5.50±2.10	4.00±0.91‡	4.00±1.29	0.82±0.45‡	0.82±0.45‡	0.58±0.25
$L GABA$ (μm)	0.21±0.01	0.19±0.02	0.19±0.002	0.21±0.01	0.23±0.01	0.23±0.01	0.27±0.01**
$L_{non-GABA}$ (μm)	0.21±0.01	0.21±0.02	0.18±0.01	0.21±0.04	0.18±0.07	0.18±0.07	0.15±0.06

Data are expressed as mean ± sem. † significantly different from other cell types in control animals (ANOVA). ‡ significantly different from each other in control animals (ANOVA). * significantly different from the same cell type in control animals (one tailed t-test). ** significantly different from the same cell type in control animals (two tailed t-test). N_L is the number ($\times 10^{-2}/\mu\text{m}$) and L_L is the total length of synaptic contacts normalized to the cell perimeter sampled. $L GABA$ is the mean length of synaptic contacts.

CHAPITRE SIXIÈME

**UNE PROCÉDURE DE FIXATION POUR L'INVESTIGATION
ULTRASTRUCTURALE DES CONNEXIONS SYNAPTIQUES DANS LE
CORTEX HUMAIN PRÉLEVÉ PAR RÉSECTION**

**A Fixation Procedure for Ultrastructural Investigation of Synaptic Connections
in Resected Human Cortex**

F. Morin ^{1,3}, C. Crevier ¹, G. Bouvier ⁴, J.-C. Lacaille ^{2,3} and C. Beaulieu ^{1,3}

Départements de pathologie ¹ et de physiologie ², Centre de Recherche en Sciences Neurologiques³, Université de Montréal et Département de neurochirurgie ⁴, Hôpital Notre-Dame, Montréal, Québec, Canada.

publié dans

Brain Research Bulletin, 44: 205-210, 1997.

ABSTRACT

Electron microscopic investigations of the fine circuitry of human central nervous system require a well-preserved tissue ultrastructure. Since the deterioration of subcellular structures occurs rapidly in postmortem human brain, the use of a fixation by immersion of surgically resected human nervous tissue would be advantageous to investigate directly its synaptic circuitry. To obtain an optimal preservation of subcellular elements in immersion fixed brain tissue, different conditions of fixation were first tested on 400 μm -thick sections of rat neocortex. Parameters tested were temperature of the fixative solution, concentrations of glutaraldehyde and of cacodylate buffer with or without microwave irradiation and finally, the presence of dimethyl sulfoxide. The best ultrastructural preservation was obtained by immersing the tissue in 0.1 M cacodylate buffer, 3.0 mM CaCl_2 , 2% paraformaldehyde, 2.5% glutaraldehyde and 2.5% dimethyl sulfoxide at 37 °C for 5 minutes and then at 4 °C for 4 hours. This procedure of fixation was then applied to human neocortical tissue resected to alleviate temporal lobe epilepsy. This method led to good tissue preservation in addition to retaining the antigenicity to the inhibitory amino acid neurotransmitter, γ -aminobutyric acid (GABA). Therefore, the tissue preservation obtained would permit these chemically-defined connections to be investigated quantitatively at the electron microscopic level in resected human cortex.

Key words: Brain, synapse, electron microscopy, immunocytochemistry

INTRODUCTION

Ultrastructural studies of chemically-defined connections within the central nervous system require an adequate preservation of elements composing the synaptic complex as well as the retention of antigenicity of neuroactive molecules. This is usually achieved after an *in situ* vascular perfusion of the brain with appropriate solutions of aldehydes [see Hayat, 1981 for review]. However, the study of human nervous tissue at the subcellular level is problematic since brain specimens are usually obtained many hours postmortem. While light microscopic studies can still be performed on such material [Chan-Palay and Yasargil, 1986; Jones et al., 1992], the analysis of the fine structures of chemically-defined connections in postmortem brain may be compromised. The use of surgically resected human nervous tissue rapidly fixed by immersion could theoretically allow an analysis of the tissue at the ultrastructural level. However, while the preservation of the tissue is considerably improved compared to postmortem material, the fixation by immersion still results in significant damage, particularly in the core of the resected tissue block. To minimize these effects, many techniques have been used over the years varying from perfusing the resected human brain tissue through its overlying blood vessels [Chan-Palay and Yasargil, 1986], to exposing the tissue to microwave irradiation to accelerate the fixation rate [Boon and Kok, 1987; Boon et al., 1988; Leong et al., 1985]. Using these methods, immunocytochemical demonstration of various neuroactive molecules

in human cortical tissue has been possible [Beach et al., 1987; Chan-Palay and Yasargil, 1986; Jones et al., 1992; Kisvarday et al., 1986, 1990; Schiffmann et al., 1988; Vinters et al., 1994]. However, ultrastructural analyses of human nervous tissue have been scarce [Babb et al., 1991; DeFelipe et al., 1993; del Rio and DeFelipe, 1994, 1995; Kisvarday et al., 1986, 1990; Sutula et al., 1989].

The aim of the present study was to design a procedure of fixation by immersion which would preserve the subcellular elements and be suitable for quantitative investigations [Beaulieu et al., 1994] of the synaptic circuitry of the human cerebral cortex. Given the low availability of human tissue, the different techniques of fixation were first compared in neocortical tissue of adult rats. The procedure giving the best tissue ultrastructure was then applied to an electron microscopic investigation of human cortical tissue obtained by surgical resection. Subsequently, we verified whether this method of fixation allowed the study of GABAergic connections in the human cerebral cortex.

METHODS

Brain tissue of adult rat

A series of fixation tests were performed on neocortical tissue of 7 Long-Evans male rats (200-300 g). The animals were deeply anesthetized with sodium pentobarbital (100 mg/100 g; i.p.) before being sacrificed by decapitation. Brains

were quickly removed from the skull and extensively washed in cold (4 °C) oxygenated minimum essential medium eagle (MEM, Sigma) to remove the blood. Coronal 400 µm-thick sections of the cerebral cortex were rapidly cut on a manual tissue slicer (Stoelting Co.) and transferred to the MEM solution at 4 °C. Each section was then fixed by immersion following one of the protocols given below. The delay time between the removal of the brain from the skull and the time of fixation were carefully monitored for each tissue section.

In previous ultrastructural studies with *in situ* vascular perfusion, cortical tissue was obtained from animals perfused through the ascending aorta with a fixative solution containing 2% paraformaldehyde (PFA), 2.5% glutaraldehyde (GTA), 3.0 mM CaCl₂ in 0.1 M cacodylate buffer (CB, pH 7.4, room temperature). This fixation provided good ultrastructural preservation of the subcellular elements and a high antigenicity for amino-acid neurotransmitters [Beaulieu et al., 1994]. Preliminary experiments have demonstrated that the immersion fixation of fresh rat cortical tissue in this solution led to important alterations of the fine ultrastructure and to an inconsistent level of antigenicity. Therefore, variations of this method of fixation were compared in order to obtain optimal ultrastructural preservation of rat cortical tissue.

In a first series of tests, the technique of microwave irradiation was applied to evaluate the effect of six different fixative solutions on the preservation of the tissue ultrastructure. The first solution was that routinely used for vascular perfusion. From

this original solution, we also modified: 1) the osmolarity of the cacodylate buffer to 0.075 M and 0.125 M, 2) the concentration of the glutaraldehyde (4.0% and 6.0%), and finally 0.8 M sucrose was added to the solution as proposed by Hayat [1981]. Each tissue section was placed separately in a Petri dish containing 5 ml of the fixative solution at either room temperature or at 4 °C. The fixation was then carried out in a microwave (at 100% power) for a given period of time (either 6, 8 or 12 seconds). A standard domestic microwave was used (General Electric, 800 Watts) in which the rotating glass platform had been removed and a beaker containing 300 ml of cool tap water was placed in the corner [Login and Dvorak, 1985]. After microwave irradiation, the Petri dish containing the tissue slice was put on ice for 1 hour. On average, ten tissue sections were fixed for each test.

In a second series of tests, rat neocortical tissue was fixed by immersion in the first fixative solution described above (2% PFA, 2.5% GTA, 3.0 mM CaCl₂ in 0.1 M CB) to which either 0.25% or 2.5% of dimethyl sulfoxide (DMSO) was added. In addition, the temperature at which the fixation was carried out was varied. The first method consisted of placing the tissue for 5 minutes in the fixative preheated at 37 °C and then at 4 °C for 4 hours. The second technique also involved immersing the tissue for 5 minutes in the fixative solution preheated at 37 °C, but then to postfix it for 4 hours at room temperature. Lastly, the third and fourth protocols consisted of fixing the tissue for 4 hours, at either room temperature or 4 °C.

Tissue sections fixed with the different protocols were rinsed in 0.1 M CB for 12 hrs at 4 °C. They were then postfixed in 1% osmium tetroxide dissolved in 0.1 M phosphate buffer (PB; pH 7.4; room temperature) for 30 minutes, and in a buffered solution of 1% osmium tetroxide and 1.5% potassium ferrocyanide for another 10 minutes. After an extensive wash in PB, the sections were dehydrated in ascending concentrations of ethanol before being embedded in Durcupan ACM (Fluka) resin. Ultrathin sections (gray interference color) of the tissue section were cut on a ultramicrotome (Ultracut S, Reichert), mounted on single slot grids coated with pioloform, contrasted with lead citrate, and examined under a CM-100 electron microscope. The ultrastructural preservation of the tissue obtained with various protocols was evaluated using specific criteria. First, the general appearance of the tissue was examined at low magnification (x3 000-5 000), focusing mainly on the condition of cellular structures and extracellular matrix, degree of vacuolization and destruction of the myelin. Then, the preservation of the myelin laminae and of the subcellular structures such as mitochondria, microtubules, synaptic contacts and vesicles were examined at higher magnification (x15 000-35 000).

Fixation of Resected Human Temporal Cortex

Human neocortical tissue was obtained during surgical treatment of five patients to alleviate temporal lobe epilepsy. Informed consent was obtained in all cases. The patients were healthy individuals with no evidence of other neurological disorder. The epileptic foci were located deep in the temporal lobe, in the

hippocampus or amygdala. Since no neuropathological sign of abnormality was detected in the resected superior temporal gyrus (areas 21, 22 and 38 of Brodmann), the neocortical tissue examined was considered normal.

The human cortical tissue obtained from biopsy of the first two patients was fixed according to the protocol which gave the best reliability and ultrastructural results in the tests of immersion-fixation performed on rat tissue. Immediately after removal of the cortical region, a small block of superior temporal cortex extending from the pia to the white matter was quickly dissected from a larger cortical area and rinsed in cold oxygenated MEM. Then, 400 μm -thick sections were cut using a manual tissue slicer and put for 5 minutes in the fixative solution (2% PFA, 2.5% GTA, 2.5% DMSO, 3.0 mM CaCl₂ in 0.1 M CB) preheated at 37 °C and then at 4 °C for 4 hours. Because the technique of tissue slicing causes damage to the surface of the section and also requires time to perform, the cortical tissue collected from the other patients was processed differently. A 15x15 mm tissue section from a straight portion of the cortex and in which the white-gray matter could be clearly identified was dissected from a larger tissue section and rinsed in cold oxygenated MEM. Then, a 5x5 mm cortical column extending from the pia to the white matter was cut with a razor blade and put for 5 minutes in the fixative solution preheated at 37 °C and then at 4 °C for 4 hours. Using this last method, the time from which the tissue was resected to when it was placed in the fixative solution never exceeded 5 minutes. After fixation, tissue blocks were washed in 0.1 M PB and cut on a vibratome in 100 μm -thick sections. Smaller blocks extending from the pia mater to the beginning of

the white matter were then made using a binocular microscope. Subsequently, blocks that were not perpendicular to the six cortical layers were discarded. The tissue was embedded in resin and processed for electron microscopic (EM) examination to evaluate the quality of the ultrastructure.

Finally, the presence of GABA in neurons and synaptic terminals was tested on ultrathin sections of resected human cortex using a postembedding immunoperoxidase and immunogold method described previously [Beaulieu, 1993; Beaulieu et al., 1994].

RESULTS

Brain tissue of adult rats

The first series of tests, using microwave irradiation, examined the effects of 1) the buffer osmolarity, 2) the concentration of glutaraldehyde and 3) the duration of fixation in the microwave. All tests were carried out on three separate occasions to verify the reliability of our results. We first compared three osmolarities of the cacodylate buffer (0.075, 0.1 and 0.125 M) in the original fixative solution; i.e. containing 2% PFA, 2.5% GTA, 3.0 mM CaCl₂ (pH 7.4). A good preservation of the myelin, cellular organelles and membranes was obtained with a buffer osmolarity of 0.1 M in the original fixative (Fig. 1A), whereas extensive structural alterations of the tissue were observed at both lower (0.075 M, Fig. 1B) and higher (0.125 M)

osmolarities. The effect of different glutaraldehyde concentration (2.5, 4.0, 6.0%) in the fixative solution was also tested. At higher concentrations (4.0 and 6.0%), glutaraldehyde was detrimental to the tissue ultrastructure which was probably due to the increased osmolarity of the fixative (not shown). Finally, the addition of 0.8 M sucrose in the original solution did not yield a superior preservation compared to the original fixative (not shown).

The duration of exposure in fixative to microwave irradiation also had a significant effect on the preservation of the ultrastructure. Best results were obtained when 400 μm -thick rat neocortical sections were exposed to microwave irradiation for 12 seconds, leading to a final temperature of fixative of around 40 °C (not shown). However, as a general rule, it proved difficult to obtain reliable results with the use of the microwave since under the same test conditions, the temperature of the fixative measured after microwave treatment was highly variable. This discrepancy in the final temperature of the fixative solution occurred even though conditions such as volume of the solution, starting temperature, and size of the tissue block were standardized. Therefore, the unreliability of the microwave led us to perform a second series of tests to find an alternative procedure.

In this second series of tests, our aim was to enhance the penetration rate of the aldehydes through the depth of tissue blocks by 1) using fixation solutions of different temperatures and, 2) adding dimethyl sulfoxide (DMSO) to the fixative solution. All tests were performed on four separate occasions. Superior ultrastructural

preservation was obtained when neocortical sections were placed for 5 minutes in the fixative preheated at 37 °C and then at 4 °C for 4 hours, compared to tissue fixed at either room temperature or 4 °C for 4 hours, or at 37 °C for 5 minutes and then at room temperature for 4 hours (Fig. 2). The combination of DMSO and an appropriate temperature of fixation provided the best possible ultrastructural preservation in rat neocortical tissue, at least with the fixation by immersion (Fig. 3). Furthermore, measurements made on sections before fixation and after the resin embedding, showed that this fixation protocol did not induce any detectable shrinkage of the tissue (not shown). This optimal protocol was subsequently applied to surgically resected human cortical tissue.

Ultrastructural preservation of human temporal cortex

The fixation by immersion of surgically resected human cortical tissue with the protocol described in the previous paragraph (37 °C for 5 minutes and then at 4 °C for 4 hours) preserved the ultrastructural appearance of the subcellular elements throughout the full depth of tissue blocks (Fig. 4). In one case, DMSO was omitted in the fixative (Fig. 3B). When the cortex was examined at the center of the tissue block and compared to tissue fixed in the presence of DMSO (Fig. 3A), a better continuity between the tissue organelles and apposition between cell membranes was found when 2.5% DMSO was included to the fixative solution. Particularly, elements composing the synaptic complex were very well preserved (see also Fig. 3A). However, it should be noted that some alterations of the tissue ultrastructure could be

seen in the material. For instance, some mitochondria and cytoskeletal elements (particularly microtubules) were slightly damaged and vacuoles were present in many cellular compartments.

The immunoreactivity of cellular and subcellular elements for the inhibitory amino acid transmitter, GABA, was also verified in the human neocortical tissue and found to be preserved using our fixation protocol (Fig. 5).

DISCUSSION

This study described a fixation procedure which was suitable for electron microscopic investigation of human cortical tissue obtained from biopsy. Using this protocol, subcellular elements were well-preserved and tissue antigenicity to GABA was observed, such that electron microscopic studies of these chemically-defined circuits in human cortical tissue can be made. This method of fixation was rapid and simple, and did not require the use of sophisticated apparatus. It should be noted that even though the ultrastructure was well preserved, this protocol of fixation still induced structural alterations. Therefore, one should be cautious not to confound these effects with ultrastructural changes induced by disease. For instance, the arrangement of microtubules in dendritic shafts was affected following our protocol of fixation (see Fig. 4). It is therefore likely that a detailed localization of cytoskeletal proteins (such as microtubule-associated proteins) would be difficult to perform on such material. However, we are confident that the ultrastructural elements composing

the synaptic complex were well preserved. In preliminary analyses, counts of synaptic contacts were obtained from series ($n=9$) of two consecutive sections of resected human cortex, suggesting that this fixative protocol may be adequate for quantitative analyses of synaptic circuitry in resected human tissue [Beaulieu, 1993; Beaulieu et al., 1992; 1994].

The presence of paraformaldehyde and glutaraldehyde in appropriate concentrations in the buffer is critical in obtaining a well-preserved ultrastructure and a good antigenicity for amino-acid transmitters in vascular perfused animals [reviewed in Hayat, 1981; Beaulieu et al., 1992, 1994]. A major limitation of fixation by immersion is that the aldehydes must pass through the tissue permeability barrier. The addition of a solvent such as dimethyl sulfoxide likely accelerated the penetration of the fixative agents (particularly at 37 °C) within the tissue by weakening this barrier [Franz and Van Bruggen, 1967; Jacob et al., 1964]. This may have prevented the deterioration and breakdown of existing structures particularly in the core of the tissue block. As Sandborn et al., [1969, 1975] have previously suggested, the use of dimethyl sulfoxide improves the preservation of membranes, increases the continuity between the organelles and allows a greater precision of enzyme localization. This procedure therefore provides good tissue preservation in addition to retaining the antigenicity of amino acid neurotransmitters. Since a recent study reported that the immunodetection of many antigenic sites (even of sensitive antigens) was possible after a fixation with 3.5% glutaraldehyde [Mrini et al., 1995], the proposed protocol may also be appropriate for the immunocytochemical detection of other substances.

In conclusion, this procedure allows the demonstration of GABAergic connections at the electron microscopic level in human nervous tissue, in addition to providing a method with which quantitative ultrastructural studies of these connections [Beaulieu, 1993; Beaulieu et al., 1992, 1994] can be carried out in human epilepsy research. This technique may also be applied to the study of such chemically-defined abnormalities in other human neurological disorders.

ACKNOWLEDGEMENTS

We are grateful to Marthe Mercier and Rhéal Daigle of the Hôpital Notre-Dame for their help. This work was supported by the Fonds de la Recherche en Santé du Québec (FRSQ; J.-C. L.), the Medical Research Council of Canada (MRCC; J.-C. L. and C.B.), the Savoy Foundation (F.M.), a Research Center grant from the Fonds pour la Formation de Chercheurs et l'Aide à la Recherche (FCAR) to the Groupe de Recherche sur le Système Nerveux Central and an Équipe de Recherche grant from the FCAR (J.-C. L.). We would like to thank S. Nurse and A. Chapman for helpful comments on the manuscript.

REFERENCES

- Babb, T. L.; Kupfer, W. R.; Pretorius, J. K.; Crandall, P. H.; Levesque, M. F. Synaptic reorganization by mossy fibers in human epileptic fascia dentata. *Neuroscience* 42: 351-363; 1991.
- Beach, T. G.; Tago, H.; Nagai, T.; Kimura, H.; McGeer, P. L.; McGeer, E. G. Perfusion-fixation of the human brain for immunohistochemistry. *J. Neurosci. Meth.* 19: 183-192; 1987.
- Beaulieu, C.; Kisvarday, Z.; Somogyi, P.; Cynader, M.; Cowey, A. Quantitative distribution of GABA-immunopositive and -immunonegative neurons and synapses in the monkey striate cortex (area 17). *Cereb. Cortex.* 2: 295-309; 1992.
- Beaulieu, C. Numerical data on neurons in adult rat neocortex with special reference to the GABA population. *Brain Res.* 609: 284-292; 1993.
- Beaulieu, C.; Campistron, G.; Crevier, C. Quantitative aspects of the GABA circuitry in the primary visual cortex of the adult rat. *J. Comp. Neurol.* 339: 559-572; 1994.
- Boon, M. E.; Kok, L. P. *Microwave cookbook of pathology: the art of microscopic visualization*, 2nd ed., Leiden: Coulomb Press Leyden; 1987.
- Boon, M. E.; Marani, E.; Adriolo, P. J. M.; Steffelaar, J. W.; Bots, G. Th. A.; Kok, L. P. Microwave irradiation of human brain tissue: production of microscopic slides within one day. *J. Clin. Path.* 41: 590-593; 1988.
- Chan-Palay, V.; Yasargil, G. Immunocytochemistry of human brain tissue with a polyclonal antiserum against neuropeptide Y. *Anat. Embryol.* 174: 27-33; 1986.

- DeFelipe, J.; Sola, R. G.; Marco, P.; del Rio, M. del R.; Pulido, P.; Ramon y Cajal, S. Selective changes in the microorganization of the human epileptogenic neocortex revealed by parvalbumin immunoreactivity. *Cereb. Cortex* 3: 39-48; 1993.
- del Rio, M. R.; DeFelipe, J. A study of SMI 32-stained pyramidal cells, parvalbumin immunoreactive chandelier cells, and presumptive thalamocortical axons in the human temporal neocortex. *J. Comp. Neurol.* 342: 389-408; 1994.
- del Rio, M. R.; DeFelipe, J. A light and electron microscopic study of calbindin D-28k immunoreactive double bouquet cells in the human temporal cortex. *Brain Res.* 690: 133-140; 1995.
- Franz, T. J.; Van Bruggen, J. T. A possible mechanism of action of DMSO. *Ann. N.Y. Acad. Sci.* 141: 302-309; 1967.
- Hayat, M. A. Fixation for Electron Microscopy. New York: Academic Press; 1981.
- Jacob, S. W.; Bischel, M. B.; Herschler, R. J. Dimethyl sulfoxide: effects on the permeability of biologic membranes (preliminary report). *Curr. Therap. Res.* 6: 193-198; 1964.
- Jones, E. G.; Hendry, S. H. C.; Liu, X.- B.; Hodgins, S.; Potkin, S. G.; Tourtellotte, W. W. A method for fixation of previously fresh-frozen human adult and fetal brains that preserves histological quality and immunoreactivity. *J. Neurosci. Meth.* 44: 133-144; 1992.
- Kisvarday, Z. F.; Adams, C. B. T.; Smith, A. D. Synaptic connections of axo-axonic (chandelier) cells in human epileptic temporal cortex. *Neuroscience* 19: 1179-1186; 1986.

- Kisvarday, Z. F.; Gulyas, A.; Beroukas, D.; North, J. B.; Chubb, I. W.; Somogyi, P. Synapses, axonal and dendritic patterns of GABA-immunoreactive neurons in human cerebral cortex. *Brain* 113: 793-812; 1990.
- Leong, A. S.; Daymon, M. E.; Milios, J. Microwave irradiation as a form of fixation for light and electron microscopy. *J. Path.* 146: 313-321; 1985.
- Login, G. R.; Dvorak, A. M. Microwave energy fixation for electron microscopy. *Am. J. Pathol.* 120: 230-243; 1985.
- Mrini, A.; Moukles, H.; Jacomy, H.; Bosler, O.; Doucet, G. Efficient immunodetection of various protein antigens in glutaraldehyde-fixed brain tissue. *J. Histochem. Cytochem.* 43: 1285-1291; 1995.
- Sandborn, E. B.; Makita, T.; Lin, K.- N. The use of dimethyl sulfoxide as an accelerator in the fixation of tissues for ultrastructural and cytochemical studies and in freeze etching of cells. *Anat. Record.* 163: 255; 1969.
- Sandborn, E. B.; Stephens, H.; Bendayan, M. The influence of dimethyl sulfoxide on cellular ultrastructure and cytochemistry. *Ann. N.Y. Acad. Sci.* 243: 122-138; 1975.
- Schiffmann, S.; Campistron, G.; Tugendhaft, P.; Brotchi, J.; Flament-Durand, J.; Geffard, M.; Vanderhaeghen, J. -J. Immunocytochemical detection of GABAergic nerve cells in the human temporal cortex using a direct gamma-aminobutyric acid antiserum. *Brain Res.* 442: 270-278; 1988.
- Sutula, T.; Cascino, G.; Cavazos, J.; Parada, I.; Ramirez, L. Mossy fiber synaptic reorganization in the epileptic human temporal lobe. *Ann. of Neurol.* 26: 321-330; 1989.

Vinters, H. V.; Secor, D. L.; Read, S. L.; Frazee, J. G.; Tomiyasu, U.; Stanley, T. M.; Ferreiro, J. A.; Akers, M. A. Microvasculature in brain biopsy specimens from patients with Alzheimer's disease: an immunohistochemical and ultrastructural study. *Ultrastruct. Path.* 18: 333-348; 1994.

Figure 1: Effect of osmolarity. Electron micrographs showing rat neocortical tissue fixed by immersion in cacodylate buffer osmolarity of 0.1 M (A) and 0.075 M (B) in a fixative solution containing 2% PFA, 2.5% GTA, 3.0 mM CaCl₂. Note the high degree of vacuolization (asterisks) in the tissue fixed with the lower osmolarity buffer (B). In particular, many cellular organelles, (especially mitochondria) and membranes were damaged in the low osmolarity fixative solution. Scale bar 1 μ m.

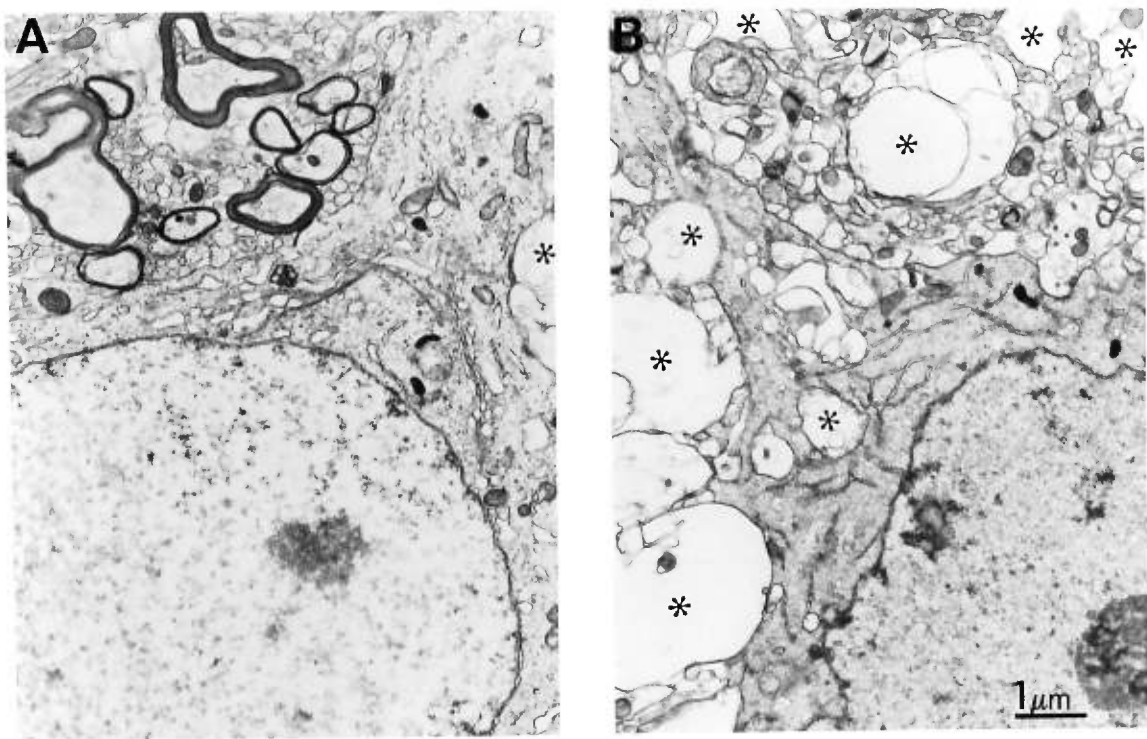
Figure 2: Effect of temperature. Electron micrographs showing rat neocortical tissue fixed by immersion in a fixative solution containing 2% PFA, 2.5% GTA, 3.0 mM CaCl₂, 2.5% DMSO in 0.1 M cacodylate buffer at 4 °C for 4 hrs (A) or at 37 °C for 5 min and then at 4 °C for 4 hrs (B). Note first that the general appearance of these two procedures on the tissue ultrastructure was not strikingly different. However, the linearity of the cellular membranes, the definition of the synaptic membranes, and the preservation of the myelin were consistently better when the initial 5 min fixation period at 37 °C was added to the procedure. Note the presence of ribosomes (indicated by open arrow) on rough endoplasmic reticulum in B. Scale bar 0.5 μ m.

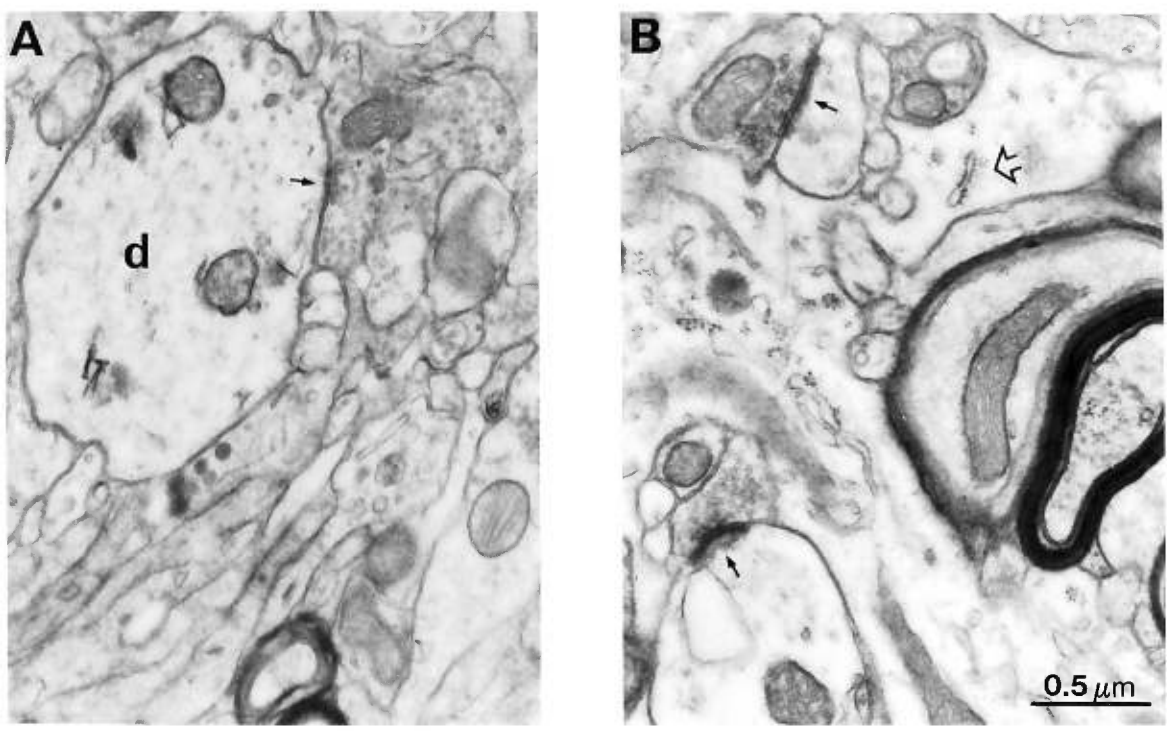
Figure 3: Effect of the dimethyl sulfoxide (DMSO). Electron micrographs showing human temporal cortex fixed by immersion in a fixative solution containing 2% PFA, 2.5% GTA, 3.0 mM CaCl₂ in 0.1 M cacodylate buffer at 37 °C for 5 min and then at 4 °C for 4 hrs. Tissue shown in (A) was fixed with 2.5% DMSO while the tissue in (B) was fixed without DMSO. The presence of DMSO in the fixative solution greatly improved the preservation of the ultrastructure. Figure A shows Type I and II

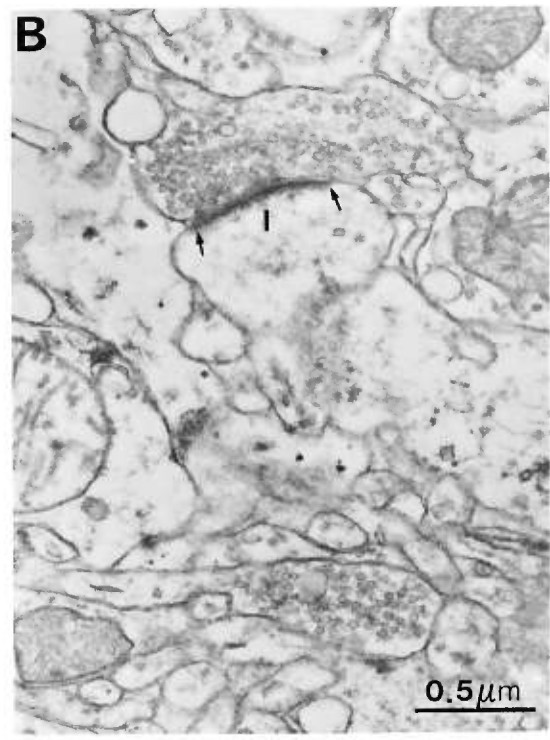
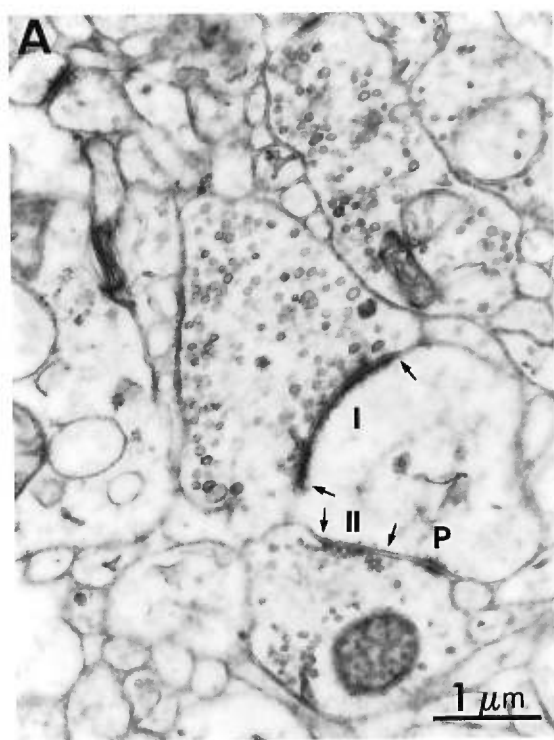
synapses as well as a puncta adherens (P) made on a dendritic spine. Synaptic vesicles, pre- and post-synaptic membranes, the presence of the postsynaptic density or of cell organelles such as the spine apparatus were all present and easily recognizable at the electron microscopic level. Note in the neocortical tissue shown in Figure B that the continuity between the tissue organelles and apposition between cell membranes is not as well delimited as in Figure A. Scale bar 1 μm (A) and 0.5 μm (B).

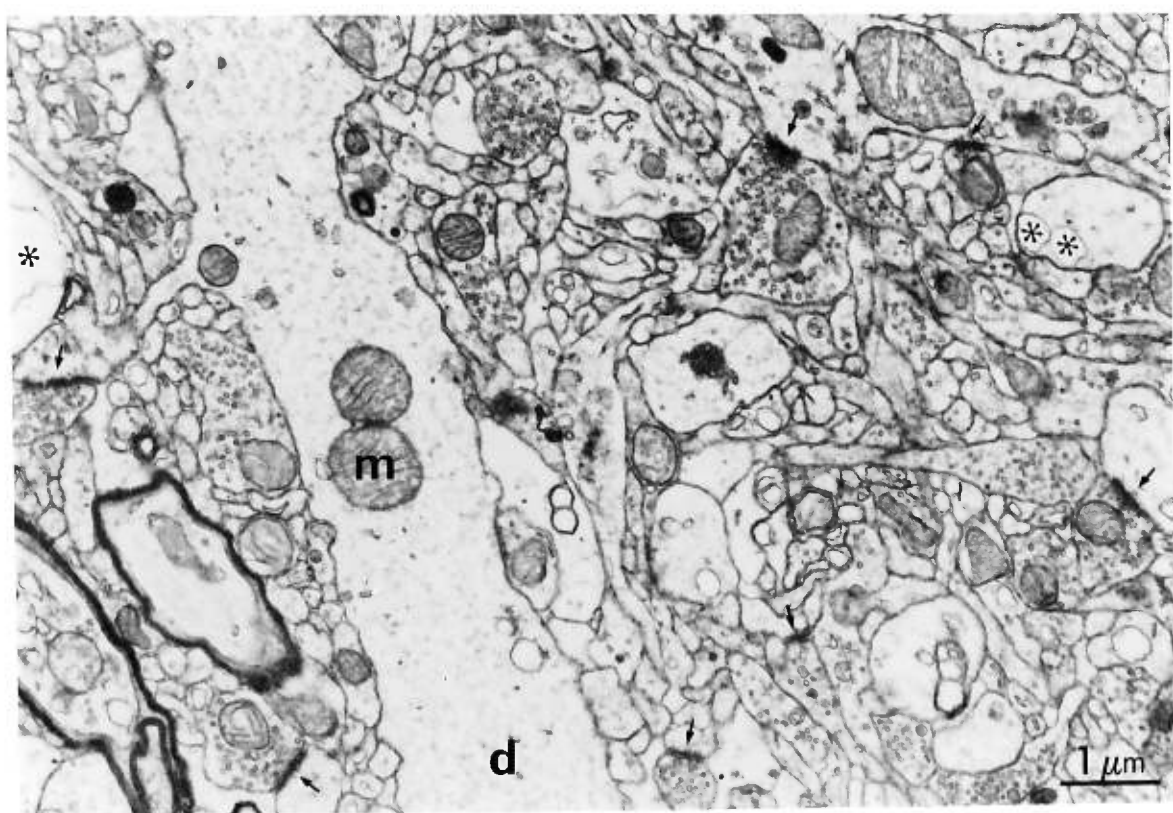
Figure 4: Overall appearance of human neocortical tissue fixed with the proposed protocol. This figure shows a representative view of the tissue taken in cortical layer II-III of human temporal cortex. The elements forming the synaptic complex were all well-preserved. However, some mitochondria (m) and cytoskeletal elements were slightly damaged and a number of vacuoles were present (asterisks) in the tissue. Synaptic contacts are indicated by small arrows. Scale bar 1 μm .

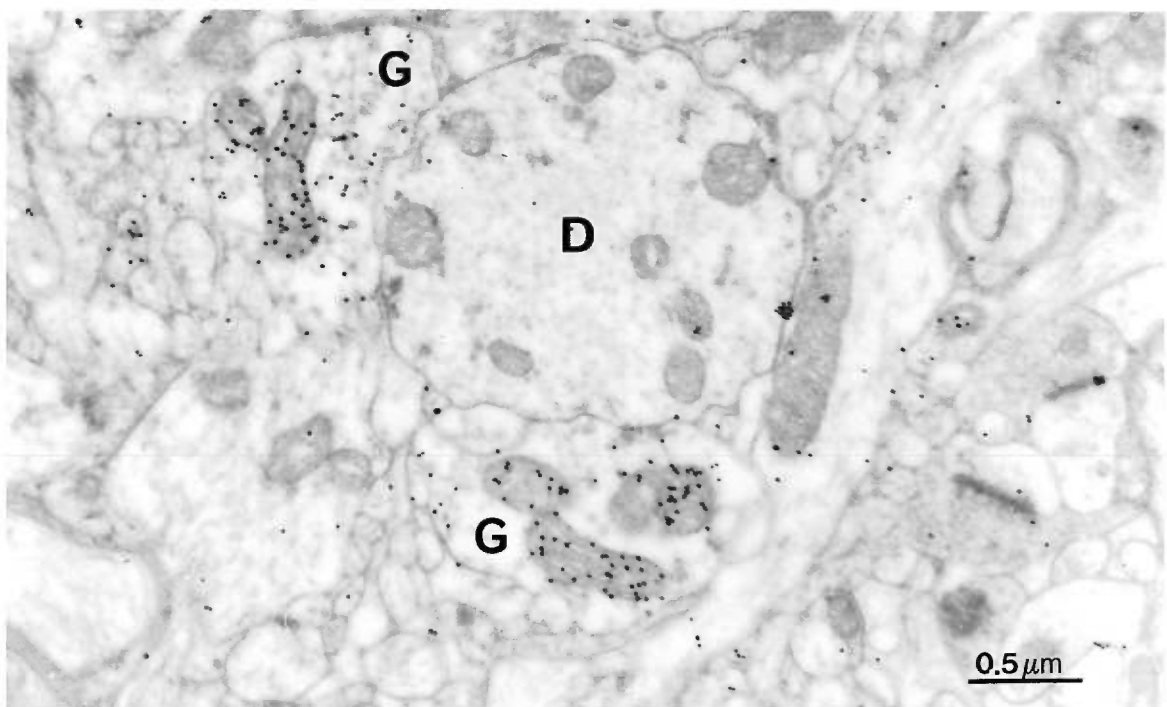
Figure 5: GABA-immunoreactivity in human neocortical tissue fixed with the proposed protocol. The demonstration of GABA profiles was done using the postembedding immunogold technique. Note the specificity of the gold labelling over mitochondria in two GABA-immunopositive axon terminals (G) apposed on a GABA-negative dendritic trunk (D). Scale bar 0.5 μm .











CHAPITRE 7

DISCUSSION GÉNÉRALE

7 DISCUSSION GÉNÉRALE

7.1 L'hippocampe du rat normal

Nos travaux physiologiques ont démontré, à l'aide d'enregistrement *patch clamp* en configuration cellule entière, que les propriétés intrinsèques des cellules pyramidales diffèrent de celles des interneurones situés dans les couches oriens et l'alveus (O/A), pyramidale (PYR) et lacunosum-moleculare (LM) chez le rat juvénile (Morin et al. 1996). Par contre, les propriétés intrinsèques des trois groupes d'interneurones sont semblables (Morin et al. 1996). De plus, nos résultats ont indiqué que les courants postsynaptiques non-NMDA, NMDA et GABA_A ne diffèrent pas dans les trois groupes d'interneurones et les cellules pyramidales, à l'exception des courants postsynaptiques NMDA dont la cinétique est plus lente dans les interneurones O/A (Morin et al. 1996).

7.1.1 La caractérisation morphologique des cellules pyramidales et des interneurones

Nos travaux ont montré que, chez le rat juvénile, la morphologie des interneurones des couches O/A, PYR et LM diffère (Morin et al. 1996). Le corps cellulaire des interneurones O/A, PYR et LM est de forme multipolaire, mais chaque groupe d'interneurones présente une arborisation dendritique et axonale spécifique (Morin et al. 1996). Les dendrites des interneurones O/A sont surtout situées dans la couche oriens, ainsi que quelquefois dans la couche radiatum, tandis que leur axone s'arborise dans les couches oriens, pyramidale et radiatum (Morin et al. 1996). Les

dendrites des interneurones PYR sont situées dans les couches oriens et radiatum, tandis que leur axone a des branches dans les couches pyramidale et radiatum (Morin et al. 1996). Les arborisations dendritiques et axonales des interneurones LM sont situées dans les couches radiatum et lacunosum-moleculare (Morin et al. 1996). La morphologie de ces trois groupes d'interneurones concorde avec les données morphologiques déjà rapportées chez l'animal adulte (Schwartzkroin et Kunkel 1985; Lacaille et al. 1987; Kawaguchi et Hama 1988; Lacaille et Schwartzkroin 1988a; Lacaille et Williams 1990; Buhl et al. 1994), ainsi que chez l'animal juvénile (McBain et al. 1994; Williams et al. 1994). Nos résultats suggèrent donc que les caractéristiques morphologiques de ces différents sous-types d'interneurones sont déjà établies chez le rat âgé de deux à trois semaines (Morin et al. 1996). La différenciation morphologique des interneurones O/A, PYR et LM indique que les circuits inhibiteurs de la région CA1 sont hétérogènes chez le rat juvénile. Ainsi, chaque sous-type d'interneurone possède une certaine organisation anatomique qui lui permet de jouer un rôle fonctionnel distinct selon l'origine de ses afférences et les cibles de son axone.

7.1.2. Les propriétés intrinsèques des cellules pyramidales et des interneurones

7.1.2.1 Potentiel d'action, résistance d'entrée et après-hyperpolarisation

Nos travaux physiologiques ont démontré que certaines propriétés intrinsèques des cellules pyramidales, notamment l'amplitude et la durée du potentiel d'action ainsi que la résistance d'entrée, diffèrent de celles des interneurones O/A, PYR et LM

(Morin et al. 1996). Ces différences observées dans nos travaux concordent généralement avec les observations faites chez l'animal adulte lors d'enregistrement intracellulaire (Schwartzkroin et Mathers 1978; Kawaguchi et Hama 1987; Lacaille et al. 1987; Lacaille et Schwartzkroin 1988a; Lacaille et Williams 1990; Lacaille 1991), ainsi que chez l'animal juvénile en enregistrement *patch clamp* en configuration cellule entière (Williams et al. 1994). Par contre, des travaux faits à l'aide d'enregistrements intracellulaires chez l'animal adulte ont montré que la durée du potentiel d'action est semblable dans les cellules pyramidales et interneurones LM (Lacaille et Schwartzkroin 1988a), tandis que les études faites à l'aide d'enregistrements *patch clamp* en configuration cellule entière chez le rat juvénile ont indiqué que les cellules pyramidales ont un potentiel d'action de plus longue durée que les interneurones LM (Morin et al. 1996). Ces différences peuvent être dues à l'utilisation de techniques d'enregistrement différentes (intracellulaire versus cellule entière), à l'âge des animaux, et à la température à laquelle les enregistrements ont été faits (Williams et al. 1994; Morin et al. 1996).

D'autres propriétés intrinsèques diffèrent entre les cellules pyramidales et les interneurones : les après-hyperpolarisations (AHP) qui succèdent au potentiel d'action. Nos travaux physiologiques ont démontré la présence d'après-hyperpolarisation rapide (AHP_r) et d'une après-hyperpolarisation de moyenne durée (AHP_m) dans les interneurones O/A, PYR et LM (Morin et al. 1996). De plus, nos travaux ont révélé que l'amplitude de l' AHP_r et de l' AHP_m est plus prononcée dans les interneurones que dans les cellules pyramidales (Morin et al. 1996). Des AHPs plus prononcées dans les interneurones O/A (Lacaille et al. 1987), PYR

(Schwartzkroin et Mathers 1978) et LM (Kawaguchi et Hama 1987; Lacaille et Schwartzkroin 1988a) que dans les cellules pyramidales ont déjà été rapportées lors d'enregistrements intracellulaires chez le rat adulte. Par contre, ces AHPs avaient une apparence monophasique. D'autres travaux faits à l'aide d'enregistrement *patch clamp* en configuration cellule entière ont rapporté des AHPs biphasiques dans les interneurones O/A (Zhang et McBain 1995) et LM (Williams et al. 1994) chez le rat juvénile. De plus, des AHPs rapides et de moyenne durée ont aussi été observées dans les cellules pyramidales chez le rat adulte (Storm 1989, 1990). Des travaux ont démontré que les diverses composantes des AHPs dans les cellules pyramidales sont produites par différentes conductances potassiques activées par le Ca^{2+} (Storm 1989).

Ainsi, la présence de conductances potassiques distinctes dans les cellules pyramidales et les interneurones peut contribuer aux différences de la fréquence de décharge et de l'accommodation de la fréquence de décharge durant une dépolarisation soutenue observées dans ces neurones.

7.1.2.2 Réponses produites par injection de courant

Nos données physiologiques suggèrent également que les interneurones et les cellules pyramidales répondent différemment à des injections de courant. Premièrement, une constante de temps plus rapide a été observée dans les interneurones comparativement aux cellules pyramidales (Morin et al. 1996), ce qui confirme les données rapportées lors d'enregistrement intracellulaire (Schwartzkroin et Mathers 1978; Lacaille et al. 1987; Lacaille et Schwartzkroin 1988a). De plus, nos travaux démontrent que l'application d'un courant dépolarisant, à un potentiel

membranaire près du potentiel de repos, produit un train de potentiel d'action régulier dans les interneurones mais des réponses en bouffées avec accomodation dans 50% des cellules pyramidales (Morin et al. 1996). De plus, l'injection de courant dépolarisant à des potentiels membranaires hyperpolarisés ne modifie pas les réponses en décharge régulière dans les trois groupes d'interneurones (Morin et al. 1996). Par contre, lors d'enregistrements intracellulaires chez le rat adulte, l'injection de courant dépolarisant provoque des réponses en bouffée dans les interneurones LM lorsque le potentiel de membrane est hyperpolarisé, mais une décharge régulière près du potentiel membranaire de repos (Kawaguchi et Hama 1988; Lacaille et Schwartzkroin 1988a). Cette absence de réponses en bouffée sensibles au voltage a aussi été observée par Williams et ses collaborateurs (1994) et ne concorde donc pas avec les observations rapportées chez l'animal adulte (Kawaguchi et Hama 1988; Lacaille et Schwartzkroin 1988a). Toutefois, certaines différences de conditions expérimentales comme l'âge des animaux, la température à laquelle les enregistrements ont été faits, ainsi que la technique d'enregistrement utilisée (intracellulaire versus cellule entière) peuvent aussi expliquer l'absence de réponses en bouffée (Williams et al. 1994; Morin et al. 1996).

Nos données physiologiques indiquent également la présence d'un courant entrant activé par une hyperpolarisation (réponse à rectification entrante) dans les trois groupes d'interneurones et dans les cellules pyramidales (Morin et al. 1996). De plus, un rebond post-inhibiteur dépolarisant est observé à la fin des impulsions de courant hyperpolarisant dans les interneurones et les cellules pyramidales (Morin et al. 1996). Ces données sont en accord avec des travaux précédents rapportant la présence d'une

conductance à rectification entrante et d'un rebond post-inhibiteur dans les interneurones O/A et LM ainsi que dans les cellules pyramidales de la région CA1 (Lacaille et Williams 1990; Williams et al. 1994; Maccaferri et McBain 1996). La conductance potassique I_h explique la rectification entrante et le rebond post-inhibiteur des cellules pyramidales (Storm 1990) et des interneurones O/A (Maccaferri et McBain 1996). Cette même conductance serait aussi présente dans les interneurones PYR et LM et produirait les réponses à rectification entrante et de rebond post-inhibiteur dans ces cellules.

En conclusion, nos données physiologiques indiquent que les propriétés intrinsèques des cellules pyramidales diffèrent de celles des interneurones O/A, PYR et LM chez le rat juvénile, ce qui suggère que les conductances responsables de ces propriétés intrinsèques sont exprimées chez le rat âgé de 15 à 22 jours (Morin et al. 1996). Par contre, nos travaux démontrent que les propriétés intrinsèques des interneurones LM sont semblables à celles des interneurones O/A et PYR (Morin et al. 1996). Ces observations sont en désaccord avec les données obtenues chez l'animal adulte indiquant que les propriétés intrinsèques des interneurones LM diffèrent de celles des interneurones O/A et PYR chez l'animal adulte (Lacaille et al. 1987; Kawaguchi et Hama 1988; Lacaille et Schwartzkroin 1988a). Donc, la différenciation des propriétés intrinsèques des interneurones LM semble seulement partielle chez le rat juvénile, car leurs propriétés diffèrent de celles des cellules pyramidales mais pas de celles des interneurones O/A et PYR (Morin et al. 1996).

7.1.3. Les courants postsynaptiques excitateurs dans les cellules pyramidales et les interneurones

Plusieurs études physiologiques ont démontré que la stimulation des afférences de la région CA1 provoque des réponses postsynaptiques excitatrices dans les cellules pyramidales et les différents sous-types d'interneurones chez le rat adulte (Schwartzkroin et Mathers 1978; Knowles et Schwartzkroin 1980; Ashwood et al. 1984; Lacaille et al. 1987; Collingridge et al. 1988; Kawaguchi et Hama 1988; Lacaille et Schwartzkroin 1988a,b; Hestrin et al. 1990). Nos travaux ont indiqué que les courants postsynaptiques excitateurs (CPSE) sont formés de composantes AMPA et NMDA dans les cellules pyramidales et les interneurones (Morin et al. 1996). Tel que déjà rapporté (Sah et al. 1990), nos données ont suggéré que les propriétés des CPSE AMPA sont semblables dans les cellules pyramidales et les trois groupes d'interneurones (Morin et al. 1996). Par contre, il a été démontré que la cinétique des CPSE AMPA spontanés est plus rapide dans les interneurones de la région CA3 de l'hippocampe et du cortex visuel que dans les cellules pyramidales (Hestrin 1993; McBain et Dingledine 1993). De plus, des données physiologiques et moléculaires ont récemment indiqué que les récepteurs AMPA des cellules principales et des interneurones de l'hippocampe diffèrent (Geiger et al. 1995). La discordance entre nos résultats et ceux des autres études (Hestrin 1993; McBain et Dingledine 1993; Geiger et al. 1995) pourrait être liée à la présence de mécanismes AMPA distincts dans les interneurones de différentes régions ou à des différences entre les courants spontanés et ceux provoqués par l'activation de nombreuses fibres afférentes.

Nos travaux ont également démontré que les propriétés des CPSE NMDA des cellules pyramidales et des trois groupes d'interneurones sont généralement semblables, à l'exception du temps de montée qui est plus lent dans les interneurones O/A (Morin et al. 1996). Nos données concordent avec des résultats précédents indiquant que le temps de montée des CPSE NMDA est plus lent dans les interneurones O/A que dans les interneurones de la couche moléculaire et les cellules pyramidales (Perouansky et Yaari 1993). Le temps de montée plus lent des CPSE NMDA dans les interneurones O/A par rapport aux autres interneurones pourrait refléter leur cinétique d'activation plus lente (Perouansky et Yaari 1993).

En résumé, nos travaux suggèrent que les mécanismes liés aux CPSE AMPA et NMDA sont semblables dans les cellules pyramidales et les trois groupes d'interneurones chez le rat juvénile, sauf pour certains mécanismes liés aux CPSE NMDA, qui semblent spécifiques aux interneurones O/A. Puisque les interneurones GABAergiques immunopositifs pour la parvalbumine et la somatostatine de la couche oriens sont préférentiellement lésés après le traitement à l'AK (Best et al. 1993; Morin et al. 1998a), il est donc possible que les propriétés particulières des récepteurs NMDA de ces interneurones contribuent à les rendre plus vulnérables.

7.1.5. Les courants postsynaptiques inhibiteurs dans les cellules pyramidales et les interneurones

La stimulation des afférences de la région CA1 produit aussi des courants postsynaptiques inhibiteurs (CPSI) dans les cellules pyramidales et les différents sous-types d'interneurones (Schwartzkroin et Mathers 1978; Knowles et

Schwartzkroin 1980; Alger et Nicoll 1982; Alger 1984; Ashwood et al. 1984; Lacaille et al. 1987; Kawaguchi et Hama 1988; Lacaille et Schwartzkroin 1988a,b; Lacaille 1991). Nos données ont montré que les CPSI GABA_A sont semblables dans les cellules pyramidales et les trois groupes d'interneurones chez le rat juvénile (Morin et al. 1996). Par contre, chez le rat adulte, les réponses synaptiques GABAergiques sont moins prédominantes que les réponses excitatrices dans les interneurones O/A (Lacaille et al. 1987), PYR (Schwartzkroin et Mathers 1978) et LM (Lacaille et Schwartzkroin 1988a) enregistrés intracellulairement, contrairement à ce qui a été rapporté dans les cellules pyramidales (Alger et Nicoll 1982; Collingridge et al. 1984). Toutefois, des réponses inhibitrices marquées et similaires à celles des cellules pyramidales ont été observées dans les interneurones PYR lors d'une autre étude plus récente réalisée chez le rat adulte (Lacaille 1991), en accord avec nos données. Une étude récente a démontré que les propriétés des CPSI GABA_A spontanés de certains sous-types d'interneurones de la région CA1 sont différentes (Hajos et Mody 1997). Il semble donc que certains mécanismes GABAergiques soient spécifiques à des sous-types d'interneurones distincts, toutefois ces différences n'étaient pas apparentes dans les réponses globales étudiées dans nos travaux.

Ces différences pourraient avoir une importance fonctionnelle puisque la cinétique des réponses GABA_A dans les interneurones semble déterminer la fréquence de l'activité oscillatoire générée par les circuits inhibiteurs de l'hippocampe (Traub et al. 1996; Wang et Buzsaki 1996). Ainsi, l'hétérogénéité des synapses GABA pourrait contribuer aux patrons d'oscillations distincts associés à différents comportements chez l'animal (Traub et al. 1996; Wang et Buzsaki 1996).

7.2. L'hippocampe du rat traité à l'acide kaïnique

Nos travaux anatomiques et physiologiques suggèrent que plusieurs types de changements se produisent dans les circuits inhibiteurs de la région CA1 de l'hippocampe après le traitement à l'AK, mais que ces modifications sont spécifiques à certains sous-types d'interneurones. De plus, certains changements contribuent à la désinhibition des cellules pyramidales (Morin et al. 1998a,b), tandis que d'autres servent plutôt à rétablir l'inhibition dans les cellules pyramidales (Morin et al. 1998b). Ainsi, la désinhibition des cellules pyramidales peut être provoquée par 1) la perte des interneurones dans la couche oriens et l'alveus, et 2) la réduction des courants postsynaptiques excitateurs dans les interneurones de la couche lacunosum-moleculare. Les changements qui tendent à rétablir l'inhibition sont 1) les modifications de cinétique des courants GABA_A monosynaptiques des cellules pyramidales et leur conductance inchangée, malgré une perte d'interneurones, et 2) la cinétique modifiée des courants postsynaptiques excitateurs des interneurones O/A et leur conductance intacte, malgré une déafférentation partielle.

7.2.1. La perte de cellules dans l'hippocampe épileptique

Le modèle de l'AK est fréquemment utilisé pour étudier les mécanismes sous-jacents à l'épilepsie, car ce modèle reproduit la perte de certains neurones du hile et des cellules pyramidales de la région CA3 observée chez les épileptiques (Nadler 1981; Ben-Ari 1985).

Nos travaux anatomiques ont indiqué que le traitement à l'AK provoque une perte sélective des interneurones immunopositifs pour la DAG dans la couche oriens et l'alveus de la région CA1 (Morin et al. 1998a), mais pas dans les couches radiatum et lacunosum-moleculare (Morin et al. 1998a). Nos observations sont donc en accord avec celles de Franck et collaborateurs (1988) indiquant que les interneurones immunopositifs pour la DAG sont toujours présents dans les couches pyramidale, radiatum et lacunosum-moleculare après le traitement à l'AK (Franck et al. 1988). Dans notre étude, la perte sélective des interneurones immunopositifs pour la DAG dans la couche oriens et l'alveus laisse supposer que le traitement à l'AK ne produit pas une réduction généralisée de l'immunoréactivité à la DAG (Morin et al. 1998a). En utilisant la coloration de Nissl, cette hypothèse a été confirmée par l'observation d'une perte cellulaire des interneurones dans la couche oriens et l'alveus, mais pas dans les couches radiatum et lacunosum-moleculare (Morin et al. 1998a). Les interneurones de la couche oriens et l'alveus qui dégénèrent suite au traitement à l'AK correspondent probablement aux interneurones horizontaux qui contiennent la somatostatine, puisque la perte de ces neurones a déjà été rapportée chez le rat traité à l'AK (Best et al. 1993). La réduction partielle des interneurones immunopositifs pour la DAG dans la couche pyramidale (Morin et al. 1998a) concorde avec la perte de neurones contenant la parvalbumine dans la région CA1 (Best et al. 1993). Des travaux anatomiques et physiologiques ont suggéré que les interneurones horizontaux sont impliqués dans l'inhibition rétroactive des cellules pyramidales (McBain et al. 1994; Blasco-Ibanez et Freund 1995; Macafferri et McBain 1995). La perte des interneurones GABAergiques de la couche oriens et l'alveus devrait donc contribuer à

une perte partielle d'inhibition des cellules pyramidales de la région CA1 et ainsi contribuer à l'activité épileptiforme après le traitement à l'AK. Ainsi, nos travaux suggèrent que la perte d'interneurones GABAergiques suite au traitement à l'AK semble spécifique à certains interneurones impliqués dans l'inhibition rétroactive, et n'affecte pas ceux qui produisent l'inhibition proactive.

7.2.2. Les propriétés intrinsèques des cellules pyramidales et des interneurones après le traitement à l'AK

Les changements des propriétés intrinsèques provoqués par le traitement à l'AK sont sujets à controverse. Certaines études intracellulaires ont indiqué une diminution des après-hyperpolarisations lentes et une augmentation de la résistance d'entrée dans les cellules pyramidales chez les rats traités à l'AK (Franck et Schwartzkroin 1985; Franck et al. 1988; Nakajima et al. 1991), tandis que d'autres travaux n'ont pas observé ces changements (Williams et al. 1993; Perez et al. 1996). Nos enregistrements de *patch clamp* en configuration cellule entière ont aussi indiqué que les propriétés intrinsèques des cellules pyramidales ne sont pas modifiées suite au traitement à l'AK (Morin et al. 1998b), ce qui concorde avec les résultats précédents issus de notre laboratoire (Williams et al. 1993; Perez et al. 1996). Nos travaux ont également indiqué que les propriétés intrinsèques des interneurones O/A et LM sont inchangées après le traitement à l'AK (Morin et al. 1998b). Nos résultats sont en accord avec l'observation d'une résistance d'entrée inchangée dans les interneurones de la couche pyramidale suite au traitement à l'AK lors d'enregistrements intracellulaires (Franck et al. 1988), ainsi qu'avec les propriétés intrinsèques intactes

des interneurones des couches oriens, radiatum et lacunosum-moleculare dans le modèle d'épilepsie du *status epilepticus* (Rempe et al. 1997).

Nos observations suggèrent donc que l'activité épileptiforme de la région CA1 chez les animaux traités à l'AK n'est pas causée par des changements des propriétés intrinsèques des cellules pyramidales ou des interneurones, mais plutôt par des modifications au niveau des mécanismes synaptiques de l'hippocampe.

7.2.3. Les modifications de la transmission synaptique excitatrice suite au traitement à l'AK

Nos travaux ont montré que les courants postsynaptiques excitateurs sont modifiés dans certains sous-types d'interneurones suite au traitement à l'AK (Morin et al. 1998b). En effet, la conductance des CPSE non-NMDA et NMDA est diminuée dans les interneurones LM après le traitement à l'AK (Morin et al. 1998b), et cette perte est spécifique à ces interneurones puisque la conductance des CPSE est inchangée dans les interneurones O/A (Morin et al. 1998b). Cette perte de réponse excitatrice dans les interneurones LM concorde avec les observations anatomiques qui ont démontré une dégénérescence des contacts synaptiques excitateurs sur les interneurones LM après le traitement à l'AK (Kunkel et al. 1988).

La réduction de réponse excitatrice dans certains interneurones inhibiteurs de la région CA1 concorde avec l'hypothèse des cellules inhibitrices dormantes du gyrus dentelé proposée par Sloviter (1991). Cette hypothèse stipule que l'activité épileptiforme du gyrus dentelé est due à une désinhibition des cellules principales, causée par une perte d'afférences excitatrices aux interneurones inhibiteurs (Sloviter

1987, 1991). Dans la région CA1 du rat traité à l'AK, une perte des afférences excitatrices sur les interneurones LM pourrait également contribuer à la réduction de l'inhibition polysynaptique dans les cellules pyramidales et à leur hyperexcitabilité (Franck et al. 1988; Williams et al. 1993). Toutefois, dans la région CA1, la perte des afférences excitatrices est spécifique aux interneurones LM et n'affecte pas les interneurones O/A. De plus, la perte de réponse excitatrice aux interneurones inhibiteurs ne s'applique peut-être pas à tous les modèles d'épilepsie, puisque d'autres travaux ont rapporté que les réponses synaptiques excitatrices des interneurones sont inchangées dans le modèle du *status epilepticus* (Rempe et al. 1997). Ce modèle d'épilepsie provoque par contre une perte plus généralisée des neurones de l'hippocampe, ce qui laisse supposer que la perte sélective des fibres collatérales de Schaffer semble être le facteur déterminant contribuant à la réduction de l'excitation sur les interneurones LM dans le modèle d'épilepsie de l'AK (Morin et al. 1998b).

Bien que la conductance des CPSE ne soit pas modifiée dans les interneurones O/A après le traitement à l'AK, nos données ont indiqué que le temps de descente de ces CPSE est plus rapide (Morin et al. 1998b). Ces différences de cinétique des CPSE suggèrent la présence de changements à ces synapses excitatrices après le traitement à l'AK. Ces données sont en accord avec des observations préliminaires suggérant aussi que la cinétique des CPSE spontanés dans les interneurones O/A est modifiée suite au traitement à l'AK (Perez et Lacaille 1997). Puisque la conductance des CPSE est inchangée dans les interneurones O/A, malgré leur déafférentation partielle due à la perte des fibres afférentes provenant de la région CA3 après le traitement à l'AK (Lacaille et al. 1987), les changements de cinétique des CPSE dans ces interneurones

pourraient indiquer que des changements compensatoires se sont produits aux synapses excitatrices des interneurones O/A (Morin et al. 1998b). Le bourgeonnement extensif des fibres collatérales des axones des cellules pyramidales de la région CA1 suite au traitement à l'AK (Perez et al. 1996) pourrait être impliqué dans la formation de nouvelles synapses excitatrices et compenser la perte des synapses provenant de la région CA3 (Morin et al. 1998b). Ainsi, la formation de nouvelles synapses pourrait contribuer à une conductance inchangée des CPSE, tandis que la présence de nouvelles synapses ayant des propriétés différentes pourrait expliquer les changements de cinétique des CPSE (Morin et al. 1998b). Ces changements compensatoires pourraient contribuer au rétablissement des potentiels postsynaptiques inhibiteurs dans les cellules pyramidales à de longs intervalles (deux à quatre mois) après le traitement à l'AK (Franck et Schwartzkroin 1985; Franck et al. 1988; Nakajima et al. 1991).

7.2.4. Les modifications des synapses GABAergiques après le traitement à l'AK

Il a été démontré à l'aide d'enregistrements intracellulaires que les réponses inhibitrices polysynaptiques des cellules pyramidales de la région CA1 sont diminuées après le traitement à l'AK (Franck et al. 1988; Williams et al. 1993; Perez et al. 1996). Nos données ont montré que l'amplitude et la conductance des CPSI GABA_A monosynaptiques des cellules pyramidales et des interneurones O/A et LM sont inchangées après le traitement à l'AK (Morin et al. 1998b). Nos observations suggèrent donc qu'une perte d'inhibition monosynaptique n'est pas responsable de la désinhibition des cellules pyramidales après le traitement à l'AK (Morin et al. 1998b).

Nos conclusions concordent avec celles d'autres travaux montrant aussi une inhibition monosynaptique intacte dans les cellules pyramidales de la région CA1 chez les rats traités à l'AK (Williams et al. 1993; Esclapez et al. 1997), ainsi que dans d'autres modèles d'épilepsie (Mangan et al. 1995; Mangan et Lothman 1996). Par contre, nos résultats ont indiqué que la cinétique des CPSI GABA_A monosynaptiques est plus rapide dans les cellules pyramidales des animaux traités à l'AK, ce qui suggère la présence de changements compensatoires aux synapses GABAergiques (Morin et al. 1998b). De plus, la présence d'une conductance des CPSI GABA_A intacte, malgré une perte d'interneurones immunopositifs pour la DAG dans la couche oriens et l'alveus (Morin et al. 1998a), suggèrent que des changements compensatoires se sont produits aux synapses GABAergiques après le traitement à l'AK (Morin et al. 1998b). Par contre, la nature de ces changements compensatoires est toujours inconnue. Ces changements pourraient impliquer la formation de nouvelles synapses inhibitrices sur les cellules pyramidales suite au bourgeonnement des axones des interneurones GABAergiques, tel qu'observé dans le gyrus dentelé (Davenport et al. 1990), ou une modification des propriétés des synapses GABA sur les cellules pyramidales (Morin et al. 1998b).

Certaines évidences sont en accord avec la présence de changements fonctionnels aux récepteurs GABA_A dans le modèle d'épilepsie du *status epilepticus* (Kapur et Coulter 1995; Gibbs et al. 1997; Kapur et Macdonald 1997). Dans le modèle de la pilocarpine, l'expression de l'ARN_m des sous-unités $\alpha 2$ et $\alpha 5$ des récepteurs GABA_A est diminuée dans les neurones de la région CA1, tandis que l'expression des sous-

unités $\alpha 1$, $\beta 2$ ou $\gamma 2$ est inchangée (Houser et Esclapez 1996; Rice et al. 1996; Vick et al. 1996). De plus, des travaux physiologiques ont montré que les courants GABA sont réduits dans les cellules pyramidales dissociées de la région CA1 après *status epilepticus* (Kapur et Coulter 1995; Gibbs et al. 1997), tandis que l'efficacité du GABA à produire des courants GABA_A est augmentée (Kapur et Coulter 1995; Gibbs et al. 1997). Ces travaux ont aussi montré que la potentialisation des courants GABA par les benzodiazépines est réduite (Gibbs et al. 1997). Il semble donc que, dans ce modèle d'épilepsie, les récepteurs GABA_A subissent des modifications moléculaires et fonctionnelles qui pourraient contribuer à des changements fonctionnels au niveau de la transmission synaptique GABAergique.

7.2.5. Les contacts synaptiques GABA sur les interneurones et les cellules pyramidales sont modifiés après le traitement à l'AK

Plusieurs études anatomiques ont suggéré que la perte de contacts synaptiques inhibiteurs sur les cellules pyramidales pourrait contribuer à l'activité épileptiforme des cellules principales dans les modèles d'épilepsie (Ribak et al. 1979, 1982; Houser et al. 1986). Chez l'humain, certains ont observé une perte similaire (Marco et al. 1997) dans le cortex, par contre d'autres ont rapporté que les neurones et contacts synaptiques inhibiteurs sont toujours présents dans l'hippocampe épileptique (Babb et al. 1989). Dans le modèle du rat traité à l'AK, une perte des interneurones immunopositifs pour la somatostatine et la parvalbumine a été observée (Best et al. 1993), en accord avec nos travaux (Morin et al. 1998a). Cette perte d'interneurones

inhibiteurs et par conséquent la perte de leurs contacts synaptiques sur les cellules pyramidales devrait contribuer à l'hyperexcitabilité des cellules principales après le traitement à l'AK (Best et al. 1994). Par contre, nos données ultrastructurales n'ont indiqué aucune perte de contacts synaptiques périsomatiques GABA sur les cellules pyramidales, mais plutôt une augmentation de leur longueur moyenne après le traitement à l'AK (Morin et al. 1998c). Ces résultats suggèrent donc une augmentation de l'inhibition périsomatique sur les cellules pyramidales. Ces observations sont difficiles à concilier avec la perte des contacts synaptiques immunopositifs pour la parvalbumine rapportée sur les cellules pyramidales du rat traité à l'AK (Best et al. 1994). Toutefois, une étude récente a démontré que la perte des neurones immunopositifs pour la parvalbumine n'est pas nécessairement corrélée à une perte de neurones GABAergiques chez la gerbille prédisposée aux crises épileptiques (Scotti et al. 1997). L'activité épileptiforme pourrait donc diminuer l'intensité de l'immunoréactivité pour la parvalbumine sans nécessairement causer la mort des neurones contenant la parvalbumine (Scotti et al. 1997).

Nos données ultrastructurales suggèrent donc que l'hyperexcitabilité des cellules pyramidales après le traitement à l'AK n'est pas due à une diminution de l'inhibition périsomatique des cellules pyramidales (Morin et al. 1998c). Par ailleurs, nos travaux ont indiqué que les courants postsynaptiques GABA_A monosynaptiques sont inchangés dans les cellules pyramidales chez les rats traités à l'AK (Morin et al. 1998b). Nos données physiologiques ne reflètent donc pas l'augmentation de l'inhibition périsomatique observée anatomiquement aux cellules pyramidales (Morin et al. 1998c). Toutefois, la présence de courants postsynaptiques inhibiteurs

inchangés combinée à une augmentation de l'inhibition périsomatique pourrait suggérer une perte de synapses inhibitrices sur les dendrites des cellules pyramidales (Morin et al. 1998c). La perte d'interneurones GABAergiques de la couche oriens et l'alveus chez les rats traités à l'AK est compatible avec une telle réduction de synapses dendritiques inhibitrices, puisque ces interneurones, immunopositifs pour la somatostatine, forment normalement des contacts synaptiques sur les dendrites des cellules pyramidales (Blasco-Ibanez et Freund 1995).

Dans un deuxième temps, nos travaux ont aussi montré que le nombre et la longueur totale des contacts synaptiques GABA sont augmentés dans les interneurones LM après le traitement à l'AK, ce qui suggère une augmentation de l'inhibition périsomatique (Morin et al. 1998c). Cette augmentation de l'inhibition périsomatique des interneurones LM concorde avec l'hypothèse de désinhibition qui postule que l'activité épileptiforme chez la gerbille est causée par une augmentation de l'inhibition des neurones inhibiteurs (Peterson et al. 1985; Farias et al. 1992). Par contre, nos résultats physiologiques n'ont pas montré d'augmentation des courants postsynaptiques GABA_A dans les interneurones LM après le traitement à l'AK (Morin et al. 1998b). Ces données physiologiques semblent donc en désaccord avec l'augmentation de l'inhibition périsomatique observée au niveau ultrastructural dans les interneurones LM. Toutefois, l'augmentation des synapses GABA périsomatiques en présence de courants postsynaptiques inhibiteurs inchangés pourrait indiquer une perte de synapses inhibitrices sur les dendrites des interneurones LM suite au traitement à l'AK. Les interneurones horizontaux de la couche oriens font des contacts synaptiques inhibiteurs sur les dendrites des cellules pyramidales dans la

couche lacunosum-moleculare (Blasco-Ibanez et Freund 1995). Leur perte, suite au traitement à l'AK (Best et al. 1993), pourrait contribuer à une réduction des synapses inhibitrices sur les dendrites des interneurones LM, si ces interneurones horizontaux formaient aussi des contacts synaptiques avec les interneurones inhibiteurs.

7.2.6. Les contacts synaptiques non-GABA sont inchangés après le traitement à l'AK

Nos données ultrastructurales ont aussi indiqué que le nombre et la longueur des contacts synaptiques périsomatiques non-GABA sont inchangés dans les interneurones et les cellules pyramidales après le traitement à l'AK (Morin et al. 1998c). Il est bien établi que le traitement à l'AK provoque la dégénérescence des fibres afférentes de la région CA1 (Nadler 1981). Toutefois, six à huit semaines après le traitement à l'AK, une réapparition des synapses excitatrices est observée dans la région CA1, et il a été suggéré que cette synaptogénèse est due au bourgeonnement des fibres Schaffer résistantes au traitement à l'AK (Nadler et al. 1980). Ces changements compensatoires pourraient expliquer l'absence de modifications de contacts synaptiques périsomatiques non-GABA chez les animaux traités à l'AK (Morin et al. 1998c). Toutefois, nos données ultrastructurales ne nous permettent pas de déterminer s'il y a eu perte et réapparition de synapses périsomatiques non-GABA, ou une absence de changement après le traitement à l'AK.

Nos observations suggérant que les contacts synaptiques périsomatiques non-GABA sont intacts suite au traitement à l'AK sont en accord avec nos données physiologiques qui indiquent une amplitude et conductance des CPSE inchangées dans les cellules pyramidales et les interneurones O/A après le traitement à l'AK

(Morin et al. 1998b). Nos données ultrastructurales sont aussi en accord avec les évidences indiquant que l'activation synaptique des interneurones de la région CA1 est intacte chez les animaux traités à l'AK (Esclapez et al. 1997). Par contre, nos travaux physiologiques ont montré que la cinétique des CPSE est modifiée dans les interneurones O/A suite au traitement à l'AK, ce qui suggère certains changements à leurs synapses excitatrices (Morin et al. 1998b). Puisque les synapses périsomatiques non-GABA sont inchangées dans ces interneurones, des modifications compensatoires survenant aux synapses situées sur leurs dendrites pourraient être responsables des modifications de la cinétique des courants synaptiques excitateurs.

Nos données ultrastructurales ont aussi montré que le nombre des contacts synaptiques périsomatiques non-GABA sur les interneurones LM est inchangé après le traitement à l'AK (Morin et al. 1998c). Ces observations semblent en désaccord avec nos données physiologiques indiquant que les courants postsynaptiques excitateurs sont diminués dans ces interneurones après le traitement à l'AK (Morin et al. 1998b). Toutefois, le nombre inchangé de synapses périsomatiques non-GABA sur les interneurones LM pourrait aussi indiquer que des modifications se sont produites au niveau des synapses dendritiques de ces interneurones.

7.2.7 L'épilepsie du lobe temporal chez l'humain

Chez les épileptiques, certains travaux anatomiques ont rapporté une perte des synapses inhibitrices sur le corps cellulaire et le segment initial de l'axone des cellules pyramidales (Marco et al. 1997), tandis que d'autres observations ont démontré que les neurones et contacts synaptiques inhibiteurs sont toujours présents

(Babb et al. 1989). De plus, d'autres travaux ont rapporté une perte d'interneurones immunopositifs pour la somatostatine chez les patients épileptiques (Robbins et al. 1991; de Lanerolle et al. 1989). Ainsi, la perte des interneurones inhibiteurs chez les épileptiques reste donc sujet à controverse.

Nos travaux anatomiques ont permis la mise au point d'une technique de fixation compatible avec l'immunoréactivité pour le GABA à partir de tissu cortical prélevé chez des patients épileptiques lors d'une chirurgie du lobe temporal. La compatibilité de cette méthode de fixation avec l'immunocytochimie pour le GABA pourrait permettre de quantifier les neurones GABA dans l'hippocampe à partir de tissu prélevé d'épileptiques et de déterminer si une perte spécifique d'interneurones inhibiteurs de l'hippocampe est présente dans l'épilepsie du lobe temporal, comme nos travaux chez le rat traité à l'AK l'ont suggéré (Morin et al. 1998a). Ces techniques pourraient également permettre une analyse ultrastructurale quantitative des contacts synaptiques périsomatiques GABA et non-GABA sur les neurones de la région CA1 afin d'examiner si l'épilepsie du lobe temporal est accompagnée de changements à ces synapses (Morin et al. 1998c). Ces travaux permettraient de déterminer si les changements aux synapses périsomatiques GABA dans les interneurones LM et les cellules pyramidales chez le rat traité à l'AK sont également retrouvés dans des neurones similaires de l'hippocampe des épileptiques.

7.2.8 Perspectives d'avenir

Les résultats obtenus dans cette thèse suggèrent plusieurs avenues de recherche intéressantes. Dans un premier temps, chez le rat normal, nos données

physiologiques indiquent que la stimulation des fibres afférentes de la région CA1 produit des courants postsynaptiques inhibiteurs GABA_A qui sont semblables dans les différents interneurones examinés. Par contre, des évidences anatomiques suggèrent que certaines afférences inhibitrices des interneurones de la région CA1 proviennent de différentes sources : certaines proviennent d'interneurones inhibiteurs qui font des contacts synaptiques préférentiellement sur d'autres interneurones (Acsady et al. 1996a,b; Gulyas et al. 1996), d'autres proviennent des fibres afférentes GABAergiques du septum (Freund et Antal 1988). Cette diversité des afférences inhibitrices pourrait être associée à une hétérogénéité des propriétés des synapses inhibitrices des interneurones. Il serait donc intéressant de faire une analyse détaillée des propriétés des synapses inhibitrices dans différents sous-types d'interneurones en caractérisant leurs réponses synaptiques spontanées et miniatures. Les courants postsynaptiques GABA_A spontanés pourraient être étudiés à l'aide d'enregistrement *patch clamp* en configuration cellule entière en présence d'antagonistes des récepteurs ionotropiques au glutamate, tandis que les courants miniatures, reflétant l'activation de synapses unitaires, seraient examinés en présence de la tetrodoxine pour bloquer les canaux Na⁺ et prévenir la libération du GABA qui est dépendante des potentiels d'action. Certaines données préliminaires suggèrent que les propriétés des CPSI spontanés GABA_A diffèrent dans les interneurones (Nurse et Lacaille 1996). En effet, la cinétique des CPSIs semble différente (temps de montée plus lent et temps de descente plus rapide) dans certains interneurones. De plus, la fréquence des CPSI GABA_A spontanés semble plus rapide dans certains interneurones de la couche oriens et l'alveus (Nurse et Lacaille 1996). Ainsi, l'analyse détaillée des propriétés des

courants postsynaptiques GABA_A spontanés et miniatures pourrait mettre en évidence des différences fonctionnelles aux synapses GABAergiques propres à certains interneurones.

Dans un deuxième temps, dans le modèle d'épilepsie de l'AK, nos données physiologiques ont indiqué des changements au niveau des courants postsynaptiques excitateurs dans les interneurones O/A et LM, ainsi qu'au niveau des courants postsynaptiques inhibiteurs dans les cellules pyramidales. Afin de différencier les modifications dues aux effets aigus du traitement à l'AK des changements compensatoires, les courants postsynaptiques excitateurs et inhibiteurs devraient être étudiés deux à trois jours après le traitement à l'AK en utilisant les mêmes techniques que dans cette thèse. Ainsi, les présumés changements compensatoires devraient être absents à ce court intervalle.

De plus, afin de confirmer la présence de changements au niveau des synapses excitatrices unitaires des interneurones O/A deux semaines après le traitement à l'AK, une étude détaillée des CPSE miniatures permettrait de caractériser les propriétés des synapses excitatrices dans les interneurones O/A après le traitement à l'AK. Les CPSE miniatures dans les interneurones O/A pourraient être étudiés à l'aide d'enregistrement *patch clamp* en configuration cellule entière en présence de l'antagoniste des récepteurs GABA_A et de la tétrodoxine. Ensuite, pour déterminer si ces changements sont dus aux effets aigus du traitement à l'AK ou à des changements compensatoires, les CPSE miniatures devraient être examinés deux à trois jours après le traitement à l'AK. Enfin, afin de déterminer l'origine des synapses excitatrices qui sont modifiées suite au traitement à l'AK, une étude des CPSE produits par

stimulation minimale dans les interneurones O/A pourrait être réalisée en présence des antagonistes des récepteurs GABA_A (BIC). Des travaux récents ont démontré la présence de récepteurs présynaptiques mGluR7 sensibles à L-2-amino-4-phosphonobutyrate (AP4) aux terminaisons des cellules pyramidales. Ces récepteurs sont préférentiellement colocalisés aux synapses sur les interneurones immunopositifs pour la somatostatine dans la couche oriens et l'alveus (Shigemoto et al. 1996). L'étude des CPSE, sensibles à l'agoniste AP4, dans les interneurones O/A permettrait de déterminer si les synapses excitatrices qui sont modifiées suite au traitement à l'AK proviennent des fibres axonales des cellules pyramidales ou des afférences de la région CA1.

Enfin, nos données ultrastructurales suggèrent indirectement que le traitement à l'AK pourrait provoquer une perte des synapses GABA sur les dendrites des cellules pyramidales et des interneurones LM. Une étude ultrastructurale quantitative des synapses dendritiques GABA chez des rats témoins et des animaux traités à l'AK permettrait de vérifier cette hypothèse. Un marquage immunocytochimique des interneurones LM avec la calbindine pourrait permettre l'identification de ce type d'interneurone et la reconstruction de leurs dendrites. L'analyse quantitative des synapses GABA sur ces dendrites pourrait être accomplie à l'aide des techniques d'immunocytochimie contre le GABA en coupes séries et de microscopie électronique. Une analyse quantitative similaire pourrait être faite sur les dendrites des cellules pyramidales (GABA-immunonégatives). Une telle étude détaillée des synapses GABA sur les dendrites des interneurones LM et des cellules pyramidales

permettrait de déterminer directement si le traitement à l'AK provoque une perte de leurs synapses dendritiques GABAergiques.

Les travaux présentés dans cette thèse contribuent donc à l'avancement des connaissances quant au rôle des interneurones inhibiteurs dans l'hippocampe du rat normal ainsi que dans le modèle d'épilepsie de l'AK, et contribuent à mieux comprendre les mécanismes qui sous-tendent l'épilepsie du lobe temporal chez l'humain.

CHAPITRE 8

BIBLIOGRAPHIE GÉNÉRALE

8 BIBLIOGRAPHIE GÉNÉRALE

Acsady, L., Arabadzisz, D. and Freund, T. F. Correlated morphological and neurochemical features identify different subsets of vasoactive intestinal polypeptide-immunoreactive interneurons in rat hippocampus. *Neuroscience* 73: 299-315, 1996a.

Acsady, L., Arabadzisz, D. and Freund, T. F. Different populations of vasoactive intestinal polypeptide-immunoreactive interneurons are specialized to control pyramidal cells or interneurons in the hippocampus. *Neuroscience* 73: 317-334, 1996b.

Alger, B.E. and Nicoll, R.A. Feed-forward dendritic inhibition in rat hippocampal pyramidal cells studied in vitro. *J. Physiol. (Lond.)* 328: 105-123, 1982.

Alger, B.E. Characteristics of a slow hyperpolarizing synaptic potential in rat hippocampal pyramidal cells in vitro. *J. Neurophysiol.* 52: 892-910, 1984.

Andersen, P., Eccles, J.C. and Loynard, Y. Location of synaptic inhibitory synapses on hippocampal pyramids. *J. Neurophysiol.* 27: 592-607, 1964.

Ascher, P. and Nowak, L. The role of divalent cations in the *N*-methyl-*D*-aspartate responses of mouse central neurones in culture. *J. Physiol. (Lond.)* 399: 247-266, 1988.

Ashwood, T.J., Lancaster, B. and Wheal, H.V. In vivo and in vitro studies on putative interneurons in the rat hippocampus: possible mediators of feed-forward inhibition. *Brain Res.* 293: 279-291, 1984.

Ashwood, T.J. and Wheal, H.V. Extracellular studies on the role of *N*-methyl-D-aspartate receptors in epileptiform activity recorded from the kainic acid-lesioned hippocampus. *Neurosci. Lett.* 67: 147-152, 1986.

Ashwood, T.J. and Wheal, H.V. The expression of *N*-methyl-D-aspartate-receptor-mediated component during epileptiform synaptic activity in the hippocampus. *Br. J. Pharmacol.* 91: 815-822, 1987.

Babb, T.L., Pretorius, J.K., Kupfer, W.R. and Crandall, R.H. Glutamate decarboxylase-immunoreactive neurons are preserved in human epileptic hippocampus. *J. Neurosci.* 9: 2563-2574, 1989.

Baimbridge, K.G. and Miller, J.J. Immunohistochemical localization of calcium-binding protein in the cerebellum, hippocampal formation and olfactory bulb of the rat. *Brain Res.* 245: 223-229, 1982.

Baude, A., Nusser, Z., Roberts, J.D., Mulvihill, E., McIlhinney, R.A. and Somogyi, P. The metabotropic glutamate receptor (mGluR1 alpha) is concentrated at

- perisynaptic membrane of neuronal subpopulations as detected by immunogold reaction. *Neuron* 11: 771-787, 1993.
- Ben-Ari, Y. Limbic seizure and brain damage produced by kainic acid: mechanisms and relevance to human temporal lobe epilepsy. *Neuroscience* 14: 375-403, 1985.
- Best, N., Mitchell, J., Bainbridge, K. G. and Wheal, H. V. Changes in parvalbumin-immunoreactive neurons in the rat hippocampus following a kainic acid lesion. *Neurosci. Lett.* 155: 1-6, 1993.
- Best, N., Mitchell, J. and Wheal, H. V. Ultrastructure of parvalbumin-immunoreactive neurons in the CA1 area of the rat hippocampus following a kainic acid injection. *Acta Neuropathol.* 87: 187-195, 1994.
- Blasco-Ibanez, J.M. and Freund, T.F. Synaptic input of horizontal interneurons in stratum oriens of the hippocampal CA1 subfield: structural basis of feed-back activation. *Eur. J. Neurosci.* 7: 2170-2180, 1995.
- Buckmaster, P.S., Kunkel, D.D., Robbins, R.J. and Schwartzkroin, P.A. Somatostatin immunoreactivity in the hippocampus of mouse, rat, guinea pig and rabbit. *Hippocampus* 4: 167-180, 1994.

Buhl, E.H., Han, Z.-S., Lorinczi, Z., Stezhka, V.V., Karnup, S.V. and Somogyi, P. Physiological properties of anatomically identified axo-axonic cells in the rat hippocampus. *J. Neurophysiol.* 71: 1289-1307, 1994.

Buhl E.H., Cobb S.R., Halasy K. and Somogyi P. Properties of unitary IPSPs evoked by anatomically identified basket cells in the rat hippocampus. *Eur. J. Neurosci.* 7: 1989-2004, 1995.

Buhl, E.H., Otis, T.S. and Mody, I. Zinc-induced collapse of augmented inhibition by GABA in a temporal lobe epilepsy model. *Science* 271: 369-373, 1996.

Collingridge, G.L. Inhibitory post-synaptic currents in rat hippocampal CA1 neurons. *J. Physiol. (Lond.)* 356: 551-564, 1984.

Collingridge, G.L., Herron, C.E. and Lester, R.A.J. Synaptic activation of N-methyl-D-aspartate receptors in the schaffer collateral-commissural pathway of rat hippocampus. *J. Physiol. (Lond.)* 399: 283-300, 1988.

Cronin, J., Obenhaus, A., Houser, C.R. and Dudek, F.E. Electrophysiology of dentate granule cells after kainate-induced synaptic reorganization of the mossy fibers. *Brain Res.* 573: 305- 310, 1992.

Curtis, D.R., Duggan, A.W., Felix, D. and Johnston, G.A. GABA, bicuculline and central inhibition. *Nature* 226: 1222-1224, 1970.

Davenport, C.J., Brown, W.J. and Babb, T.L. GABAergic neurons are spared after intrahippocampal kainate in the rat. *Epilepsy Res.* 5: 28-42, 1990.

Davies, J., Francis, A.A., Jones, A.W. and Watkins, J.C. 2-Amino-5-phosphonovalerate (2APV), a potent and selective antagonist of amino acid-induced and synaptic excitation. *Neurosci. Lett.* 21 : 77-81, 1981.

Davis, C.H, Pozza, M.F. and Collingridge, G.L. CGP 55845A: a potent antagonist of GABA_B receptors in the CA1 region of rat hippocampus. *Neuropharmacol.* 32: 1071-1073, 1993.

de Lanerolle, N.C., Kim, J.H., Robbins, R.J. and Spencer D.D. Hippocampal interneuron loss and plasticity in human temporal lobe epilepsy. *Brain Res.* 495: 387-395, 1989.

Engel, J. Jr. *Seizures and Epilepsy*, (Publ.) F.A. Davis Company, MA, 1989, pp. 536.

Esclapez, M., Hirsch, J.C., Khazipov, R., Ben-Ari, Y. and Bernard C. Operative GABAergic inhibition in hippocampal CA1 pyramidal neurons in experimental epilepsy. *Proc. Natl. Acad. Sci. (USA)* 94: 12151-12156, 1997.

Farias, P.A., Low, S.Q., Peterson, G.M. and Ribak, C.E. Morphological evidence for altered synaptic organization and structure in the hippocampal formation of seizure-sensitive gerbils. *Hippocampus* 2: 229-245, 1992.

Franck, J.E. and Schwartzkroin, P.A. Do kainate-lesioned hippocampi become epileptogenic? *Brain Res.* 389: 309-313, 1985.

Franck, J.E., Kunkel, D.D., Baskin, D.G. and Schwartzkroin, P.A. Inhibition in kainate-lesioned hyperexcitable hippocampi: physiologic, autoradiographic and immunocytochemical observations. *J. Neurosci.* 8: 1991-2002, 1988.

Freund, T.F. and Antal, M. GABA-containing neurons in the septum control inhibitory interneurons in the hippocampus. *Nature* 336: 170-173, 1988.

Freund, T.F. and Buzsáki, G. Interneurons of the hippocampus. *Hippocampus* 6: 347-470, 1996.

Fukuzako, H. and Izumi, K. Clinical aspects of the epilepsies. In: *GABA Mechanisms in Epilepsy*, Tunnicliff, G. et Raess, B.U., Wiley-Liss, Inc., 1991, p. 1-30.

Geiger, J.R.P., Melcher, T., Koh, D.-S., Sakmann, B., Seeburg, P.H., Jonas, P. and Monyer, H. Relative abundance of subunit mRNAs determines gating and Ca^{2+}

permeability of AMPA receptors in principal neurons and interneurons in rat CNS. *Neuron* 15: 193-204, 1995.

Gibbs, J.W., Shumate, M.D. and Coulter, D.A. Differential epilepsy-associated alterations in postsynaptic GABA_A receptor function in dentate granule cells and CA1 neurons. *J. Neurophysiol.* 77: 1924-1938, 1997.

Goddard, G.V., McIntyre, D.C. and Leech, C.K. A permanent change in brain function resulting from daily electrical stimulation. *Exp. Neurol.* 25: 295-330, 1969.

Gulyas, A.I., Toth, K., Danos, P. and Freund, T.F. Subpopulations of GABAergic neurons containing parvalbumin, calbindin D-28k, and cholecystokinin in the rat hippocampus. *J. Comp. Neurol.* 312: 371-378, 1991.

Gulyas, A.I., Miles, R., Hajos, N. and Freund, T.F. Precision and variability in postsynaptic target selection of inhibitory cells in the hippocampal CA3 region. *Eur. J. Neurosci.* 5: 1729-1751, 1993.

Gulyas, A.I., Hajos, N. and Freund, T.F. Interneurons containing calretinin are specialized to control other interneurons in the rat hippocampus. *J. Neurosci.* 16: 3397-3411, 1996.

Hajos, N. and Mody, I. Synaptic communication among hippocampal interneurons: properties of spontaneous IPSCs in morphologically identified cells. *J. Neurosci.* 17: 8427-8442, 1997.

Halasy, K., Buhl, E.H., Lorinczi, Z., Tamas, G. and Somogyi, P. Synaptic target selectivity and input of GABAergic basket and bistratified interneurons in the CA1 area of the rat hippocampus. *Hippocampus* 6: 306-329, 1996.

Herron, C.E., Williamson, R. and Collingridge, G.L. A selective *N*-methyl-D-aspartate antagonist depresses epileptiform activity in rat hippocampal slices. *Neurosci. Lett.* 61: 225-260, 1985.

Hestrin, S., Nicoll, R.A., Perkel, D.J. and Sah, P. Analysis of excitatory synaptic action in pyramidal cells using whole-cell recording from rat hippocampal slices. *J. Physiol. (Lond.)* 422: 203-225, 1990.

Hestrin, S. Different glutamate receptor channels mediate fast excitatory synaptic currents in inhibitory and excitatory cortical neurons. *Neuron* 11: 1083-1091, 1993.

Honore, T., Davies, S.N., Drejer, J., Fletcher, E.J., Jacobsen, P., Lodge, D. and Nielsen, F.E. Quinoxalinediones: Potent competitive non-NMDA glutamate receptor antagonists. *Science* 241: 701-703, 1988.

Houser, C.R., Harris, A.B. and Vaughn, J.E. Time course of the reduction of GABA terminals in a model of focal epilepsy: a glutamic acid decarboxylase immunocytochemical study. *Brain Res.* 383: 129-145, 1986.

Houser, C.R. and Esclapez, M. Vulnerability and plasticity of the GABA system in the pilocarpine model of spontaneous recurrent seizures. *Epilepsy Res.* 26: 207-218, 1996.

Kapur, J. and Coulter, D.A. Experimental status epilepticus alters γ -aminobutyric acid type A receptor function in CA1 pyramidal neurons. *Ann. Neurol.* 38: 893-900, 1995.

Kapur, J. and Macdonald, R.L. Rapid seizure-induced reduction of benzodiazepine and Zn^{2+} sensitivity of hippocampal dentate gyrus cell $GABA_A$ receptors. *J. Neurosci.* 17: 7532-7540, 1997.

Kawaguchi, Y. and Hama, K. Two subtypes of non-pyramidal cells in rat hippocampal formation identified by intracellular recording and HRP injection. *Brain Res.* 411: 190-195, 1987.

Kawaguchi, Y. and Hama, K. Physiological heterogeneity of nonpyramidal cells in rat hippocampal CA1 region. *Exp. Brain Res.* 72: 494-502, 1988.

Knowles, W.D. and Schwartzkroin, P.A. Axonal ramifications of hippocampal CA1 pyramidal cells. *J. Neurosci.* 1: 1236-1241, 1980.

Knowles, W.D. and Schwartzkroin, P.A. Local circuit synaptic interactions in hippocampal brain slices. *J. Neurosci.* 1: 318-322, 1981.

Kosaka, T., Katsumaru, H., Hama, K., Wu, J.-Y. and Heizmann, C.W. GABAergic neurons containing the Ca^{2+} -binding protein parvalbumin in the rat hippocampus and dentate gyrus. *Brain Res.* 419: 119-130, 1987.

Kosaka, T., Wu, J.Y. and Benoit, R. GABAergic neurons containing somatostatin-like immunoreactivity in the rat hippocampus and dentate gyrus. *Exp. Brain Res.* 71: 388-398, 1988.

Kunkel, D.D., Lacaille, J.-C. and Schwartzkroin, P.A. Ultrastructure of stratum lacunosum-moleculare interneurons of hippocampal CA1 region. *Synapse* 2: 382-394, 1988.

Kunkel, D.D. and Schwartzkroin, P.A. Ultrastructural characterization and GAD co-localization of somatostatin-like immunoreactive neurons in CA1 of rabbit hippocampus. *Synapse* 2 : 371-381, 1988.

Lacaille, J.-C., Mueller, A.L, Kunkel, D.D. and Schwartzkroin, P.A. Local circuit interactions between oriens-alveus interneurons and CA1 pyramidal cells in hippocampal slices: electrophysiology and morphology. *J. Neurosci.* 7: 1979-1993, 1987.

Lacaille, J.-C. and Schwartzkroin, P.A. Stratum lacunosum-moleculare interneurons of hippocampal CA1 region: I. Intracellular response characteristics, synaptic responses, and morphology. *J. Neurosci.* 8: 1400-1410, 1988a.

Lacaille, J.-C. and Schwartzkroin, P.A. Stratum lacunosum-moleculare interneurons of hippocampal CA1 region: I. Intrasomatic and intradendritic recording of local circuit synaptic interactions. *J. Neurosci.* 8: 1411-1424, 1988b.

Lacaille, J.-C., Kunkel, D.D. and Schwartzkroin, P.A. Electrophysiological and morphological characterization of hippocampal interneurons. In: *The Hippocampus-New Vistas*, edited by V. Chan-Palay and C. Kohler. New York: Liss, 1989, p.287-305.

Lacaille, J.-C. and Williams, S. Membrane properties of interneurons in stratum oriens/alveus of the CA1 region of rat hippocampus. *Neuroscience* 36: 349-359, 1990.

Lacaille, J.-C. Postsynaptic potentials mediated by excitatory and inhibitory amino acids in interneurons of stratum pyramidale of the CA1 region of rat hippocampal slices in vitro. *J. Neurophysiol.* 66: 1441-1454, 1991.

Lancaster, B. and Wheal, H.V. Chronic failure of inhibition of the CA1 area of the hippocampus following kainic acid lesions of the CA3/CA4 area. *Brain Res.* 295: 317-324, 1984.

Lorente de Nō, R. Studies on the structure of the cerebral cortex II. Continuation of the study of the ammonic system. *J. Psychol. Neurol. (Lpz)* 46: 113-177, 1934.

Lothman, E.W., Bertram, E.H., Bekenstein, J.W. and Perlin, J.B. Self-sustaining limbic status epilepticus induced by "continuous" hippocampal stimulation: electrographic and behavioral characteristics. *Epilepsy Res.* 3: 107-119, 1989.

Maccaferri, G. and McBain, C.J. Passive propagation of LTD to stratum oriens-alveus inhibitory neurons modulates the temporoammonic input to the hippocampal CA1 region. *Neuron* 15: 137-145, 1995.

Maccaferri, G. and McBain, C.J. The hyperpolarization-activated current (I_h) and its contribution to pacemaker activity in rat CA1 hippocampal stratum oriens-alveus interneurones. *J. Physiol. (Lond.)* 497: 119-130, 1996.

Mangan, P.S., Rempe, D.A. and Lothman, E.W. Changes in inhibitory neurotransmission in the CA1 region and dentate gyrus in a chronic model of temporal lobe epilepsy. *J. Neurophysiol.* 74: 829-840, 1995.

Mangan, P.S. and Lothman, E.W. Profound disturbances of pre- and postsynaptic $GABA_B$ receptor-mediated processes in region CA1 in a chronic model of temporal lobe epilepsy. *J. Neurophysiol.* 76: 1282-1296, 1996.

Marco, P., Sola, R. G., Ramón y Cajal , S. and DeFelipe, J. Loss of inhibitory synapses on the soma and axon initial segment of pyramidal cells in human epileptic peritumoural neocortex: implications for epilepsy. *Brain Res. Bull.* 44: 47-66, 1997.

McBain, C.J. and Dingledine, R. Heterogeneity of synaptic glutamate receptors on CA3 stratum radiatum interneurones of rat hippocampus. *J. Physiol. (Lond.)* 462: 373-392, 1993.

McBain, C.J., Dichiara, T.J. and Kauer, J.A. Activation of metabotropic glutamate receptors differentially affects two classes of hippocampal interneurons and potentiates excitatory synaptic transmission. *J. Neurosci.* 14: 4433-4445, 1994.

McNamara, J.O. Cellular and molecular basis of epilepsy. *J. Neurosci.* 14: 3413-3425, 1994.

Misgeld, U. and Frotscher, M. Postsynaptic GABAergic inhibition of non-pyramidal neurons in the guinea pig hippocampus. *Neuroscience* 19:193-206, 1986.

Morin, F., Beaulieu, C. and Lacaille, J.-C. Membrane properties and synaptic currents evoked in CA1 interneuron subtypes in rat hippocampal slices. *J. Neurophysiol.* 76: 1-16, 1996.

Morin, F., Beaulieu, C. and Lacaille, J.-C. Selective loss of GABA neurons in area CA1 of the rat hippocampus after intraventricular kainate. *Epilepsy. Res.* 32: 363-369, 1998a.

Morin, F., Beaulieu, C. and Lacaille, J.-C. (1998b) Cell-specific alterations in synaptic properties of hippocampal CA1 interneurons after kainate treatment. *J. Neurophysiol.*, in press.

Morin, F., Beaulieu, C. and Lacaille, J.-C. (1998c) Alterations of perisomatic GABA synapses on hippocampal CA1 inhibitory interneurons and pyramidal cells in the kainate model of epilepsy, submitted.

Nadler, J.V., Perry, B.W., Gentry, C. and Cotman C.W. Loss and reacquisition of hippocampal synapses after selective destruction of CA3-CA4 afferents with kainic acid. *Brain Res.* 191: 387-403, 1980.

Nadler, J.V. Kainic acid as a tool for the study of temporal lobe epilepsy. *Life Sci.* 29: 2031-2042, 1981.

Nakajima, S., Franck, J.E., Bilkey, D. and Schwartzkroin, P.A. Local circuit synaptic interactions between CA1 pyramidal cells and interneurons in the kainate-lesioned hyperexcitable hippocampus. *Hippocampus* 1: 67-78, 1991.

Nurse, S. and Lacaille, J.-C. Properties of miniature IPSCs in CA1 interneurons of the rat hippocampus in vitro. *Soc. for Neurosci. Abstr.* 22: 670, 1996.

Perez, Y., Morin, F., Beaulieu, C. and Lacaille, J.-C. Axonal sprouting of CA1 pyramidal cells in hyperexcitable hippocampal slices of kainate-treated rats. *Eur. J. Neurosci.* 8: 736-748, 1996.

Perez, Y. and Lacaille, J.-C. Spontaneous excitatory postsynaptic currents in hippocampal CA1 interneurons in the kainate model of epilepsy. *Soc. Neurosci. Abstr.* 23: 2153, 1997.

Perouansky, M. and Yaari, Y. Kinetic properties of NMDA receptor-mediated synaptic currents in rat hippocampal pyramidal cells versus interneurons. *J. Physiol. (Lond.)* 465: 223-244, 1993.

Peterson, G.M., Ribak, C.E. and Oertel, W.H. A regional increase in the number of hippocampal GABAergic neurons and terminals in the seizure-sensitive gerbil. *Brain Res.* 340: 384-389, 1985.

Ramón y Cajal , S. *Histologie du système nerveux de l'homme et des vertébrés.* Maloine, Paris, 1911.

Rempe, D.A., Bertram, E.H., Williamson, J.M. and Lothman, E.W. Interneurons in area CA1 stratum radiatum and stratum oriens remain functionally connected to excitatory synaptic input in chronically epileptic animals. *J. Neurophysiol.* 78: 1504-1515, 1997.

Represa, A., Jorquera, I., Le Gal La Salle, G. and Ben-Ari, Y. Epilepsy induced collateral sprouting of hippocampal mossy fibers: does it induce the

development of ectopic synapses with granule cell dendrites? *Hippocampus* 3: 257-268, 1993.

Ribak, C.E., Vaughn, J.E. and Saito, K. Immunocytochemical localization of glutamic acid decarboxylase in neuronal somata following colchicine inhibition of axonal transport. *Brain Res.* 140: 315-332, 1978.

Ribak, C.E., Harris, A.B., Vaughn, J.E. and Roberts, E. Inhibitory, GABAergic nerve terminals decrease at sites of focal epilepsy. *Science* 205: 211-214, 1979.

Ribak, C.E., Bradburne, R.M. and Harris, A.B. A preferential loss of GABAergic, symmetric synapses in epileptic foci: A quantitative ultrastructural analysis of monkey neocortex. *J. Neurosci.* 2: 1725-1735, 1982.

Ribak, C.E., Nitsch, R. and Seress, L. Proportion of parvalbumin-positive basket cells in the GABAergic innervation of pyramidal and granule cells of the rat hippocampal formation. *J. Comp. Neurol.* 300: 449-461, 1990.

Rice, A., Rafiq, A., Shapiro, S.M., Jakoi, E.R., Coulter, D.A. and DeLorenzo, R.J. Long-lasting reduction of inhibitory function and γ -aminobutyric acid type A receptor subunit mRNA expression in a model of temporal lobe epilepsy. *Proc. Natl. Acad. Sci. (USA)* 93: 9665-9669, 1996.

Robbins, R.J., Brines, M.L., Kim, J.H., Adrian, T., deLanerolle, N., Welsh, S. and Spencer, D.D. A selective loss of somatostatin in the hippocampus of patients with temporal lobe epilepsy. *Ann. Neurol.* 29: 325-332, 1991.

Sah, P., Hestrin, S. and Nicoll, R.A. Properties of excitatory postsynaptic currents recorded in vitro from rat hippocampal interneurons. *J. Physiol. (Lond.)* 430: 605-616, 1990.

Schwartzkroin, P.A. and Mathers, L.H. Physiological and morphological identification of a nonpyramidal hippocampal cell type. *Brain Res.* 157: 1-10, 1978.

Schwartzkroin, P.A. and Kunkel, D.D. Morphology of identified interneurons in the CA1 regions of guinea pig hippocampus. *J. Comp. Neurol.* 232: 205-218, 1985.

Schwartzkroin, P.A. Origins of the epileptic state. *Epilepsia* 38: 853-858, 1997.

Scotti, A.L., Kalt, G., Bollag, O. and Nitsch, C. Parvalbumin disappears from GABAergic CA1 neurons of the gerbil hippocampus with seizure onset while its presence persists in the perforant path. *Brain Res.* 760: 109-117, 1997.

Shigemoto, R., Kulik, A., Roberts, J.D.B., Ohishi, H., Nusser, Z., Kaneko, T. and Somogyi, P. Target-cell-specific concentration of a metabotropic glutamate receptor in the presynaptic active zone. *Nature* 381: 523-525, 1996.

Shin, C.S. and McNamara, J.O. Mechanisms in epilepsy. *Annu. Rev. Med.* 45: 379-389, 1994.

Sik, A., Penttonen, M., Ylinen, A. and Buzsaki, G. Hippocampal CA1 interneurons: an *in vivo* intracellular labeling study. *J. Neurosci.* 15: 6651-6665, 1995.

Sloviter, R.S. "Epileptic" brain damage in rats induced by electrical stimulation of the perforant path. I. Acute electrophysiological and light microscopic studies. *Brain Res. Bull.* 10: 675-697, 1983.

Sloviter, R.S. and Naviler, G. Immunocytochemical localization of GABA-, cholecystokinin-, vasoactive intestinal polypeptide-, and somatostatin-like immunoreactivity in the area dentata and hippocampus of the rat. *J. Comp. Neurol.* 256: 42-60, 1987.

Sloviter, R.S. Calcium-binding protein (calbindin-D28k) and parvalbumin immunocytochemistry: localization in the rat hippocampus with specific reference to the selective vulnerability of hippocampal neurons to seizure activity. *J. Comp. Neurol.* 280: 183-196, 1989.

Sloviter, R.S. Permanently altered structure, excitability, and inhibition after experimental status epilepticus in the rat: the "dormant basket cell" hypothesis and its possible relevance to temporal lobe epilepsy. *Hippocampus* 1: 41-66, 1991.

Sloviter, R.S. Possible functional consequences of synaptic reorganization in the dentate gyrus of kainate-treated rats. *Neurosci. Lett.* 137: 91-96, 1992.

Somogyi, P., Nunzi, M.G., Gorio, A. and Smith, A.D. A new type of specific interneuron in the monkey hippocampus forming synapses exclusively with the axon initial segments of pyramidal cells. *Brain Res.* 259: 137-142, 1983.

Somogyi, P., Hodgson, A.J., Smith, A.D., Nunzi, M.G., Gorio, A. and Wu, J.-Y. Different populations of GABAergic neurons in the visual cortex and hippocampus of cat contain somatostatin- or cholecystokinin-immunoreactive material. *J. Neurosci.* 4: 2590-2603, 1984.

Storm, J.F. An afterhyperpolarization of medium duration in rat hippocampal pyramidal cells. *J. Physiol. (Lond.)* 409: 171-190, 1989.

Storm, J.F. Potassium currents in hippocampal pyramidal cells. In: *Understanding the Brain Through the Hippocampus*, edited by J. Storm-Mathisen, J. Zimmer, and O. P. Ottersen. New York: Elsevier, 1990, p.161-188.

Sundstrom, L.E., Mitchell, J. and Wheal, H.V. Bilateral reorganisation of mossy fibers in the rat hippocampus after a unilateral intracerebroventricular kainic acid injection. *Brain Res.* 609: 321-326, 1993.

Tauck, D.L. and Nadler, J.V. Evidence of functional mossy fiber sprouting in hippocampal formation of kainic acid-treated rats. *J. Neurosci.* 5: 1016-1022, 1985.

Thompson, S.M. Modulation of inhibitory synaptic transmission in the hippocampus. *Prog. Neurobiol.* 42: 575-609, 1994.

Toth, K. and Freund, T.F. Calbindin D28k-containing nonpyramidal cells in the rat hippocampus: their immunoreactivity for GABA and projection to the medial septum. *Neuroscience* 49: 793-805, 1992.

Traub, R.D., Whittington, M.A., Colling, S.B., Buzsaki, G. and Jefferys, J.G.R. Analysis of gamma rhythms in the rat hippocampus in vitro and in vivo. *J. Physiol. (Lond.)* 493: 471-484, 1996.

Turner, D.A. and Wheal, H.V. Excitatory synaptic potentials in kainic-acid denervated rat CA1 pyramidal neurons. *J. Neurosci.* 11: 2786-2794, 1991.

Turski, L., Ikonomidou, C., Turski, W.A., Bortolotto, Z.A. and Cavalheiro, E.A. Review: Cholinergic mechanisms and epileptogenesis. The seizures induced by pilocarpine: A novel experimental model of intractable epilepsy. *Synapse* 3: 154-171, 1989.

Vick, R.S., Rafiq, A., Coulter, D.A., Jakoi, E.R. and DeLorenzo, R.J. GABA_A $\alpha 2$ mRNA levels are decreased following induction of spontaneous epileptiform discharges in hippocampal-entorhinal cortical slices. *Brain Res.* 721: 111-119, 1996.

Wang, X.-J. and Buzsaki, G. Gamma oscillation by synaptic inhibition in a hippocampal interneuronal network model. *J. Neurosci.* 15: 6402-6413, 1996.

Wasterlain, C.G., Farber, D.B. and Fairchild, M.D. Synaptic mechanisms in the kindled epileptic focus: A speculative synthesis. *Adv. Neurol.* 44: 411-433, 1986.

Williams, S., Vachon, P. and Lacaille, J.-C. Monosynaptic GABA-mediated inhibitory postsynaptic potentials in CA1 pyramidal cells of hyperexcitable

hippocampal slices from kainic acid-treated rats. *Neuroscience* 52: 541-554, 1993.

Williams, S., Samulack, D.D., Beaulieu, C. and Lacaille, J.-C. Membrane properties and synaptic responses of interneurons located near the stratum lacunosum-moleculare/radiatum border of area CA1 in whole-cell recordings from rat hippocampal slices. *J. Neurophysiol.* 71: 2217-2235, 1994.

Zhang, L. and McBain, C.J. Potassium conductances underlying repolarization and after-hyperpolarization in rat CA1 hippocampal interneurones. *J. Physiol. (Lond.)* 488: 661-672, 1995.

CHAPITRE 9

APPENDICE

APPENDICE I

Contribution de l'étudiant pour chacun des articles inclus dans cette thèse.

A) Propriétés membranaires et courants synaptiques générés dans des sous-types d'interneurones de la région CA1 dans des tranches d'hippocampe chez le rat

J'ai effectué les chirurgies animales, les expériences électrophysiologiques, l'analyse des données, ainsi que la rédaction du manuscrit.

B) Perte sélective des neurones GABA dans la région CA1 de l'hippocampe chez le rat après injection intraventriculaire de l'acide kaïnique

J'ai effectué les chirurgies animales, les expériences d'immunocytochimie, la collection et l'analyse des données, ainsi que la rédaction du manuscrit.

C) Altérations spécifiques des propriétés synaptiques des interneurones de la région CA1 de l'hippocampe après le traitement à l'acide kaïnique

J'ai effectué les chirurgies animales, les expériences électrophysiologiques, l'analyse des données, ainsi que la rédaction du manuscrit.

D) Altérations des synapses périsomatiques GABA dans les interneurones inhibiteurs et les cellules pyramidales de la région CA1 de l'hippocampe dans le modèle d'épilepsie de l'acide kaïnique

J'ai effectué les chirurgies animales, les expériences d'immunocytochimie et de microscopie électronique, la collection et l'analyse des données, ainsi que la rédaction du manuscrit.

E) Une procédure de fixation pour l'investigation ultrastructurale des connexions synaptiques dans le cortex humain prélevé par résection

J'ai effectué la préparation histologique du tissu animal, la collection de tissu humain à l'hôpital, les expériences histologiques immunocytochimiques et de microscopie électronique, la collection et l'analyse des données, ainsi que la rédaction du manuscrit.